

**ENGINE PERFORMANCE, EMISSION AND CORROSION OF
BIODIESEL–BIOETHANOL–DIESEL BLENDS FROM
JATROPHA CURCAS–*CEIBA PENTANDRA* MIXED OIL**

SURYA DHARMA

**FACULTY OF ENGINEERING
UNIVERSITY OF MALAYA
KUALA LUMPUR**

2018

**ENGINE PERFORMANCE, EMISSION AND
CORROSION OF BIODIESEL–BIOETHANOL–DIESEL
BLENDS FROM *JATROPHA CURCAS–CEIBA
PENTANDRA* MIXED OIL**

SURYA DHARMA

**THESIS SUBMITTED IN FULFILMENT
OF THE REQUIREMENTS
FOR THE DEGREE OF DOCTOR OF PHILOSOPHY**

**FACULTY OF ENGINEERING
UNIVERSITY OF MALAYA
KUALA LUMPUR**

2018

UNIVERSITY OF MALAYA

ORIGINAL LITERARY WORK DECLARATION

Name of Candidate : **Surya Dharma**

Registration/Matric No : **KHA140114**

Name of Degree : **Doctor of Philosophy (Ph.D)**

Title of Project/Research Report/Dissertation/Thesis ("This Work")

Engine Performance, Emission and Corrosion of Biodiesel–Bioethanol–Diesel Blends from *Jatropha Curcas-Ceiba Pentandra* Mixed Oil.

Field of Study : **Energy**

I do solemnly and sincerely declare that:

- (1) I am the sole author/writer of the work;
- (2) This work is original;
- (3) Any use of any work in which copyright exists was done by way of fair dealings and any expert or extract from or reference to or reproduction of any copyright work has been disclosed expressly and sufficiently and the title of the work and its authorship has been acknowledged in this work;
- (4) I do not have any actual knowledge nor do I ought to reasonably to know that the making of this work constitutes an infringement of any copyright work;
- (5) I hereby assign all and every rights in the copyright to this work to the University of Malaya (UM), who henceforth shall be the owner of the copyright in this work and that any reproduction or use in any form or by any means whatsoever is prohibited without the written consent of UM having been first had and obtained actual knowledge;
- (6) I am fully aware that if in the course of making this work I have infringed any copyright whether internationally or otherwise, I may be subject to legal action or any other action as may be determined by UM.

Candidate's Signature

Date: 18/09/2017

Subscribed and solemnly declared before,

Witness Signature

Date: 18/09/2017

Name: **Dr. MOHD NASHRUL MOHD ZUBIR**
Designation **Senior Lecturer**
Department of Mechanical Engineering
Faculty of Engineering
University of Malaya

**ENGINE PERFORMANCE, EMISSION AND CORROSION OF
BIODIESEL–BIOETHANOL–DIESEL BLENDS FROM *JATROPHA CURCAS*–
CEIBA PENTANDRA MIXED OIL**

ABSTRACT

The increasing world population growth, energy crisis and environmental damage due to the use of fossil fuels are the main issues we face today, motivating many researchers to develop environmentally friendly, renewable and biodegradable fuels such as biodiesel. Biodiesel can be produced from various types of raw materials such as edible oil, non-edible oil, waste oil and animal fats. Numerous efforts have been made to increase the production and improve the properties of biodiesel by mixing several types of feedstock. The main objectives of this study are to optimize production, analyze engine performance and exhaust emissions, and investigate the corrosion of biodiesel produced from mixtures of crude *J. curcas* and *C. pentandra* oils. The selection of mixed compositions is based on the properties of crude oil mixtures. The biodiesel was produced using a two-step process, whereas the *J. curcas* and *C. pentandra* oil mixture was esterified with sulfuric acid (H_2SO_4) and the product of the esterification process was converted into methyl esters through alkali-catalysed transesterification. The optimization of the methyl ester yield through transesterification process was through surface methodology based on Box-Behnken experimental design. The parameters such as methanol-to-oil ratio, agitation speed and concentration of the potassium hydroxide catalyst were evaluated in optimization biodiesel production. Based on the results, the optimum operating parameters for transesterification of the J50C50 oil mixture at 60 °C over a period of 2 hours were as follows: methanol-to-oil ratio: 30%, agitation speed: 1300 rpm and catalyst concentration: 0.5 wt.%. These optimum operating parameters gave the highest yield for the J50C50 biodiesel with a value of 93.33%. The physicochemical properties of the optimized J50C50 biodiesel

fulfil the requirements given in the ASTM D6751 and EN 14214 standards. Experimental study was done regarding engine performance and exhaust emission using single cylinder direct injection engine. The fuel used was biodiesel-diesel and biodiesel-bioethanol-diesel fuel blends. Parameters that became the object of observation included brake specific fuel consumption, engine torque, brake power, exhaust gas temperature, brake thermal efficiency, CO, CO₂, and NO_x emissions, as well as smoke opacity. The results showed that the small content of biodiesel and bioethanol in the mixture had properties and performance close to diesel fuel, but significantly reduced the CO₂ and smoke opacity. Analysis of corrosion behavior was done to analyse the effect of biodiesel and bioethanol on the degradation of machine components. A static immersion test method for 2000 hours was considered as appropriate to see the effect of mixed fuel on the corrosion of mild steel coupons. A series of tests was performed to see changes in mild steel coupons due to corrosion, such as scanning electron microscope, energy dispersive x-ray, fourier transform infrared, and properties testing. In conclusion, it is known that the rate of corrosion is influenced by the percentage of biodiesel and bioethanol content in the fuel mixture. The addition of biodiesel and bioethanol in a small percentage has a relatively similar corrosion rate with diesel fuel.

Keyword: *Biodiesel; Bioethanol; Performance; Emissions; Corrosion.*

PRESTASI ENJIN, PELEPASAN DAN KAKISAN CAMPURAN BIODIESEL- BIOETANOL-DIESEL DARI *JATROPHA CURCAS*-POKOK KEKABU OIL CAMPURAN

ABSTRAK

Peningkatan pertumbuhan penduduk dunia, krisis tenaga dan kerosakan alam sekitar akibat penggunaan bahan api fosil adalah isu utama yang harus dihadapi hari ini. Inilah yang mendasari ramai penyelidik untuk membangunkan bahan api mesra alam, diperbaharui dan biodegradable seperti biodiesel. Biodiesel boleh dihasilkan dari pelbagai jenis bahan mentah, seperti minyak makan, minyak tidak boleh dimakan, minyak sisa dan lemak haiwan. Pelbagai usaha telah dibuat untuk meningkatkan jumlah pengeluaran dan memperbaiki sifat-sifat biodiesel, salah satunya adalah dengan mencampurkan beberapa jenis bahan mentah. Objektif utama kajian ini adalah untuk mengoptimumkan pengeluaran, menganalisis prestasi enjin dan pelepasan ekzos, dan menyiasat kesan kakisan bahan api yang dihasilkan daripada campuran minyak mentah *J. curcas* dan *C. pentandra*. Pemilihan campuran campuran adalah berdasarkan sifat-sifat campuran minyak mentah. Tambahan pula, biodiesel dihasilkan dengan menggunakan proses dua langkah, di mana campuran *J. curcas* dan *C. pentandra* diserap pertama dengan asid sulfurik (H_2SO_4), dan produk proses esterifikasi ditukar kepada metil ester (biodiesel) Melalui transesterification alkali-catalysed. Untuk mengoptimumkan hasil biodiesel yang dihasilkan pada proses transesterifikasi dengan menggunakan metodologi permukaan berdasarkan rancangan eksperimen Box-Behnken. Parameter pengeluaran seperti nisbah methanol-ke-minyak, kelajuan agitasi dan kepekatan pemangkin kalium hidroksida menjadi parameter pengoptimuman. Berdasarkan hasilnya, parameter operasi optimum untuk transesterifikasi campuran minyak J50C50 pada $60^\circ C$ dalam tempoh 2 jam adalah seperti berikut: nisbah metanol-ke-minyak: 30%, kelajuan agitasi: 1300 rpm dan kepekatan pemangkin: 0.5 Wt.%. Parameter

operasi optimum ini memberikan hasil tertinggi untuk biodiesel J50C50 dengan nilai 93.33%. Sifat fizikokimia biodiesel J50C50 yang dioptimumkan memenuhi kehendak yang diberikan dalam piawaian ASTM D6751 dan EN 14214. Kajian eksperimen mengenai prestasi enjin dan pelepasan ekzos menggunakan enjin suntikan langsung silinder tunggal. Bahan api yang digunakan ialah campuran bahan bakar biodiesel-diesel dan campuran bahan bakar biodiesel-bioethanol-diesel. Parameter yang menjadi obyek pemerhatian termasuk penggunaan bahan bakar khusus injap, tork enjin, kuasa brek, suhu gas ekzos, kecekapan terma brek, CO, CO₂, dan pelepasan NO_x, serta kelegapan asap. Keputusan menunjukkan bahawa kandungan kecil biodiesel dan bioethanol dalam campuran mempunyai ciri-ciri dan prestasi yang dekat dengan bahan api diesel, tetapi dengan ketara mengurangkan CO₂ dan kelegapan asap. Analisi tingkah laku kakisan bertujuan untuk melihat kesan biodiesel dan bioethanol pada degradasi komponen mesin. Kaedah ujian rendaman statik untuk 2000 jam dianggap sesuai untuk melihat kesan bahan api campuran pada kakisan kupon keluli ringan. Satu siri ujian dilakukan untuk melihat perubahan kupon keluli ringan disebabkan oleh kakisan, seperti mikroskop elektron imbasan, sinaran dispersif tenaga, inframerah transformasi empatier, dan ujian sifat. Kesimpulannya, diketahui bahawa kadar kakisan dipengaruhi oleh peratusan kandungan biodiesel dan bioethanol dalam campuran bahan bakar. Tambahan biodiesel dan bioethanol dalam peratusan kecil mempunyai kadar kakisan yang agak sama dengan bahan api diesel.

Kata kunci: *Biodiesel; Bioethanol; Prestasi; Pelepasan; Kakisan.*

ACKNOWLEDGEMENTS

I would like to thank to almighty Allah S.W.T, the creator of the world for giving me the fortitude and aptitude to complete this thesis.

I would like to special thanks to my supervisors Professor Dr. Masjuki Haji Hassan and Dr. Ong Hwai Chyuan for their helpful guidance, encouragement and assistance throughout this works. I also express my gratitude to the Ministry of Higher Education (MOHE) for HIR Grant for the financial support through project no. UM.C/HIR/MOHE/ENG/60 (D0000060-16001). I also would like to convey appreciation to all lectures and staff of the Department of Mechanical Engineering, University of Malaya for preparing and giving opportunity to conduct this research. I also would like to thank all members in “Centre Energy of Sciences” research group for their valuable ideas and discussion.

Last but not least, take pleasure in acknowledgment the continued encouragement and moral support of my beloved wife (Isma Fitriani Lubis), my sons (Rafi, Rifqi and Raihan), my parents (Alm. Jumin SP and Almh. Ponisah), my father and mother in law, my brothers, my sister, my other family members, Prof. Dr. T.M. Indra Mahlia, Dr. Susan, Mr. Abdi, Mr. Fitranto Kusumo, Mr. Ayat, Mr. Priyonggo Suseno, Jassinnee Millano and all of my friends. Their help, advice and ideas had contributed a lot toward the success of this thesis.

TABLE OF CONTENTS

ABSTRACT	iii
ABSTRAK.....	v
ACKNOWLEDGEMENTS.....	vii
TABLE OF CONTENTS.....	viii
LIST OF FIGURES	xiii
LIST OF TABLES.....	xvii
LIST OF SYMBOLS AND ABBREVIATIONS.....	xix
LIST OF APPENDICES.....	xxi
CHAPTER 1: INTRODUCTION.....	1
1.1 Overview	1
1.2 Research background.....	2
1.3 Objectives.....	6
1.4 Contributions of the study.....	7
1.5 Thesis outline	8
CHAPTER 2: LITERATURE REVIEW.....	10
2.1 Introduction	10
2.2 Feasibility of biodiesel and bioethanol feedstocks	13
2.3 Biodiesel feedstocks	15
2.3.1 Edible vegetable oils.....	18
2.3.2 Non edible vegetable oil feedstock	20
2.3.2.1 Jatropha curcas L.	20
2.3.2.2 Ceiba pentandra L.	21
2.3.3 Waste or recycled oils	22
2.3.4 Animal fats.....	23
2.4 Bioethanol feedstocks	24
2.4.1 First-generation bioethanol.....	25

2.4.2	Second-generation bioethanol (lignocellulosic materials).....	26
2.4.3	Third-generation bioethanol.....	27
2.5	Properties of biodiesel and petroleum diesel.....	28
2.5.1	Kinematic viscosity.....	28
2.5.2	Density.....	29
2.5.3	Acid value.....	30
2.5.4	Flash point.....	31
2.5.5	Cloud point and pour point.....	31
2.5.6	Calorific value.....	32
2.5.7	Oxidation stability.....	33
2.5.8	Cetane number.....	34
2.5.9	Iodine value.....	35
2.6	Properties of bioethanol and gasoline.....	35
2.7	Properties of biodiesel–bioethanol–petroleum diesel blends.....	37
2.8	Optimization esterification-transesterification using response surface methodology (RSM).....	39
2.9	Engine performance and emissions characterization.....	40
2.9.1	Biodiesel–petroleum diesel blends.....	40
2.9.2	Bioethanol–gasoline blends.....	42
2.9.3	Biodiesel–bioethanol–petroleum diesel blends.....	45
2.10	Corrosion.....	46
2.10.1	Corrosion behaviour of metals and their alloys immersed in biodiesels ...	46
2.10.2	Corrosion behaviour of metals and their alloys immersed in ethanol/bioethanol.....	50
2.11	Summary.....	51

CHAPTER 3: METHODOLOGY	52
3.1 Introduction	52
3.2 Materials.....	54
3.3 Experimental setup for esterification and transesterification	54
3.4 Measurement of physicochemical properties	55
3.5 Biodiesel production	56
3.5.1 <i>J. curcas</i> – <i>C. pentandra</i> crude oil mixtures	56
3.5.2 Mixing and degumming crude oil	57
3.5.3 Esterification	57
3.5.4 Transesterification.....	58
3.6 Optimization biodiesel production	58
3.7 Fatty acid composition and Fourier transform infrared spectrum of the <i>J. curcas</i> - <i>C. pentandra</i> biodiesel.....	60
3.8 Physicochemical properties of <i>J. curcas</i> , <i>C. pentandra</i> and <i>J. curcas</i> - <i>C. pentandra</i> biodiesels.....	61
3.9 Biodiesel diesel fuel blend	61
3.10 Biodiesel-bioethanol-diesel fuel blend	62
3.11 Experimental procedure for engine test and emissions.....	63
3.12 Corrosion testing.....	65
3.13 Material for corrosion test.....	65
3.14 Corrosion analysis	66
3.15 Summary	67
CHAPTER 4: RESULTS AND DISCUSSION	68
4.1 Introduction	68

4.2	Physicochemical properties of crude oil mixtures.....	68
4.3	Biodiesel production and optimization	71
4.3.1	Properties of the J50C50 biodiesel.....	71
4.3.1.1	Fatty acid composition and Fourier transform infrared spectrum of the J50C50 biodiesel	71
4.3.1.2	Physicochemical properties of J. curcas, C. pentandra and J50C50 biodiesels	74
4.3.2	Optimization of the J50C50 biodiesel yield using response surface methodology	79
4.3.2.1	Quadratic regression model.....	80
4.3.2.2	Effect of methanol-to-oil ratio	86
4.3.2.3	Effect of agitation speed.....	87
4.3.2.4	Effect of catalyst concentration	87
4.3.3	Summary	89
4.4	Engine performance and exhaust emission	90
4.4.1	Biodiesel-diesel and biodiesel-bioethanol-diesel fuel blending	90
4.4.2	Errors and uncertainties analysis.....	94
4.4.3	Engine performance analysis	95
4.4.3.1	Brake specific fuel consumption.....	95
4.4.3.2	Engine torque.....	97
4.4.3.3	Brake power.....	100
4.4.3.4	Exhaust gas temperature.....	101
4.4.3.5	Brake thermal efficiency	103
4.4.4	Exhaust emissions	106
4.4.4.1	Nitrogen oxides.....	106
4.4.4.2	Carbon monoxide.....	108

4.4.4.3 Carbon dioxide.....	110
4.4.4.4 Smoke opacity	113
4.4.5 Summary.....	115
4.5 Biodiesel-diesel fuel blends and biodiesel-bioethanol-diesel fuel blends corrosion	116
4.5.1 Corrosion rate.....	116
4.5.2 Surface characteristics	120
4.5.3 Effects of corrosion on fuel properties	128
4.5.3.1 Total acid number	128
4.5.3.2 Kinematic viscosity and density	130
4.5.3.3 Fourier transform infrared (FTIR)	133
4.5.4 Summary.....	138
CHAPTER 5: CONCLUSION AND RECOMMENDATIONS.....	139
5.1 Conclusion.....	139
5.2 Recommendations.....	141
References	143
List of Publications and Papers Presented.....	176
Appendix	179

LIST OF FIGURES

Figure 2.1: Total world energy consumption by energy source for 1990–2040 (EIA, 2016).....	11
Figure 2.2: Delivered transportation energy consumption by country grouping, 2012–2040 (quadrillion Btu) (EIA, 2016).....	12
Figure 2.3: Energy-related carbon dioxide emissions, 1990–2040 (billion metric tons) (EIA, 2016)	13
Figure 2.4: Breakdown of expenditure required for biodiesel production (Ahmad et al., 2011; Lin, L. et al., 2011)	16
Figure 2.5: Classification of biodiesel feedstocks (Atabani et al., 2012; Mofijur, Atabani, et al., 2013)	17
Figure 2.6: Types of feedstocks used for bioethanol production (de Souza et al., 2013).....	25
Figure 2.7: Phase behaviour of an ethanol–biodiesel–petroleum diesel blend (Fernando et al., 2004; Hansen et al., 2005).....	38
Figure 3. 1: Methodolgy glowchart	53
Figure 3.2: Tree, fruits, seeds and crude oil of: (a) <i>J. curcas</i> and (b) <i>C. pentandra</i>	54
Figure 3.3: Apparatus for esterification and transesterification of crude <i>J. curcas</i> – <i>C. pentandra</i> oil to methyl ester	55
Figure 3.4: Schematic layout of the single-cylinder direct injection diesel engine set-up	63
Figure 4.1: Fourier transform infrared spectrum of the J50C50 biodiesel.....	73
Figure 4.2: Plot of the experimental versus predicted J50C50 biodiesel yield	83
Figure 4.3: Residual plots: (a) normal probability plot of studentized residuals, (b) plot of the studentized residuals versus the predicted biodiesel yield and (c) outlier <i>t</i> plot.....	85

Figure 4.4: Three-dimensional surface plot which shows the combined effects of: (a) methanol-to-oil ratio and catalyst concentration, (b) agitation speed and methanol-to-oil ratio, and (c) catalyst concentration and agitation speed on the J50C50 biodiesel yield.	88
Figure 4.5: Variation of the brake specific fuel consumption for (a) biodiesel-diesel blends with different percentage of J50C50 biodiesel and (b) biodiesel-bioethanol-diesel blends at full load and various engine speeds	97
Figure 4.6: Variation of the engine torque for (a) biodiesel-diesel blends with different percentage of J50C50 biodiesel, and (b) biodiesel-bioethanol-diesel blends at full load and various engine speeds	99
Figure 4.7: Variation of the brake power for (a) biodiesel-diesel blends with different percentage of J50C50 biodiesel, and (b) biodiesel-bioethanol-diesel blends at full load and various engine speeds	101
Figure 4.8: Variation of the exhaust gas temperature for (a) biodiesel-diesel blends with different percentage of J50C50 biodiesel, and (b) biodiesel-bioethanol-diesel blends at full load and various engine speeds	103
Figure 4.9: Variation of the brake thermal efficiency for (a) biodiesel-diesel blends with different percentage of J50C50 biodiesel, and (b) biodiesel-bioethanol-diesel blends at full load and various engine speeds	105
Figure 4.10: Variation of the NO _x emissions for (a) biodiesel-diesel blends with different percentage of J50C50 biodiesel, and (b) biodiesel-bioethanol-diesel blends at full load and various engine speeds	107
Figure 4.11: Variation of the CO emissions for (a) biodiesel-diesel blends with different percentage of J50C50 biodiesel, and (b) biodiesel-bioethanol-diesel blends at full load and various engine speeds	110

Figure 4.12: Variation of the CO ₂ emissions for (a) biodiesel-diesel blends with different percentage of J50C50 biodiesel, and (b) biodiesel-bioethanol-diesel blends at full load and various engine speeds	112
Figure 4.13: Variation of the smoke opacity for (a) biodiesel-diesel blends with different percentage of J50C50 biodiesel, and (b) biodiesel-bioethanol-diesel blends at full load and various engine speeds	114
Figure 4.14: Corrosion rate of mild steel in (a) biodiesel-diesel blends, and (b) biodiesel-bioethanol-diesel blends after immersion for 400, 800, 1200, 1600 and 2000 hours	117
Figure 4.15: Photographs of mild steel coupons are immersed in some fuel mixtures with the immersion time duration of (a) 0 hour (as receipt), (b) 400 hours, (c) 2000 hours.	120
Figure 4.16: Optical photograph (1000 ×) showing the morphology of corrosion products in the surface of mild steel after immersion 400 h at ambient temperature for (a) B0, (b) B10, (c) B20, (d) B30, (e) B40, (f) B50, (g) B10BE5, (h) B20BE8, (i) B30BE10, (j) B40BE13 and (k) B50BE15 ...	122
Figure 4.17: Optical photograph (1000 ×) showing the morphology of corrosion products in the surface of mild steel after immersion 2000 h at ambient temperature for (a) B0, (b) B10, (c) B20, (d) B30, (e) B40, (f) B50, (g) B10BE5, (h) B20BE8, (i) B30BE10, (j) B40BE13 and (k) B50BE15 ...	123
Figure 4.18: Elemental composition of mild steel as received (a) and mild steel after immersion 2000 hours at ambient temperature for (b) B0, (c) B10, (d) B20, (e) B30, (f) B40, (g) B50, (h) B10BBE5, (i) B20BE8, (j) B30BE10, (k) B40BE13, and (l) B50BE15.	124
Figure 4.19: Changes in total acid number (TAN) of (a) J50C50 biodiesel-diesel fuel blends and (b) J50C50 biodiesel-bioethanol-diesel fuel blends before and	

after exposure to mild steel at ambient temperature for 0, 400, 800, 1200, 1600 and 2000 hours of immersion.....	129
Figure 4.20: Changes in viscosity of (a) J50C50 biodiesel-diesel fuel blends and (b) J50C50 biodiesel-bioethanol-diesel fuel blends before and after exposure to mild steel at ambient temperature for 0, 400, 800, 1200, 1600 and 2000 hours of immersion.....	131
Figure 4.21: Changes in density (a) J50C50 biodiesel-diesel fuel blends and (b) J50C50 biodiesel-bioethanol-diesel fuel blends before and after exposure to mild steel at ambient temperature for 0, 400, 800, 1200, 1600 and 2000 hours of immersion.	132
Figure 4.22: Main features of the FTIR spectrum of J50C50 biodiesel-diesel fuel sediment caused by exposure to mild steel to some fuel mixtures (a) Diesel fuel, (b) B10, (c) B20, (d) B30, (e) B40, (f) B50, (g) B10BE5, (h) B20BE8, (i) B30BE10, (j) B40BE13, and (k) B50BE15	134

LIST OF TABLES

Table 2.1: World bioethanol production from 2012 to 2015	15
Table 2.2: World biodiesel production from 2012 to 2015.....	15
Table 2.3: Potential feedstocks for biodiesel production in various countries.....	18
Table 2.4: Composition of various types of lignocellulosic-biomass materials.....	27
Table 2.5: Physicochemical properties of methanol, ethanol, gasoline and bioethanol .	36
Table 2.6: Review of material corrosion tests for some types of biodiesel	49
Table 3.1: List of apparatus used for properties test.....	56
Tabel 3.2: Box-Behnken coded and uncoded independent variables for optimization of the transesterification process parameters for the <i>J. curcas</i> - <i>C. pentandra</i> oil mixture	59
Tabel 3.3: Description of biodiesel-diesel blending	62
Tabel 3.4: Description of for biodiesel-bioethanol-diesel blending	63
Tabel 3.5: Technical specifications of the engine	64
Tabel 3.6: Technical specifications of the gas analyser.....	64
Tabel 3.7: Mild steel composition	66
Table 4.1: Physicochemical properties of <i>Jatropha</i> , <i>Jatropha curcas</i> and <i>Ceiba</i> <i>pentandra</i> crude oils as well as various crude oil mixtures	70
Table 4.2: Comparison of the fatty acid composition of the J50C50 biodiesel with other biodiesels.....	72
Table 4.3: Wavenumber, functional group, band assignment and absorption intensity of the absorption peaks detected in the Fourier transform infrared spectrum of the J50C50 biodiesel.....	73
Table 4.4: Comparison of the physicochemical properties of J50C50 biodiesel before optimization with diesel and other biodiesels	77
Table 4.5: Physicochemical properties of the J50C50 biodiesel after optimization.....	79

Table 4.6: Experimental design for optimization of the transesterification process parameters for the <i>J. curcas</i> - <i>C. pentandra</i> oil mixture	80
Table 4.7: Results obtained from analysis of variance	82
Table 4.8: The properties of J50C50 biodiesel, biodiesel-diesel fuel blends and biodiesel-bioethanol-diesel fuel blends	93
Table 4.9: List of measurement accuracy and percentage uncertainties	95
Table 4.10: Wavenumber, functional group, band assignment and absorption intensity of the absorption peaks detected in the Fourier transform infrared spectrum of the J50C50 biodiesel-diesel fuel blends	137

University of Malaya

LIST OF SYMBOLS AND ABBREVIATIONS

Symbol	Description	Unit
A	Area of specimen	cm ²
AV	Acid value	mg KOH/g
Bsfc	Brake specific fuel consumption	g/kWh
BMEP	Brake mean effective pressure	Pa
BTE	Brake thermal efficiency	%
CO	Carbon monoxide	% vol.
CO ₂	Carbon dioxide	% vol.
CR	Corrosion rate	mm/year
D	Density of metal	g/cm ³
EGT	Exhaust gas temperature	°C
HC	Hydrocarbons	ppm
HSU	Hartridge smoke units	%
K _w	Ionization constant	—
MW	Molecular weight	g/mol
NO _x	Nitrogen oxides	ppm
n	Normality	—
N	speed	Rev/min
CR	Corrosion rate	mm/year
Q _{hvc}	Heating value of uel	kJ/kg
S15	Sulfur grade 15	ppm
S500	Sulfur grade 500	ppm
—	Speed agitation	rpm
T	Transmission	%
—	Reaction time	hour
—	Reaction temperature	°C
V	Volume	liter
V _d	Volume displacement	liter
\dot{m}	Flow rate mass	kg/s
MW	Molecular weight	g/mol
w	Weight	g
W	Brake power	kW
—	Yield ester	%
—	Reaction time	hour
—	Reaction temperature	°C
ρ	Density	kg/m ³
π	Constanta pi	—
τ	Torque	Nm

ANN	Artificial neural networks
ANOVA	Analysis of variance
ASTM	American Society for Testing and Materials
B0	Diesel 100%
B10	10% biodiesel + 90% diesel fuel
B20	20% biodiesel + 80% diesel fuel
B30	30% biodiesel + 70% diesel fuel
B40	40% biodiesel + 60% diesel fuel
B50	50% biodiesel + 50% diesel fuel
B100	Biodiesel 100%
B10BE5	10% biodiesel + 5% bioethanol + 85% diesel fuel
B20BE8	20% biodiesel + 8% bioethanol + 72% diesel fuel
B30BE10	30% biodiesel + 10% bioethanol + 60% diesel fuel
B40BE13	40% biodiesel + 13% bioethanol + 47% diesel fuel
B50BE15	50% biodiesel + 15% bioethanol + 35% diesel fuel
BEA	Bosch emissions analysis
Ca	Calcium
CaCl ₂	Calcium chloride
EDX	Energy dispersive x-ray
EN	European standard
FAC	Fatty acid composition
FAME	Fatty acid methyl ester
FFA	Free fatty acid
FTIR	Fourier transform infrared
GHG	Greenhouse gases
H ₂ SO ₄	Sulphuric acid
H ₃ PO ₄	Phosphoric acid
IEO	The International Energy Outlook
J90C10	<i>J. curcas</i> and <i>C. pentandra</i> biodiesel (90:10 wt.%)
J80C20	<i>J. curcas</i> and <i>C. pentandra</i> biodiesel (80:20 wt.%)
J50C50	<i>J. curcas</i> and <i>C. pentandra</i> biodiesel (50:50 wt.%)
J20C80	<i>J. curcas</i> and <i>C. pentandra</i> biodiesel (20:80 wt.%)
J10C90	<i>J. curcas</i> and <i>C. pentandra</i> biodiesel (10:90 wt.%)
MPOB	Malaysian Palm Oil Board
OECD	Organization for Economic Cooperation and Development
PM	Particulate matter
RSM	Response surface methodology
SEM	Scanning electron microscope
TAN	Total acid number

LIST OF APPENDICES

Appendix A: Sample calculation esterification and transesterification.....	179
Appendix B: Standard procedure engine performance and emission.....	181
Appendix C: Photo of measurement characterization of biodiesel properties test.....	190
Appendix D: Sample calculation engine performance at 1900 rpm.....	195
Appendix E: Corrosion Test.....	212

University of Malaya

CHAPTER 1: INTRODUCTION

1.1 Overview

Energy crisis has become an important issue in recent years and focused investigation in many countries throughout the world. Economic growth coupled with the increasing standard of living have made energy an important factor in supporting human life, especially after the Industrial Revolution in the last few centuries (Atabani et al., 2012). The International Energy Outlook (IEO) projected growth in energy demand worldwide to increase from 549 quadrillion British thermal units (Btu) in 2012 to 629 quadrillion Btu in 2020 and 815 quadrillion Btu in 2040, an increase of as much as 48% in 2012–2040 (EIA, 2016). In 2016, British Petroleum noted that oil demand has increased nearly 20 Mb/d over the outlook, with increased use in Asia for both transportation and industrial sectors (Petroleum, 2016). The transportation sector is known to use petroleum and other conventional fuels as a dominant energy source resulting in increased energy consumption at an average annual rate of 1.4%, from 104 quadrillion Btu in 2012 to 155 quadrillion Btu in 2040 (EIA, 2016).

The rapid growth of transport and the corresponding increasing use of energy by sector plays a crucial role in the daily activities around the world (Ong et al., 2012). Unfortunately, these activities have a negative impact on changing the environment through its increasing greenhouse gases (GHG) emissions, as it was noted that 18.5% of emissions in Europe in 2012 resulted from this sector (Eurostat, 2015). This causes deep concern; the Kyoto Protocol targets for 2020 greenhouse gas emissions from the transportation sector as 20% below the 1990 levels for all EU-27 countries of the European Union. Several attempts are made to pursue this aim such as by reducing energy use, improving energy efficiency and carbon sequestration, and decarbonisation of energy supply to the expansion of renewable energy (Nanaki et al., 2012).

1.2 Research background

The limited oil resources, increasing energy demand, soaring oil prices, negative environmental impacts and global warming became a major issue in the world today, which are all due to the world's dependence on fossil fuels (Ileri et al., 2016; Kannan et al., 2011). These concerns encourage researchers to develop biofuels such as biodiesel and bioethanol as renewable and environmentally friendly alternative fuels to supply the energy needs (Agarwal, Gupta, et al., 2015; Qi et al., 2011). Besides that, both have the functional properties similar to petroleum fuel (Pang et al., 2006). In addition, the development of biodiesels and bioethanol will also reduce our dependency on fossil fuels, which in turn, helps in reducing the negative impact fossil fuels have always caused (Mofijur, Masjuki, Kalam, Atabani, et al., 2013). Substituting even a small fraction of total consumption by alternative fuels will have a significant economic and environmental impact (Anand et al., 2011).

Biodiesel is one of the most promising alternative fuels to replace diesel and bioethanol is regarded as a potential fuel to substitute gasoline (Ghisi et al., 2011). Biodiesel can be obtained from various sources, both edible and non-edible vegetable oil, waste oil and animal fat which can be generated through the process of transesterification of triglycerides present in vegetable oil with alcohol in the presence of alkaline or acidic catalysts (Campanelli et al., 2010; Dharma, Ong, et al., 2016; Lin, Y.-C. et al., 2011). Meanwhile, bioethanol can be obtained from the conversion of microbial lignocellulosic biomass through fermentation of some types of biomass such as lignocellulosic biomass, starchy and sucrose-containing raw materials (Sebayang et al., 2016).

Biodiesel is one of the most frequently used alternatives to solve this problem. It is renewable, biodegradable, non-toxic, and has properties similar to diesel fuel. However, it does not have sulfur and aroma in its composition (Fazal et al., 2011a,

2012; Haseeb et al., 2011). Biodiesel is defined as the mono-alkyl esters of vegetable oils or animal fats, produced by transesterification reactions. Vegetable oil mainly consists of triglyceride molecules which gives the oil its high viscosity. Due to the high viscosity of neat vegetable oils, they are not used as fuel as it causes operational problems in diesel engine, such as formation of deposits in fuel nozzle, because of the poorer atomization upon injection into the combustion chamber (Fazal et al., 2011a; Knothe, 2010). To reduce the viscosity to make the fuel usable in a diesel engine, neat oil is converted to three monoalkyl esters (three separated long chain carbon molecules) by transesterification. Normally, this reaction is performed using methanol in basic homogeneous catalysts which is faster than acidic catalysts (Silitonga, Masjuki, Mahlia, Ong, Atabani, et al., 2013). The glycerol formed as the product biodiesel is removed. There are many potential vegetable oils to be used as sources of biodiesel, including soybean oil, sunflower oil, cottonseed oil, and rapeseed oil. (Silitonga, Masjuki, Mahlia, Ong, Chong, et al., 2013). Besides, a few non-edible raw materials are also allowed to be used as biodiesel feedstocks such as *Jatropha curcas*, *Ceiba pentandra*, *Calophyllum inophyllum*, *Moringa oleifera* and *Croton megalocarpus* (Mofijur, Masjuki, Kalam, Atabani, et al., 2013). The difference between diesel fuel and biodiesel lies in their chemical properties. Diesel is composed of hundreds of with different boiling points while biodiesel contains fewer compounds, primarily C16–18 carbon chain length alkyl esters, depending on the type of vegetable oil (Atabani, Silitonga, et al., 2013). Composition of the fuel has significant influences on its properties. Biodiesel has higher flash point and cetane number and it provides good lubricity compared to diesel fuel (Knothe, 2005). Combustion of biodiesel fuel in general produces lower smoke, particulate matter, carbon monoxide and hydrocarbon emissions than diesel, while the engine efficiency is either unaffected or improved (Qi et al., 2010; Qi et al., 2009). However, NO_x emissions from biodiesel and diesel fuel blend are higher than diesel in

most cases, especially at high speeds and loads (Chen et al., 2018; Vieira da Silva et al., 2017). In addition, the compatibility of biodiesel materials is a rising concern (Fazal et al., 2011a, 2012), as the composition and unsaturated molecules can amplify corrosion and material degradation. In automobile applications, biodiesel has contact with various kinds of materials, which can be grouped to three major categories: (1) ferrous alloys, (2) non-ferrous alloys, and (3) polymers. Metallic materials can reduce corrosion and wear in contact with biodiesel.

Bioethanol is a type of biofuel and it is generally perceived that bioethanol is one of the solution to address pollution issues resulting from the burning of fossil fuels (Maryana et al., 2014). Bioethanol can be produced from various edible feedstocks such as corn, sugar cane, cassava, starch cellulose, beet and barley sugar (Shahir et al., 2014). Bioethanol produced from these edible feedstocks is also known as first-generation bioethanol. Owing to the increasing use of land mass for the cultivation of crops for bioethanol feedstocks as well as growing concern over food shortages, bioethanol is also produced from non-edible feedstocks (lignocellulosic materials). Such bioethanol is known as second-generation bioethanol which is cheaper and more environmental-friendly compared to first-generation bioethanol (Romaní et al., 2013). However, the third-generation bioethanol appears to be a more viable alternative compared the 1st and 2nd generations such as macroalgae, microalgae and seaweed to be used as feedstocks (Tan et al., 2014). These feedstocks do not compete with other crops for arable land and water. In addition, algae fuels can produce energy per hectare up to more than 30–100 times compared with terrestrial plants such as corn and soybean (Ashokkumar et al., 2015).

In its application, bioethanol can be mixed into diesel fuel. The mixing of bioethanol with diesel fuel has its own challenges because bioethanol has density, viscosity, cetane amount and lower calorific value than diesel (Aydogan et al., 2013).

The presence of bioethanol in diesel fuel has several advantages such as not requiring major modifications to the diesel engine used, significantly led to a reduction in exhaust emissions such as smoke opacity, particulate matter (PM) and NO_x (Pidol et al., 2012; Tan et al., 2014; Torres-Jimenez et al., 2011). In compression ignition engines, the addition of ethanol or methanol into the fuel is used as an additive or fuel mixture (Yilmaz, Vigil, Benalil, et al., 2014). In addition, the presence of bioethanol in diesel fuel has deficiencies such as generating increased thermal efficiency and specific fuel consumption, reducing engine power, decreases lubrication, lowers cetane number and solubility, causing higher heat of vaporization, and auto-ignition temperature, hygroscopic properties of ethanol can lead to increased moisture content in fuel mixtures that can lead to corrosion and growth of aqueous microorganisms (Torres-Jimenez et al., 2011; Yilmaz, Vigil, Donaldson, et al., 2014). In addition, the presence of ethanol and methanol in diesel fuel causes imperfections in the fuel mixture (Yilmaz, Vigil, Donaldson, et al., 2014). Bioethanol can form a stable solution in diesel fuel only in vol.% (Anand et al., 2011).

These technical constraints in the use of ethanol–diesel fuel blend had inspired many researchers to innovate by adding additives (emulsifier) to improve the solubility, but this would have a bad effect on the properties of the mixture (Shahir et al., 2015). Biodiesel is one of the additives that can be completely miscible in diesel or ethanol, and able to enhance the solubility of ethanol in diesel fuel at any temperature (Thangavelu et al., 2016). In this case, the addition of biodiesel to ethanol-diesel fuel blend as a binder or emulsifier is excellent. This mixture is also known to reduce emissions of particulate matter and NO_x as well as capable of causing an increase in CO and HC, especially at lower loads (Yilmaz, Vigil, Benalil, et al., 2014). Several studies researched diesel fuel blended with biodiesel and ethanol and their application in diesel engines such as Yilmaz and Vigil (2014) that compared some types of potential

mixtures for diesel fuels including biodiesel and alcohol. The results showed that the addition of the alcohol can reduce NO_x emissions and BSFC, while the value of CO, HC and the exhaust gas temperature of the engine is increased. Hulwan et al. (2011) studied diesel-ethanol-biodiesel blends in 3 cylinders, CI diesel engine. It is known that the addition of ethanol may lead to an increase in brake specific fuel consumption and thermal efficiency, reduction of smoke up to 70%, reduction in NO emissions, while increasing emissions of CO at low engine load and causes a slight decrease in the high load. Mofijur et al. (2016) stated that the content of the mixture is efficient, namely (5–10% ethanol) with (20–25% biodiesel) in diesel fuel, which can reduce emissions while being safe for the environment. In addition to affecting engine performance and emissions, the fuel mixture also affects the material in a diesel engine. Haseeb et al. (2011) reported that the fuel mixture leads to corrosion on some engine components such as tank, fuel filters, fuel feed pumps and some parts in the fuel line. The quality of ethanol is known to have a high influence on the effects of corrosion that occurs in the material (Shahir et al., 2014).

1.3 Objectives

The need of oil in the world continues to rise at this time, so making it necessary to look for other sources to be made substitutes for fossil fuels. Among many renewable resource, biodiesel and bioethanol are the most suitable options to meet these needs because they can be produced from edible, non-edible, waste or recycle oil, and animal fat.. A large number of studies have been carried out to investigate the effects of using biodiesel or bioethanol on engine performance and emissions. Despite the abundance of articles related to biodiesels and bioethanol, there are only a few studies which focused on biodiesel–bioethanol–diesel fuel blends. Hence, the purpose of this study is to assess the feasibility of using crude *Jatropha curcas-Ceiba pentandra* mixture oil as biodiesel feedstock, production/optimization, as well as blending biodiesel with bioethanol and

diesel fuel to the engine performance and emission, and material corrosion. Therefore, the main objectives of this research are as follows:

1. To analyze the characterizations of biodiesel from *Jatropha curcas* and *Ceiba pentandra* biodiesel blend with bioethanol.
2. To investigate the production of biodiesel through optimization of transesterification process and whether it possesses appropriate biodiesel standards in accordance with ASTM D6751 or EN / ISO 14214.
3. To investigate the effects of biodiesel-diesel fuel blends and biodiesel-bioethanol-diesel fuel blends on the changes of properties, engine performance and exhaust emissions.
4. To analyze the development of corrosion behavior on mild steel immersed in biodiesel-diesel fuel blends and biodiesel-bioethanol-diesel fuel blends.

1.4 Contributions of the study

This study contributes to the physicochemical properties, production processes, optimization analysis, engine performance and emissions testing, as well as corrosion on the material. This study is of the effort to increase biodiesel production as well as to explore other raw materials sourced from non-edible feedstocks. Mixture of two or more types of feedstocks is a breakthrough to anticipate the scarcity and high cost of feedstocks in biodiesel production. Although this study uses two types of non-edible feedstocks, namely *jatropha curcas* and *ceiba pentandra*, the methodologies and stages of biodiesel production process can still be applied to other raw materials. A summary of the original contribution of this research can be seen in the following points:

1. Combining two or more types of biodiesel feedstocks is highly enabling and shows great potential in increasing the production and improvement of biodiesel properties.

2. The production parameters used in the optimization process can also be applied to other raw materials. It aims to reduce production costs, processing time, and to obtain optimal biodiesel yield.
3. Provide input in the use of biodiesel-bioethanol-diesel fuel mixture as an alternative fuel for diesel engines, gas emission characteristics and corrosion behavior.

1.5 Thesis outline

This thesis presents some experimental results relating to the biodiesel production, engine performance and emission, as well as corrosion material using *Jatropha curcas*-*Ceiba pentandra* biodiesel and bioethanol blends. This thesis is also divided to five chapters as shown below.

Chapter 1 provides background information on the study, objectives, contributing research and thesis outline.

Chapter 2 presents a review of the literature related study consisted of an overview of the energy, renewable energy, biodiesel, bioethanol, as well as the feasibility of biodiesel and bioethanol feedstocks. Overall reviews obtained from several sources related such as journal articles, conference papers, research reports, surveys and predictions from credible institutions.

Chapter 3 describes the research methodology consisted of a description of the material, the process of selecting the percentage mixture of both crude oil, the biodiesel production process, process optimization, characterization of biodiesel, characterization of biodiesel-diesel fuel blend, the characterization of biodiesel-bioethanol-diesel fuel blend, engine performance and emissions, observations corrosion in materials.

Chapter 4 covers the results and discussion of the research methodology conducted.

Results and discussion involves choosing the percentage of crude *Jatropha*

curcas-Ceiba pentandra mixture oil, biodiesel production, parameter optimization, characterization of biodiesel properties, characterization of the properties of biodiesel-diesel fuel blend, characterization properties of biodiesel-bioethanol-diesel fuel blend, engine performance and emissions, as well as observation of corrosion in materials.

Chapter 5 provides conclusions from a study consisting of research conclusions and recommendations for future work.

University of Malaya

CHAPTER 2: LITERATURE REVIEW

2.1 Introduction

During the last few decades, energy plays an important role in supporting the global economy. Energy is defined as the ability to perform tasks and can be found in various forms such as chemical, thermal, electrical, mechanical, gravitational, nuclear, glowing, sound, and motion (Bilgen, 2014). Sectors that depend on energy include agriculture, industrial service and transport sectors. The energy source has many forms; the first is fossil energy, such as oil, coal and natural gas, non-renewable resource. Fossil fuels are formed when prehistoric plants and animals died and progressively buried by layers of rock. The second one is nuclear energy; this energy uses sustainable nuclear fission to generate heat and electricity, and currently supplying about 6% of the world energy, and 13–14% of the world's electricity. The third is renewable energy sources such as wind, solar, geothermal and hydropower, which are claimed as clean energy revolution, securing the future of energy (Energy, 2016). Global energy demand and resource consumption is projected to increase over the next few decades, even though it is experiencing a slowdown in the last few years (Bilgen, 2014). In 2016, the IEO conducted an analysis to project an increase in energy consumption of all fuel sources until 2040 as shown in **Figure 2.1**. It is known that the world consumption for renewable energy increased from 86.99 quadrillion Btu in 2020 to 131.36 quadrillion Btu by 2040. Meanwhile, liquid fuel also increased from 204.17 quadrillion Btu in 2020, to 246.04 quadrillion Btu in 2040 (EIA, 2016).

Fossil fuels dominate world energy demand numbering about 80%. This is due to the adaptability of fuel, high combustion efficiency, availability, reliability, and handling facilities from fossil fuels are better compared to other fuel types (Atabani, Mahlia, Badruddin, et al., 2013). The transport sector is highly dependent on oil, and it is known that the global consumption of liquid transportation fuels reached 2.9 Terra

Watt (TW) from petroleum (Caspeta et al., 2013). Energy consumption in the transport sector increases at an average annual rate of 1.4%. **Figure 2.2** shows the condition of the energy consumption of the transport sector between 2012–2040. It is known that the countries of the OECD (Organization for Economic Cooperation and Development) accounted for 55% of total energy consumption and the non-OECD (Organization for Economic Cooperation and Development) accounted for 45%. In 2020, the transportation energy consumption for OECD and non-OECD are projected to be equal. However, in 2040, the non-OECD region projected will increase up to 61% of global transportation energy consumption or equal to 94 quadrillion Btu (EIA, 2016).

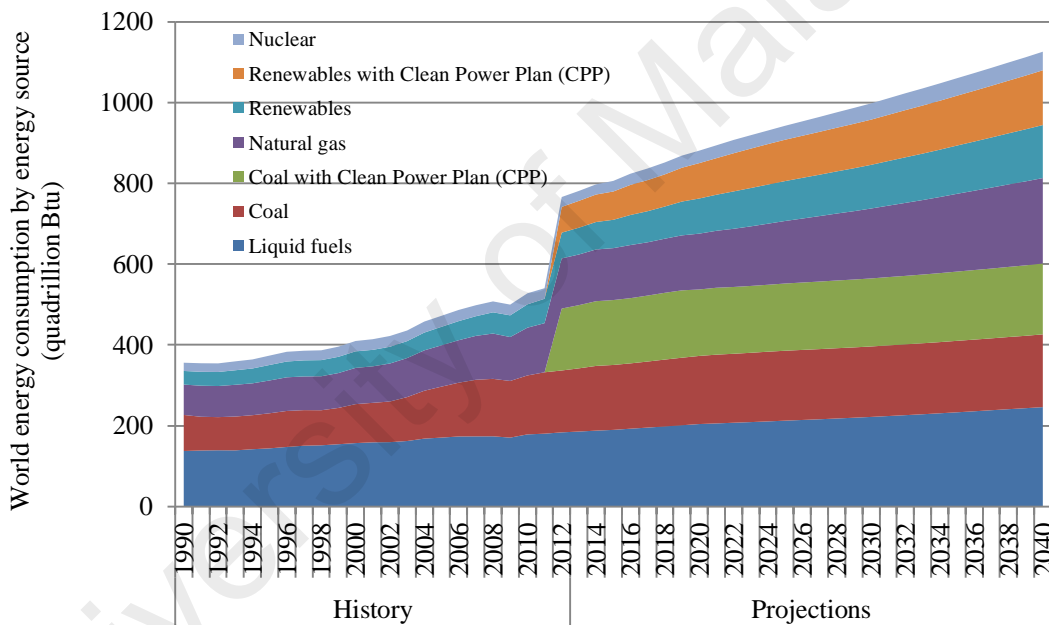


Figure 2.1: Total world energy consumption by energy source for 1990–2040 (EIA, 2016)

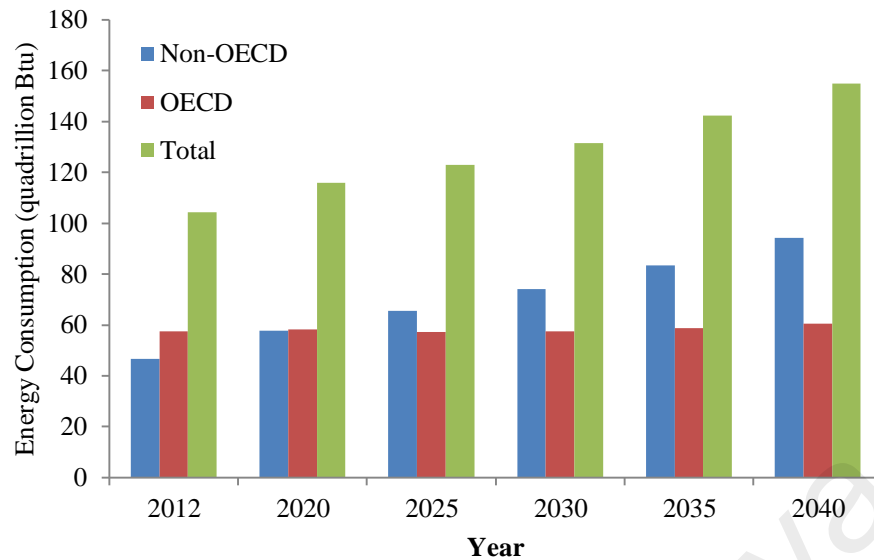


Figure 2.2: Delivered transportation energy consumption by country grouping, 2012–2040 (quadrillion Btu) (EIA, 2016).

Increased energy consumption due to the current global population continues to rise by more than 1.5 billion over the last two decades (Council, 2013). Dependence on fossil fuels causes it to dwindle in number, as well as causing environmental damage and global warming (Ileri et al., 2016; Kannan et al., 2011). Transportation sector is known as a major energy and user the largest emitter, of more than 20% of global greenhouse gas (GHG) emissions (Mofijur et al., 2016; Solís et al., 2013). It is believed that the growth of CO₂ emissions from the transportation sector is faster than the total CO₂ emissions. Total CO₂ emissions from fossil fuels increased by approximately 38% from 20.9 gigatonnes (Gt) in 1990 to 28.8 GT in 2007, while emissions from the transport sector increased from 45% in the same year (Saboori et al., 2014). **Figure 2.3** shows the amount of carbon dioxide emissions (CO₂) from OECD and non-OECD for the year 2012–2040 (EIA, 2016).

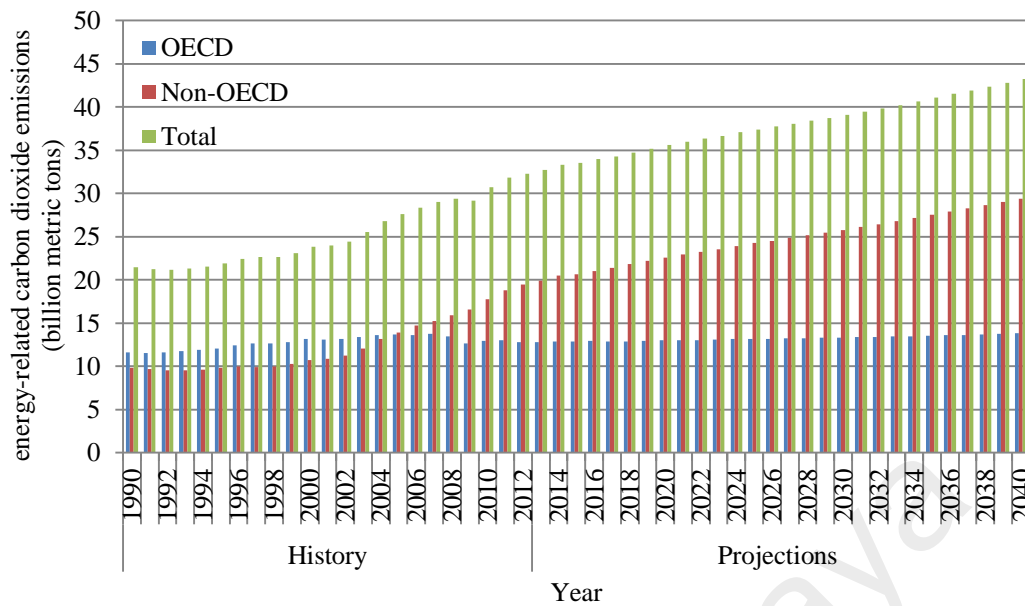


Figure 2.3: Energy-related carbon dioxide emissions, 1990–2040 (billion metric tons) (EIA, 2016)

2.2 Feasibility of biodiesel and bioethanol feedstocks

The steady growth of the world population over the years coupled with the increasing use of energy derived from fossil fuels leads to a critical need for renewable and sustainable sources of energy. Biofuel is one of the alternative sources of energy to fulfil this need (Gupta et al., 2015). Biofuels are alternative fuels with great potential, providing energy security and bringing benefits to the economy and environment (Cheng et al., 2011; Nigam et al., 2011). A number of countries have already put policies related to biofuel production and large-scale acquisition of lands into force (Bracco, 2015). For instance, India has been actively exploring biofuels since 2001 and a policy was issued in 2009 whereby 20% of the national diesel fuel requirements will be fulfilled by biofuels in 2017 (Gunatilake et al., 2014). The production of biodiesels from non-edible feedstocks such as *Jatropha* and *Pongamia* oils is expected to increase the energy security in India (Altenburg, 2010). An energy policy has also been implemented in China with the issuance of the Renewable Energy Law in January 2006 along with a series of regulations (Peidong et al., 2009). China has set a target in which 15% of the energy use is derived from renewable sources by year 2020 (Ji, 2015).

Energy policies are also enforced in the USA, which is evidenced by the strong support given by the US government through the promulgation of the 2005 Energy Policy Act. In addition, the USA is rich in raw materials for biofuel production and therefore, it is likely that the USA will be the world's largest biodiesel producer. It is projected that the USA will supply a total of 36 billion gallons (136 billion litres) of biofuels to the international market in 2022 (Ziolkowska, 2014).

In 1999, Malaysia introduced a renewable energy programme known as the Five-Fuel Diversification Strategy, whereby palm oil is chosen as the biodiesel feedstock (Jayed et al., 2011). Malaysia is one of the leading producers of palm oil in the world, making up 42.3% of global palm oil production. The Government of Malaysia established agencies such as the Malaysian Palm Oil Board (MPOB) in order to ensure the sustainability of palm oil (Yusoff et al., 2013). The Five-Fuel Diversification Strategy continued until 2006 when the Ministry of Plantation Industries and Commodities Malaysia implemented the 'National Biofuel Policy' in anticipation of the rising demand for fuels in the transportation sector, which involved encouraging the use of diesel fuel blended with 5% palm biodiesel (Jayed et al., 2011). Energy policies are also enforced in Indonesia, whereby the Government of Indonesia aims to substitute transportation fuels with 10% biofuels by year 2010. In response to this policy, 5.52 million hectares of unused lands were developed for energy production crops (Dillon et al., 2008; Jayed et al., 2011).

The Organisation for Economic Cooperation and Development (OECD) released a list of bioethanol and biodiesel-producing countries from 2012 to 2015, as shown in **Table 2.1.** and **Table 2.2.** (Organisation for Economic Co-operation and Development (OECD), 2015). It can be seen that there is a growth in bioethanol and biodiesel production in recent years for all countries. It is evident that the USA is consistent in the

development of bioethanol and biodiesel, producing 66,763.06 million litres of bioethanol and 4,986.91 million litres of biodiesel in 2015.

Table 2.1: World bioethanol production from 2012 to 2015

Country	millions of litres			
	2012	2013	2014	2015
United States of America	56,552.46	58,571.11	61,851.90	66,763.06
Brazil	25,755.84	28,370.26	31,393.59	34,485.14
China	9,361.44	9,455.04	9,516.79	9,600.72
India	2,580.77	2,774.36	2,927.53	3,085.56
Canada	1,732.04	1,827.61	1,908.22	2,001.72
Thailand	967.98	1,093.39	1,218.08	1,342.68
Pakistan	634.95	631.73	671.53	704.07
Argentina	564.15	595.29	646.38	673.03
Ukraine	440.79	513.61	578.55	643.03
Republic of South Africa	459.01	513.95	568.37	622.85

Table 2.2: World biodiesel production from 2012 to 2015

Country	millions of litres			
	2012	2013	2014	2015
United States of America	4,782.05	5,001.45	4,999.23	4,986.91
Argentina	3,173.94	3,282.36	3,400.22	3,544.98
Brazil	2,521.36	2,589.43	2,659.35	2,731.15
Indonesia	526.74	633.56	736.89	1,033.83
Thailand	748.59	809.08	880.04	945.35
India	471.05	559.86	652.09	742.91
Australia	657.00	665.15	673.04	680.75
Colombia	536.94	575.15	620.78	662.90
Malaysia	282.23	430.53	527.88	598.45
Canada	230.90	267.35	300.35	331.34

2.3 Biodiesel feedstocks

There are various feedstocks available for biodiesel production (Mofijur, Masjuki, Kalam, Atabani, et al., 2013). At present, there are more than 350 types of oil-bearing crops around the world which are identified as potential feedstocks for biodiesel production (Silitonga, Masjuki, Mahlia, Ong, Atabani, et al., 2013). One of the main requirements in biodiesel production is to reduce the overall production cost and upscale the production of biodiesels (Mofijur, Atabani, et al., 2013). Biodiesel production is

generally dependent on several factors, which include the availability and price of the feedstocks as well as conversion cost. The availability of feedstocks accounts for 75% of the overall biodiesel production cost. The breakdown of the expenditure required for biodiesel production is shown in **Figure 2.4** (Ahmad et al., 2011; Lin, L. et al., 2011).

Biodiesel feedstocks can be classified into four major groups, namely edible vegetable oils, non-edible vegetable oils (include microalgae and macroalgae), waste or recycled oils, and animal fats. These feedstocks are summarized in **Figure 2.5** (Atabani et al., 2012; Mofijur, Atabani, et al., 2013).

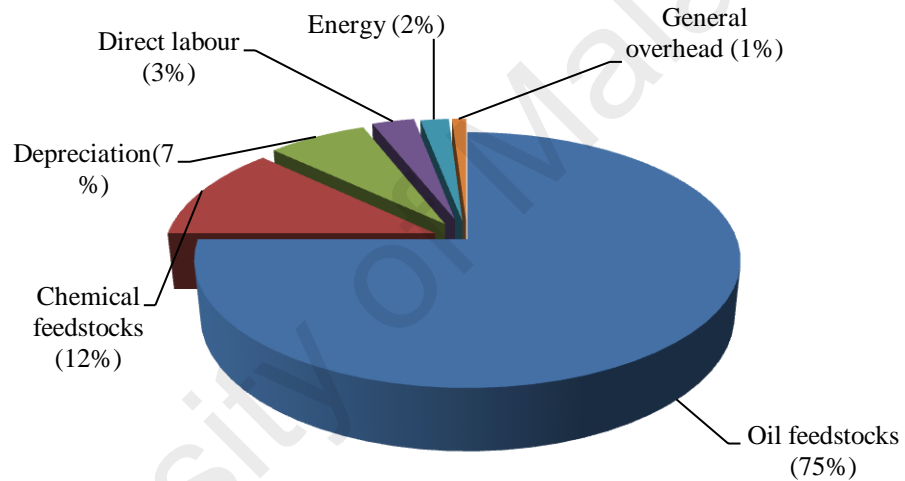


Figure 2.4: Breakdown of expenditure required for biodiesel production (Ahmad et al., 2011; Lin, L. et al., 2011)

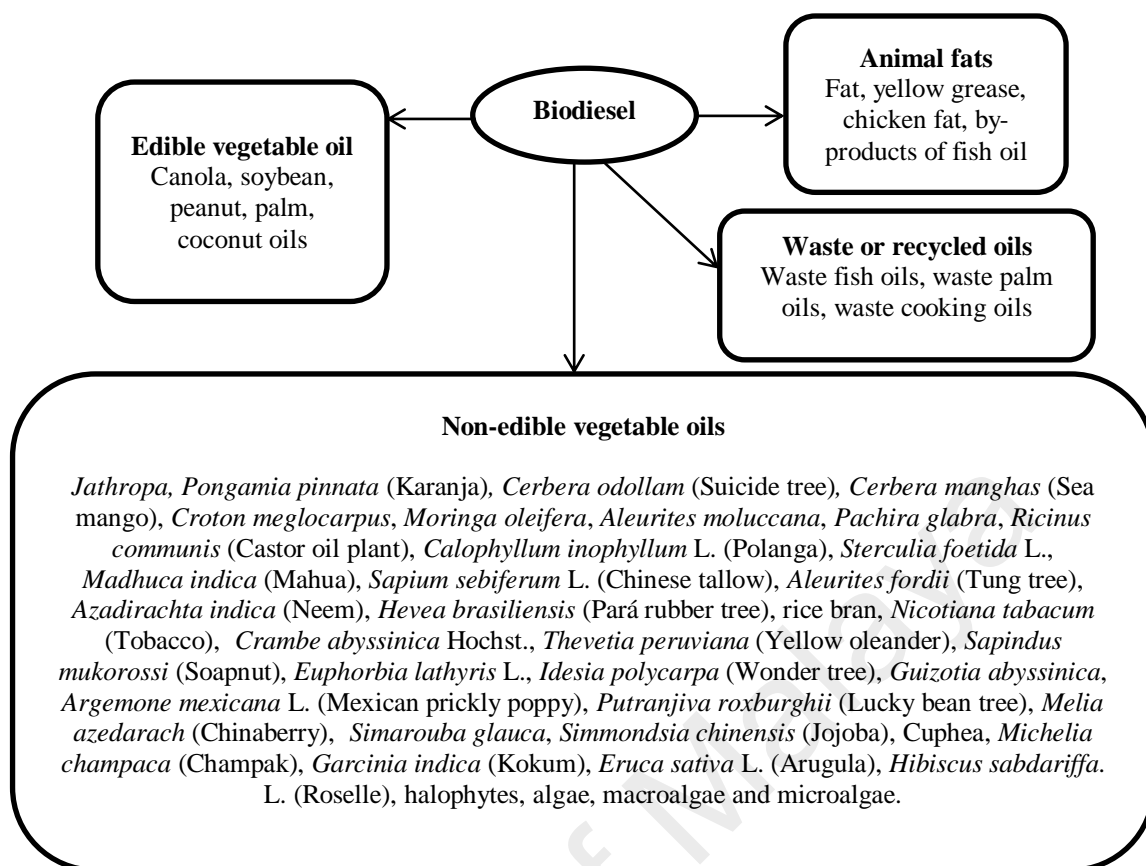


Figure 2.5: Classification of biodiesel feedstocks (Atabani et al., 2012; Mofijur, Atabani, et al., 2013)

Table 2.3 shows the potential feedstocks for biodiesel in various countries (Silitonga, Masjuki, Mahlia, Ong, Chong, et al., 2013). An initial evaluation of the physicochemical properties of the edible and non-edible feedstocks is important in order to investigate the feasibility of these feedstocks for biodiesel production. The physicochemical properties of edible and non-edible feedstocks can be found in many papers pertaining to biodiesels and a brief treatment is given in the following subsections.

Table 2.3: Potential feedstocks for biodiesel production in various countries

Country	Feedstock
Argentina	Soybean oil
Brazil	Soybean oil/palm oil/castor oil/cotton oil
Canada	Rapeseed oil/animal fats/soybean oil/yellow grease/tallow/mustard oil/flax oil
China	<i>Jatropha</i> oil/waste cooking oil/rapeseed oil
France	Rapeseed/sunflower oil
Germany	Rapeseed oil
Greece	Cottonseed oil
India	<i>Jatropha</i> oil/ <i>Pongamia pinnata</i> (karanja) oil/soybean oil/ rapeseed oil/sunflower oil/peanut oil
Indonesia	Palm oil/ <i>Jatropha</i> oil/coconut oil
Ireland	Frying oils/animal fats
Italy	Rapeseed oil/sunflower oil
Japan	Waste cooking oils
Malaysia	Palm oil
Mexico	Animal fats/waste cooking oils
New Zealand	Waste cooking oils/tallow
Philippines	Coconut oil/ <i>Jatropha</i> oil
Singapore	Palm oil
Spain	Linseed oil/sunflower oil
Sweden	Rapeseed oil
Thailand	Palm oil/ <i>Jatropha</i> oil/coconut oil
UK	Rapeseed oil/Waste cooking oils
USA	Soybean oil/waste cooking oil/peanut oil

2.3.1 Edible vegetable oils

Biodiesels are one of the solutions to overcome the depletion of oil reserves and address environmental issues associated with the burning of fossil fuels. Biodiesels are largely derived from vegetable oils and they are produced through transesterification of triglycerides present in the vegetable oils with alcohol in the presence of an alkaline or acidic catalyst (Campanelli et al., 2010). Vegetable oils such as palm, coconut, canola, soybean and sunflower oils are commonly used as feedstocks for biodiesel production (Likojar et al., 2014). Each vegetable oil has its own advantages. For instance canola, which can produce oil contains up to 992 kg per hectare (Dyer et al., 2010). Biodiesels produced from canola and rapeseed oils have replaced up to 80% of total diesel in the European Union (Rosillo-Calle et al., 2009). The addition of up to 5% of canola

biodiesel into diesel fuel has been proven to reduce CO emissions significantly (Roy et al., 2013).

Soybean oil is a vegetable oil which is used as the main raw material for biodiesel production in the USA (Corseuil et al., 2011). The use of soybean biodiesel reduces CO emissions by 46% as well as the amount of unburned hydrocarbons (HCs) (Özener et al., 2014). The higher the proportion of soybean biodiesel in the biodiesel–diesel blend, the higher the cloud point cold filter plugging point and acid value (Qi and Lee, 2014).

Peanut (*Arachis hypogea L.*) biodiesel is produced in China, India, the USA as well as other regions in the world (Moser, 2012). Peanut is an annual plant which is grown widely in the Mediterranean region (Aydin, 2007). Peanut biodiesel is shown to be capable of improving the cold flow properties of the fuel (Pérez et al., 2010). Moreover, peanut biodiesel–methanol blends are capable of boosting the performance of diesel engines (Tosun et al., 2014).

Sunflower (*Helianthus annuus*) is an edible material with high purity, low volatility and low free fatty acids (Banerjee et al., 2014). It is known that 2.4 kg of sunflower seeds can produce 0.96 kg of biodiesel (Iglesias et al., 2012). Sunflower seed oil is the third largest in terms of the annual oil extraction with an average oil yield of approximately 14×10^6 t. This makes sunflower seed oil valuable for both food and biodiesel production. Sunflower seed oil ranks fourth in terms of annual edible oil production with a value of 15×10^6 t (Koutinas et al., 2014).

Oil palm (*Elaeis guineensis*) is native to West Africa and it can be largely found in the wild. Oil palm has also been cultivated as an agricultural crop because it is an excellent raw material for both food and biodiesel production (Acevedo et al., 2015). Palm biodiesel–diesel blends appear to be promising alternative fuels for diesel engines and have gained much attention in Indonesia, Malaysia and Thailand (Mofijur et al., 2014). Blends consisting of 10% palm biodiesel and 90% diesel are currently used in

diesel engines. However, blends containing higher percentage of palm biodiesel have also been used in diesel engines without the need for engine modifications (Fazal et al., 2013b).

2.3.2 Non edible vegetable oil feedstock

The increasing demand for biofuels produced from edible vegetable oils has been much debated among scientists, researchers, environmentalists and policymakers owing to the growing concern on the use of agricultural lands for fuel production, rather than food (da Silva César et al., 2015). The use of vegetable oils for biodiesel production disrupts the balance between market demands and food supply, which in turn, increases the price of oils and biodiesels (Nizah et al., 2014). For this reason, non-edible oils are now being considered as biodiesel feedstocks, eliminating the dependency on edible vegetable oils for fuel production. *Jatropha curcas*, *Cerbera odollam* (sea mango) *Ceiba pentandra* and karanja oils are examples of non-edible biodiesel feedstocks (Silitonga, Masjuki, Mahlia, Ong, Chong, et al., 2013).

2.3.2.1 *Jatropha curcas* L.

Jatropha curcas, abbreviated as *J. curcas* non-edible oil appears to be a feasible feedstock for biodiesel production since this plant be cultivated on barren lands that are inhospitable for other plants to thrive (Al Basir et al., 2015). *J. curcas* is a small tree or large shrub, belonging to the family Euphorbiaceae comprising around eight hundred species, which in turn belongs to some 321 genera (Atabani, Mahlia, Badruddin, et al., 2013). *J. curcas* can grow up to a height of 8–10 m in favourable conditions with low to high rain-fall climate between 250 and 3000 mm (Kabbashi et al., 2015). The length and width of the green leaves of this plant measures around 6 and 15 cm, respectively. The leaves have three to seven shallow lobes and are arranged alternately with spiral phyllotaxis (Kalam et al., 2012). Approximately 35 to 40% and 50 to 60% of *J. curcas* oil is found in the seeds and kernels whereas the amount of saturated and unsaturated

fatty acid content in *J. curcas* oil is roughly 21 and 79% (Takase et al., 2015). *J. curcas* oil is composed of 44.5, 35.4, 13.0 and 5.8% of oleic acid, linoleic acid, palmitic acid and stearic acid, respectively. It can be seen that the amount of unsaturated fatty acids (oleic and linoleic acids) is rather high and therefore, *J. curcas* oil has high cold flow properties (Ong et al., 2014). Since *J. curcas* oil has high free fatty acid (FFA) content exceeding 1%, pre-treatment is required to reduce the FFA content to less than 1% (Sulistyo et al., 2015).

2.3.2.2 *Ceiba pentandra* L.

Ceiba pentandra, abbreviated as *C. pentandra* and more commonly known as *kapok* and *kekabu*, is a silk-cotton tree belonging to the *Malvaceae* family. Even though *C. pentandra* is native to tropical regions in America and West Africa, it is now found in Asian countries such as West India, Pakistan, Indonesia, Malaysia, Vietnam and the Philippines (Ong, L. K. et al., 2013; Rashid et al., 2014; Silitonga, Ong, et al., 2013). Some parts of *C. pentandra* have high economic value since they can be used as timber whereas the pods contain 17% of fibres which can be used to manufacture pillows and mattresses (Ong, L. K. et al., 2013). *C. pentandra* is a drought-resistant plant which is naturally found in humid, tropical regions. The pods of this tree are rough, pendulous capsules containing seeds varying from 25 to 28 wt.%. Each fruit and seed yields an average of 1,280 kg/ha of oil (Ong et al., 2014). In addition, the fibres of *C. pentandra* contain 36 to 64% of cellulose which is used to produce cellulosic ethanol (Tye et al., 2012). The possibility of transforming *C. pentandra* into biodiesel is known since 1931, when Dr. C.L. Alsberg discovered that the saturated and unsaturated fatty acid content in *C. pentandra* oil is 17.15 and 76.32%, respectively (Vedharaj et al., 2013). The amount of monoalkyl fatty acid esters present in biodiesels (specifically fatty acid methyl esters and fatty acid ethyl esters) make them a promising alternative fuel in compression-ignition (diesel) engines (Atabani, Silitonga, et al., 2013). However, *C.*

pentandra contains a pair of cyclopropene fatty acids (malvalic acid) which are more reactive than the double bond carbon chains (polyunsaturated fatty acids) (Silitonga, Ong, et al., 2013). In addition, the cyclopropene fatty acids present in *C. pentandra* results in higher viscosity, which leads to faster oxidation of the biodiesel compared to palmitic acid (Bindhu et al., 2012).

2.3.3 Waste or recycled oils

The high cost of feedstocks is a factor which hinders the commercialization of biodiesels and therefore, end users are still heavily reliant on petroleum diesels (Al-Hamamre et al., 2014). The cost of edible vegetable oils for feedstocks constitutes 70–95% of the total biodiesel production cost and this is highly undesirable for biodiesel production (Farooq et al., 2015). For this reason, much research is carried out to use waste cooking oils or recycled oils as raw materials for biodiesel production because they are relatively inexpensive compared to pristine oils (Nurfitri et al., 2013). The use of waste cooking oils does not only reduce the cost of feedstocks, but it also helps in solving issues related to the disposal of used oils (Xue, 2013). The total cost of biodiesel production can be reduced by 60–90% by using waste cooking oils (Talebian-Kiakalaieh et al., 2013).

The physicochemical properties of waste cooking oils are similar to those of vegetable oils (Gui et al., 2008). However, it shall be noted here that waste cooking oils have been heated to a temperature range of 160–200 °C for extended periods, which will alter some of their physicochemical properties. This includes an increase in the oils' kinematic viscosity and specific heat, as well as changes in their colour and surface tension. In addition, it can be expected that there will be the formation of fats in the oils (Kulkarni et al., 2006). In order to improve the physicochemical properties of waste cooking oils, a two-step process can be used for biodiesel production (esterification,

followed by transesterification), depending on the free fatty acid content and moisture content of the oils (Math et al., 2010).

Biodiesel blends containing up to 20% of biodiesel produced from waste cooking oils have characteristics similar to those of diesel, particularly with regards to their spray and combustion characteristics in diesel engines (Lin et al., 2013). However, the use of waste cooking oils is not without drawbacks. For instance, the use of waste cooking oils as feedstocks inhibits the separation of fatty acid methyl esters from glycerol, as well as results in the formation of dimer acid, polymers and glycerides (Talebian-Kiakalaieh et al., 2013). In addition, saponification (such as the formation of soap and water) reduces the iodine value and increases the kinematic viscosity of the biodiesels produced from waste cooking oils (Ruiz-Méndez et al., 2008). More importantly, the methyl ester yield is reduced because of the high water content of waste cooking oils (Sirisomboonchai et al., 2015). These issues need to be addressed when using waste cooking oils as feedstocks for biodiesel production.

2.3.4 Animal fats

Animal fats are mainly derived from animal rendering processes, in which the by-products of animals are processed to produce useful raw such as animal fats. Animal fats include lard as well as fat from chicken, turkey and other poultry (Adewale et al., 2015). Animal fats are an inexpensive source of lipids which can be used for biodiesel production, whereby 0.78 t of biodiesel can be produced from 1 t of animal fats (Awad et al., 2014; Awad et al., 2013). At present, 80% of biodiesels are produced from vegetable oils while the remaining 20% are produced from animal fats in the following countries: Malaysia, Indonesia, Argentina, the USA, Brazil, the Netherlands, Germany, the Philippines, Belgium and Spain (Banković-Ilić et al., 2014). There are a number of advantages when waste animal fats are used for biodiesel production and these include reducing the cost of feedstocks as well as increasing food security (Adewale et al.,

2015). However, the high degree of saturated fatty acids present in animal fats requires complex processing techniques and these saturated fatty acids affects the physicochemical properties of the biodiesel. This disadvantage is compensated by the fact that biodiesels derived from animal fats produce low NO_x emissions compared to other biodiesels due to their high saturated fatty acid content and cetane numbers (Yanowitz et al., 2009). Moreover, the high degree of saturated fatty acids increases the oxidation stability of the biodiesel (Ramírez-Verduzco et al., 2012). More importantly, biodiesels produced from animal fats have properties that approximate those of diesel and these biodiesels can be used readily in CI engines without the need for engine modifications (Adewale et al., 2015).

2.4 Bioethanol feedstocks

Bioethanol can be produced from various types of feedstocks. First-generation bioethanol are produced from agricultural raw materials containing sugar and starch (Shahir et al., 2014). However, second-generation bioethanol are produced from lignocellulosic materials containing sugar such as sugar cane, molasses, sugar beet and fruits. These lignocellulosic materials may also be processed directly into bioethanol by fermentation (Romaní et al., 2013). Pre-treatments such as milling, hydrolysis and detoxification are not necessary to produce bioethanol from sugar cane and molasses (Balat et al., 2008). Third-generation bioethanol are produced from seaweed or algae and they offer several advantages over other types of bioethanol such as high area productivity, elimination of competition of lands for cultivation of biofuel crops as well as recycling carbon dioxide (CO₂) (Sebayang et al., 2016; Tan et al., 2014). The various types of feedstocks used for bioethanol production are summarized in **Figure 2.6** (de Souza et al., 2013).

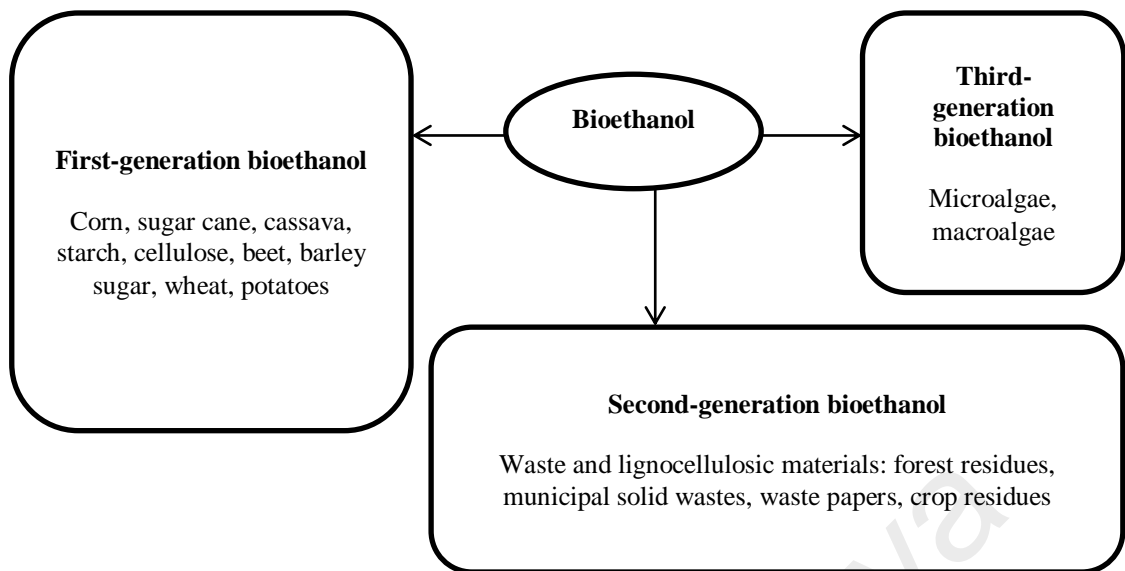


Figure 2.6: Types of feedstocks used for bioethanol production (de Souza et al., 2013)

2.4.1 First-generation bioethanol

First-generation bioethanol are bioethanol produced from edible feedstocks such as cassava, sugar cane, corn and soybeans (Shahir et al., 2014). Cassava (*Manihot esculenta Crantz*) belongs to the *Euphorbiaceae* family and it is a tropical, perennial plant which grows on poor or depleted soils (Jansson et al., 2009). Cassava is being actively promoted as one of the potential raw materials for bioethanol compared to other bioethanol feedstocks (Liu et al., 2013). Cassava is a major source of calories for more than 1 billion people in developing countries and therefore, the exploitation of cassava for industrial starch and bioethanol in tropical regions results in major concerns over food security (Chetty et al., 2013). As an energy plant with high starch content, cassava gives superior conversion ratio for bioethanol production compared to other crops (Kristensen et al., 2014).

Bioethanol is produced from the fermentation of sugars in the form of sucrose, starch or lignocellulose present in sugar cane (Dias et al., 2011). Sugar cane is an ideal bioethanol feedstock since processing sugar cane is more economical compared to

maize (Macedo et al., 2008). In Brazil, bioethanol has been produced from sugar cane since a few decades ago (Dias et al., 2013).

Corn or maize (*Zea mays*) is also used to produce bioethanol and the production of bioethanol from starch sources is a common practice in North America (Limayem et al., 2012). Corn is a preferable feedstock for bioethanol production due to its composition: starch 76.75% (w/w), proteins 6.35% (w/w), lipids 5.86% (w/w), ash 0.70% (w/w) and water 10.34% (w/w) (Nikolić et al., 2009). In fact, the energy content of corn is higher than the energy required to produce ethanol (Mojović et al., 2006). In addition, the average loss of ethanol yield for corn is considerably low (3–23%), depending on the quality of the grains (Singh, 2012).

2.4.2 Second-generation bioethanol (lignocellulosic materials)

Lignocellulosic materials can be categorized into four groups based on its type of source: (1) forest residues, (2) municipal solid wastes, (3) waste papers and (4) crop residues (Balat, 2011). A number of studies have been carried out to produce bioethanol from various types of lignocellulosic material wastes such as corn stover (Agarwal, Dhar, et al., 2015), rice straws (Binod et al., 2010), sugar cane bagasse (Gutiérrez-Rivera et al., 2015) and cassava residues (Kristensen et al., 2014). Lignocellulosic materials are preferable for bioethanol production in order to reduce the dependency on edible feedstocks which are also used for food production (Conde-Mejia et al., 2012). The chemical composition of lignocellulosic materials is known to affect the efficiency of biofuel production during the conversion process (de Souza et al., 2013). The chemical composition and structure of lignocellulosic materials are dependent on genetic and environmental variations. Lignocellulosic materials consist of cellulose, hemicellulose, lignin and ash (Balat, 2011). The chemical composition of several types of lignocellulose materials is summarized in **Table 2.4** (Balat, 2011; Sarkar et al., 2012). In bioethanol production, the ethanol yield is directly related to cellulose,

hemicellulose and individual sugar concentrations in the raw materials (Karunanithy et al., 2008). It shall be noted here that lignin cannot be used for bioethanol production (Balat, 2011)..

Table 2.4: Composition of various types of lignocellulosic-biomass materials (% dry weight)

Material	Cellulose	Hemicellulose	Lignin	Ash	Extractives
Green algae	20–40	20–50	–	–	–
Cotton	80–95	5–20	–	–	–
Grasses	25–40	25–50	10–30	–	–
Hardwoods	45 ± 2	30 ± 5	20 ± 4	0.6 ± 0.2	5 ± 3
Hardwood bark	22–40	20–38	30–55	0.8 ± 0.2	6 ± 2
Softwoods	42 ± 2	27 ± 2	28 ± 3	0.5 ± 0.1	3 ± 2
Softwood bark	18–38	15–33	30–60	0.8 ± 0.2	4 ± 2
Cornstalks	39–47	26–31	3–5	12–16	1–3
Rice straws	32–47	19–27	5–24	12.4	–
Bagasse	65 (Total carbohydrate)		18.4	2.4	–
Wheat straws	37–41	27–32	13–15	11–14	7 ± 2
Newspapers	40–55	25–40	18–30	–	–
Chemical pulp	60–80	20–30	2–10	–	–

2.4.3 Third-generation bioethanol

Algae can be categorized as microalgae or macroalgae based on their morphology and size (Jones et al., 2012). The productivity, scalability and continuity are the primary factors for one to select either microalgae or macroalgae as bioethanol feedstocks (Chen et al., 2015). Several studies have shown that both microalgae and macroalgae are potential feedstocks for biodiesel and bioethanol (Chen et al., 2015). Microalgae are unicellular, free-floating microorganisms which create filaments and form colonies. Microalgae are also able to adapt well in extreme ecological habitats (Oncel, 2013). Photosynthesis results in rapid growth of microalgae in the sea and these microalgae have high energy content (Singh et al., 2011). Algae offer a number of advantages over other feedstocks since they do not require freshwater or any lands for survival and they are biodegradable (Noraini et al., 2014). In addition, algae are non-toxic and they contain a low percentage of lignin and hemicellulose compared to lignocellulosic

materials (Mood et al., 2013). Algae have high sugar content (min. 50%) and low lignin content which are important for the fermentation process in order to attain high ethanol yields (Wi et al., 2009).

2.5 Properties of biodiesel and petroleum diesel

The fatty acid composition is the main chemical property which influences the engine injection, combustion and emission characteristics of the biodiesel (Sorate et al., 2015). In addition, the high saturated fatty acid content and low unsaturated fatty acid content of various feedstocks help improve the physicochemical properties of the biodiesel (Altun et al., 2014). The kinematic viscosity, density, cetane number, calorific value, flash point, cloud point and pour point are the important physicochemical properties which need to be considered when producing biodiesels for use in diesel engines (Ashraful et al., 2014; Gandure et al., 2014). The quality of biodiesel is assessed by its measuring its physicochemical properties in accordance with the methods outlined in the ASTM D6751 and EN14214 standards (Ahmad et al., 2014).

2.5.1 Kinematic viscosity

Kinematic viscosity is defined as the resistance of a fluid towards the direction of the flow (Knothe et al., 2011). Kinematic viscosity is indicative of the fluidity or thickness of the oil and it is determined by measuring the time required for a particular oil to pass through an orifice of a specific size (Atabani, Mahlia, Badruddin, et al., 2013). In general, a high kinematic viscosity is undesirable because it reduces the intake stroke, which delays the mixing of air with fuel in the combustion chamber (Ashraful et al., 2014). The kinematic viscosity is determined according to the method given in the ASTM D445 standard (Sanford et al., 2009). In addition, a high kinematic viscosity reduces the speed of fuel injection and the difference in the fuel density becomes significant, resulting in an increase in the average diameter of the oil droplets (Agarwal, Dhar, et al., 2015). Aliche et al. (2015) conducted rheological characterization of

biodiesel at low temperatures and they discovered that gelling typically occurs at low temperatures such that the mechanical behaviour of the biodiesel becomes viscoplastic. The kinematic viscosity of petroleum diesel and biodiesel is 3.21 and 5.0 mm²/s, respectively (Bari et al., 2015).

According to Černoch et al. (2010) the kinematic viscosity depends on the amount of free glycerol, free fatty acids and glycerides present in the biodiesel as well as temperature (Geacai et al., 2015). There is an increase in the oxidation of the fuel at high temperatures which in turn increases the fuel viscosity resulting from the Diels-Alder reaction, forming dimers and polymers (Lin et al., 2014). In addition, the kinematic viscosity of the biodiesel depends on the transesterification process, whereby a lower kinematic viscosity indicates that the transesterification process has been carried out effectively (de Almeida et al., 2015). Since the kinematic viscosity is indicative of the fluidity of the biodiesel, this property has a direct impact on the atomization of the fuel when the fuel is injected into the combustion chamber (Rocabruno-Valdés et al., 2015).

2.5.2 Density

Density is an important physical property for biodiesels because it is used to determine the precise volume of fuel which needs to be injected into the combustion chamber (Verduzco, 2013). The density affects the fuel injection process and it is related to the cetane number, calorific value and kinematic viscosity of the fuel (Gülüm et al., 2015). The density is dependent on the fatty acid composition and purity of the biodiesel (Martínez et al., 2014). In general, decreasing the degree of unsaturated fatty acids improves the density of the biodiesel (Martínez et al., 2014). However, the density of the biodiesel can be decreased by the presence of low-density contaminants such as methanol, ethanol or other solvents (Martínez et al., 2014). The density of the biodiesel

is determined according to the method given in the ASTM D 1298 standard (Chattopadhyay et al., 2013).

Chhetri et al. (2012) compared three types of biodiesel (such as canola, *Jatropha* and soapnut biodiesels) and discovered that the density of the biodiesels increases with an increase in temperature and pressure (Prieto et al., 2015). The density of petroleum diesel decreases by 3.5% for fuel temperatures more than 60 °C. In contrast, the density for biodiesels decreases by a larger amount compared to petroleum diesel, with a decrease within a range of 5.0–5.5% (Gautam et al., 2015). According to Agarwal, Dhar, et al. (2015) the fuel density is an important property since it influences the injection characteristics of the engine such as the total mass of fuel injected as well as pressure waves. It shall be highlighted here that the fuel density may also affect the production, transportation and distribution processes that take place in the internal combustion engine (Barabás, 2015). In diesel engines, the fuel is injected into the combustion chamber volumetrically and therefore, variations in density will have a direct impact on the power output and fuel consumption of the engine, as well as engine emissions (Gülüm et al., 2015).

2.5.3 Acid value

Acid value is a measure of the number of carboxylic acid groups in a chemical compounds and can be used to measure the amount of acid present (Yaakob et al., 2014). This parameter is used to see the degradation of biodiesel that is directly related to the stability. The acid value is the quantity basis and expressed as mg KOH required to neutralize 1 g of FAME (Kaya et al., 2009). Free fatty acids are the saturated or unsaturated monocarboxylic acids that occur naturally in fats, oils or greases but are not attached to glycerol backbones (Saloua et al., 2010). High acid content can cause severe corrosion in the fuel supply system of the engine. Standard ASTM D664 and EN 14104

for a maximum acid value of approved biodiesel is 0.50 mg KOH/g (Silitonga, Masjuki, Mahlia, Ong, Atabani, et al., 2013).

2.5.4 Flash point

Flash point is the temperature at which the fuel will ignite when it is exposed to either spark or flame. Even though the flash point does not have a direct impact on the combustion characteristics, increasing the flash point ensures safe storage and transportation of the fuel (Carareto et al., 2012). The flash point is defined as the minimum temperature at which a fuel produces sufficient vapour to burn momentarily, resulting in the first flash (Chattopadhyay et al., 2013). The flash point is measured according to the method given in the ASTM D93 standard and in general, the flash point is inversely proportional to the volatility of the fuel (Boog et al., 2011; Carareto et al., 2012). The main purpose of specifying the flash point is to ensure that the biofuel is sufficiently purified in which excess methanol or ethanol is removed from the biofuel. It shall be noted that even the slightest amount of residual methanol or ethanol in the biofuel will result in a significantly depressed flash point (Hoekman et al., 2012). The European Norm specifies that the flash point and combustion point for biodiesel should be within the range of 161–188 °C and 179–200 °C, respectively, based on the assumption that the biodiesel does not contain any residual alcohol (Martínez et al., 2014). According to Mittelbach et al. (2004) the decrease in flash point of the biodiesel results from the presence of alcohol residue and other low boiling-point solvents. Indeed, Černoch et al. (2010) observed that the presence of carbon residue and other impurities has an effect on the flash point of the biodiesel.

2.5.5 Cloud point and pour point

The cloud point is the temperature at which wax crystals first become visible when the fuel is cooled. The cloud point is measured when wax crystals begin to form upon cooling the fuel (Atabani, Mahlia, Masjuki, et al., 2013; Mejía et al., 2013). The

presence of solidified wax thickens the oil, which clogs the fuel filters and injectors in internal combustion engines. Furthermore, the solidified wax accumulates on the cold surface of the engine parts, forming an emulsion with water (Dwivedi et al., 2014). For this reason, the cloud point is also an indicator of the tendency of the oil to plug filters or small orifices at cold operating temperatures (Dwivedi et al., 2014).

In contrast, the pour point is the lowest temperature at which the fuel is still able to flow. In general, biodiesels with higher saturated fatty acid content will have a higher pour point. One of the main issues concerning the use of biodiesels is their poor physicochemical properties at low temperatures, particularly biodiesels produced from palm oil containing stearic and palmitic acids. It has been shown that the higher the unsaturated fatty acid content, the poorer the physicochemical properties of the biodiesel at low temperatures (Mejía et al., 2013).

In general, biodiesels have higher cloud point and pour point compared to petroleum diesel (Torres-Jimenez et al., 2011). According to Imahara et al. (2006) the cloud point of a biodiesel can be determined from the amount of saturated chains that are separated from unsaturated chains. To date, blending biodiesels with diesel fuel is the most common method used to improve the cold flow properties of the fuel since the diesel fuel acts as a solvent when crystals, waxes or gels form in the fuel (Mejía et al., 2013).

2.5.6 Calorific value

The calorific value is the value that indicates the amount of available energy content in the fuel (Ashraful et al., 2014). The calorific value of the fuel properties is very important to determine the ability of a very high heat release during the combustion process, and is closely related to the engine performance. It is known that, the higher of calorific value indicates the higher of heat released during the combustion

process and consequently improve engine performance (Ghazali et al., 2015). The calorific value is obtained through testing using calorimetric bomb. Generally, the calorific value of biodiesel is lower (39–41 MJ/kg) compared with other liquid fuels such as petrol (46 MJ/kg), diesel fuel (43 MJ/kg) or oil (42 MJ/kg), but higher than coal (32–37 MJ/kg) (Oliveira et al., 2013). The calorific value of biodiesel is lower than that of diesel because of its higher oxygen content (Puhan et al., 2009; Ramadhas, A. et al., 2005; Ramadhas, A. S. et al., 2005).

2.5.7 Oxidation stability

Oxidation stability is the tendency of the fuel to react with oxygen at ambient temperature, and it reflects the relative vulnerability of the fuel degraded by oxidation (Pullen et al., 2012). According to Dunn (2005) biodiesels have lower oxidation stability compared to petroleum diesel. The FAME content and the existence of natural antioxidants in the feedstocks used for biodiesel production are the factors which affect the oxidation stability of biodiesels (Schober et al., 2004). The auto-oxidation of FAMES is a chain reaction which involves three basic steps: initiation, propagation and termination (Chen et al., 2011). Oxidation is characterized by a free radical mechanism which generates hydroperoxides, short-chain carboxylic aldehydes, ketones and acids (Orozco et al., 2013). These radical peroxides generate new radicals in the esters which bind oxygen in the air, and the hydroperoxides grow rapidly to the propagation stage. The formation of decomposed by-products occurs at an exponential rate during the auto-oxidation phase (Sorate et al., 2015).

The main factors which leads to oxidation in biodiesels are the presence of oxygen and metal traces, the amount of unsaturated fatty acid chains as well as high temperatures (Jain et al., 2011). Oxidation increases the kinematic viscosity of the biodiesel, which in turn, clogs fuel injectors and filters and leads to engine malfunction (Dantas et al., 2011). However, the addition of antioxidants have been proven to slow

down degradation of the fuel due to oxidation and the presence of these antioxidants do not have a significant effect on the physicochemical properties of the biodiesel (Fattah et al., 2014). The effects of oxidation on the quality of the biodiesel can be determined by taking into account the concentration of the antioxidants, amount of fatty acids as well as total glycerine content (Sorate et al., 2015).

Oxidation stability is measured according to the method in the EN 14112 standard. In this method, 3 g of samples are analysed in heating condition at 110 °C with constant airflow (10 L/h) using an instrument called Biodiesel Rancimat (Chen et al., 2011). The airflow passes through the sample, creating bubbles in the flask which contains deionized or distilled water. This drags the volatile carboxylic acids (breakdown products) which solubilize and increase the conductivity of the water (da Silva Araújo et al., 2014). The response is a curve which shows the conductivity versus time, in which two tangents intersect at a point, which corresponds to the timescale, induction period or oxidation stability (da Silva Araújo et al., 2014).

2.5.8 Cetane number

Cetane number is a relative measure of the time delay between the injection and auto-ignition of the fuel (Ramírez-Verduzco et al., 2012). Cetane number is used as an indicator of the quality of fuel combustion during the ignition process (Rocabruno-Valdés et al., 2015). Cetane number may be represented by the elapsed time between the start of fuel injection and the onset of ignition (Iqbal et al., 2015). In general, it is desirable if the fuel has a high cetane number for CI engines (Sajjad et al., 2014). Cetane number can be controlled by the addition of 0.25 vol% of additives or by changing the composition of the hydrocarbons (Vilutienė et al., 2015).

2.5.9 Iodine value

The iodine value is an index number of the double bonds present in the molecules of the biodiesel. The iodine value is used to measure the degree of unsaturated fatty acids present in the biodiesel and it is expressed by the grams of iodine reacting with 100 grams of the biodiesel (Wang, L.-b. et al., 2012). The iodine value affects the oxidation stability of the biodiesel. In general, biodiesels with high concentrations of unsaturated fatty acid chains will usually have high iodine values and therefore, the fuels are more susceptible to oxidative degradation (Tubino et al., 2013). According to Love et al. (2009) the peak NO_x concentration increases significantly with the amount of iodine and therefore, there is a strong correlation between the chemical structure of the fuel and NO_x emissions.

2.6 Properties of bioethanol and gasoline

Bioethanol is an oxygenated fuel which contains 35% oxygen and this reduces particulate matter and NO_x emissions from combustion (Balat et al., 2008). In general, bioethanol has higher octane number, higher enthalpy (heat of evaporation), higher flame speed and a wider flammable range compared to gasoline (Manzetti et al., 2015). These properties result in a higher compression ratio, shorter burning time and leaner combustion engines (Yoon et al., 2012). These are some of the advantages of using bioethanol in internal combustion engines (Manzetti et al., 2015).

In addition, ethyl tertiary butyl ether is produced synthetically from bioethanol, and it serves as an octane enhancer which reduces exhaust emissions (Balat, 2011). Blending gasoline with 10% of bioethanol improves the physicochemical properties of the fuel for SI engines in accordance with the EN 228 standard (Balat, 2009). Several studies have shown that blending ethanol with gasoline improves engine torque, engine power and thermal efficiency braking (Najafi et al., 2009; Yoon et al., 2009). However bioethanol has its own disadvantages. The energy content of bioethanol is only 66% of

the energy content for gasoline, which indicates that bioethanol has lower energy density. In addition, bioethanol is corrosive, miscible with water and toxic to the ecosystem. Bioethanol also has low flame luminosity and low vapour pressure, making cold starts difficult (Balat, 2007). However, Masum et al. (2013) highlighted that bioethanol has high octane number and therefore, the fuel is able to withstand high compression before detonation/ignition. It is known that premature ignition of the fuel can cause damage to the engine. The physicochemical properties of methanol, ethanol, gasoline and bioethanol are summarized in **Table 2.5** (Balat, 2011; Yoon et al., 2011, 2012).

Table 2.5: Physicochemical properties of methanol, ethanol, gasoline and bioethanol

Property	Methanol (CH ₃ OH)	Ethanol (C ₂ H ₅ OH)	Gasoline (C ₄ –C ₁₂)	Bioethanol
Molecular weight (g/mol)	32	46	~114	46.07
Specific gravity	0.789 (298 K)	0.788 (298 K)	0.739 (288.5 K)	–
Vapour density relative to air	1.1	1.59	3.0–4.0	–
Liquid density (g/cm ³ at 298 K)	0.79	0.79	0.74	0.792
Boiling point (K)	338	351	300–518	351.5
Melting point (K)	175	129	–	–
Heat of evaporation (Btu/lb)	472	410	135	367.13
Heating value (kBTU/gal)				
Lower heating value (LHV)	58	74	111	–
Higher heating value (HHV)	65	85	122	–
Tank design pressure (psig)	15	15	15	–
Viscosity (cP)	0.54	1.2	0.56	–
Flash point (K)	284	287	228	–
Flammable/explosion limits				
(%) Lower flammable limit (LFL)	6.7	3.3	1.3	–

Table 2.5: Continued

(%) Upper flammable limit (UFL)	36	19	7.6	–
Auto-ignition temperature (K)	733	636	523–733	696
Solubility in H ₂ O (%)	Miscib. (100%)	Miscib. (100%)	Negl. (~0.01)	–
Azeotrope with H ₂ O	None	95% EtOH	Immiscible	–
Peak flame temperature (K)	2143	2193	2303	–
Minimum ignition energy in air (mJ)	0.14	0.23	–	–
Oxygen (wt%)	–	–	0	35
Octane number (RON)	–	–	86–94	105–108

2.7 Properties of biodiesel–bioethanol–petroleum diesel blends

In general, biodiesel–bioethanol–petroleum diesel blends produce lower carbon monoxide (CO), carbon dioxide (CO₂) and particulate matter up to 40% (Fernando et al., 2004). The solubility of bioethanol–biodiesel–petroleum diesel blends is influenced by two factors: temperature and water content. The components of these blends can be mixed easily at ambient temperatures but they will separate at temperatures below 10 °C (Hansen et al., 2005). To overcome the separation of biodiesel–bioethanol–petroleum diesel blends can be done in two ways that is to add emulsifier or by adding co-solvent. An emulsifier can be added to prevent separation of the different fuels in the blend, which will suspend small droplets of ethanol in the petroleum diesel. Meanwhile, a co-solvent can be added into the blend, which acts as a bridging agent and produces a homogeneous mixture through molecular compatibility and bonding (Shahir et al., 2014). **Figure 2.7** shows the phase behaviour of an ethanol–biodiesel–petroleum diesel blend (Fernando et al., 2004). It can be seen from **Figure 2.7** that bioethanol, biodiesel and petroleum diesel can be blended at room temperature, provided that the percentage volume of petroleum diesel is less than 20%, since the three components of the blend fall within the one-phase region (Fernando et al., 2004; Hansen et al., 2005).

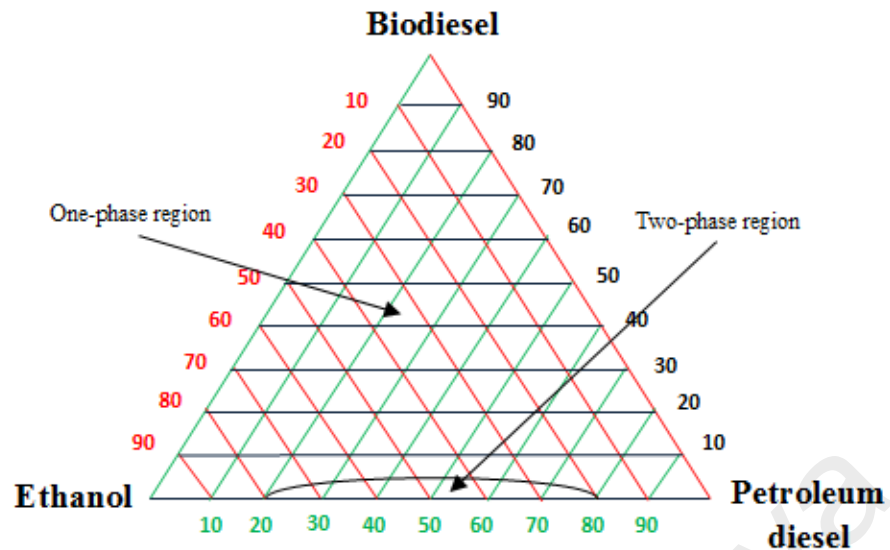


Figure 2.7: Phase behaviour of an ethanol–biodiesel–petroleum diesel blend (Fernando et al., 2004; Hansen et al., 2005)

It is known that the temperature and purity of bioethanol affects the phase formed in biodiesel–bioethanol–petroleum diesel blends (Chotwichien et al., 2009). In general, the inter-solubility of the components in these blends decreases with a decrease in temperature (Pidol et al., 2012). It has been shown that blends composed of 15% biodiesel, 5% bioethanol and 85% diesel have a calorific value close to that of petroleum diesel (Kim et al., 2010). According to Lapuerta et al. (2009) blending biodiesel, bioethanol and petroleum diesel results in an unstable formation of two liquid phases which may be a gelatinous interphase or gelatinous phase at the bottom of the glass cell. Chotwichien et al. (2009) investigated the effect of blending ethanol and butanol with palm biodiesel and diesel at various temperatures. They observed that blending bioethanol (up to 10%) with diesel at 10 °C results in good solubility but decreases the density, kinematic viscosity and cetane number of the fuel. However, this can be compensated by the addition of biodiesel into the blend.

2.8 Optimization esterification-transesterification using response surface methodology (RSM)

Biodiesel production from oil seeds can be obtained by extraction, purification (degumming, deacidification, dewaxing, and dehydration) and transesterification (Lin, C.-Y. et al., 2011; Pradhan et al., 2012; Wang, R. et al., 2012). These processes constitute up to 70% of the total biodiesel production cost in order to produce and refine the biodiesel from the feedstock (Pradhan et al., 2012; Zeng et al., 2008). There are many factors affecting the biodiesel production process such as methanol-to-oil molar ratio, the amount of catalyst, reaction temperature, reaction time and speed agitation. Therefore, it is necessary to optimize those factors aiming to minimize the cost of biodiesel production process (Micic et al., 2015). Response surface methodology (RSM) is a statistical tool used to investigate the effect of either an independent variable or a combination of independent variables on the dependent variable of a process (Betiku et al., 2015; Boey et al., 2013; Chellamboli et al., 2014). In this context, if the 'process' is the 'biodiesel production', then the independent variables are the operating parameters that influences biodiesel production such as the methanol-to-oil molar ratio, catalyst concentration, reaction time, reaction temperature and agitation speed (Chellamboli et al., 2014; Ong, H. et al., 2013). Hence, the dependent variable of the process is the biodiesel yield.

RSM can be used to optimize the operating parameters in order to achieve maximum biodiesel yield by means of a mathematical model. The use of RSM results in significant time and cost savings since the biodiesel yield can be predicted by simply tweaking the operating parameters, and this reduces the need to execute a large number of experiments which are costly in terms of time, money and effort. The experiment model of biodiesel synthesis developed is able to simulate the reaction under various transesterification conditions with good estimations of errors. This is helpful when mass

production of biodiesel needed (Ghadge et al., 2006). RSM has been shown to be a reliable tool which provides statistically acceptable results (Micic et al., 2015). This tool has been implemented effectively by a number of researchers to optimize biodiesel production using various feedstocks. For instance, Betiku et al. (2014) optimized the two-step biodiesel production process from neem oil using RSM and ANN and the results showed that the biodiesel yield is 99.1 and 98.7%, respectively. Optimization using response surface methodology based on the Box-Behnken also successfully applied to production of biodiesel from waste cooking oil, it is known that the accuracy of prediction models was 99.5% (Hamze et al., 2015). In addition, some parameters such as methanol/oil ratio, temperature, time, and amount of catalyst were variable that is used by Dwivedi et al. (2015) to optimize *P. pinnata* oil. From these studies it was known that the catalyst concentration, reaction time and the methanol/oil molar ratio has a significant impact on the biodiesel yield.

2.9 Engine performance and emissions characterization

2.9.1 Biodiesel–petroleum diesel blends

One of the main advantages of biodiesels is their high lubricity, which helps reduce friction losses and improve brake power. In addition, biodiesels have high cetane number, low sulphur content and oxygen content within a range of 10–11 %wt (Sundaresan et al., 2007). However, a high percentage volume of biodiesel in biodiesel–petroleum diesel blends can decrease engine performance due to the increase in kinematic viscosity and density as well as decrease in calorific value (Haşimoğlu et al., 2008; Qi et al., 2009). In terms of durability, biodiesels are considered superior to petroleum diesel since they have lower soot formation and higher lubricity, which will reduce particulate emissions (Xue et al., 2011a).

However, according to Mofijur, Masjuki, Kalam, Atabani, et al. (2013) the burning of biodiesels over long hours will degrade engine components such as hoses,

gaskets, O-rings, elastomer seals, adhesives and plastics since the rubber, adhesives and plastics will begin to break down. The addition of biodiesel into diesel fuel also increases the tendency of fuel filter blockage (Fazal et al., 2011a). This is due to the formation of wax crystals in the diesel fuel and the amount of wax crystals increases with a further decrease in temperature, which will eventually clog fuel filters and injectors. The accumulation of the wax crystals results in fuel gelation and the fuel eventually stops flowing (Fernando et al., 2007). Bari (2014) studied the performance of a four-stroke diesel engine powered metrobus fuelled by ultra-low sulphur diesel (ULSD) blended with 20% biodiesel. The results showed that the engine torque and engine power of the 20% biodiesel–diesel blend are similar to those for ULSD. In addition, the UHC and CO emissions are reduced for this blend, however, the NO_x emissions increases by 4.4%. Rashedul et al. (2014) reported that the biodiesel fuel reduces CO emissions by 27.7% compared to diesel at high loads. However, the UHC and NO_x emissions of the biodiesel fuel increases by 15.8 and 19.5% respectively, at low loads.

Özener et al. (2014) observed the performance, emission and combustion characteristics of biodiesels (up to 50% of biodiesel-diesel blends) in direct injection (DI) diesel engine with an engine speed from 1200 to 3000 rpm. The results showed that a decline in engine torque by 1–4% results in a significant reduction of CO emissions. The reduction of CO emissions and significant increase of NO_x emissions is due to the high oxygen content of the biodiesel, which leads to advanced injection process (Jindal et al., 2015). Moreover, biodiesels lead to lower ignition delay and lower premixed combustion phase, and they can be used readily in diesel engines without any engine modifications. Kumar, N. et al. (2015) reported that biodiesel–diesel blend (B40) can be used successfully in a modified engine during an endurance test up to 512 h.

Furthermore, the increase in the premixed combustion phase and fuel spray can reduce carbon deposition.

In general, the heat release rate is one of the indicators of the fuel combustion characteristic and it depends on the ignition delay and fuel properties (Oo et al., 2015). Analysis of the combustion and heat released by the biodiesel is used to reduce both energy and fuel consumption and attain acceptable engine performance parameters (Gumus, 2010). Teoh et al. (2014) investigated the effect of biodiesel blends on the combustion characteristics of a diesel engine with a common-rail cylinder at various operation loads. The results showed that the peak of the apparent heat release rate (AHRR) is lower for the biodiesel blends at low operation loads. However, the peak of the AHRR for the biodiesel blends is comparable to that for diesel at high operation loads. In addition, the biodiesel blends reduce ignition delay and speed up the burning time for all engine operation loads.

Mangus et al. (2015) observed the combustion characteristics of several types of biodiesels in a CI engine. The results showed that increasing the percentage volume of biodiesel in the biodiesel–diesel blend reduces the heat release rate and the premixed combustion phase over a longer duration, which is due to the increase in fuel kinematic viscosity. The increase in the combustion duration is also a consequence of the flash point and low volatility due to the increase in fuel kinematic viscosity (Gumus, 2010). Özçelik et al. (2015) found that the maximum heat release rate (HRR) is 35 J/crank angle degree for a 1.9 multi-jet diesel engine operating at an engine speed of 2500 and 4000 rpm using biodiesel.

2.9.2 Bioethanol–gasoline blends

At present, bioethanol–gasoline blends are widely used as alternative fuels in the transportation sector (Costa et al., 2011). The high octane number and density of

bioethanol–gasoline blends increases the brake thermal efficiency and compression ratio of the engine without pre-ignition (Costa et al., 2011). In addition, it is possible to achieve better combustion in the combustion chamber due to the high oxygen content of bioethanol, which reduces CO and UHC emissions (Najafi et al., 2009; Topgül et al., 2006). A number of studies have been conducted over the years to determine the performance, emissions and durability of bioethanol–gasoline blends (Bayraktar, 2005). Yücesu et al. (2006) discovered that E40 and E60 bioethanol–gasoline blends reduce exhaust emissions significantly, whereby the average UHC emission is reduced by 16.45%.

However, ethanol fuels are not without limitations even though they are widely used in the transportation sector. Yoon et al. (2009) investigated the performance of a four-cylinder SI engine fuelled with E85G15, E100 and G100 fuels and the results showed that an ethanol-blended fuel tend to reduce CO, CO₂ and UHC emissions, but not NO_x emissions. In addition, they observed a 10% decrease in the brake mean effective pressure (BMEP) for the E85G15 fuel. In contrast, the decrease in the BMEP is more significant for the E100 fuel, with a value of 25%. According to Turner et al. (2011) bioethanol–gasoline blends offer several benefits, whereby they reduce engine exhaust emissions and improve the efficiency of engines. It has been shown that a lower percentage volume of bioethanol in bioethanol–gasoline blends increases the vapour pressure in SI engines and reduces the heavy fractions for high blends. The addition of bioethanol also decreases the brake specific fuel consumption (BSFC), but it increases the brake thermal efficiency and volumetric efficiency (Najafi et al., 2009).

Al-Hasan (2003) investigated the effect of bioethanol–gasoline blends on the performance of a four-cylinder SI engine (TOYOTA Tercel-3A). The results showed that the bioethanol–gasoline blend containing 20% bioethanol reduces the BSFC by 5% compared to gasoline. The addition of bioethanol into gasoline increases the engine

speed and overall brake power, decreases the engine torque and results in loss of fuel economy and mileage since the energy value of bioethanol is lower than that for gasoline (Tangka et al., 2011). However, bioethanol with a high octane rating can also be used to modify the research octane number (RON) of gasoline. This gives greater thermal efficiency and/or more aggressive turbocharging to the engine and therefore, the engine can be downsized with a higher compression ratio (Anderson et al., 2012).

Costagliola et al. (2013) investigated the effect of bioethanol–gasoline blends (0, 10, 20, 30 and 85%) on the combustion efficiency of a SI engine. They observed that there is no significant difference in the combustion development whereas the global efficiency is slightly improved with an average value of roughly +5%. The addition of ethanol into gasoline also decreases the duration of combustion initiation due to the fact that ethanol has a faster laminar flame velocity (Costagliola et al., 2013).

Turkcan et al. (2013) investigated the effect of second injection timing on the performance of homogeneous charge compression ignition (HCCI) engine using gasoline mixed with an alcohol (such as ethanol and methanol). The results showed that there is a significant decrease in the maximum cylinder gas pressure and the maximum heat release rate. In addition, the combustion initiation is delayed with retarded second fuel injection timing. In another study, Turkcan et al. (2014) investigated the effect of various parameters on the performance of a DI HCCI engine and the observations were focused on the start of the first and second injection. The results showed that the start of the first injection has a significant effect on the cylinder gas pressure and heat release rate. In addition, increasing the ethanol content in the bioethanol–gasoline blends decreases the maximum cylinder gas pressure compared to gasoline for the test conditions considered in their study.

2.9.3 Biodiesel–bioethanol–petroleum diesel blends

It is expected that the addition of biodiesel or bioethanol into petroleum diesel will enhance the physicochemical properties of the fuel (Yilmaz, Vigil, Donaldson, et al., 2014). According to Zhu et al. (2011) biodiesel–bioethanol–petroleum diesel blends improve the engine performance and increase the brake thermal efficiency of four-cylinder DI diesel engines. The addition of bioethanol helps reduce NO_x and particulate emissions from diesel engines (Labeckas et al., 2014; Zhu et al., 2011). Yilmaz (2012) revealed that the biodiesel–ethanol/methanol–diesel blends showed higher brake specific fuel consumption than diesel. The addition of bioethanol and biodiesel into the mixture also results in brake specific fuel consumption considerably when compared to baseline diesel (Hulwan et al., 2011). Barabas et al. (2010) highlighted that biodiesel–bioethanol–petroleum diesel blends decrease CO and UHC emissions. The decrease in particulate emissions is due to the higher oxygen content of the fuel which lowers the air/fuel stoichiometric ratio. This reduces the aromatic content of the fuel which in turn, reduces carbonaceous soot (Su et al., 2013). According to Labeckas et al. (2014) fuel oxygenation is important to increase auto-ignition delay and combustion pressure, as well as to reduce CO emissions and smoke opacity.

However, the effect of bioethanol–biodiesel–petroleum diesel blends on material durability is of primary concern. Armas et al. (2011) found that the use of ethanol–biodiesel–petroleum diesel fuel affects the durability of the fuel injection pumps and injection nozzles to a similar extent as that for diesel fuel. The differences between the effective sections of the holes of the nozzles before and after the test are below of 0.1 µm for both fuels. Kannan et al. (2011) tested the durability of injection pumps and nozzle injectors of a single-cylinder DI diesel engine fuelled by ethanol–biodiesel–diesel blends and the results revealed that the ethanol–biodiesel–diesel blends have the same effect on the durability of these engine components as that for diesel.

2.10 Corrosion

2.10.1 Corrosion behaviour of metals and their alloys immersed in biodiesels

Corrosion is measured using the method outlined in the ASTM D130 standard, which involves comparing the changes in colour of copper strips with respect to time, volume and temperature for the biodiesel or bioethanol (Fernando et al., 2007; Singh et al., 2012). According to Fazal et al. (2013a) corrosion of the copper occurs with an increase in the time in which the copper is immersed in the biodiesel. The immersion time was set at 200, 300, 600, 1200 and 2880 h and the temperature range was 25–27 °C.

Haseeb, Sia, et al. (2010) investigated the corrosion rate of commercially pure copper and bronze immersed in B0, B50 and B100 biodiesel–diesel blends within a range of 25–30 °C. The immersion time was 2640 h. They also compared the corrosion rate of the copper and bronze samples immersed in these fuels at a temperature of 60 °C over a period of 840 h. The results showed that the corrosion rate is dependent on the percentage volume of biodiesel in the biodiesel–diesel blend. In general, the copper and bronze samples immersed in the biodiesel–diesel blends have higher corrosion levels compared to those immersed in petroleum diesel, (Fazal et al., 2013b; Sorate et al., 2015) which is due to the higher unsaturated fatty acid content of the biodiesels such as oleic and linoleic acids. Both of these unsaturated fatty acids are prone to react with metals, resulting in corrosion (Atabani, Silitonga, et al., 2013; Haseeb, Masjuki, et al., 2010).

It has also been shown that the degradation of fuel is dependent on the type of metal to which the fuel is exposed as well as water absorption, auto-oxidation and microbial attacks during storage of the fuel (Bhardwaj et al., 2014). Fazal et al. (2010b) investigated the corrosion behaviour of copper, aluminium and stainless steel test coupons immersed in palm biodiesel at 80 °C. The immersion test was carried out over

a period of 600 and 1200 h, whereby the fuels were stirred continuously at an agitation speed of 250 rpm using a magnetic stirrer. The corrosion rate of copper, aluminium and steel was found to be 0.586, 0.202 and 0.015 mils per year (mpy), respectively.

Even though corrosion of engine components is a common issue which needs to be addressed, several researchers have noted that there are no specific tolerance limits for corrosion of engine components (Hu et al., 2012a; Singh et al., 2012). In general, increasing the percentage volume of biodiesel in biodiesel–petroleum diesel blends will increase the level of corrosion and oxidation stability (Sorate et al., 2015). Copper alloys are more susceptible to corrosion compared to iron and aluminium alloys (Sorate et al., 2015). Hu et al. (2012a) observed the occurrence of corrosion on copper, mild carbon steel, aluminium and stainless steel samples upon exposure to rapeseed biodiesel and the corrosion level is more severe for copper and mild carbon steel samples immersed in rapeseed biodiesel. In contrast, the corrosion level is minor for aluminium and stainless steel – the effect is similar to that for samples immersed in commercial diesel fuel. This is attributed to the formation of a thin oxide layer on the surface of the aluminium and stainless steel, which serves as barrier that prevents these metals from further oxidation, resulting in a minor corrosion effect. The results indicated that chemical corrosion is the primary mechanism of corrosion and the products of corrosion are metal oxides and salts of fatty acids – the latter product is the consequence of the reaction between the metal oxides in the oxide layer of the metals and the fatty acids present in the rapeseed biodiesel.

According to Singh et al. (2012) biodiesel reduces auto-oxidation and therefore, it is the presence of moisture that increases the corrosion rate. This is due to the formation of a new phase and secondary products by degradation of the metal strip upon exposure to biodiesel–mineral diesel blends. Advanced anode reaction can be used to identify the characteristics of electrochemical metal corrosion and block a number of rusty areas on

the metal. This helps prevent corrosion of engine components due to exposure to biodiesel (Wang, W. et al., 2012). The summary of corrosion testing from several studies using different biodiesel as shown in **Table 2.6** (Deyab, 2016; Fasogbon et al., 2016; Fazal et al., 2011c; Hu et al., 2012b; Jin et al., 2015; Kaul et al., 2007; Krishnamurthy, 2013; Sterpu et al., 2012).

University of Malaya

Table 2.6: Review of material corrosion tests for some types of biodiesel

Ref.	Biodiesel feedstock	Material	Blend with diesel fuel	Immersed/ corrosion time	Condition, temperature (°C), and method	Corrosion rate																				
(Ononiwu et al., 2015)	Ghee Butter (Mann Shanu)	Mild steel	41,5%, 39.5% and diesel fuel	30 days	Temp. 30, 35, 40, 45, 50 °C, static immersion test.	3.6–4.4 mpy, biodiesel is more corrosive than diesel fuel																				
(Kaul et al., 2007)	P. glabra, S. oleoides, M. indica and J. curcas	Piston metal, and liner metal	P. Glabra, S. Oleoides, M. Indica and J. Curcas biodiesel	7200 h	Ambient temperature, static immersion test.	<table border="1"> <thead> <tr> <th></th> <th>Piston (mpy)</th> <th>Liner (mpy)</th> </tr> </thead> <tbody> <tr> <td>Undoped diesel (petro)</td> <td>0.0058</td> <td>0.0065</td> </tr> <tr> <td>Biodiesel JC oil</td> <td>0.0117</td> <td>0.0784</td> </tr> <tr> <td>Biodiesel Karanja</td> <td>0.0058</td> <td>0.0065</td> </tr> <tr> <td>Biodiesel Mahua</td> <td>0.0058</td> <td>0.0065</td> </tr> <tr> <td>Biodiesel Salvadoria</td> <td>0.1236</td> <td>0.1329</td> </tr> </tbody> </table>		Piston (mpy)	Liner (mpy)	Undoped diesel (petro)	0.0058	0.0065	Biodiesel JC oil	0.0117	0.0784	Biodiesel Karanja	0.0058	0.0065	Biodiesel Mahua	0.0058	0.0065	Biodiesel Salvadoria	0.1236	0.1329		
	Piston (mpy)	Liner (mpy)																								
Undoped diesel (petro)	0.0058	0.0065																								
Biodiesel JC oil	0.0117	0.0784																								
Biodiesel Karanja	0.0058	0.0065																								
Biodiesel Mahua	0.0058	0.0065																								
Biodiesel Salvadoria	0.1236	0.1329																								
(Hu et al., 2012b)	Rapeseed oil	copper, mild carbon steel, aluminum, and stainless steel	Rapeseed biodiesel, diesel fuel	60 days	Temp. 43 °C, static immersion test.	Copper= 0.02334 mm/year, mild carbon steel= 0.01819 mm/year, aluminum= 0.00324 mm/year, and stainless steel= 0.00087 mm/year																				
(Jin et al., 2015)	Palm	ASTM 1045 mild steel	Palm biodiesel, diesel fuel	30, 60 and 120 days	27, 50 and 80 °C, static immersion test.	0.002–0.12 mm/year, biodiesel is more corrosive than diesel, high temperature more corrosive than room temperature,																				
(Fasogbon et al., 2016)	Used cooking oil	copper-magnesium alloy, mild steel, aluminium, and stainless steel	B0, B20, B40, B60, B80, and B100	<ul style="list-style-type: none"> • 965 hours at room temperature (25-30 °C. • 8 hours for 40 °C, 60 °C, 80 °C, and 100 °C. 	Room temperature (25-30 °C) and 40, 60, 80, and 100 °C, static immersion test.	<table border="1"> <thead> <tr> <th></th> <th>Fuel</th> <th>At room temp. (mm/y)</th> <th>At 100 °C (mm/y)</th> </tr> </thead> <tbody> <tr> <td>copper-magnesium alloy</td> <td>B100</td> <td>0.005627</td> <td>0.35151</td> </tr> <tr> <td>aluminium</td> <td>B100</td> <td>0.003644</td> <td>0.319652</td> </tr> <tr> <td>mild steel</td> <td>B100</td> <td>0.00377</td> <td>0.12408</td> </tr> <tr> <td>stainless steel</td> <td>B100</td> <td>0.000112</td> <td>0.094817</td> </tr> </tbody> </table>		Fuel	At room temp. (mm/y)	At 100 °C (mm/y)	copper-magnesium alloy	B100	0.005627	0.35151	aluminium	B100	0.003644	0.319652	mild steel	B100	0.00377	0.12408	stainless steel	B100	0.000112	0.094817
	Fuel	At room temp. (mm/y)	At 100 °C (mm/y)																							
copper-magnesium alloy	B100	0.005627	0.35151																							
aluminium	B100	0.003644	0.319652																							
mild steel	B100	0.00377	0.12408																							
stainless steel	B100	0.000112	0.094817																							
(Sterpu et al., 2012)	Sunflower oil, rapeseed oil and corn oil	Carbon steel	Sunflower, rapeseed and corn biodiesel	1176 h (49 days)	Room temperature (25–30 °C), static immersion test.	Sunflower= 0.000855 mm/year, rapeseed= 0.000760 mm/year, and corn biodiesel= 0.001164 mm/year.																				
(Krishnamurthy, 2013)	Pongamia pinnata	Copper and brass	Pongamia pinnata biodiesel	100 h	Room temperature, static immersion test and at the rotation speed of 500 rpm.	Copper in condition static immersion= 0.219 mpy, and rotation speed= 2.704 mpy. Brass in condition static immersion= 0.201 mpy, and rotation speed= 1.502 mpy.																				

2.10.2 Corrosion behaviour of metals and their alloys immersed in ethanol/bioethanol

It has been reported that engine components can become susceptible to corrosion upon exposure to bioethanol (Surisetty et al., 2011). Since bioethanol is a type of alcohol, it absorbs water, which accelerates the corrosion of metals. In addition, bioethanol may contain other impurities such as organic acids resulting from bacterial contamination during the fermentation process which also accelerates the corrosion of metals. In addition, the structural composition of bioethanol–gasoline blends can change during the liquid phase and this change is dependent on the fluid temperature, atmospheric pressure, the amount of polar components in the gasoline as well as aromatic substances (Yahagi et al., 1984). According to Shahir et al. (2014) the severity of corrosion is influenced by the quality of the bioethanol. Corrosion due to ethanol can be divided into the following categories: (1) general corrosion which is caused by ionic dirt (chloride and acetic acid), (2) dry corrosion which is caused by the polarity of the ethanol molecules, and (3) wet corrosion which is caused by azeotropic water, which oxidizes a variety of metals.

Corrosion is undesirable in engine components because it can damage the metal surface (Baena et al., 2012). Even though anti-corrosive compounds can be used to reduce the effects of corrosion resulting from the use of bioethanol–gasoline blends, these compounds may alter the exhaust emission profiles of the blends, such that they introduce new emission products to the environment (Manzetti et al., 2015). Boniatti et al. (2013) and Cao et al. (2013) discovered that the bioethanol results in holes, pores and cracks on the surface of AISI 4140 steel due to the decrease in oxidation stability of the fuel. Krüger et al. (2012) observed the occurrence of corrosion on the surface of the aluminium alloys immersed in bioethanol–gasoline blends, which is attributed to the high boiling point of the bioethanol, which severely corrodes the metal surface.

Likewise, Park et al. (2014) also observed the occurrence of corrosion on the surface of aluminium alloys immersed in bioethanol–gasoline blends at 100 °C. *In situ* two-electrode electrochemical impedance spectroscopy (EIS) was used to assess the corrosion and the results showed that the polarization of the aluminium alloys increases during the initial period of immersion due to the formation of boehemite film (γ -AlOOH). However, the polarization of the aluminium alloys decreases thereafter due to the initiation of the reaction of aluminium alkoxide.

2.11 Summary

The literature review describes some research related to the feasibility, potential and development of renewable fuels such as biodiesel and bioethanol.

This chapter also explains the types of raw materials that have been developed by some previous researchers to produce biodiesel derived from edible vegetable oil (soybean, peanut, oil palm, sunflower, etc) raw materials, non edible oil (jatropha curcas, ceiba pentandra, etc), waste or recycle oil, and animal fat. Meanwhile, bioethanol can be developed from several types of raw materials including first generation (corn, sugar cane, cassava, starch, cellulose, beet, barley sugar, wheat, potatoes), second-generation bioethanol (waste and lignocellulosic materials: forest residues, municipal solid wastes, waste papers, crop residues), and third-generation bioethanol (microalgae and macroalgae).

Some characteristics of fuel properties including kinematic viscosity, density, acid value, flash point, cloud point and pour point, calorific value, oxidation stability, cetane number, and iodine value are also reviewed in depth in this section. In addition, the effects of using biodiesel, bioethanol and blends with diesel fuel are also discussed in detail and focused, including engine performance and corrosion progression in materials.

CHAPTER 3: METHODOLOGY

3.1 Introduction

In this study, the methodology was based on research stages in accordance with the groove that had been planned. It began with studying an extensive literature relating to the production of biodiesel, optimization, fuel properties, bioethanol, blending biodiesel-diesel fuel, blending biodiesel-bioethanol-diesel fuel, engine performance and exhaust emissions, material corrosion, cited from various sources such as thesis, books, journals, published, reports and conference proceedings. This chapter also discusses the selection of the percentage of the better mixture of biodiesel produced from two kinds of non-edible material namely *Jatropha curcas-Ceiba pentandra* crude oil, as well as the optimization of production based on several parameters, namely methanol-to-oil ratio, agitation speed, and catalyst percentage. The properties and characteristics of biodiesel were investigated using equipment that follows the standards of ASTM and EN. In addition, analysis of the characteristics and properties of biodiesel-diesel fuel blends, and biodiesel-bioethanol-diesel fuel blends were also done. The ability of biodiesel and mixtures thereof with diesel and bioethanol as a fuel was also tested using a Yanmar 120M TF single cylinder four strokes engines. The experiments were conducted at the Energy Efficiency and Heat Engine Laboratory, Department of Mechanical Engineering, University of Malaya. In addition, corrosion testing was also performed by immersing of mild steel coupons into biodiesel-diesel fuel blends, and biodiesel-bioethanol-diesel fuel blends up to 2000 h of immersion and then observed corrosion behaviour by using SEM and EDX. The methodology adapted in this research is shown in **Figure 3.1**. The complete studies and methodologies of experiment Interpretations are discussed in the following sections.

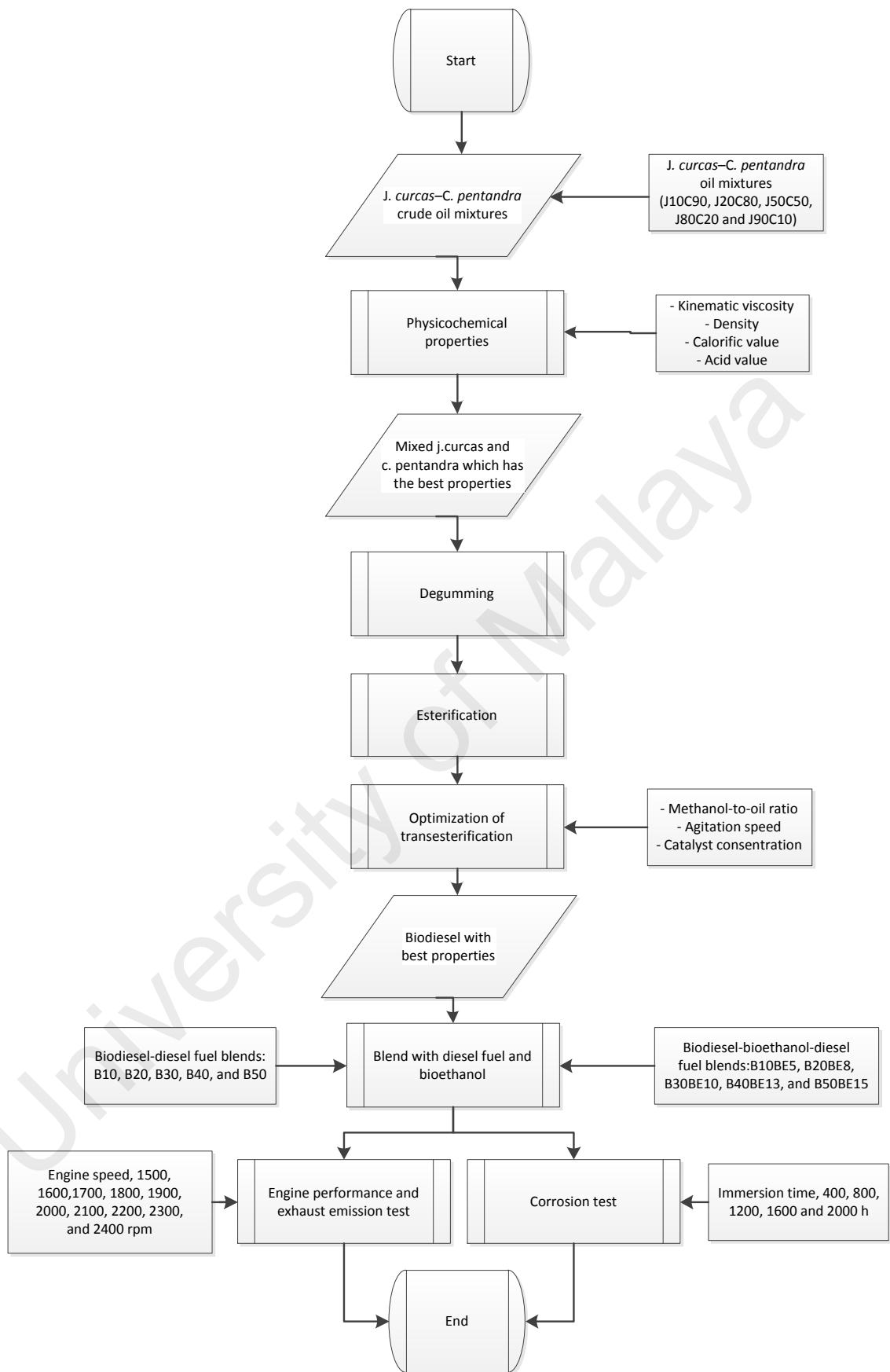


Figure 3. 1: Methodolgy glowchart

3.2 Materials

J. curcas crude oil was purchased from Kebumen, West Java, Indonesia, whereas *C. pentandra* crude oil was purchased from Probolinggo, East Java, Indonesia. Bioethanol was purchased from Bogor, West Java, Indonesia. The reagents used in the preparation of the biodiesel are as follows: methanol (purity: 99.9%), sulphuric acid (H_2SO_4 , purity: > 98.9%), phosphoric acid (H_3PO_4 20%), potassium hydroxide pellets (KOH, purity: 99%), calcium chloride anhydrous (CaCl_2 99%), sodium sulphate anhydrous (Na_2SO_4 99%) and sodium hydrogen carbonate (NaHCO_3). Whatman filter papers (Filtres Fioroni, France) were purchased from Metta Karuna Enterprise, Kuala Lumpur, Malaysia, were used for filtering the biodiesel samples. **Figure 3.2** shows the photographs of *J. curcas* and *C. pentandra* trees, fruits, seeds and crude oils.



(a) From left to right: *J. curcas* tree, fruits, seeds and crude oil



(b) From left to right: *C. pentandra* tree, fruits, seeds and crude oil

Figure 3.2: Tree, fruits, seeds and crude oil of: (a) *J. curcas* and (b) *C. pentandra*

3.3 Experimental setup for esterification and transesterification

Both the esterification and transesterification of the *J. curcas*–*C. pentandra* oil mixtures were carried out using a 500 ml three-neck round bottom flask equipped with

a reflux condenser. The condenser is used to maintain the evaporation of methanol during the reaction. The three-neck round bottom flask was placed onto a hot plate magnetic stirrer (Model: IKA CMAG HS7). A thermometer was immersed in one neck of the flask using a rubber stand to verify and control the temperature. **Figure 3.3** shows the experimental apparatus for esterification and transesterification process of crude the *J. curcas*–*C. pentandra* oil.

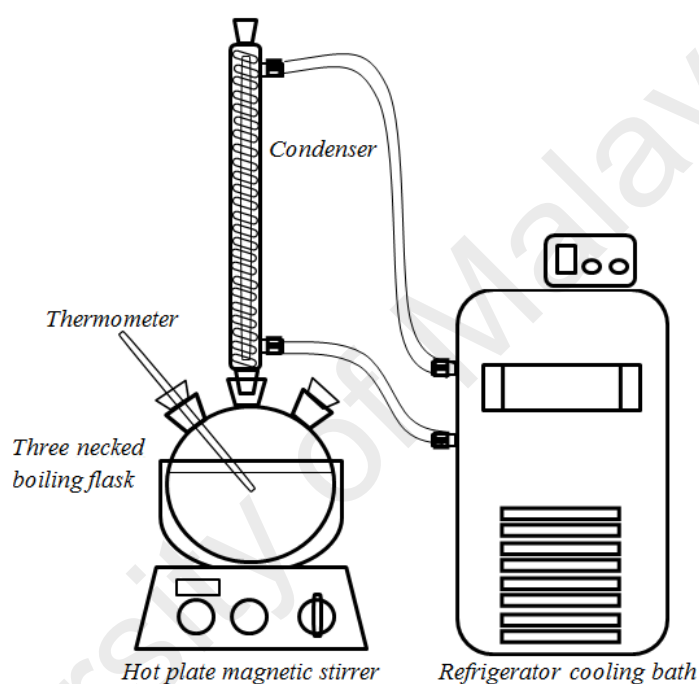


Figure 3.3: Apparatus for esterification and transesterification of crude *J. curcas*–*C. pentandra* oil to methyl ester

3.4 Measurement of physicochemical properties

The physical and chemical properties of the oil were in accordance with ASTM D6751 or EN 14214 standards. Testing is done to crude oil, biodiesel, and fuel mixture.

Table 3.1 shows a summary of equipment used in this study to analyze the properties.

Each test was repeated three times and the average value was calculated for each sample. The mean average measurement was calculated using Eq. 3.1 as below:

$$Avr = \frac{R_1 + R_2 + R_3}{\Delta R} \quad (3.1)$$

Where, Avr= average result, R1-3 = results, ΔR = number of test

Table 3.1: List of apparatus used for properties test

Property	Apparatus	Standard method	Accuracy
Kinematic viscosity	NVB classic (Normalab, France), Stabinger Viscometer	ASTM D445	$\pm 0.01 \text{ mm}^2/\text{s}$
Density	DM40 LiquiPhysics™ density meter (Mettler Toledo, Sw)	ASTM D127	$\pm 0.1 \text{ kg/m}^3$
Flash point	NPM 440 Pensky-martens flash point tester (Normalab,	ASTM D93	$\pm 0.1 \text{ }^\circ\text{C}$
Cloud and pour point	NTE 450 Cloud and pour point tester (Normalab, Franc	ASTM D2500	$\pm 0.1 \text{ }^\circ\text{C}$
Calorific value	6100EF Semi auto bomb calorimeter (Perr, USA)	ASTM D240	$\pm 0.001 \text{ MJ/kg}$
Acid number and iodine value	Automation titration rondo 20 (Mettler Toledo, Switz	ASTMD664	$\pm 0.001 \text{ mg KOH/g}$
Copper strip corrosion (3 h at 50°C)	Seta copper corrosion bath 11300-0 (Stanhope-Seta, UK)	ASTM D130	–
Sulphate ash content	Professional laboratory furnace Model L40/11 (Nabertherm,Germany)	ASTM D874	$\pm 0.001\%$
Sulfur content (S 15 grade and S500 grade)	Multi EA 5000 (Analytical jena, Germany)	ASTM D6667	–
Oxidation stability, 110°C	873 Rancimat (Metrohm, Switzerland)	EN 14112	$\pm 0.01 \text{ hour}$
FAME content	Agilent 7890 gas chromatograph (Agilent, USA)	EN 14110	$\pm 0.008\%$ or 0.0008 min
Cetane number	92000- 3 Ignition quality tester (IQT™) (Stanhope-Seta, UK)	ASTM D6890	± 0.1
Water content	837 KF coulometer (Metrohm, Switzerland)	EN ISO 12937	$\pm 0.001\% \text{ vol.}$

3.5 Biodiesel production

3.5.1 J. curcas–C. pentandra crude oil mixtures

A total of five J. curcas–C. pentandra oil mixtures (J10C90, J20C80, J50C50, J80C20 and J90C10) were prepared in this study, in which the amount of J. curcas and C. pentandra crude oils in weight percent (wt.%) was varied in order to determine and compare the properties of the oil mixtures. Properties tests, such as acid value, viscosity at 40 °C, calorific and density at 15 °C, carried out on various of J. curcas-C. pentandra crude oil mixtures. Oil mixture which has the most excellent properties then performed optimization process.

3.5.2 Mixing and degumming crude oil

The *J. curcas* and *C. pentandra* crude oils were mixed in order to improve the oxidation stability of the final product. In general, crude oils contain varying amounts of phosphatides (known as gums) and these phosphatides need to be removed from the oils since they are undesirable for biodiesel production. The process of removing phosphatides from crude oils is called degumming process. In this process, a mixture of crude oil (a mixture of *J. curcas* and *C. pentandra* crude oils which have the characteristics and properties of the most well) was preheated at 60 °C for 15 minutes. Following this, 2 vol.% of phosphoric acid (H_3PO_4 20%) was added into the oil mixture and heated at 60 °C over a period of 30 minutes with an agitation speed of 800 rpm. This was followed by a simple filtration process for at least 4 hours, in which the formation of phosphatides (gums) can be observed at the bottom of the flask. The gums were separated from the oil mixture and the oil mixture was washed several times with distilled water at 40 °C. The excess water was evaporated from oil mixture using a vacuum pump for 30 minutes in order to prevent oxidation of the oil mixture.

3.5.3 Esterification

J. curcas-*C. pentandra* biodiesel production takes place in a two-step process: (1) acid-catalysed esterification and (2) alkali-catalysed transesterification. The esterification process is also known as pre-treatment and the main purpose of this process is to reduce the amount of free fatty acids present in the oil mixture to less than 1%. In this process, 1% (v/v) of sulphuric acid (H_2SO_4) was added into 200 ml of degummed *J. curcas*-*C. pentandra* oil mixture. The esterification process was carried out over a period of 3 hours using the following operating parameters: methanol-to-oil ratio: 30%, temperature: 60 °C and agitation speed: 1200 rpm. Once the reaction was complete, the products were poured into a separating funnel in order to separate excess methanol, H_2SO_4 and impurities. After a few hours, the upper layer containing excess

methanol and , while the esterified *J. curcas-C. pentandra* oil mixture is at the bottom layer. Following this, esterified *J. curcas-C. pentandra* oil mixture was heated at 60 °C in a rotary evaporator under vacuum conditions for 1 hour to remove methanol and water residues present in the oil mixture.

3.5.4 Transesterification

Esterified *J. curcas-C. pentandra* oil mixture was measured and preheated to a temperature of 60 °C using a heating circulator. Following this, 1 wt.% of potassium hydroxide (KOH), which is an alkaline catalyst, was dissolved in methanol, noting that the methanol-to-oil ratio was 30%. This KOH-methanol solution was then added into the heated oil and the reaction continues over a period of 2 hours. The oil mixture was stirred constantly at 800 rpm using an overhead stirrer during the transesterification process and the temperature was kept constant at 60 °C. Once the reaction was complete, the methyl ester (biodiesel) was poured into a separating funnel for 6 hours in order to separate glycerol from the methyl ester. The excess methanol, glycerol and impurities contained in the high-density bottom layer were removed in this stage. Following this, the methyl ester was poured into a rotary evaporator to remove methanol residues, and then washed with distilled water several times to remove entrained glycerol and impurities. In this process, 50% (v/v) of distilled water at 50 °C was sprayed over the surface of the methyl ester and stirred slowly. The methyl ester was further purified to remove excess water and methanol using a vacuum pump at 60 °C, and finally filtered using a filter paper.

3.6 Optimization biodiesel production

Response surface methodology (RSM) with Box-Behnken experimental design was used to optimize the *J. curcas-C. pentandra* biodiesel yield using Design-Expert® software version 9.0.4.1 (Stat-Ease Inc., Minneapolis, USA). This software is a tool dedicated for design of experiments (DOE). The following operating parameters, such

as methanol-to-oil ratio (*A*), agitation speed (*B*) and catalyst concentration (*C*), were varied in order to maximize the *J. curcas-C. pentandra* biodiesel yield or methyl ester yield (*y*). The coded and uncoded levels of the Box-Behnken independent variables for optimization of the transesterification process parameters for the *J. curcas-C. pentandra* oil mixture are presented in **Table 3.2**. These experiments enable one to determine the effect of each independent variable (such as methanol-to-oil ratio, agitation speed and catalyst concentration) and the interaction between these variables on the dependent variable (such as *J. curcas-C. pentandra* biodiesel yield). The experimental data were analysed using response surface regression which is given by the following polynomial:

$$Y = b_o + \sum_{i=1}^k b_i X_i + \sum_{i=1}^k b_{ii} X_i^2 + \sum_{i_i > j}^k \sum_j^k b_{ij} X_i X_j + e \quad (3.2)$$

In **Eq. 3.2**, *Y* is the response factor, *X_i* is the independent factor, *b_o* is the intercept, *b_i* is the first-order coefficient of the model, *b_{ii}* is the quadratic coefficient of the *ith* factor; *b_{ij}* is the linear coefficient of the model for the interaction between the *ith* and *jth* factor, *k* is the number of factors studied and optimized in the experiment, and *e* is the experimental error attributed to *Y*.

Table 3.2: Box-Behnken coded and uncoded independent variables for optimization of the transesterification process parameters for the *J. curcas-C. pentandra* oil mixture

Factor	Units	Level		
		-1	0	+1
Methanol-to-oil ratio (<i>A</i>)	mol/mol	30	50	70
Speed agitation (<i>B</i>)	rpm	800	1300	1800
Catalyst concentration (<i>C</i>)	wt. %	0.50	1.25	2.00

3.7 Fatty acid composition and Fourier transform infrared spectrum of the *J. curcas-C. pentandra* biodiesel

The fatty acid composition of the *J. curcas-C. pentandra* biodiesel were determined using gas chromatography. Gas chromatography system was equipped with a ZB-wax 30 m capillary column (inner diameter: 0.25 mm, film thickness: 0.25 μm , split ratio: 1:20) with a flame ionization detector. High-purity helium was used as the carrier gas, and the temperature of the detector and injector was 250 $^{\circ}\text{C}$. The oven temperature was initially maintained at 100 $^{\circ}\text{C}$ for 10 minutes, and then increased at a rate of 15 $^{\circ}\text{C}/\text{min}$ and held at a final temperature of 240 $^{\circ}\text{C}$ for 15 minutes. The fatty acid composition of the biodiesel was analysed in accordance with the procedures outlined in the biodiesel standards.

The *J. curcas-C. pentandra* yield biodiesel was determine by fatty acid methyl ester content, which is given by the following equation:

$$FAME = \frac{(\sum A) - A_{EI}}{A_{EI}} \times \frac{C_{EI} \times V_{EI}}{m} \times 100\% \quad (3.3)$$

In **Eq. 3.3**, *FAME* represents the fatty acid methyl ester content (%), $\sum A$ is the sum of the peak areas of the fatty acid methyl ester content from C_{14} to $\text{C}_{24:1}$, A_{EI} is the peak area of the internal standard, (*i.e.* palmitic acid methyl ester), C_{EI} is the concentration of the palmitic acid methyl ester (mg/mL), V_{EI} is the volume of the palmitic acid methyl ester (mg/mL), and m is the weight of the biodiesel sample (g).

J. curcas-C. pentandra yield biodiesel can be determined using the following equation:

$$BY_{JCCP} = \frac{FAME \times W_{cmb}}{W_{cmo}} \times 100\% \quad (3.4)$$

In Eq. 3.4, BY_{JCCP} represents the biodiesel yield, $FAME$ is the fatty acid methyl ester content (%), W_{cmb} is the weight of the *J. curcas-C. pentandra* biodiesel produced from the transesterification process (g) and W_{cmo} is the weight of the *J. curcas-C. pentandra* crude oil mixture.

J. curcas-C. pentandra biodiesel was then characterized using Fourier transform infrared (FTIR) spectrometer (Model: TENSOR 27, Bruker Optics Inc, USA) equipped with a detector having a spectral range 11,000–350 cm^{-1} . The FTIR spectrum was analysed using OPUS Spectroscopy software supplied with the instrument. The absorption bands of the FTIR spectrum enable one to identify the long-chain fatty acid esters present in the *J. curcas-C. pentandra* biodiesel sample.

3.8 Physicochemical properties of *J. curcas*, *C. pentandra* and *J. curcas-C. pentandra* biodiesels

The physicochemical properties of the *J. curcas*, *C. pentandra* and *J. curcas-C. pentandra* biodiesels (*i.e.* kinematic viscosity at 40 °C, density at 15 °C, flash point, pour point, cloud point, cold filter plugging point, calorific value, acid value, copper strip corrosion, oxidation stability at 110 °C, FAME content and cetane number) were determined and compared with the physicochemical properties of diesel fuel. The physicochemical properties of biodiesel produced from transesterification of the *J. curcas-C. pentandra* oil mixture at optimum conditions were also measured and compared with the physicochemical properties of biodiesel before optimization.

3.9 Biodiesel diesel fuel blend

The *J. curcas-C. pentandra* biodiesel was blended with commonly diesel fuel at five different ratios of biodiesel, *i.e.* 10, 20, 30, 40, and 50 vol%. The biodiesel-diesel blends were labelled accordingly as B10, B20, B30, B40, and B50, respectively. Both of these fuels were blended in a glass beaker at 30 °C at a stirring speed of 2000 rpm for

30 min in order to obtain a homogeneous blend. The fuel properties of the J50C50 biodiesel and biodiesel-diesel blends were determined in accordance with the ASTM D6751 and EN 14214 standard test methods. Several tests were performed to determine the physicochemical properties of the J50C50 biodiesel and its blends such as density, kinematic viscosity, calorific value, pour point, and flash point. The process of determining the physicochemical properties of the fuel is also known as characterization of the fuel. The estimated test list for biodiesel-diesel fuel blended is shown in **Table 3.3**.

Tabel 3.3: Description of biodiesel-diesel blending

Fuel samples	Samples description
B0	100% diesel fuel
B10	10% biodiesel + 90% diesel fuel
B20	20% biodiesel + 80% diesel fuel
B30	30% biodiesel + 70% diesel fuel
B40	40% biodiesel + 60% diesel fuel
B50	50% biodiesel + 50% diesel fuel

3.10 Biodiesel-bioethanol-diesel fuel blend

In this study, bioethanol is also used as a mixture of fuel, bioethanol added to biodiesel-diesel fuel mixture with a certain level. Mixing fuel (bioethanol-biodiesel-diesel fuel) is performed at a temperature of 30 °C with a stirring speed of 2000 rpm in a glass beaker for 30 minutes. The estimated test list for biodiesel-bioethanol-diesel fuel blended is shown in **Table 3.4**.

Tabel 3.4: Description of for biodiesel-bioethanol-diesel blending

Fuel samples	Samples description
B0	100% diesel fuel
B10BE5	10% biodiesel + 5% bioethanol + 85% diesel fuel
B20BE8	20% biodiesel + 8% bioethanol + 72% diesel fuel
B30BE10	30% biodiesel + 10% bioethanol + 60% diesel fuel
B40BE13	40% biodiesel + 13% bioethanol + 47% diesel fuel
B50BE15	50% biodiesel + 15% bioethanol + 35% diesel fuel

3.11 Experimental procedure for engine test and emissions

In this study, YANMAR TF-120 direct injection diesel engine was used as the test engine. The schematic layout of the diesel engine with all of the instruments installed is shown in **Figure 3.4** and the engine technical specifications are summarized in **Table 3.5**. An eddy current dynamometer with the following specifications (maximum power: 20 kW, rated torque: 80 Nm, rated speed: 10,000 rpm) was connected to the engine. The engine was also connected to an automatic data acquisition system which measures and records the engine performance parameters (i.e. BSFC, engine torque, brake power, EGT, and BTE) at full load conditions and various engine speeds.

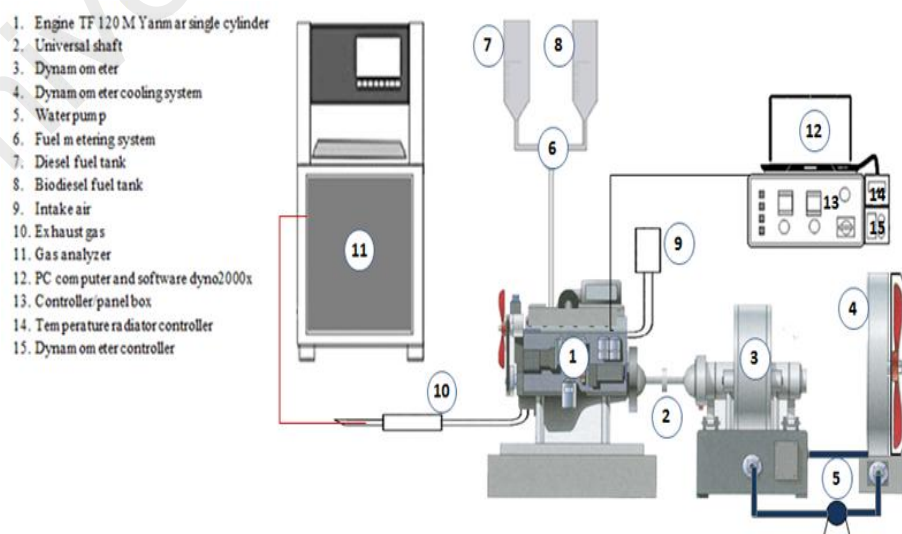


Figure 3.4: Schematic layout of the single-cylinder direct injection diesel engine set-up

Tabel 3.5: Technical specifications of the engine

Type	Specifications
Injection system	Direct injection
Number of cylinders	One
Type of cooling system	Water cooling
Cylinder bore (mm)	92
Stroke (mm)	96
Displacement (L)	0.638
Compression ratio	17.7:1
Max. power (kW)	7.7
Max. engine speed (rpm)	2400
Injection timing (deg.)	bTDC 17.0
Injection pressure (kg/cm ²)	200

Moreover, the exhaust emission parameters (*i.e.* CO, CO₂, and NO_x emissions, and smoke opacity) were measured using Bosch BEA 150 portable diesel emissions analyzer. The smoke opacity measurements were carried out by collecting the exhaust fumes from the engine using a gas analyzer filter fitted with a sensor. Calibration and maintenance of the diesel emissions analyzer was conducted separately and scheduled using the gas samples supplied by Robert Bosch Sdn. Bhd., Malaysia. The specifications of BOSCH portable emission analyser are shown in **Table 3.6**.

Tabel 3.6: Technical specifications of the gas analyser

Technical data	Accuracy range (°C)	+5 to +40	
	Functional range (°C)	+5 to +45	
	Storage temperature (°C)	-25 to +60	
	Power supply	230 V, 50 Hz	
	Exhaust component	Measurement range	Resolution
Measurement ranges, resolution	CO (% vol.)	0.000–10.00	0.001
	CO ₂ (% vol.)	0.00–18.00	0.01
	HC (ppm vol.)	0–9999	1
	NO _x (ppm vol.)	0–5000	≤ 1
Smoke opacity meter module	Degree of opacity (%)	0–100%	0.10
Oil temperature	Temperature (°C)	-20 to +150	0.16

The experiments were initiated with the engine fuelled with diesel. This was done to determine the baseline characteristics of the engine and exhaust emissions. The engine was run at full throttle position within a speed range of 1500–2400 rpm. The

engine speed was incremented at 100 rpm. The Dynomax-2000 system data controller software was used to monitor the conditions of the engine. The same procedure was repeated for each biodiesel-diesel fuel blend (*i.e.* B10, B20, B30, B40 and B50) and biodiesel-bioethanol-diesel fuel blend (*i.e.* B10BE5, B20BE8, B30BE10, B40BE13 and B50BE15) and the same operating conditions were used for each experiment. The experiment was carried out in triplicate for each biodiesel-diesel blend in order to examine the repeatability and reproducibility of the data and the average value for each investigated parameter was determined. During the experiment, the fuel volumetric flow rate was measured using a fuel gauge fitted to the equipment. The engine emissions and smoke opacity were detected by a smoke sensor placed at the engine exhaust pipe. The sensor was connected directly to the Bosch BEA 150 diesel emissions analyzer in order to record the data.

3.12 Corrosion testing

Corrosion testing performed by static immersion tests at 25–30 °C (ambient temperature) for 2000 h. Metal specimens (mild steel) placed hanging using Teflon thread separately on the overall fuel mixture are of biodiesel-diesel fuel blends and biodiesel-bioethanol-diesel fuel blends. The weight loss during corrosion tests was measured using an analytical balance with four decimal precision by calculating the difference in weight before and after testing. Furthermore, observations and measurements were performed every 400 hours of immersion, to see the effect of immersion time on the rate of corrosion.

3.13 Material for corrosion test

In this study, the specimens used were mild steel formed through the process of cutting and grinding, where the specimen dimension is a diameter of 20 mm and thickness of 2 mm. To anticipate changes in the material structure due to the effect of heat on the specimen formation, the cutting was done using a wire cut machine. On the

edge of the coupon specimen created a hole with a diameter of 2 mm which serves to hang the specimen during testing corrosion. Before the immersion, the specimen coupons through the preparation process by polishing the surface of the specimen using silicon carbide abrasive paper grading (grit 400 to 1500), and thereafter washed with acetone. Finally, the specimens were rinsed with deionized water. The composition of mild steel is shown in **Table 3.7**.

Tabel 3.7: Mild steel composition

%	C	Si	S	P	Mn	Ni	Cr	Mo	V	Cu
	0.2174	0.2792	0.0154	0.0090	1.1471	0.0170	0.0224	0.0071	0.0058	0.0472
%	Sn	Al	Ti	Zr	Zn	Ca	Co	Pb	B	Fe
	0.0024	0.0353	0.0018	0.0010	0.0033	0.0013	0.0035	0.0062	0.0005	98.1670

3.14 Corrosion analysis

The rates of corrosion of metal specimens were investigated based on data measurement results entered into the equation (3.5). Difference in weight obtained from measurements then converted into the corrosion rate (CR), where the corrosion rate (mm/y) is an abbreviation of mm per year, D is the density of metal (g/cm^3), W is the weight loss (g), T is the time of immersion (hours) and A is the cross sectional area of the specimen metal surface (cm^2). The procedures and equations used in this study according to the ASTM G31-72 method for Laboratory Immersion Corrosion Testing of Metals (ASTM, 2004).

$$CR = \frac{(8.76 \times 10^4 \times W)}{D \times A \times T} \text{ (mm/year)} \quad (3.5)$$

In addition, the metal specimen surface morphology changes observed using scanning electron microscope (SEM). Elemental analysis and composition of corrosion products was studied using energy dispersive x-ray (EDX). Changes in oil properties was also observed such as total acid number (TAN) analyser, viscosity, density and Fourier transform infrared spectroscopy (FTIR).

3.15 Summary

The research methodology describes the research steps conducted in this study. The research stages begin from selecting the raw materials to the analysis of corrosive behavior on the material. The research stages can be seen in the following summaries:

1. Selection of raw material composition from *J. curcas* and *C. pentandra* crude oil mixture based on the best properties of crude oil mixture.
2. The production process through esterification of acid catalyst (sulfuric acid) and alkaline-catalyst transesterification to obtain high methyl ester yields through transesterification optimization process for several parameters, namely methanol-to-oil ratio, agitation speed and catalyst concentration. The next step was properties test such as viscosity, density, calorific value, acid value, flash point, oxidation stability, cloud point, pour point, among others.
3. Next, biodiesel was mixed with diesel fuel in several mixes, namely B10, B20, B30, B40 and B50, and added bioethanol with some percentage of 5%, 8%, 10%, 13% and 15%. Engine performance testing and exhaust gas emissions used a single cylinder diesel engine at 1500 to 2400 rpm at full load. The parameters of the investigation were BSFC, BTE, engine torque, brake power, EGT, NO_x emission, CO, CO₂, and smoke opacity.
4. Material corrosion analysis referred to the standard ASTM G31-72. The mild steel metal was immersed in a mixed fuel up to 2000 hours at 25-30 °C temperature. The corrosion rate was calculated based on the weight lost during the immersion. The corrosion on the metal surface was then observed using SEM and EDX. The influence of corrosion on fuel properties in the investigation by testing TAN, viscosity, density and FTIR.

CHAPTER 4: RESULTS AND DISCUSSION

4.1 Introduction

This chapter contains a description of the results and discussions about the production of biodiesel from *Jathropa curcas*-*Ceiba pentandra* oil mixtures. Production stage involved the selection of the best mix percentages based on the properties and characteristics based on crude oil, followed by esterification, transesterification optimization. Furthermore, the properties and characteristics of biodiesel-diesel fuel and biodiesel-bioethanol-diesel fuel were observed and analyzed. Engine performance and exhaust emissions from biodiesel-diesel fuel and biodiesel-bioethanol-diesel fuel such as torque, brake thermal efficiency, brake power, brake specific fuel consumption, exhaust gas temperature, NO_x, CO₂, CO and smoke opacity were investigated and analyzed. In addition, the development of corrosion of the material that was immersed in biodiesel-diesel fuel and biodiesel-bioethanol-diesel blends was also observed and analyzed.

4.2 Physicochemical properties of crude oil mixtures

The physicochemical properties of *Jathropa*, *J. curcas* and *C. pentandra* crude oils as well as various crude oil mixtures are presented in **Table 4.1** (Atabani, Silitonga, et al., 2013; Jena et al., 2010; Rashid et al., 2014). Based on the properties shown in **Table 4.1**, it is found that the J50C50 oil mixture is suitable to be converted into biodiesel. These properties include the lower kinematic viscosity at 40 °C and acid value, with a value of 27.220 mm²/s and 15.82 mg KOH/g, respectively. In addition, the density at 15 °C of J50C50 mixture known also lower compared to other mixture that is 908.3 kg/m³. Changes in the physicochemical properties of oil mixture also can be seen from Jena et al. (2010) which mixes *Mahua* and *Simarouba* oil. It is known that the acid value increased significantly with the increase in the percentage of *Mahua* oil in the mixture from 8.50 to 19.37 mg KOH/g. The physicochemical properties such as

viscosity, density and calorific value are affected by structural fatty acid composition (Canakci et al., 2008; Pinzi et al., 2013). Viscosity is known as the fuel properties significantly affecting the flow characteristics and the atomization of liquid fuel (Ong, H. et al., 2013). The impurities are also known to affect the viscosity such as free glycerol, free fatty acids, glycerides, and temperature (Betiku et al., 2014).

University of Malaya

Table 4.1: Physicochemical properties of *Jatropha*, *Jatropha curcas* and *Ceiba pentandra* crude oils as well as various crude oil mixtures

Properties	Crude oils				Crude oil mixtures							
	<i>Jatropha curcas</i> ^a	<i>Jatropha</i> (Atabani, Silitonga, et al., 2013)	<i>Ceiba pentandra</i> ^a	<i>Ceiba pentandra</i> (Rashid et al., 2014)	J10C90 ^a	J20C80 ^a	J50C50 ^a	J80C20 ^a	J90C10 ^a	75M25S (Jena et al., 2010)	50M50S (Jena et al., 2010)	25M75S (Jena et al., 2010)
Kinematic viscosity at 40 °C (mm ² /s)	26.610	48.095	34.450	29.320	31.530	29.740	27.220	28.860	29.270	42.20	43.94	42.54
Acid value (mg KOH/g)	20.16	–	16.80	28.71	17.27	16.66	15.82	18.18	18.69	19.37	14.38	8.50
Density at 15 °C (kg/m ³)	913.9	905.4	905.2	921.0	909.8	909.5	908.3	910.1	910.6	913	912	912
Calorific value (MJ/kg)	38.593	38.961	38.254	–	38.026	38.167	38.226	38.571	38.693	36.27	36.04	36.31

^aResult

J_{xx}C_{yy}:

J = *J. curcas*

C = *C. pentandra*

xx = Weight percentage of *J. curcas*

yy = Weight percentage of *C. pentandra*

aa M_{bb}S = *Mahua* and *simarouba* mixture (1:1 wt.%)

aa = Weight percentage of *Mahua*

bb = Weight percentage of *Simarouba*

4.3 Biodiesel production and optimization

4.3.1 Properties of the J50C50 biodiesel

4.3.1.1 Fatty acid composition and Fourier transform infrared spectrum of the J50C50 biodiesel

The fatty acid composition of the J50C50 biodiesel is shown in **Table 4.2** (Khan et al., 2015; Martínez et al., 2014). It can be seen that the J50C50 biodiesel is mostly composed of oleic acid (36.2%), linoleic acid (34.3%) and palmitic acid (18.6%), which agrees well with the findings of previous studies (Martínez et al., 2014; Sarve et al., 2015). The total unsaturated fatty acid content of the J50C50 biodiesel is found to be 72.9%, which contributes to the improved cold flow properties. However, the total saturated fatty acid content of the J50C50 biodiesel is 24.2%, which contributes to the improved oxidation stability. The composition of fatty acids and natural antioxidants in biodiesel may affect oxidation stability and cold flow properties. This can be explained that the content of unsaturated fatty acids are sensitive to oxidative degradation, as well as unsaturated fatty compounds have lower melting points than saturated fatty compounds (Knothe, 2005; Schober et al., 2004). Park et al. (2008) reported that the oxidation stability of biodiesel blended from three different kinds of biodiesels, palm, rapeseed, and soybean biodiesels decreased total content of linoleic and linolenic acid increased, and cold flow properties decreased with increasing total levels of unsaturated fatty acids. Park also added that the high content of palmitic acid showed a high oxidative stability with a value of 11.5 hr, but has poor low temperature flow properties with the CFPP value of 5.5 °C.

Table 4.2: Comparison of the fatty acid composition of the J50C50 biodiesel with other biodiesels

Common name of fatty acid	Lipid number	Biodiesel (wt.%)			
		J50C50 ^a	NSME/CPME (Khan et al., 2015)	50R50S ^(Martínez et al., 2014)	50R50HO ^(Martínez et al., 2014)
Caprylic acid	C8:0	0.1	0.1	–	–
Capric acid	C10:0	0.1	0.1	–	–
Lauric acid	C12:0	0.1	0.1	–	–
Myristic acid	C14:0	0.1	0.1	–	–
Palmitic acid	C16:0	18.6	15.3	7.4	3.9
Palmitoleic acid	C16:1	0.5	0.3	–	–
Margaric acid	C17:0	0.1	0.1	–	–
Stearic acid	C18:0	4.5	3.1	–	–
Oleic acid	C18:1	36.2	23.2	46.5	76.7
Linoleic acid	C18:2	34.3	41.0	35.1	11.9
Linolenic acid	C18:3	0.8	1.6	6.82	3.81
Arachidic acid	C20:0	0.5	0.6	–	–
Paullinic acid	C20:1	0.6	0.8	–	–
Erucic acid	C22:1	0.5	4.5	–	–
Lignoceric acid	C24:0	0.1	0.3	–	–
Saturated		24.2	19.8	7.4	3.9
Unsaturated		72.9	71.4	88.4	92.4
Total		97.1	91.2	95.8	96.3

^aResult

J_{xx}C_{yy}:

J = *J. curcas*

C = *C. pentandra*

xx = Weight percentage of *J. curcas*

yy = Weight percentage of *C. pentandra*

NSME/CPME = *N. sativa* and *C. pentandra* biodiesel

50R50S = Rapeseed and sunflower biodiesel (50:50 wt.%)

50R50HO = Rapeseed and high oleic sunflower biodiesel (50:50 wt.%)

The Fourier transform infrared spectrum of the J50C50 biodiesel is shown in **Figure 4.1**. The wavenumber, functional group, band assignment and absorption intensity of the absorption peaks detected in the Fourier transform infrared spectrum of the J50C50 biodiesel are presented in **Table 4.3**. The results prove that the J50C50 biodiesel is composed of long-chain fatty acid esters. Spectra of products transesterification process is chemically similar to precursors (refined oil), the peak of stretching C=O is 1742 cm⁻¹ located in the region of 1800–1700 cm⁻¹ is typical of esters, the spectrum is commonly encountered in FAME and refined oil (Soares et al.,

2008). In the range of 1500–900 cm^{-1} is a major region of the spectrum from biodiesel J50C50 known as the "fingerprint" which has a peak at 1245 cm^{-1} corresponds to the bending vibration $-\text{CH}_3$ (Rabelo et al., 2015).

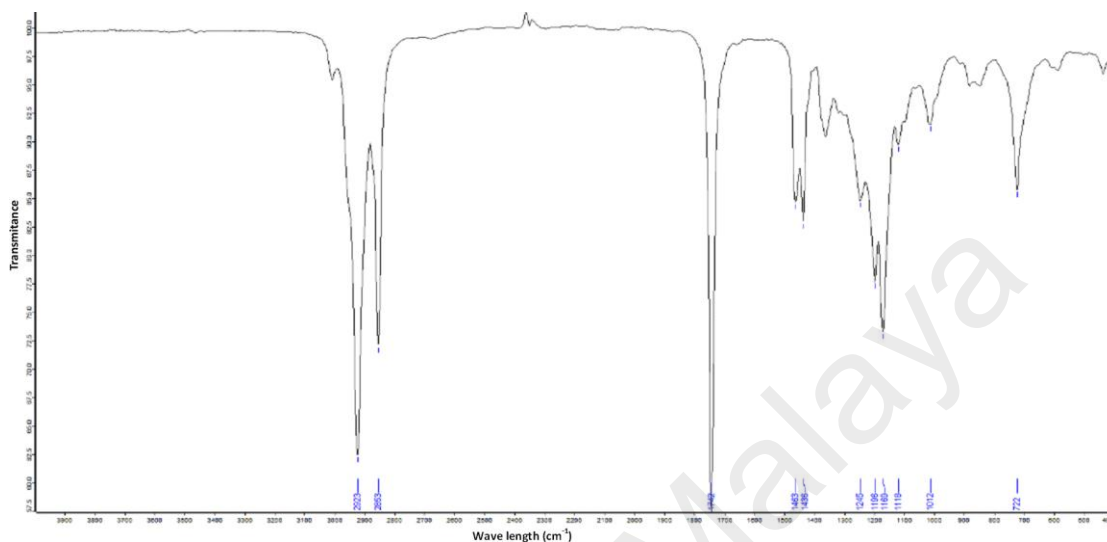


Figure 4.1: Fourier transform infrared spectrum of the J50C50 biodiesel

Table 4.3: Wavenumber, functional group, band assignment and absorption intensity of the absorption peaks detected in the Fourier transform infrared spectrum of the J50C50 biodiesel

Wavenumber (cm^{-1})	Group attribution	Vibration type	Absorption intensity
2923	$=\text{C}-\text{H}$	Asymmetric stretching vibration	Strong
2853	$-\text{CH}_2$	Symmetric stretching vibration	Strong
1742	$-\text{C}=\text{O}$	Stretching	Strong
1463	$-\text{CH}_2$	Shear-type vibration	Weak
1245	$-\text{CH}_3$	Bending vibration	Weak
1196	$\text{C}-\text{O}-\text{C}$	Anti-symmetric stretching vibration	Middling
1169	$\text{C}-\text{O}-\text{C}$	Anti-symmetric stretching vibration	Middling
1118	$\text{C}-\text{O}-\text{C}$	Anti-symmetric stretching vibration	Weak
1012	$\text{C}-\text{O}-\text{C}$	Anti-symmetric stretching vibration	Weak
722	$-\text{CH}_2$	Plane rocking vibration	Weak

4.3.1.2 Physicochemical properties of *J. curcas*, *C. pentandra* and J50C50 biodiesels

The physicochemical properties of the J50C50 biodiesel before optimization are compared with those for *J. curcas* and *C. pentandra* biodiesels, as well as biodiesels produced in other studies, and the values are tabulated in **Table 4.4**. The properties were determined according to the procedures outlined in the ASTM D6751 and EN14214 standards. The kinematic viscosity at 40 °C of the J50C50, *J. curcas* and *C. pentandra* biodiesel is found to be 4.29, 4.57 and 4.74 mm²/s, respectively, which is within the range specified in the ASTM D6751 and EN 14214 standards (1.9–6.0 mm²/s and 3.5–5.0 mm²/s, respectively). Kinematic viscosity of J50C50 lower than the pure biodiesel, it can be associated to a diminution in polymeric oxidation because of the increased saturated compounds quantity presents in the mixture (Gonçalves et al., 2012). It shall be noted here that a high kinematic viscosity is undesirable because it decreases the fluidity of the fuel, it slows down fuel injection and delays the mixing of air with fuel in the combustion chamber (Agarwal, Dhar, et al., 2015; Ashraful et al., 2014). Poor fuel atomization which causes poor cold engine start-up and ignition delay (Schober et al., 2004). In contrast, the kinematic viscosity at 40 °C for diesel is 2.96 mm²/s, which indicates that diesel has higher fluidity compared to the J50C50 biodiesel.

The density at 15 °C of the J50C50, *J. curcas* and *C. pentandra* biodiesel is found to be 866.9, 876.2 and 885.7 kg/m³, respectively, which is dependent on the fatty acid composition and purity of the biodiesel (Martínez et al., 2014). Ramírez-Verduzco et al. (2012) states that the density of fatty acids is inversely proportional to its number of carbon atoms, an increasing number of carbon resulting in reduced density to a certain extent.. The density of these biodiesels falls within the range given in the ASTM D6751 and EN14214 standards (*i.e.* 880 and 860–900 kg/m³, respectively). In contrast, diesel has a lower density at 15 °C, with a value of 846.1 kg/m³. Increased density of biodiesel causes increased viscosity, which can affect the operation of the fuel injection system

due to the delivery of a slightly greater mass of fuel in the volume metering equipment (Demirbas, 2008). The acid value of the J50C50, *J. curcas* and *C. pentandra* biodiesel is 0.04, 0.04 and 0.05 mg KOH/g, respectively. In general, a high acid value is undesirable since it can result in severe corrosion of the fuel supply system and internal combustion engine resulting from degradation of the fuel in service. Lowering the acid value can be done through a two-step pre-treatment process of esterification, wherein the amount of methanol-to-oil ratio has a very significant role (Ghadge et al., 2005). Hence, the J50C50 biodiesel is desirable since it has the lowest acid value. However, the acid value of diesel is lower compared to these biodiesels, having a value of 0.01 mg KOH/g.

The calorific value of the J50C50, *J. curcas* and *C. pentandra* biodiesel is found to be 40.21, 39.46 and 39.46 MJ/kg, respectively. Hence, the J50C50 biodiesel has a calorific value which is slightly higher than the calorific value of biodiesels derived from individual *J. curcas* and *C. pentandra* oils. Ramírez-Verduzco et al. (2012) revealed that the calorific value increased due to the increase in molecular weight decreased due to the number of double bonds increases. In general, a high calorific value is desirable since it is indicative of the energy content of the fuel. For this reason, the J50C50 biodiesel is more favourable compared to the *J. curcas* and *C. pentandra* biodiesels. However, diesel is still superior to these biodiesels in this regard, having a calorific value of 45.361 MJ/kg.

The oxidation stability at 110 °C of the J50C50, *J. curcas* and *C. pentandra* biodiesel is found to be 6.23, 14.01 and 1.76 hours, respectively. Hence, the J50C50 biodiesel has an oxidation stability which is a compromise between the *J. curcas* and *C. pentandra* biodiesels. However, the oxidation stability at 110 °C of the J50C50 biodiesel is still far from that for diesel which has an oxidation stability of 15.2 hours. Dunn (2005) also revealed that oxidation stability for biodiesel was lower compared to diesel fuel. In general, the oxidation stability is dependent on the composition of fatty

acids and natural antioxidants in the oil. It has been shown in a previous study that biodiesels with high palmitic acid content have high oxidation stability (Park et al., 2008). Based on the results shown in **Table 4.4**, it can be deduced that there is a need to improve the physicochemical properties of the J50C50 biodiesel and this can be achieved by optimizing the operating parameters of the transesterification process (Khan et al., 2015; Kumar, T. S. et al., 2015; Martínez et al., 2014; Mofijur, Masjuki, Kalam, and Atabani, 2013).

University of Malaya

Table 4.4: Comparison of the physicochemical properties of J50C50 biodiesel before optimization with diesel and other biodiesels

Property	Unit	Diesel ^a	ASTM D6751	EN 14214	Biodiesel from single feedstock				Biodiesel from multiple feedstocks		
					J. curcas ^a	JBD ^(Mofijur, Masjuki, Kalam, and Atabani, 2013)	C. pentandra ^a	Kapok ^(Kumar, T. S. et al., 2015)	J50C 50 ^a	NSME/CPME ^(Khan et al., 2015)	50R50S ^(Martínez et al., 2014)
Kinematic viscosity at 40 °C	mm ² /s	2.96	1.9–6.0	3.5–5.0	4.57	4.72	4.74	4.2	4.29	4.44	4.26
Density at 15 °C	kg/m ³	846.1	880	860–900	876.2	864.8	885.7	860.0	866.9	884.8	–
Flash point	°C	75.5	100–170 min	>120	125.5	182.5	120.5	148.0	120.5	186.5	164.0
Pour point	°C	3.0	-15 to -16	–	3.0	3.0	4.0	4.0	1.5	-1.0	–
Cloud point	°C	2.0	-3 to -12	–	2.0	3.0	4.0	-4.4	0.5	0.0	–
Cold filter plugging point	°C	0.0	-25	–	1.0	–	1.0	–	-1.2	-1.0	-5.0
Calorific value	MJ/kg	45.361	–	35	39.46	40.53	39.46	39.40	40.21	39.94	40.00
Acid value	mg KOH/g	0.017	0.05 max	0.05 max	0.04	0.05	0.05	–	0.04	0.14	0.19
Copper strip corrosion	–	1a	3 max	–	1a	–	1a	–	1a	–	–
Oxidation stability at 110 °C	Hour	15.2	3 min	6 min	14.01	3.02	1.76	–	6.23	3.27	–
FAME content	% m/m	–	–	96.5 max	98.8	–	97.3	–	98.5	–	–
Cetane index	–	49.6	47 min	51 min	59.0	51.0	56.0	51.0	56.0	–	46.3

^aResult

J_{xx}C_{yy}:

J = *J. curcas*

C = *C. pentandra*

xx = Weight percentage of *J. curcas*

yy = Weight percentage of *C. pentandra*

JBD = *Jatropha* biodiesel

NSME/CPME = *C. pentandra* and *N. sativa* biodiesel

50R50S = Rapeseed and sunflower biodiesel (50:50 wt.%)

The physicochemical properties of the J50C50 biodiesel after optimization are summarized in **Table 4.5**. It shall be noted that these are the properties of the J50C50 biodiesel produced from transesterification of *J. curcas*–*C. pentandra* crude oil mixture at a temperature of 60 °C over a period of 2 hours using the optimum operating parameters (methanol-to-oil ratio: 30%, agitation speed: 1300 rpm and KOH catalyst concentration: 0.5 wt.%) The biodiesel yield obtained from the optimum transesterification process is 93.33%.

Based on the results shown in **Table 4.5**, it is evident that there is a marked improvement in the physicochemical properties of the J50C50 biodiesel after optimization. For instance, the kinematic viscosity at 40 °C, which is 4.29 mm²/s and decreases to 3.95 mm²/s after optimization, indicating that the fluidity of the biodiesel is improved. Similarly, the density at 15 °C decreases from 866.9 to 831.2 kg/m³ after optimization. In contrast, the oxidation stability, which is initially 6.23 hours, increases significantly to 10.01 hours after optimization. However, the calorific value only shows a slight improvement from 40.21 to 40.92 MJ/kg. The acid value of the J50C50 biodiesel, which is initially 0.042 mg KOH/g (close to the maximum acid value of 0.050 mg KOH/g specified in the ASTM D6751 and EN 14214 standards) decreases further to 0.02 mg KOH/g after optimization. The flash point (*i.e.* the temperature at which the fuel ignites upon exposure to spark or flame) increases significantly from 120.5 to 196 °C after optimization. The increase in flash point of the J50C50 biodiesel is desirable since the fuel is less flammable compared to diesel which has a flash point of 75.5 °C. This makes storage and handling of the J50C50 biodiesel safer compared to diesel due to the reduced risk of fire hazards. The fatty acid methyl ester content of the J50C50 biodiesel is found to increase slightly from 98.5 to 99.1 %m/m after optimization. Overall, it can be deduced that optimization of the transesterification process parameters enhances the physicochemical properties of the J50C50 biodiesel and these properties

fulfil the specifications given in the ASTM D6751 and EN 14214 standards for biodiesel.

Table 4.5: Physicochemical properties of the J50C50 biodiesel after optimization

Property	Unit	J. <i>curcas</i> ^a	C. <i>pentandra</i> ^a	J50C50 before optimization	J50C50 after optimization
Kinematic viscosity at 40 °C	mm ² /s	4.57	4.74	4.29	3.950
Density at 15 °C	kg/m ³	876.2	885.7	866.9	831.2
Flash point	°C	125.5	120.5	120.5	196
Pour point	°C	3.0	4.0	1.5	0.5
Cloud point	°C	2.0	4.0	0.5	0.5
Cold filter plugging point	°C	1.0	1.0	-1.2	-2.0
Calorific value	MJ/kg	39.46	39.46	40.21	40.929
Acid value	mg KOH/g	0.04	0.05	0.04	0.025
Copper corrosion strip	–	1a	1a	1a	1a
Oxidation stability at 110 °C	hour	14.01	1.76	6.23	10.01
FAME content	% m/m	98.8	97.3	98.5	99.1
Cetane index	–	59.0	56.0	56.0	58

4.3.2 Optimization of the J50C50 biodiesel yield using response surface methodology

Optimizations of transesterification process based on some parameters have great influence on the result and the biodiesel production process. Some of the parameters used are methanol-to-oil ratio, agitation speed and catalyst concentration. The optimization of experimental design is presented in **Table 4.6**, which consists of 17 experimental runs.

Table 4.6: Experimental design for optimization of the transesterification process parameters for the *J. curcas*-*C. pentandra* oil mixture

Experimental run no.	A Methanol-to-oil ratio (%)	B Agitation speed (rpm)	C Catalyst concentration (%)	Experimental biodiesel yield (wt.%)	Predicted biodiesel yield (wt.%)
1	70	1300	2.00	81.27	81.09
2	50	1300	1.25	92.10	92.06
3	30	1300	0.50	93.30	93.47
4	70	1300	0.50	93.07	92.67
5	70	1800	1.25	90.84	91.37
6	50	1300	1.25	92.01	92.06
7	30	1300	2.00	81.36	81.75
8	50	1300	1.25	91.96	92.06
9	50	1800	2.00	82.51	82.15
10	30	800	1.25	91.19	90.66
11	50	1800	0.50	92.92	92.79
12	50	800	0.50	92.01	92.36
13	50	1300	1.25	91.75	92.06
14	70	800	1.25	89.29	89.33
15	50	800	2.00	79.59	79.71
16	30	1800	1.25	91.54	91.49
17	50	1300	1.25	92.88	92.06

4.3.2.1 Quadratic regression model

The quadratic regression model of the biodiesel yield using Box-Behnken experimental design is based on the uncoded levels of the independent variables. In this case, the yield of the J50C50 biodiesel is given by:

$$\begin{aligned}
 BY_{JCCP} = & 84.00644 + 0.046810A + 0.00782695B + 9.87764C + \\
 & 0.0000302021AB + 0.00237341AC + 0.00133810BC - 0.00107247A^2 - \\
 & 0.00000368210B^2 - 7.79899C^2
 \end{aligned} \tag{4.1}$$

In Eq. 4.1, BY_{JCCP} represents the biodiesel yield, A represents the methanol-to-oil ratio, B represents the agitation speed and C represents the catalyst concentration in weight percent (wt.%).

Analysis of variance (ANOVA) is carried out to determine the significance and fitness of the quadratic regression model as well as the effects of significant individual terms and their interaction on the selected responses. The ANOVA results are tabulated

in **Table 4.7**. The quadratic regression model has an F -value of 184.74 and a p -value less than 0.0001, which indicates that the model is significant at the 95% confidence level. It shall be noted here that the p -value represents the probability of error, and it is used to check the significance of each regression coefficient. The p -value is also indicative of the interaction effect of each cross product. Hence, a p -value of 0.0001 indicates that the probability of getting a large F -value due to noise is only 0.01%. ‘Prob > F ’ values less than 0.0500 indicate that the model terms are significant and therefore, the model terms B , C , B^2 and C^2 are significant. In contrast, ‘Prob > F ’ values greater than 0.1000 indicates that the model terms are not significant (Badday et al., 2013). Therefore, even though A that has a value above 0.0500, indicating that it has an effect the J50C50 biodiesel yield, the magnitude of the change caused by A is insignificant. In general, if there is large number of insignificant model terms (excluding the model terms needed to support hierarchy), model reduction by reducing the ranges of parameters may improve the model.

The lack of fit is also determined for the quadratic regression model. In general, if the quadratic regression model shows a lack of fit, this indicates that the model does not sufficiently describe the relationship between the independent variables (*i.e.* methanol-to-oil ratio, agitation speed and catalyst concentration) and the dependent variable (*i.e.* J50C50 biodiesel yield). If the model shows a lack of fit, this may be due to the exclusion of several important terms from the model or the presence of unusually large residuals arising from fitting the model. In this study, it is found that the F -value and p -value of the lack of fit parameter is 5.25 and 0.0715, respectively. The p -value of the lack of fit parameter is greater than 0.05, indicating that there is good fit between the quadratic regression model and experimental data.

Table 4.7: Results obtained from analysis of variance

Source	Sum of squares	Degrees of freedom	Mean square	F-Value	p-value (Prob > F)	Remarks
Model	366.51	9	40.72	184.74	< 0.0001	Significant
<i>A-methanol</i>	1.06	1	1.06	4.81	0.0643	
<i>B-speed</i>	4.13	1	4.13	18.72	0.0035	
<i>C-catalyst</i>	271.09	1	271.09	1229.81	< 0.0001	
<i>AB</i>	0.36	1	0.36	1.66	0.2392	
<i>AC</i>	5.070E-003	1	5.070E-003	0.023	0.8837	
<i>BC</i>	1.01	1	1.01	4.57	0.0699	
<i>A²</i>	0.77	1	0.77	3.52	0.1029	
<i>B²</i>	3.57	1	3.57	16.19	0.0050	
<i>C²</i>	81.03	1	81.03	367.60	< 0.0001	
Residual	1.54	7	0.22			
<i>Lack of fit</i>	1.23	3	0.41	5.25	0.071	Insignificant
<i>Pure error</i>	0.31	4	0.07			
Cor total	368.05	16				
R-squared	0.9958		AdjR-squared ^a	0.99		
Mean	89.37		PredR-squared ^b	0.94		
C.V. %. ^c	0.53		AdeqPrecision ^d	38.195		

^a Adjusted R²

^b Predicted R²

^c Coefficient of variation

^d Adequate precision

The coefficient of determination (R^2) reflects the variability of the dependent variable which is explained by its relationship with the independent variables (predictor variables). In general, a high R^2 value indicates that the model accounts for higher variability of the data and thus, the data points will lie closer to the regression line. In other words, a high R^2 value indicates that there is good fit between the model and experimental data. Based on the results shown in **Table 4.7**, it can be seen that the R^2 value is 0.99, which indicates that 99.58% of the variability in the J50C50 biodiesel yield is explained by the quadratic regression model.

However, it shall be noted that the R^2 value can increase with an increase in the number of predictor variables in the model and therefore, one should interpret with the value with caution. The adjusted coefficient of determination (adjusted R^2) is used to

compensate for this undesirable effect, since it does not only indicate how well the model fits with the experimental data but also accounts for the number of predictor variables. The adjusted R^2 will increase if useful predictor variables are added into the model and likewise, the adjusted R^2 will decrease upon the addition of useless predictor variables. In this study, the adjusted R^2 is found to be 0.99, as shown in **Table 4.7**, which indicates that the model accounts for 99.04% of the variability in the J50C50 biodiesel yield.

The experimental and predicted values of the J50C50 biodiesel yield are plotted in **Figure 4.2**. It is found that the differences between the experimental and predicted values are less than 0.2, indicating that there is good agreement between the model and experimental data. This finding conforms to the R^2 and adjusted R^2 obtained previously having a value close to unity. Hence, the regression model gives a good estimate of the response of the system (*i.e.* J50C50 biodiesel yield) with changes in the methanol-to-oil ratio, agitation speed and catalyst concentration.

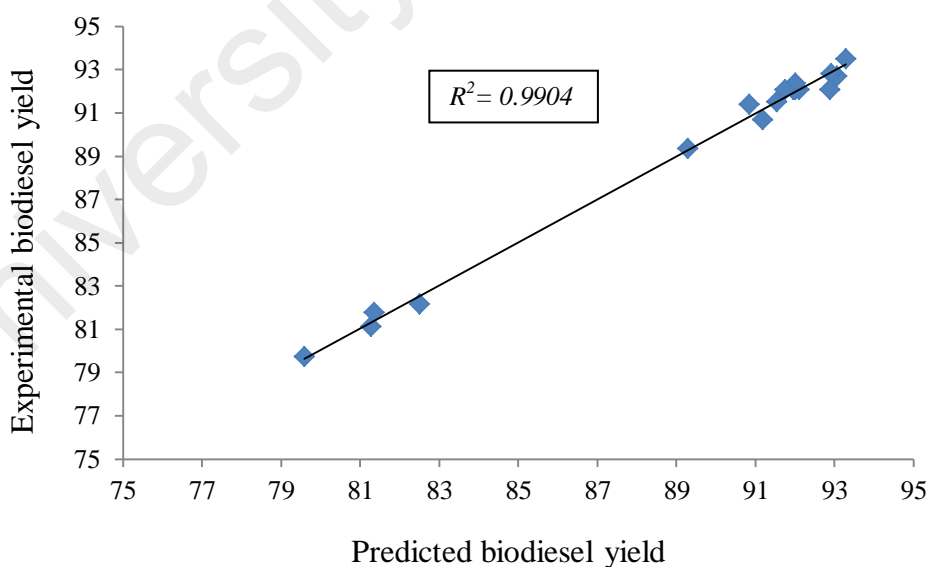


Figure 4.2: Plot of the experimental versus predicted J50C50 biodiesel yield

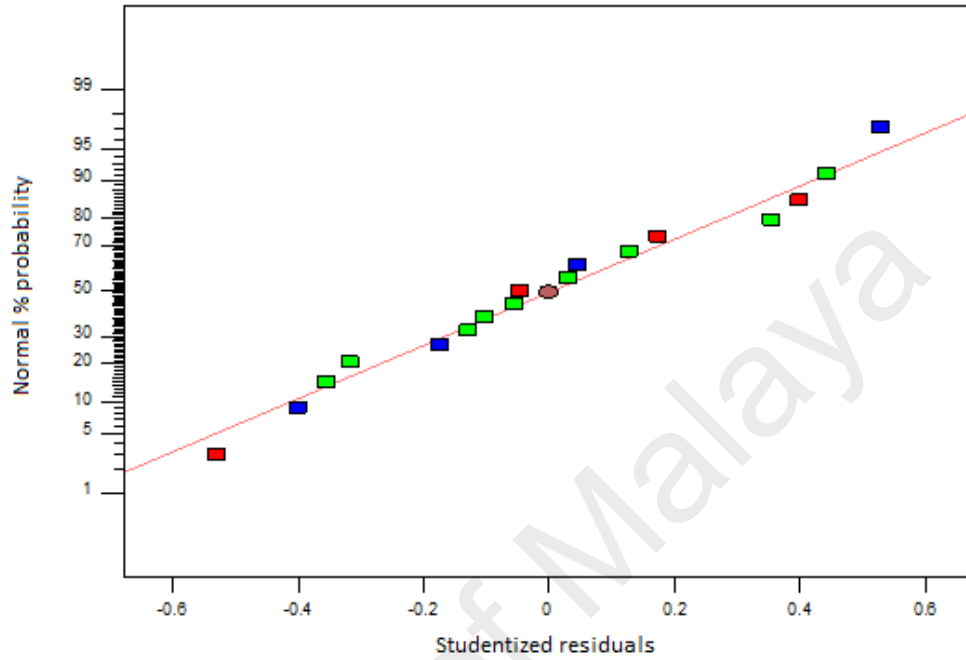
The signal-to-noise ratio is measured by the statistical parameter called 'adequate precision'. In general, an adequate precision greater than 4 is desirable. In this

study, the adequate precision is found to be 38.19, as shown in **Table 4.7**, indicating that the signal is adequate and the quadratic regression model can be used to navigate the design space. In addition, the coefficient of variation (*C.V.*) is found to be low with a value of 0.53%, which indicates that the experimental data are accurate and reliable (Shanmugaprakash et al., 2013).

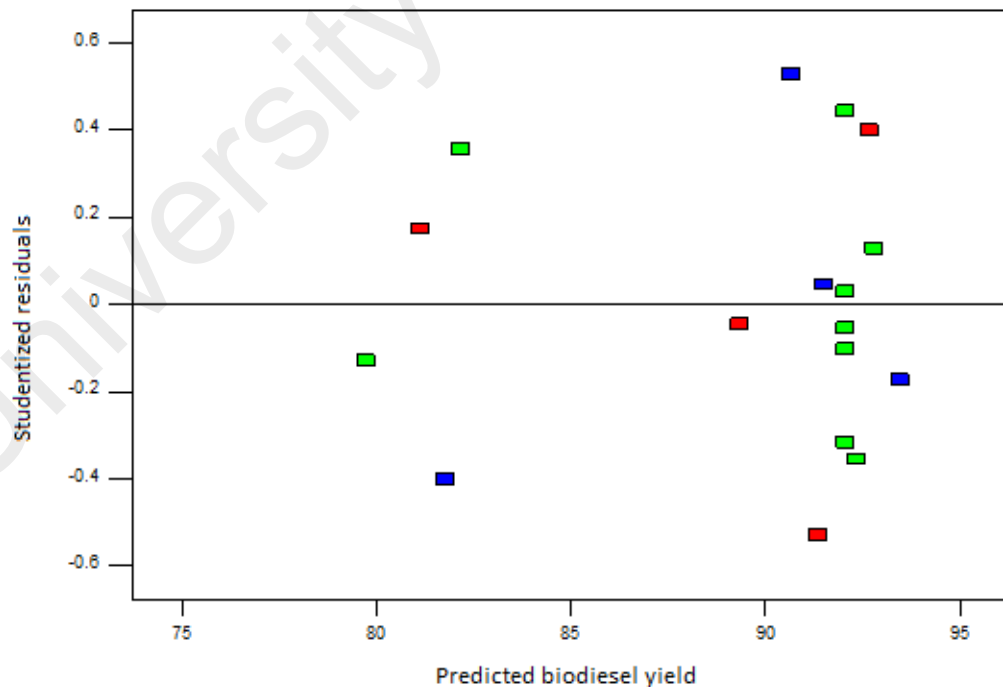
Residual is defined as the deviation between the experimental and predicted value. Hence, there is a residual for each observation in the data set. If the experimental errors are random, then it is expected that the residuals will follow a normal distribution. It is first necessary to analyse the adequacy of the quadratic regression model in order to determine whether the residuals follow a normal distribution. Hence, the residuals were normalized and divided with an estimate of their standard deviations, resulting in studentized residuals. The studentized residuals were then fitted with a normal distribution function.

Following this, the studentized residuals were predicted by the best-fit normal distribution and plotted against the studentized residuals obtained from experiments, as shown in **Figure 4.3**. It can be seen that the studentized residuals follow a normal distribution, as evidenced from the straight line in **Figure 4.3 (a)**. The studentized residuals were plotted against the predicted J50C50 biodiesel yield, as shown in **Figure 4.3 (b)**. It can be observed from **Figure 4.3 (b)** that the data points are scattered randomly in the plot, which indicates that the values of the original observations are not related to the values of the response. Hence, it can be deduced that the quadratic regression model gives an adequate description of the biodiesel production process. The outlier *t* plot for all experimental runs in the J50C50 biodiesel production is plotted in **Figure 4.3 (c)**, which indicates the value of the residual for each experimental run. One can determine which experimental run has a large residual based on this plot. It shall be noted the outlier *t* indicates the extent to which the experimental values deviate from the

predicted values. It can be observed from Figure 4.3.(c) that the entire studentized residuals lie well within the ± 3.00 interval, indicating that there is good approximation of the fitted model to the response surface.

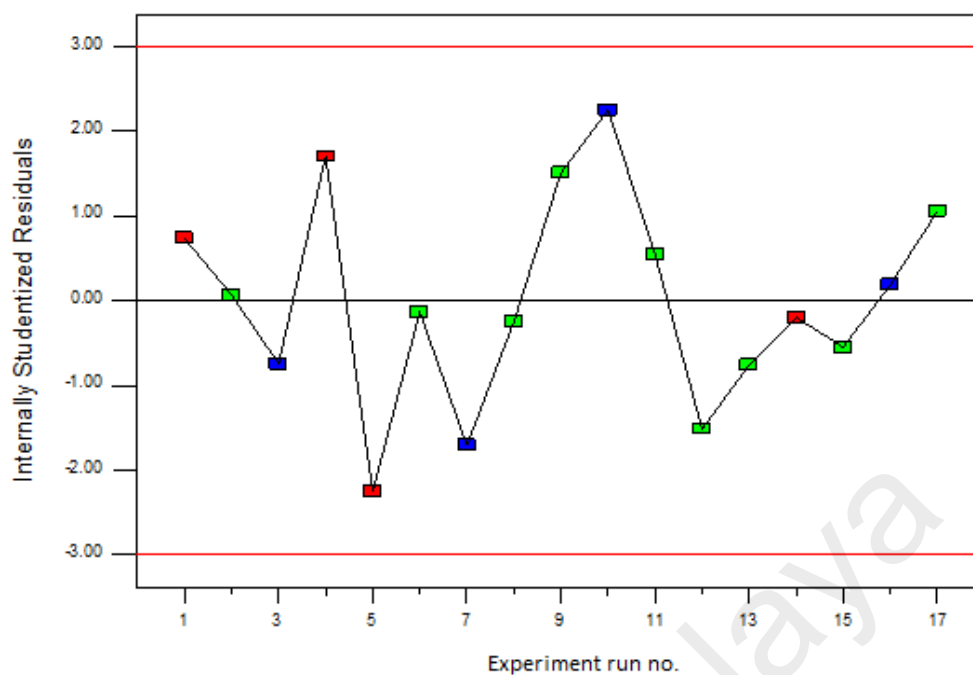


(a)



(b)

Figure 4.3: Residual plots: (a) normal probability plot of studentized residuals, (b) plot of the studentized residuals versus the predicted biodiesel yield and (c) outlier t plot



(c)

Figure 4.3: Continued

4.3.2.2 Effect of methanol-to-oil ratio

In this study, the methanol-to-oil ratio is varied at 30, 50 and 70% in order to examine the effect of methanol-to-oil ratio on the J50C50 biodiesel yield. **Figure 4.4 (a)** shows the three-dimensional surface plot of the combined effects of the methanol-to-oil ratio and catalyst concentration on the J50C50 biodiesel yield. In general, it can be observed that for a fixed catalyst concentration, increasing the methanol-to-oil ratio has an insignificant effect on the J50C50 biodiesel yield. Increasing the amount of methanol increases the time taken to extract excess methanol from the biodiesel after the transesterification process, which is attributed to the fact that methanol has one polar hydroxyl group, which works as an emulsifier and thus, improves the emulsion. The addition of methanol-to-oil ratio reduced the percentage of methyl ester yield, this behaviour indicates that the separation of glycerine and methyl esters become more difficult due to the formation emulsion (Hamze et al., 2015). This fact shows that an excessive amount of alcohol in the transesterification process will lead to increased

product, while the other side of excess methanol will help increase the solubility of glycerol resulting in lower yields (Fan et al., 2011; Kafuku et al., 2010).

4.3.2.3 Effect of agitation speed

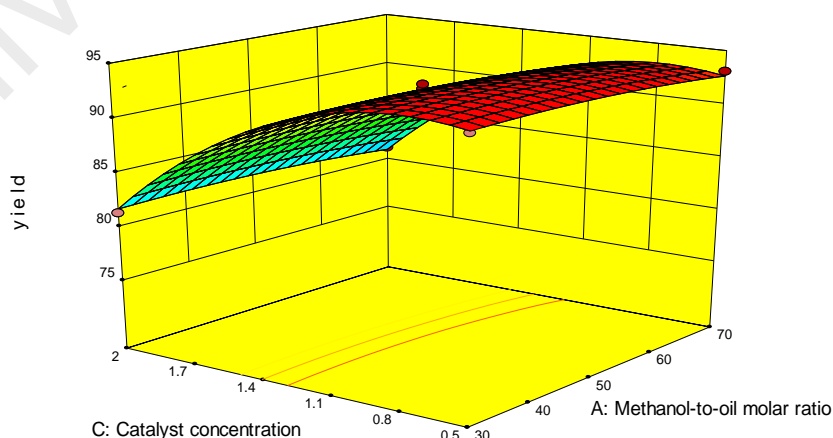
Figure 4.4 (b) shows the three-dimensional surface plot of the combined effects of the agitation speed on the J50C50 biodiesel yield, in which the agitation speed is varied at 800, 1300 and 1800 rpm. It can be seen from **Figure 4.4 (b)** that the agitation speed has an effect on the biodiesel yield, whereby the J50C50 biodiesel yield slightly increases with an increase in the agitation speed. Agitation speed (otherwise known as the mixing intensity) is known to be an important factor since it affects the homogeneity of the oil mixture once the catalyst is added into the oil for the transesterification process. Increasing the agitation speed and hence, mixing intensity, facilitates the initiation of the reaction and increases the contact area between the oil, methanol and KOH solution. In the absence of mixing, the reaction occurs only at the interface of the two layers, and this will significantly slow down the rate of reaction during the transesterification process. A number of researchers have also found that an increase in agitation speed during the transesterification process promotes the homogenization of reactants, which leads to high biodiesel yields (Meher et al., 2006; Rashid et al., 2008).

4.3.2.4 Effect of catalyst concentration

Figure 4.4 (c) shows the three-dimensional surface plot of the combined effects of catalyst concentration and agitation speed on the J50C50 biodiesel yield, in which the catalyst concentration is varied at 0.50, 1.25 and 2.00 wt.%. It is evident from **Figure 4.4 (c)** that for a fixed agitation speed, increasing the catalyst concentration decreases the J50C50 biodiesel yield. Indeed, it can be observed that the biodiesel yield decreases with an increase in catalyst concentration up to 2.00 wt.%.

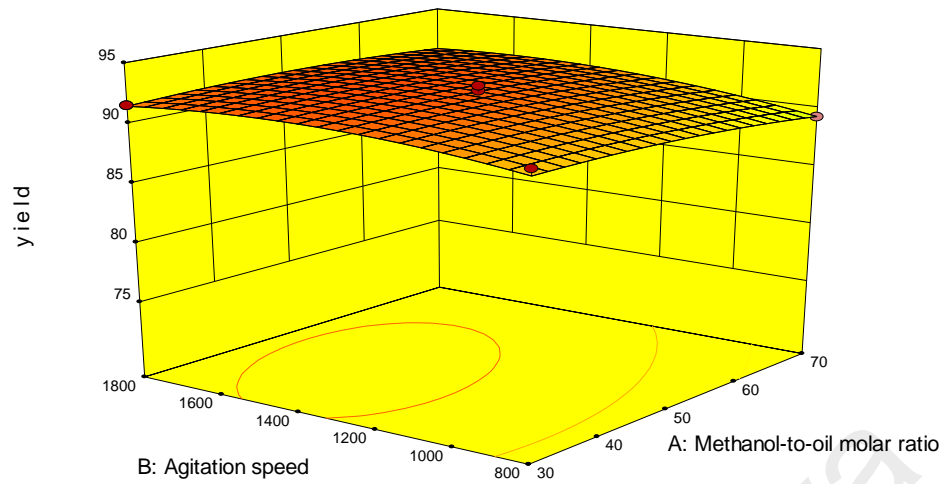
Based on the results, the biodiesel yield is within a range of 79.59–82.51 for a catalyst concentration of 2.00 wt.%. In contrast, the biodiesel yield increases with a decrease in catalyst concentration, whereby the value is within a range of 92.01–93.30 wt.%. More importantly, the biodiesel yield is highest with a value of 93.30% for the following operating parameters: methanol-to-oil ratio: 30%, catalyst concentration: 0.5% and agitation speed: 1300 rpm. This indicates that these are the optimum operating parameters for the transesterification process of the J50C50 oil mixture.

In general, the decrease in the biodiesel yield with an increase in the KOH catalyst concentration is due to the formation of soap with excessive amounts of catalyst (Leung et al., 2006). According to Zhang et al. (2003), alkali-catalysed transesterification is very sensitive to water, whereby the presence of water may cause ester saponification in alkaline conditions. In addition, excessive amounts of catalyst can lead to the formation of emulsion, which increases the viscosity of the biodiesel and induce the formation of gels (Patil et al., 2009). As it is known that KOH is the most appropriate catalyst in use in the transesterification process, the use of a catalyst limited to refined vegetable oil with less than 0.5 wt.% FFA or acid value less than 1 mg KOH/g (Betiku et al., 2015; Maran et al., 2015).

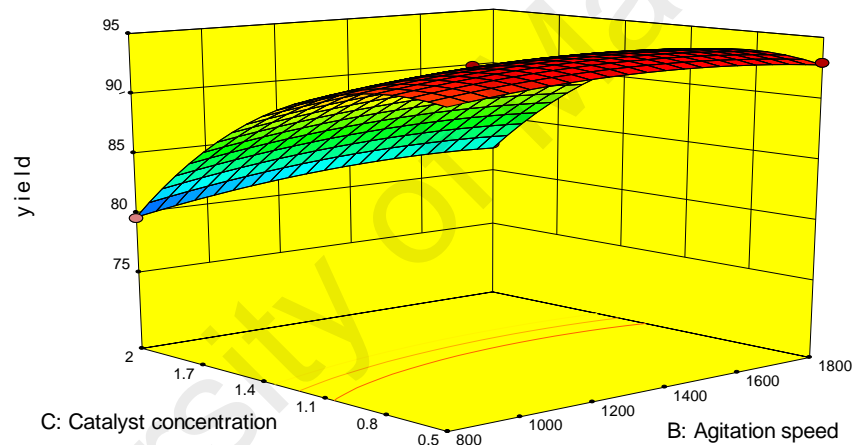


(a)

Figure 4.4: Three-dimensional surface plot which shows the combined effects of: (a) methanol-to-oil ratio and catalyst concentration, (b) agitation speed and methanol-to-oil ratio, and (c) catalyst concentration and agitation speed on the J50C50 biodiesel yield.



(b)



(c)

Figure 4.4: Continued

4.3.3 Summary

In this experiment, biodiesel production was through acid esterification and alkali-catalysed transesterification for *J.curcas*-*C. pentandra* crude oil mixtures. Some of the main findings of this test series are:

- 1 Based on properties test, J50C50 crude oil mixtures have the best properties among other crude oil mixtures, such as lower viscosity, density and acid value.

- 2 Biodiesel production conducted through transesterification optimization using response surface methodology obtained maximum parameters at constant temperature of 60 °C for 2 hours, namely: methanol-to-oil ratio: 30%, agitation speed: 1300 rpm and catalyst concentration: 0.5 wt.%. In this condition, the maximum biodiesel yield was 93.33%.
- 3 In the transesterification optimization, it appears that biodiesel yields were heavily influenced by catalyst concentration compared to other parameters such as methanol-to-oil ratio and agitation speed.
- 4 Biodiesel properties generated from the optimization process are better than without optimization, such as decreasing viscosity and density values, and increasing oxidation stability.

4.4 Engine performance and exhaust emission

4.4.1 Biodiesel-diesel and biodiesel-bioethanol-diesel fuel blending

The physicochemical properties of the crude oil, biodiesel, biodiesel-diesel fuel blends and biodiesel-bioethanol-diesel fuel blends are presented in **Table 4.8**. It is known that the kinematic viscosity measured at 40 °C and the density measured at 15 °C of the crude J50C50 oil are 27.22 mm²/s and 908.30 kg/m³, respectively. The crude J50C50 oil has a high acid value and lower calorific value, where it shows that the importance of two-step biodiesel production (acid-catalysed esterification, followed by alkaline-catalysed transesterification). This process results in a striking change in the properties of the crude J50C50 oil when it is converted into J50C50 biodiesel. The kinematic viscosity decreased up to 85%, whereas the acid value and density decreases reached 98.4% and 8.4%, respectively. In contrast, the calorific value increases of more than 5%. The J50C50 biodiesel was produced in accordance with the ASTM D6751 and EN 14214 standard test methods.

The physicochemical properties of the J50C50 biodiesel-diesel blends are also presented in **Table 4.8**. It is noticeable that the addition of the J50C50 biodiesel into diesel fuel at different ratios (10, 20, 30, 40 and 50 % vol.) alters the physicochemical properties. There is a linear change in the viscosity and density of the biodiesel-diesel fuel blends and these properties are directly proportional to the percentage of biodiesel in the blend. The flash point also shows a similar increasing trend – however, the addition of 40% of biodiesel decreases the flash point. It shall be noted though, that the flash point increases upon the addition of 50% of biodiesel into the blend. In contrast, with an increase of the percentage of biodiesel blend, it is observed with decrease in the calorific value and pour point.

Srithar et al. (2014) also observed a change in the physicochemical properties of biodiesel-diesel blends with a change in the content of biodiesel in the blend. The biodiesels were produced from mixed feedstocks (*Pongamia pinnata* and mustard oils). They discovered that a low content of biodiesel in the blend (blend A: 90% diesel, 5% PPEE and 5% MEE) has higher calorific value (~ 44 MJ/kg) and low kinematic viscosity (4.2 mm²/s), which are close to the properties of diesel fuel. Sanjid et al. (2016) also obtained similar results for biodiesels produced from a mixture of kapok and *Moringa* oils. They found that the blend composed of 5% kapok biodiesel and 5% *Moringa* biodiesel (KB5M5) has lower kinematic viscosity and density (but higher gross calorific value) compared with the blend composed of 10% kapok biodiesel and 10% *Moringa* biodiesel (KB10M10).

Meanwhile, the properties of bioethanol to the biodiesel-diesel fuel mixture are shown in **Table 4.8**. The addition of bioethanol to the mixture causes the decreasing of some fuel properties such as density, viscosity and calorific value. These results are consistent with previous research by Aydın et al. (2017) who observed changes in the fuel properties of a safflower mixture of biodiesel-bioethanol-diesel fuel. The results

show that there is a decrease in viscosity value and heating value after the addition of bioethanol up to 5% into the mixture. The declining properties of the biodiesel-bioethanol-diesel fuel blend is due to the low density, viscosity and calorific values of bioethanol. Kwanchareon et al. (2007) also adds that the fuel density is related to viscosity and combustion, if the fuel has a high density it will cause increased fuel flow resistance, resulting in high viscosity. High viscosity can lead to inferior fuel injection. Meanwhile, the calorific value of the fuel affects the output power generated during the combustion process.

University of Malaya

Table 4.8: The properties of J50C50 biodiesel, biodiesel-diesel fuel blends and biodiesel-bioethanol-diesel fuel blends

Properties	Unit	ASTM D6751	EN 14214	Diesel ^a	J. curcas ^a	C. pentandra ^a	Crude J50C50 ^a	J50C50 biodiesel ^a	Bio-ethanol ^a	(J50C50-diesel fuel) ^a					J50C50 biodiesel-bioethanol-diesel fuel				
										B10	B20	B30	B40	B50	B10BE5	B20BE8	B30BE10	B40BE13	B50BE15
Kinematic viscosity at 40 °C	mm ² /s	1.9–6.0	3.5–5.0	2.96	4.57	4.74	27.22	3.95	1.35 at 20 °C	3.55	3.75	3.89	4.08	4.23	3.27	3.25	3.36	3.42	3.4614
Density at 15 °C	kg/m ³	880	860–900	846.1	876.2	885.7	908.3	831.2	804.6	854	857.9	861.1	864.6	868.8	852.4	852.5	856.8	860.2	863
Calorific value	MJ/kg	–	35	45.36	39.46	39.46	38.22	40.92	27.6	42.76	42.43	41.41	40.75	40.17	41.581	40.543	39.590	38.261	38.117
Flash point	°C	100–170 min.	> 120	75.5	125.5	120.5	–	196	–	76.5	77.5	81.5	78.83	86.5	–	–	–	–	–
Acid value	mg KOH/g	0.5 max.	0.5 max.	0.17	0.46	0.51	15.82	0.25	–	0.36	0.37	0.44	0.46	0.47	0.37	0.37	0.47	0.47	0.46
Pour point	°C	-15 to -16	–	3	3	4	–	0.5	–	6	5.5	5	5.3	3	7	7	11	13	15
Cloud point	°C	-3 to -12	–	2	2	4	–	0.5	–	–	–	–	–	–	–	–	–	–	–
Cold filter plugging point	°C	-25	–	0	1	1	–	-2	–	–	–	–	–	–	–	–	–	–	–
Oxidation stability at 110 °C	h	3 min.	6 min.	15.2	14.01	1.76	–	10.01	–	–	–	–	–	–	–	–	–	–	–
Copper strip corrosion	–	3 max.	–	1a	1a	1a	–	1a	–	–	–	–	–	–	–	–	–	–	–
FAME content	%m/m	–	96.5 max.	–	98.8	97.3	–	99.1	–	–	–	–	–	–	–	–	–	–	–
Cetane index	–	47 min.	51 min.	49.6	59	56	–	58	–	–	–	–	–	–	–	–	–	–	–

^aResult (J50C50) = J. curcas-C. pentandra (50:50 %wt.)

4.4.2 Errors and uncertainties analysis

The uncertainties of the measured parameters can be estimated and reduced to a certain extent by careful selection and calibration of the measuring instruments, planning the experiments in a systematic manner, implementing reliable data acquisition procedures, and controlling the experimental conditions. It is important to estimate the uncertainties of the engine performance parameters (*i.e.* BSFC, engine torque, brake power, EGT, and BTE) and exhaust emission parameters (*i.e.* CO, CO₂, and NO_x emissions, and smoke opacity) since the uncertainties reflect the accuracy of these parameters. The uncertainty represents the range where it is believed that the true value of the parameter lies within this range. **Table 4.9** shown the uncertainties of all parameters are presented using propagation of errors, the total percentage uncertainty of an experimental trial can be computed as:

Overall the experimental uncertainty = square root of [(uncertainty of fuel flow measurement)² + (uncertainty of BSFC)² + (uncertainty of load)² + (uncertainty of brake power)² + (uncertainty of EGT)² + (uncertainty of BTE)² + (uncertainty of NO_x)² + (uncertainty of CO)² + (uncertainty of CO)² + (uncertainty of CO₂)² + (uncertainty of smoke opacity)²] = square root of [(2.428)² + (2.051)² + (0.405)² + (1.873)² + (0.088)² + (0.772)² + (1.24)² + (1.24)² + (1.55)² + (0.14)²] = 4.46%

The total percentage uncertainty of an experimentally found trial (the measurements were repeated 3 times for each test) can be calculated as 4.46% which is less than 5% (95% confidence level), within an acceptable range of errors and uncertainties analysis (Ruhul et al., 2016).

Table 4.9: List of measurement accuracy and percentage uncertainties

Measurement	Range	Accuracy	Measurement techniques	%Uncertainty
Load	± 600 Nm	± 0.1 Nm	Strain gauge type load cell	± 0.4
Speed	0 – 10,000 rpm	± 1 rpm	Magnetic pick up type	± 0.1
Time	–	± 0.1 s	-	± 0.2
Fuel flow	0.5 – 36 L/h	± 0.01 L/h	Positive displacement gear wheel flow meter	± 0.79
Air flow	0.25 – 7.83 kg/min	± 0.07 kg/min	Hot wire air mass meter	± 2
EGT sensor	0 – 1200 °C	± 0.3 °C	Type K thermocouple	± 0.08
Pressure Sensor	0 – 25,000 kPa	± 10 kPa	Piezoelectric crystal type	± 0.5
Emissions				
NO _x	0 – 5000 ppm	± 1 ppm	Electrochemical	± 1.24
CO	0 – 10 vol%	± 0.001 vol%	Non-dispersive infrared	± 1.55
CO ₂	0 – 18 vol%	± 0.01 vol%	Non-dispersive infrared	± 1.48
Smoke opacity	0 – 100 vol%	± 0.10 vol%	Photodiode receiver	± 0.14
Computed				
BSFC	–	± 5 g/kWh	–	± 2.05
Brake power	–	± 0.03 kW	–	± 1.87
BTE	–	± 0.2%	–	± 0.77

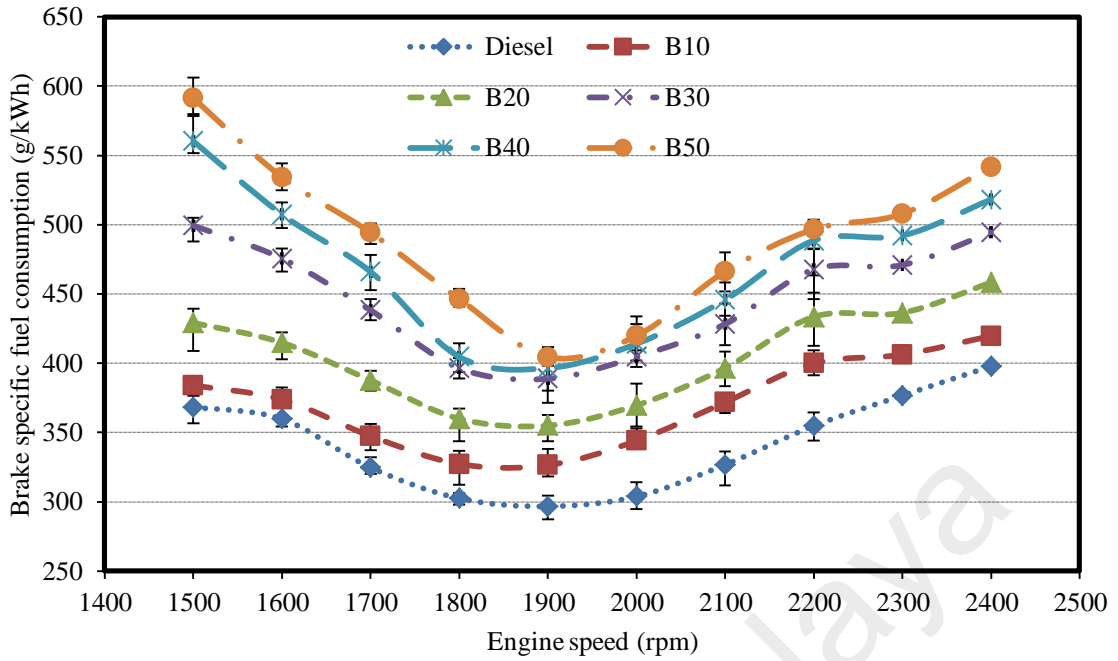
4.4.3 Engine performance analysis

4.4.3.1 Brake specific fuel consumption

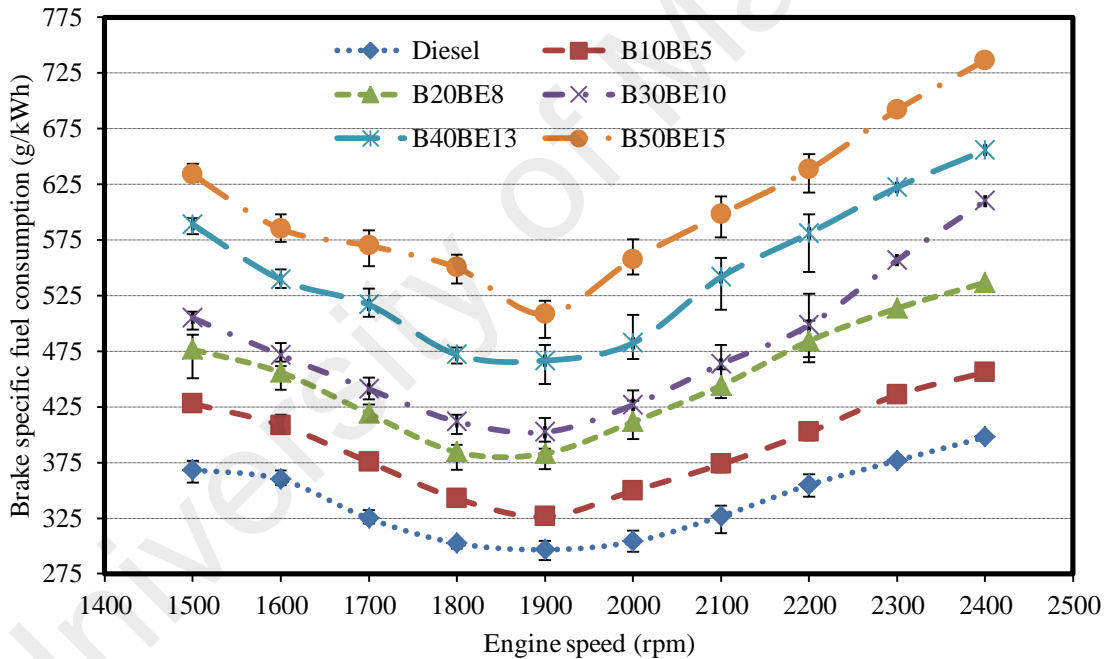
Brake specific fuel consumption (BSFC) is an important parameter used to evaluate the effect of different fuel blends on the engine performance. The BSFC of the diesel engine is dependent on the relationship between a numbers of variables: volumetric fuel injection system, fuel density, viscosity and lower heating value (LHV) (Qi, Lee, et al., 2014). The variation of the BSFC for biodiesel-diesel fuel blends and biodiesel-bioethanol-diesel fuel blends are shown in **Figure 4.5**. It is known that there is a decrease of BSFC due to the increased in engine speed. Indeed, all of the fuels tested

in this study result in a decrease in the BSFC when the engine speed varies from 1500 to 1900 rpm, followed by a slight increase thereafter up to a speed of engine at 2400 rpm. **Figure 4.5. (a)** shown that the BSFC tends to increase along with the increase of biodiesel content in the mixtures. The B50 blend has the highest BSFC whereas the diesel fuel has the lowest BSFC. These results are consistent with Srithar et al. (2014) who found that the addition of mixed *pongamia pinnata* and mustard biodiesel into diesel fuel increases the BSFC. The BSFC was found to be 419.6, 458.1, 499.2, 560.2 and 591.3 g/kWh when the content of biodiesel in the fuel blends were 10, 20, 30, 40 and 50%, respectively. In contrast, the BSFC for diesel fuel was 397.7 g/kWh. In general, the BSFC for biodiesels is higher than that for diesel fuel, whereas the calorific value of biodiesels is lower compare with diesel fuel (Atabani et al., 2014; Can, 2014; Sanjid et al., 2016). Therefore, if the engine is fueled with either biodiesels or biodiesel-diesel fuel blends, the BSFC will increase since the brake torque produced is lower due to the lower energy content of biodiesels (Canakci et al., 2009). According to Buyukkaya (2010), the fuel consumption increases linearly with an increase in the content of biodiesel in biodiesel-diesel fuel blends. However, there is a decrease in the calorific value of the biodiesel during combustion due to the high cetane number as well as variations in injection timing.

Meanwhile, the addition of bioethanol in biodiesel-diesel fuel blends can be seen in **Figure 4.5. (b)**. It is known that, there is an increase in BSFC with increased bioethanol content in the mixture. The B50BE15 or bioethanol 15% mixture has the highest BSFC reaching 736.3 g/kWh at 2400 rpm. The increase in BSFC is due to the lower of heating value of biodiesel and bioethanol compared to diesel fuel (Zhu et al., 2010). In addition, the presence of higher latent heat from bioethanol vaporization, causing lower temperatures in-cylinder and away from the top dead center (TDC), resulting in incomplete combustion (Fang et al., 2013).



(a)



(b)

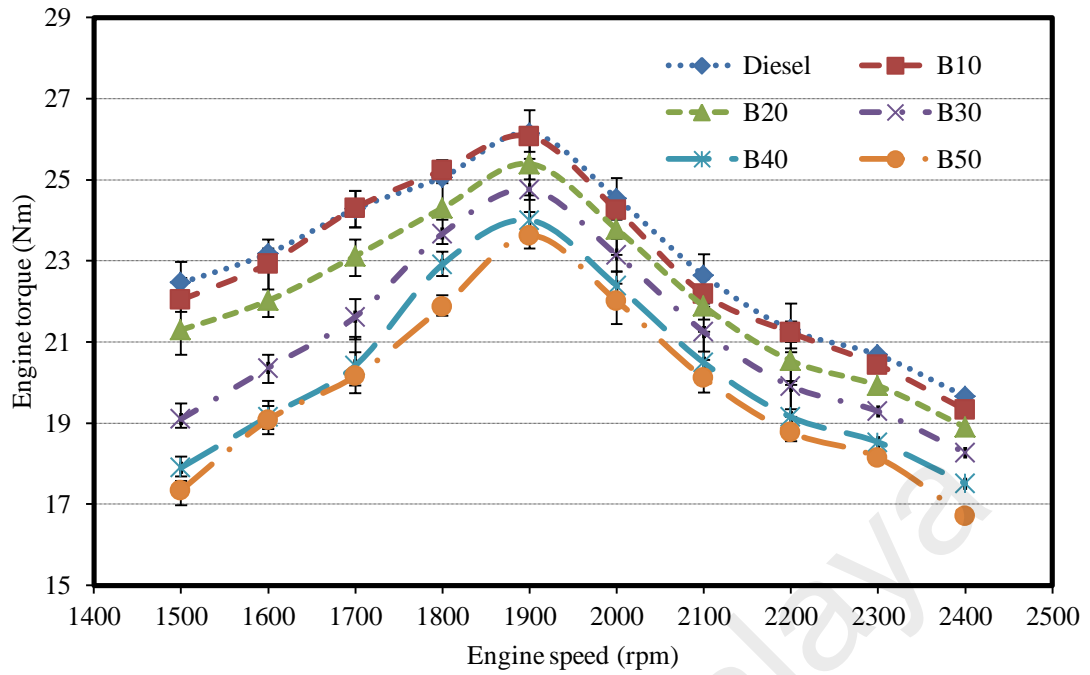
Figure 4.5: Variation of the brake specific fuel consumption for (a) biodiesel-diesel blends with different percentage of J50C50 biodiesel and (b) biodiesel-bioethanol-diesel blends at full load and various engine speeds

4.4.3.2 Engine torque

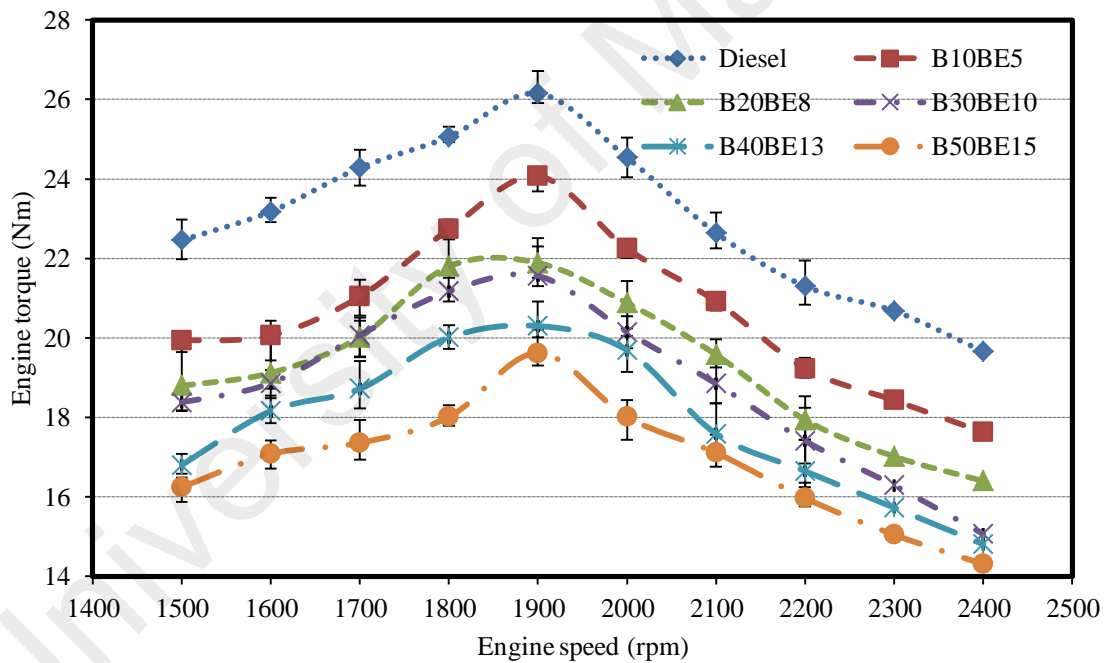
The variation of the engine torque (ET) for the J50C50 biodiesel-diesel fuel blends and J50C50 biodiesel-bioethanol-diesel fuel within an engine speed range of

1500–2400 rpm are shown in **Figure 4.6**. It is known that the ET increases with speed until it reaches a maximum value, followed by a decrease when the engine speed is further increased and this is evident from **Figure 4.6. (a) and (b)**. The diesel fuel has a maximum torque of 26.15 Nm at 1900 rpm. In the biodiesel-diesel fuel blends, the ET for the B10 blend is close to that for diesel (26.07 Nm) at the same speed. It is also apparent that the maximum engine torque is attained at an engine speed of 1900 rpm. The B20, B30, B40 and B50 mixture has a maximum engine torque of 2.9, 5.3, 8.2, and 9.7% lower than diesel fuel, respectively. In general, **Figure 4.6. (a)** shows that the ET values for biodiesel-diesel fuel blends are lower compared to that for diesel fuel. This is due to the fact that biodiesel has high viscosity, low volatility and heavier molecules and consequently, biodiesel-diesel fuel blends evaporate at a slower rate and they are more difficult to burn compared to diesel fuel (Bari, 2014). The higher fuel viscosity reduces the amount of fuel being fed into the oil pump and the engine's volumetric efficiency remains lower, which decreases engine torque (Aydin et al., 2010). In addition, the calorific value of the fuel is a crucial constraint in determining the ET. Increasing the percentage of biodiesel in biodiesel-diesel fuel blends decreases the calorific value of the resultant fuel, which in turn, lowers the ET (Ong et al., 2014).

The addition of bioethanol to the biodiesel-diesel fuel blends also affects the engine torque as shown in **Figure 4.6. (b)**. It appears that the addition of bioethanol resulted in a decrease in ET in almost every mixed composition, in which the B10BE5 mixture had the highest ET of 24.07 Nm at 1900 rpm and B50BE15 had the lowest ET of 14.31 Nm at 2400 rpm. The lower torque results in the biodiesel-bioethanol-diesel fuel blends are caused by the amount of oxygenated calories (biodiesel and bioethanol) in the fuel mixture. In addition, higher density and lower heating value in diesel biodiesel-bioethanol blended fuels, cause the lower atomization ratio (Tan et al., 2017).



(a)



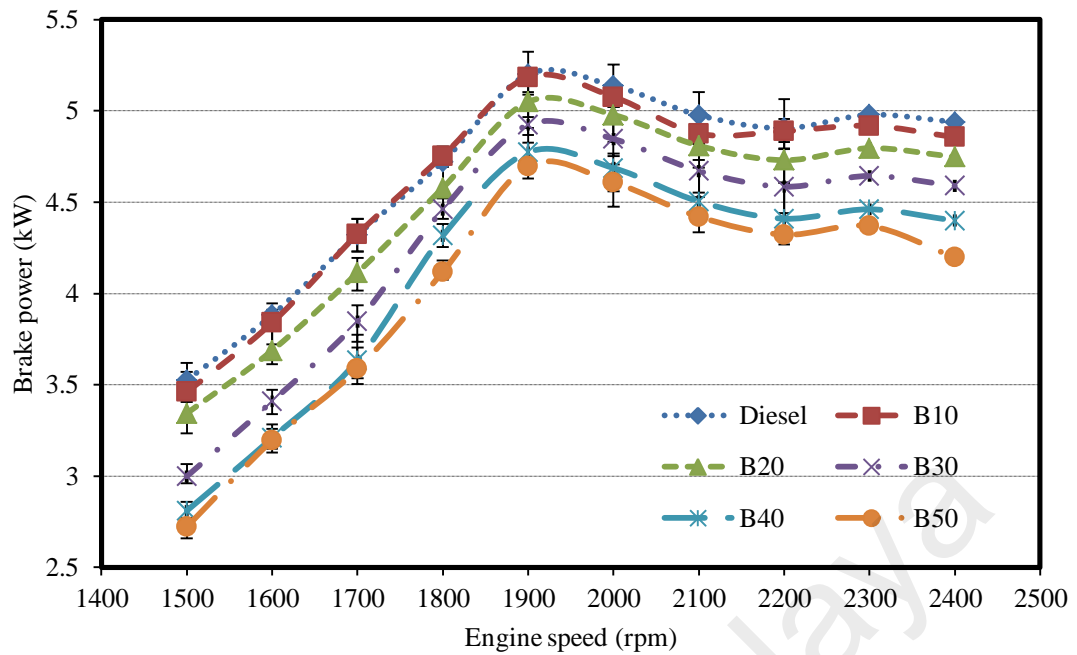
(b)

Figure 4.6: Variation of the engine torque for (a) biodiesel-diesel blends with different percentage of J50C50 biodiesel, and (b) biodiesel-bioethanol-diesel blends at full load and various engine speeds

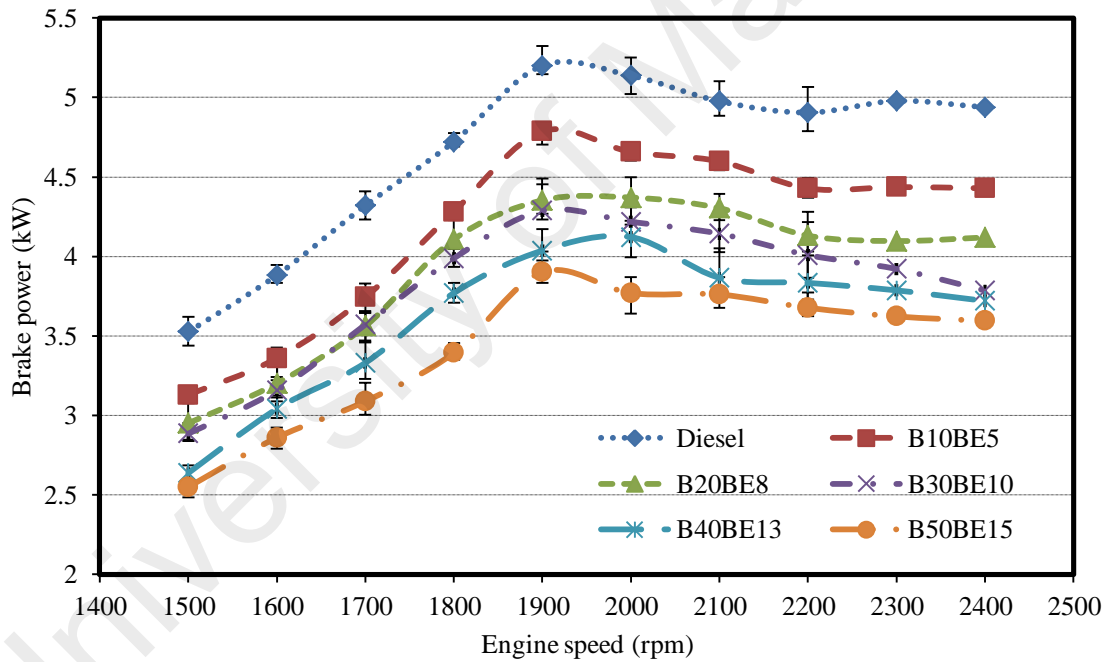
4.4.3.3 Brake power

The variation of the brake power (BP) for biodiesel-diesel blends with different percentage of J50C50 biodiesel and biodiesel-bioethanol-diesel fuel blends in the single-cylinder direct injection diesel engine are shown in **Figure 4.7**. It is known that the variation of the brake power as a function of engine speed is similar for all fuels tested in this study. **Figure 4.7. (a)** shows that the adding of J50C50 biodiesel into diesel fuel decreases the brake power – though at a smaller scale. Diesel fuel has a maximum BP highest of 5.2 kW. It is known that the addition of biodiesel into the fuel mixture causes BP decrease up to 8.11% for B50 at 1900 rpm. In addition, it is known that the BP increases with increasing engine speed. The BP reaches its peak at an engine speed of 1900 rpm, and the BP decreases at higher speeds. According to (An et al., 2013), the addition of 10% of waste cooking oil methyl ester results in the highest brake power, with a value comparable to that for diesel fuel. The reduction of BP is caused by frictional force, poor mixture formation as well as higher viscosity and density of the biodiesel (Kalam et al., 2011; Ong et al., 2014). The high viscosity and lower calorific value of the biodiesel results in uneven combustion characteristics and decreases the engine brake power (Mofijur, Masjuki, Kalam, and Atabani, 2013).

The variation of engine brake power obtained due to the addition of bioethanol to the biodiesel-diesel fuel mixture is shown in **Figure 4.7. (b)**. When compared to other bioethanol blends, B10BE5 has a better brake power engine, which is slightly lower than diesel fuel, with a maximum BP is 4.8 kW at 1900 rpm. As the figure shows, the addition of bioethanol into the mixture decreases BP for the entire mixture. It appears that the B50BE15 mixture has the lowest BP of 2.5 kW at 1500 rpm. The decline in BP values along with the increase in bioethanol content in the mixture is associated with the decreasing lower heating value of biodiesel-bioethanol fuel because the lower heating value of bioethanol and biodiesel is lower than diesel fuel (Al-Hassan et al., 2012).



(a)



(b)

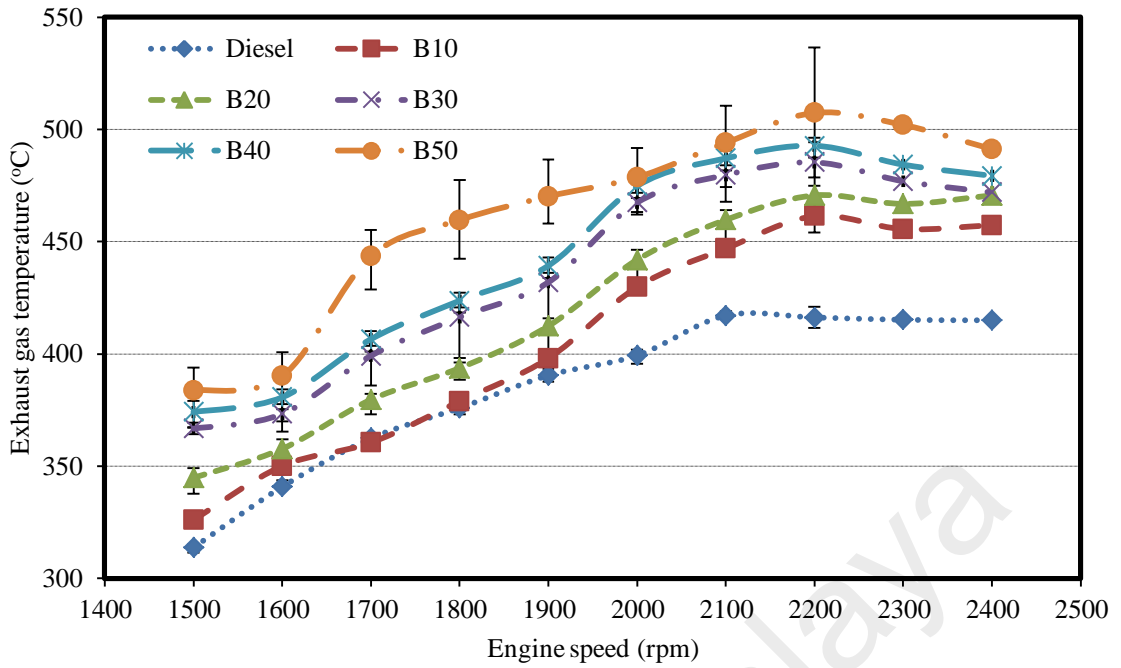
Figure 4.7: Variation of the brake power for (a) biodiesel-diesel blends with different percentage of J50C50 biodiesel, and (b) biodiesel-bioethanol-diesel blends at full load and various engine speeds

4.4.3.4 Exhaust gas temperature

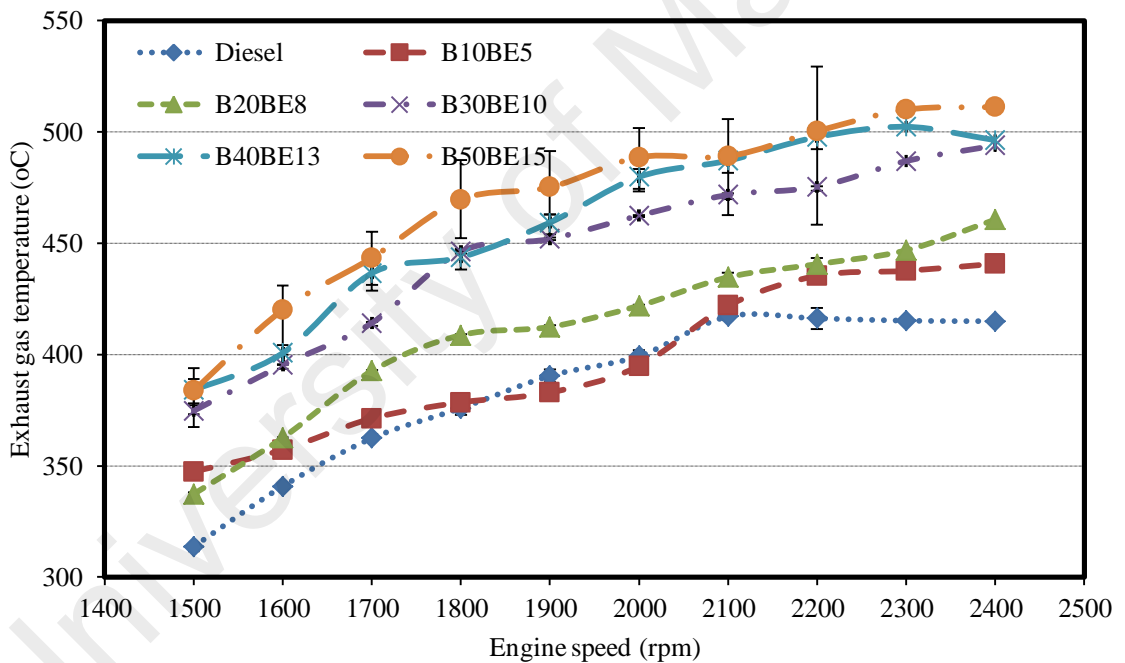
The exhaust gas temperature (EGT) is a parameter of the quality of combustion in the cylindrical combustion chamber. The increase in EGT is associated with more

amount of fuel is required by the engine to produce the extra power which is also needed to take up the additional loading (Srithar et al., 2014). The EGT is also directly related to the air/fuel ratio, which explains why a higher air/diesel fuel ratio results in higher EGT (Bora et al., 2012). The variation of the EGT for biodiesel-diesel fuel blends and biodiesel-bioethanol-diesel fuel blends within an engine speed range of 1500–2400 rpm at full load are shown in **Figure 4.8. (a) and (b)**. As the **Figure 4.7 (a)** show, the EGT increases with an increase in engine speed up to 2200 rpm, but there is a minor decrease in the EGT at higher speeds. It is apparent that the diesel fuel has lower EGT compared to the J50C50 biodiesel-diesel blends within the range of engine speeds investigated in this study. The highest EGT for diesel is 417.1 °C whereas the EGT for the B10, B20, B30, B40 and B50 blend has increased by 9.6, 12.8, 15, 18.1, 21.6%, respectively. It is clear that the percentage of biodiesel in the blend has a significant effect on the EGT. This is due to the fact that biodiesel has a higher cetane number, which results in longer ignition delay and slower burning rate (Raheman et al., 2008).

The changes of EGT with respect to engine speed due to the use of biodiesel-bioethanol-diesel fuel mixtures are shown in **Figure 4.8. (b)**. It appears that the addition of bioethanol in the fuel mixture results in a slight increase in EGT along with an increase in bioethanol content and engine speed. The occurrence of an increase in EGT on a small scale due to the presence of bioethanol causes shortened combustion duration in the combustion chamber (Yilmaz, 2012). B10BE5 has EGT very close to diesel fuel, while B50BE15 has the highest EGT that is 511.2 °C.



(a)



(b)

Figure 4.8: Variation of the exhaust gas temperature for (a) biodiesel-diesel blends with different percentage of J50C50 biodiesel, and (b) biodiesel-bioethanol-diesel blends at full load and various engine speeds

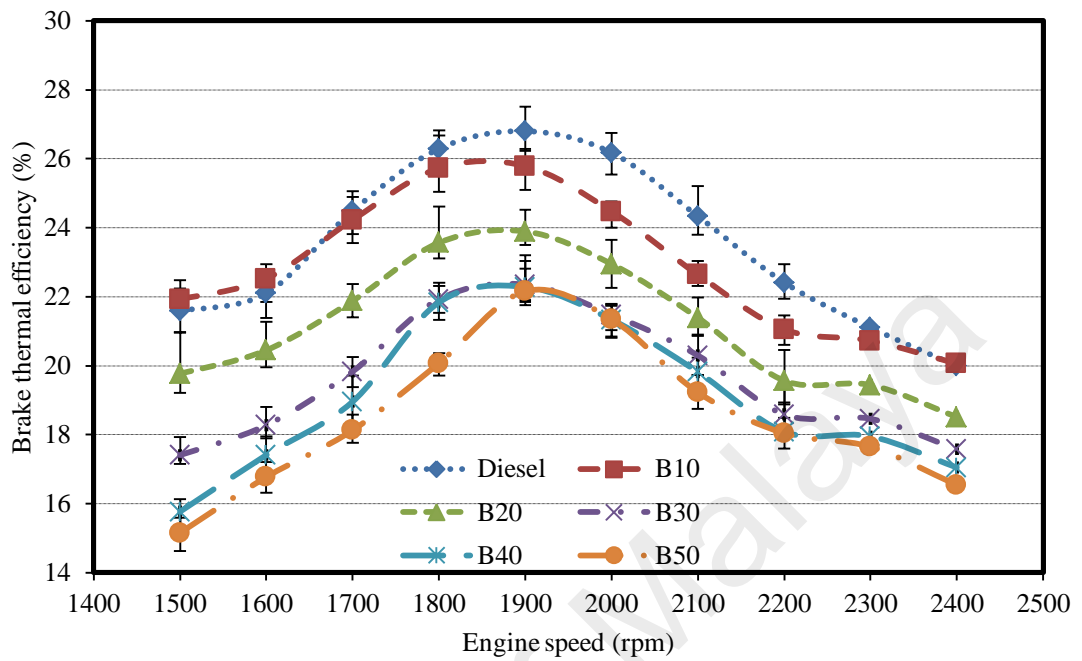
4.4.3.5 Brake thermal efficiency

The brake thermal efficiency (BTE) is used to evaluate how well the engine is able to convert heat of from combustion of fuel into mechanical energy. The BTE is

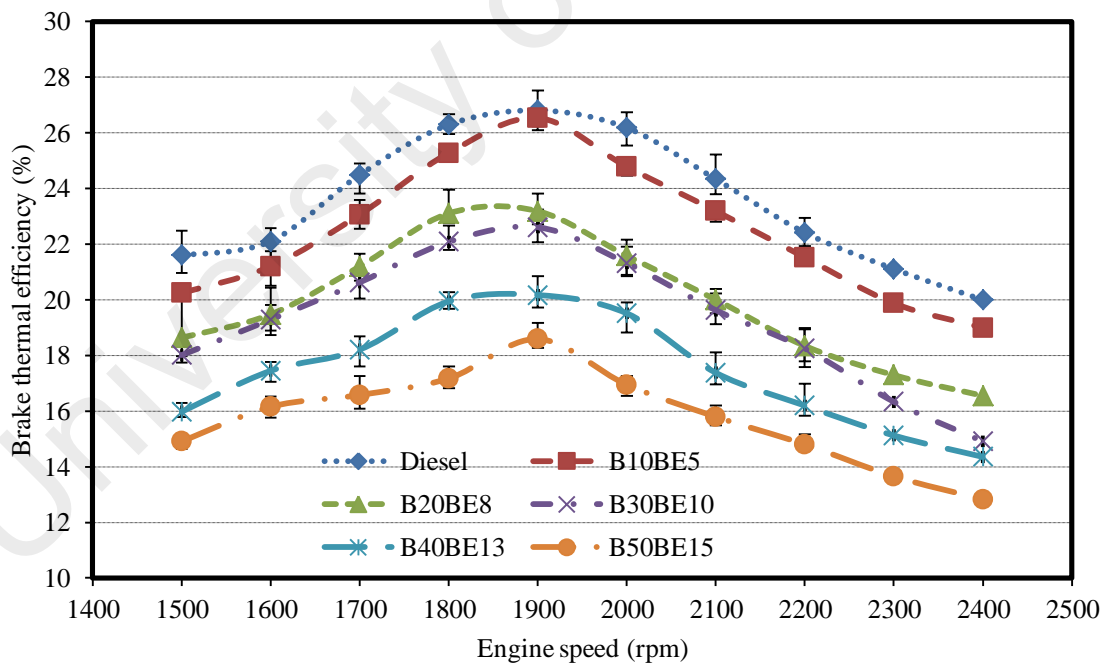
defined as the brake power of the heat engine as a function of the thermal input of the fuel. The variation of the BTE for biodiesel-diesel blends with different percentage of J50C50 biodiesel as well as the addition of bioethanol at various engine speeds is shown in **Figure 4.9**. It is known that, the increasing of engine speed caused the increase in BTE which reaches a maximum value at 1900 rpm. The BTE then decreases at speeds beyond 1900 rpm. **Figure 4.9. (a)** shows the maximum BTE is 26.75% for diesel fuel, which is 3.6% higher than that for B10 (25.79 %). The maximum BTE for the B20, B30, B40 and B50 blend is 10.7, 16.4, 16.7, and 17.2% lower than diesel fuel, respectively. These observations are consistent with the results of Ganapathy et al. (2011) who found that the *Jatropha* biodiesel has lower BTE compared to diesel fuel, which is due to poor atomization, evaporation and combustion resulting from the higher viscosity and lower volatility of biodiesel. The decrease in BTE for blends with higher percentage of biodiesel might due to the lower calorific value and higher fuel consumption (Muralidharan et al., 2011; Ramadhas, A. et al., 2005). The lower calorific value of biodiesel is caused by the presence of large amounts of oxygen in the fuel as well as the higher density of the biodiesel equated to diesel fuel (Enweremadu and Rutto, 2010) (Enweremadu et al., 2010).

Meanwhile, the addition of bioethanol in biodiesel-diesel blends provides a change to BTE. BTE tends to decrease with increasing bioethanol content in the mixture. It is seen that the decrease in BTE reached 30.6% after addition of 15% bioethanol in the mixture (B50BE15). Decreasing the BTE value due to the addition of bioethanol may be associated with lower heating values of the mixed fuel affecting fuel injections, resulting in poor atomization during the premixed combustion phase (Tan et al., 2017). The presence of bioethanol also has an impact on increasing latent heat of vaporization leads to increase the heat losses, as well as decreasing cetane numbers that

cause longer ignition delays and incomplete combustion to occur as more fuel is burned in the expansion stroke (Al-Hassan et al., 2012).



(a)



(b)

Figure 4. 9: Variation of the brake thermal efficiency for (a) biodiesel-diesel blends with different percentage of J50C50 biodiesel, and (b) biodiesel-bioethanol-diesel blends at full load and various engine speeds

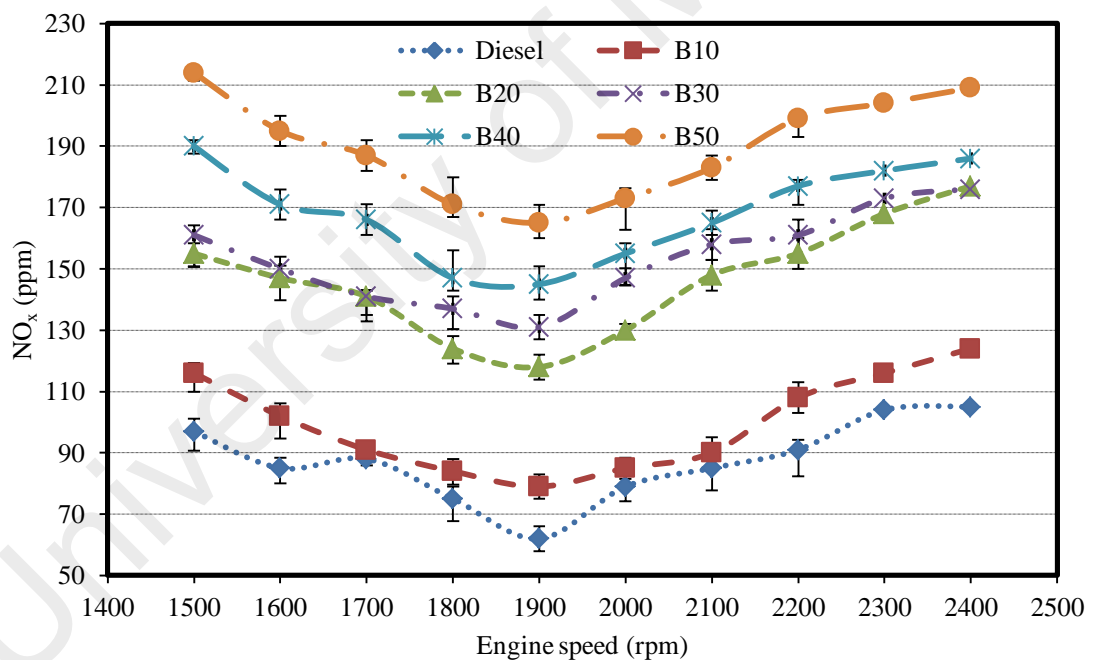
4.4.4 Exhaust emissions

4.4.4.1 Nitrogen oxides

Nitrogen oxides (NO_x) are the by-products (pollutants) are positively correlated with the temperature of combustion, which is directly influenced by the engine load (Vieira da Silva et al., 2017). In general, the formation of NO_x is directly linked with the engine parameters such as in-cylinder temperature, oxygen supply, and residence time. This is due to the high activation energy required for the combustion reaction, and this reaction is determined by the equity ratio, oxygen concentration, and combustion temperature (Özener et al., 2014). The variation of NO_x emissions for biodiesel-diesel blends and biodiesel-bioethanol-diesel fuel blends within an engine speed range of 1500–2400 rpm are shown in **Figure 4.10**. It is noticeable that the NO_x emission is higher at the extremes of the engine speed range investigated in this study for all fuels. **Figure 4.10.(a)** shows that the diesel fuel has the lowest NO_x emission (105 ppm) compared with the J50C50 biodiesel-diesel fuel blends. The NO_x emission increased by 14.29, 68.57, 67.62, 77.14 and 99.05% compared to diesel fuel, respectively for B10, B20, B30, B40 and B50. Increased emissions of NO_x due to the addition of biodiesel in line with a study conducted by Ong et al. (2014) analyzing NO_x emission changes due to the addition of biodiesel *Jatropha curcas*, *Ceiba pentandra* and *Callophyllum Inophyllum*, the average NO_x emissions increased by nearly 40% due to the addition of biodiesel. The NO_x emissions are higher for biodiesel compared to diesel fuel due to the chemically bound oxygen content in the biodiesel, which increases the formation of NO_x (Behçet, 2011). In addition, the increase in NO_x emissions can be attributed to the adiabatic temperature. Biodiesel contains higher unsaturated fatty acid content, which leads to higher adiabatic flame temperature of the fuel and this increases the NO_x emissions (Sanjid et al., 2016). Moreover, Bari (2014) stated that the present of oxygen

content in the biodiesel, higher in-cylinder temperature as well as long residence time leads to higher NO_x emissions than diesel fuel for almost all engine speeds.

The addition bioethanol showed slightly changes in NO_x emission as shown in Figure 4.10 (b). The addition of bioethanol can reduce NO_x emissions but in a small percentage. Compared to the biodiesel-diesel fuel mixture, the reduction of NO_x emissions reached 11.9, 8.65, 3.97, 4.21, and 6.69%, respectively after addition of 5, 8, 10, 13 and 15% bioethanol. However, the value of NO_x of biodiesel-bioethanol-diesel is still higher than diesel fuel. This is associated with a decrease in cetane numbers due to the addition of oxygenates. As it is known that cetane numbers have an effect on combustion, low cetane numbers lead to delayed combustion and more accumulated fuel/air mixture, resulting in increased NO_x formation (Shi et al., 2005)



(a)

Figure 4.10: Variation of the NO_x emissions for (a) biodiesel-diesel blends with different percentage of J50C50 biodiesel, and (b) biodiesel-bioethanol-diesel blends at full load and various engine speeds

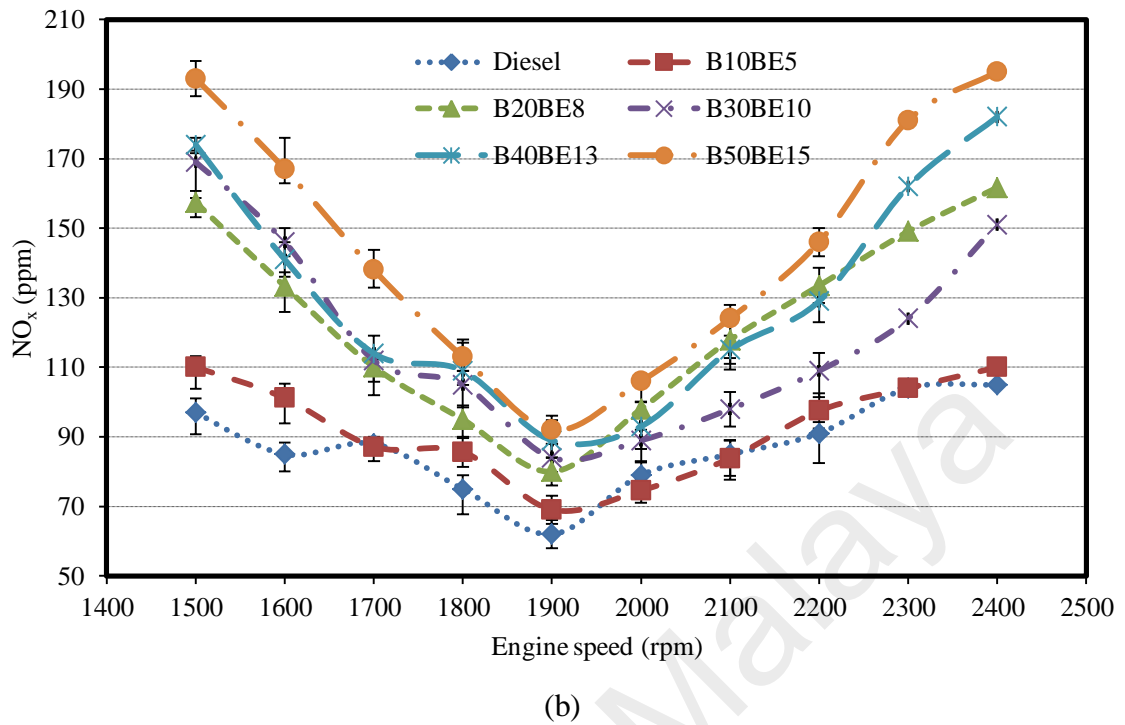


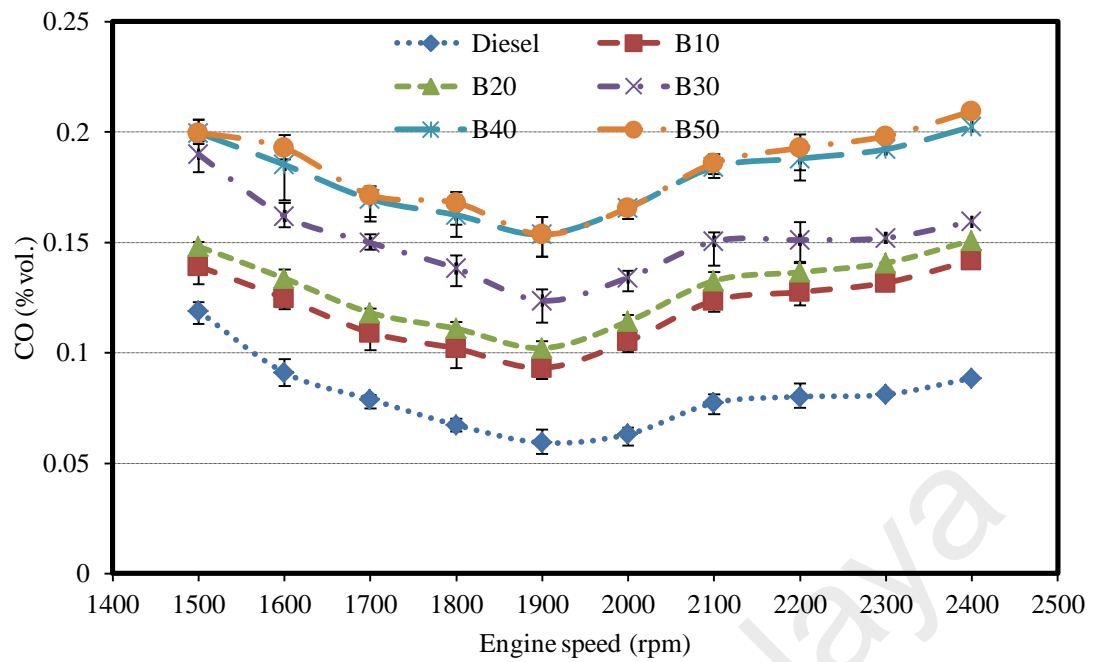
Figure 4.10: Continued

4.4.4.2 Carbon monoxide

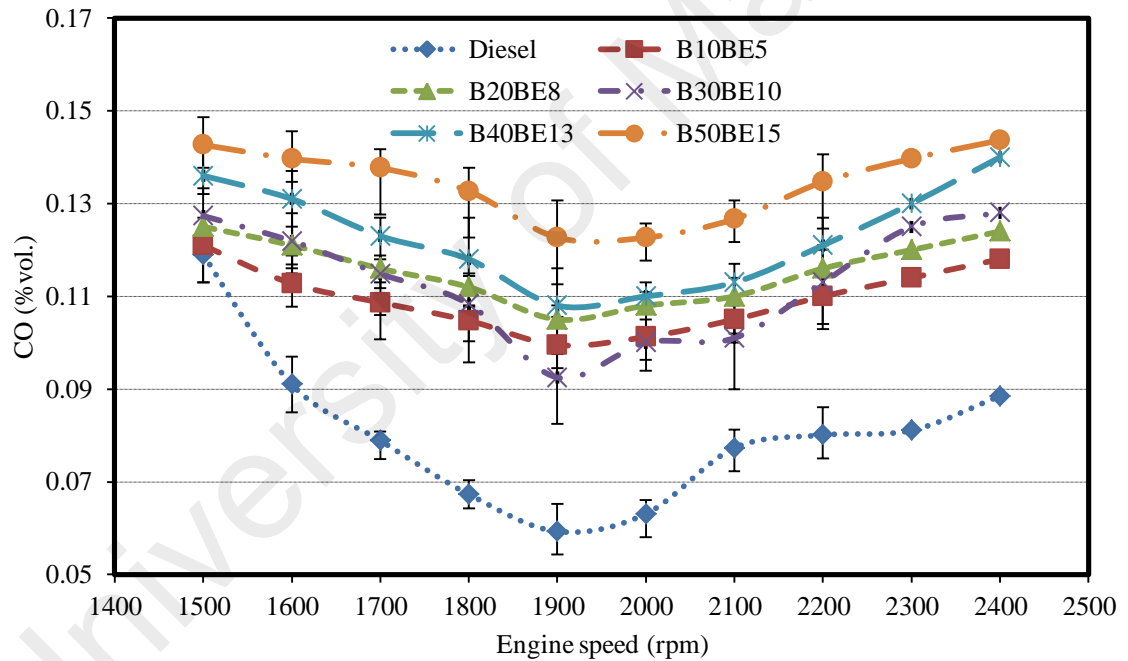
Carbon monoxide (CO) emissions are the outcomes of rich combustion with present of reduced oxygen or air in the combustion chamber (Aydın et al., 2014). The variation of the CO emissions for biodiesel-diesel fuel blends and biodiesel-bioethanol-diesel fuel blends at speed of engine in a range of 1500–2400 rpm can be seen in **Figure 4.11**. **Figure 4.11 (a)** shows that there is a minor increase of CO emissions when biodiesel is added to the diesel fuel. The average CO emissions for diesel fuel is 0.08%. Mixing up to 50% of biodiesel into diesel fuel (B50) led to increased emissions of CO up to 137.5%. The CO emission tends to decrease up to an engine speed of 1900 rpm, and the CO emission increases beyond this engine speed. Several reasons that lead the emissions of CO increase such as rising temperatures in the combustion chamber, the ratio of air/fuel, physical and chemical properties of fuel, lack of oxygen at high speeds

and the limited amount of time available to complete combustion (Muralidharan et al., 2011). In addition, injection timing, injection pressure and the type of fuel all play a role in the influencing the level of CO emissions (Sanjid et al., 2016). The high levels of CO emissions for biodiesel-diesel blends are associated with the higher density and kinematic viscosity of the biodiesel, which directly affect the pattern of the fuel spray that cause a slow combustion in the combustion chamber (Ong et al., 2014). The higher CO emission of biodiesel relative to that for diesel fuel was also observed by other researchers such as (Banapurmath et al., 2008). They found that the CO emission is 0.15, 0.12 and 0.14% for biodiesel produced from honge, *Jatropha* and sesame oil whereas the CO emission is lower for diesel fuel, with a value of 0.11%.

Variations in CO emissions with respect to bioethanol fuel, at full load and engine speed are shown in **Figure 4.11. (b)**. The overall test results showed a very significant reduction in CO emissions of 17.3, 20.7, 49.2, 48.8, and 46.78%, respectively after the addition of bioethanol of 5, 8, 10, 13 and 15%. The low CO emissions for mixed fuels containing bioethanol are associated with high oxygen amounts of bioethanol, which encourages further CO oxidation during the engine exhaust process (Subbaiah et al., 2010). It is clear that CO emissions increase at low and high engine speeds, and decrease at medium speed of 1900 rpm. Increased CO emissions at such high speeds are indirectly caused by the evaporative cooling effect of bioethanol in the emulsion, thereby causing a reduction in flame temperature and decreasing burning velocity (Tan et al., 2017).



(a)



(b)

Figure 4.11: Variation of the CO emissions for (a) biodiesel-diesel blends with different percentage of J50C50 biodiesel, and (b) biodiesel-bioethanol-diesel blends at full load and various engine speeds

4.4.4.3 Carbon dioxide

The burning of fossil fuels results in increasing concentrations of CO₂ in the atmosphere, which leads to the greenhouse effect. For this reason, it is important to

analyze the CO₂ emissions released from diesel engines (Mukhopadhyay et al., 2005; Özener et al., 2014). CO₂ is produced when the amount of oxygen present in the combustion chamber is sufficient for complete combustion (in other words, ideal combustion). However, complete combustion is rare in practice, resulting in the formation of CO as one of the by-products (Nalgundwar et al., 2016). The variation of CO₂ emissions for biodiesel-diesel blends with different percentage of J50C50 biodiesel and biodiesel-bioethanol-diesel fuel blends at the engine speed ranges from 1500 to 2400 rpm are shown in **Figure 4.12**. The results show that the diesel fuel has higher CO₂ emission (4.29 %vol.) compared to other biodiesel-diesel blends at 1900 rpm. The addition of biodiesel into diesel fuel is known to reduce CO₂ emissions. CO₂ emissions in biodiesel are lower than diesel, this is attributed to the fact that biodiesel is low carbon fuel and has a lower carbon and to hydrogen ratio than diesel fuel (Xue et al., 2011b). Indeed, the CO₂ emission decreases by 40% when 50% of J50C50 biodiesel is blended with diesel fuel. According to Ong et al. (2014), the reduction of CO₂ emissions for blends with a higher percentage of biodiesel is due to the high viscosity of biodiesel. Xue et al. (2011a) reviewed studies pertaining to the effect of biodiesel on performance of the engine and emissions and they highlighted that biodiesel can reduce CO₂ emissions by 50–80% compared to diesel fuel. This in turn, will help reduce greenhouse gas emissions on a global scale through the life cycle CO₂. In addition, the lower calorific value of biodiesel results in higher fuel consumption to produce the same power and the present of large quantity of oxygen in the biodiesel results in more carbon being oxidized into CO₂ (Bari, 2014).

Figure 4.12. (b) show the effect of bioethanol presence in biodiesel-diesel fuel mixture to CO₂ emissions. As seen in the figure that the increase in bioethanol content in line with decreasing CO₂ emissions. When compared to the biodiesel-diesel fuel mixture, the average CO₂ emissions level decreased to 59.5% after the addition of

bioethanol. Reduced of CO₂ emissions due to low carbon-to-hydrogen ratios contained in bioethanol molecules can increase the oxidation of CO molecule to CO₂, resulting in more water formation and less CO₂ gas (Tan et al., 2017).

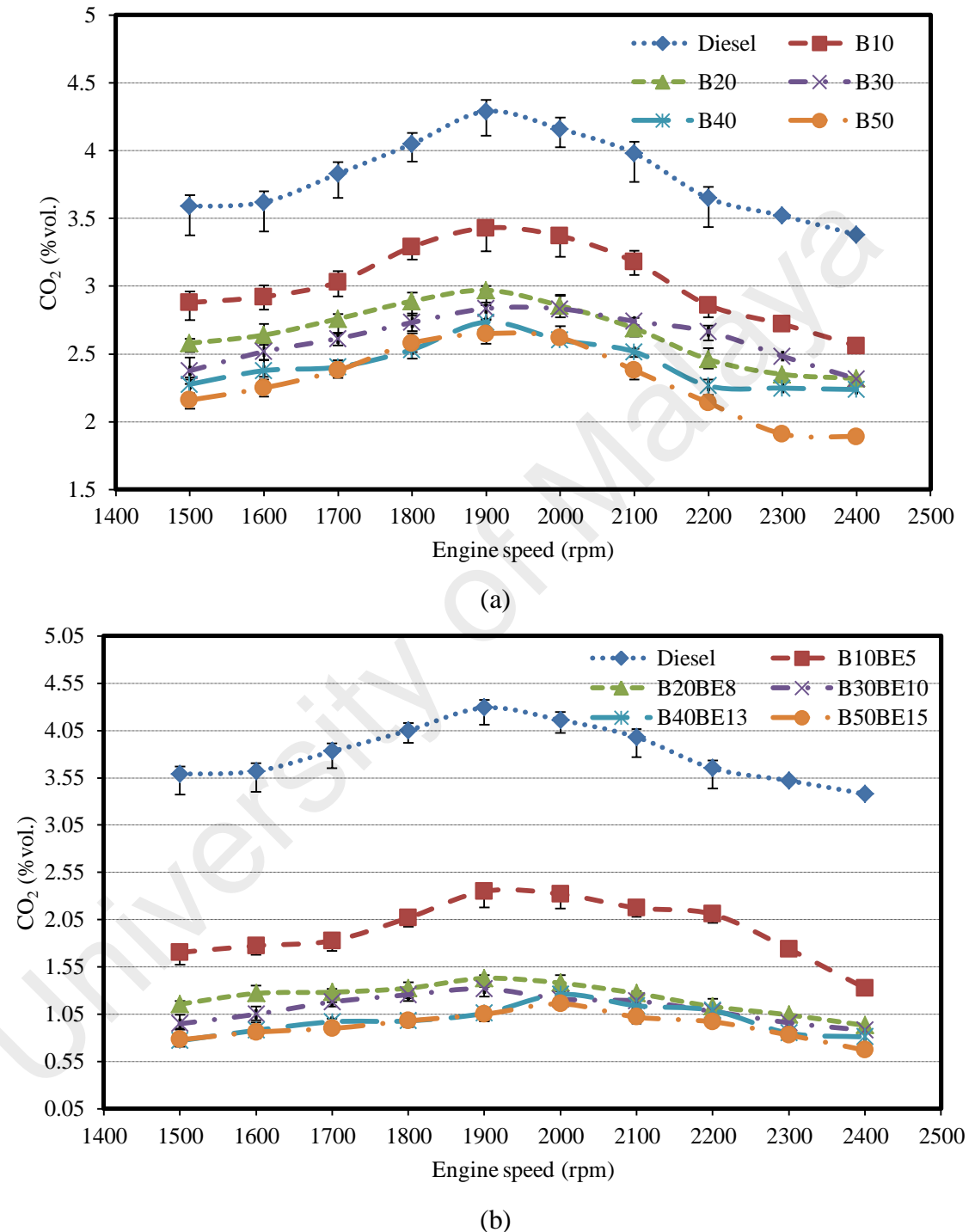


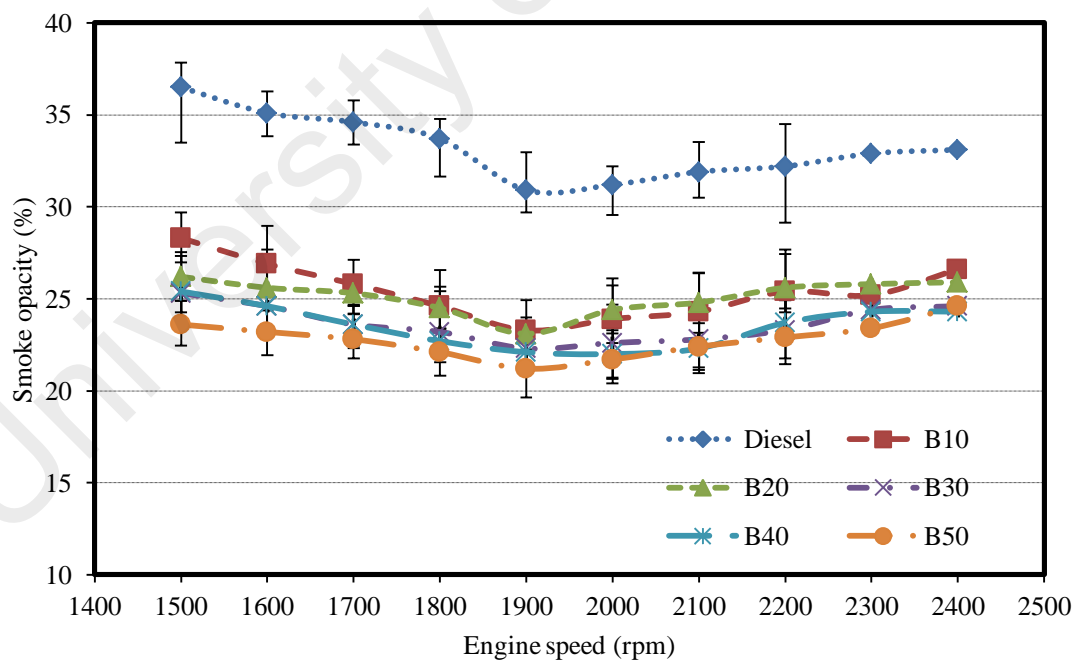
Figure 4.12: Variation of the CO₂ emissions for (a) biodiesel-diesel blends with different percentage of J50C50 biodiesel, and (b) biodiesel-bioethanol-diesel blends at full load and various engine speeds

4.4.4.4 Smoke opacity

The smoke opacity is an indicator of dry soot and particulate matter emissions. In diesel engines, the atomized fuel splits into carbon (formation of soot) during the combustion process and the carbon then oxidizes in the reaction zone (soot oxidation). The carbon particles (known as soot or smoke) form if the amount of oxygen or the local temperature does not support the oxidation process (Attia et al., 2016). The variation of the smoke opacity for J50C50 biodiesel-diesel blends and biodiesel-bioethanol-diesel fuel blends at various engine speeds are shown in **Figure 4.13**. From the **Figure 4.13. (a)** it is clear that the smoke opacity is lower for all of the biodiesel-diesel blends investigated in this study compared to diesel fuel. The diesel fuel has the highest average smoke opacity, with a value of 33.2%. Smoke opacity has decreased significantly due to the addition of biodiesel in diesel fuel. It is known that, the addition of up to 50% biodiesel (B50) causes a decrease in average smoke opacity up to 45.6%. The lower average smoke opacity values of the J50C50 biodiesel-diesel blends are attributed to the oxygen content and higher cetane index of the biodiesel (Aydin et al., 2014). According to Kakati et al. (2016), the addition of biodiesel into diesel fuel reduces its smoke opacity, which is due to the present of oxygen molecules in the biodiesel and this improves combustion. The decrease in the smoke opacity upon the addition of biodiesel is also due to the reduction of aromatic compounds in the mixture, which are precursors of soot (Lapuerta et al., 2008). Mosarof et al. (2016) reported that the addition of palm and *Calophyllum inophyllum* biodiesel into diesel fuel up to 30% reduces smoke opacity by 4.64%.

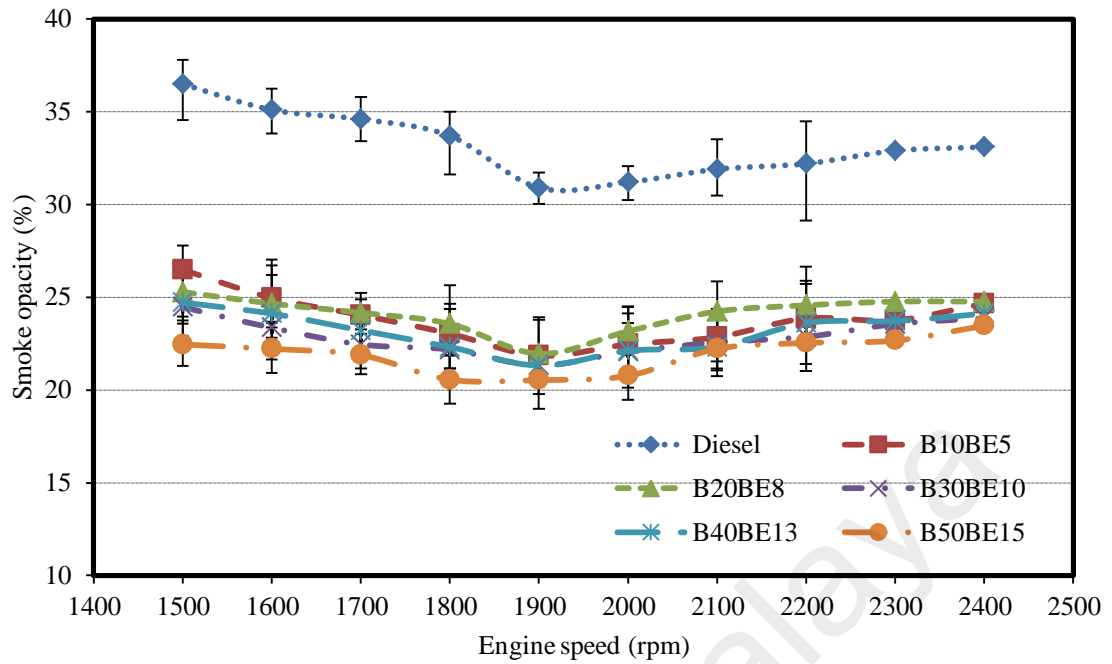
In addition, the addition of bioethanol also gives the same effect on the reduction of smoke opacity produced. As indicated by **Figure 4.13. (b)** that there is a decrease in smoke opacity due to the addition of bioethanol to the biodiesel-diesel fuel blends. The decrease in smoke opacity averaged a small percentage when compared to the use of

biodiesel-diesel fuel blends, which were 4.01, 3.35, 1.44, 3.76 and 3.79%, respectively after the addition of bioethanol of 5, 8, 10, 13 and 15%. Reduced smoke opacity in bioethanol-fueled fuels can be attributed to a decrease in maximum flame temperature in the combustion chamber due to backward injection time, this impacts on the ignition delay. The ignition delay makes fuel and air mixed homogeneously and affects the decreased amount of opacity smoke produced (Fang et al., 2013). The addition of bioethanol which is an oxygenated fuel also causes an increase in the oxygen content in the fuel, which affects the decrease in the formation of soot precursors, so that the opacity smoke produced can be reduced (Kalghatgi et al., 2006). Li et al. (2015) reported that, the decrease in soot emissions is associated with in-cylinder gas temperature and equivalence ratio, when the engine loads up and the more fuel is injected which affects to the temperature in the cylinder be higher. This is useful for soot oxidation and better combustion.



(a)

Figure 4.13: Variation of the smoke opacity for (a) biodiesel-diesel blends with different percentage of J50C50 biodiesel, and (b) biodiesel-bioethanol-diesel blends at full load and various engine speeds



(b)

Figure 4.13. Continued

4.4.5 Summary

The biodiesel bioethanol blend in the fuel mixture could affect the fuel properties. In addition, engine performance testing and exhaust gas emissions using direct injection diesel engines showed significant changes. The main findings of this test series had been compiled as follows:

- 1 The presence of biodiesel in diesel fuel affects on the properties of the fuel blends, such as increased viscosity, density, flash point and acid value. Meanwhile, the addition of bioethanol in biodiesel-diesel blends indicates a decrease in some properties, such as viscosity, density, and calorific value compared to biodiesel-diesel blends.
- 2 In engine performance testing, the engine was operated in full load at speeds ranging from 1500 rpm to 2400 rpm. The test results showed that the presence of

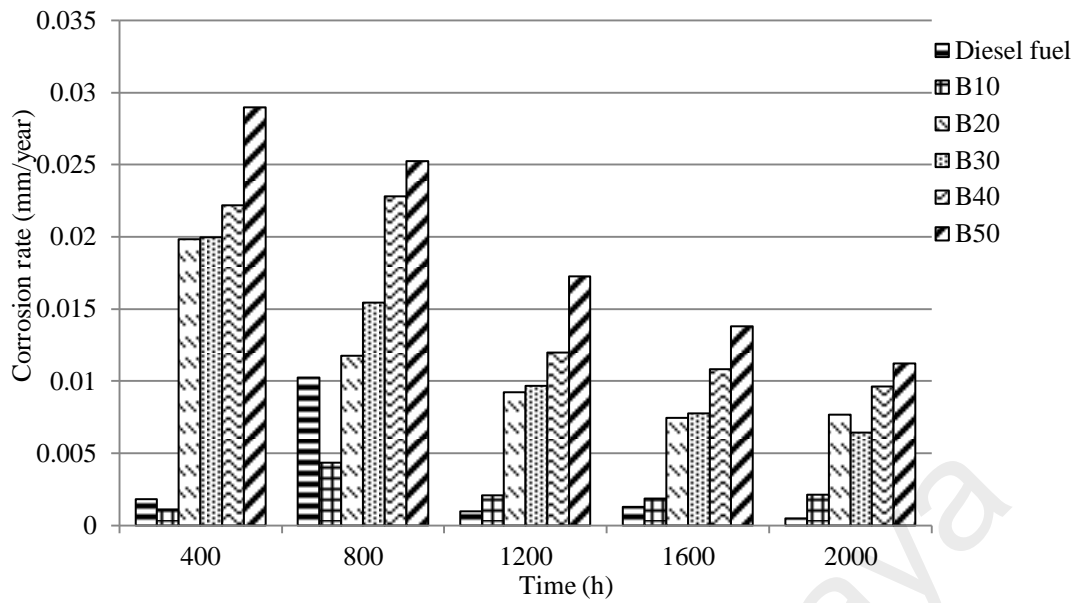
biodiesel and bioethanol in diesel fuel increased BSFC and EGT, while the engine torque, power and brake thermal efficiency tended to decrease.

- 3 NO_x emissions and CO increased after the addition of biodiesel and bioethanol, while CO₂ and smoke opacity decreased significantly.
- 4 In biodiesel-diesel fuel blends, B10 has good physicochemical properties and its similar to diesel fuel. In performance engine testing, B10 has higher engine torque, brake power and brake heat efficiency compared to other fuel mixtures, with grades of 26.07 Nm, 5.2 kW and 25.79%, respectively. B10 has better exhaust emissions compared to diesel fuel. While on biodiesel-bioethanol-diesel fuel blends, B10BE5 has better brake power, engine torque, thermal efficiency, NO_x emissions and smoke opacity than any other blends.

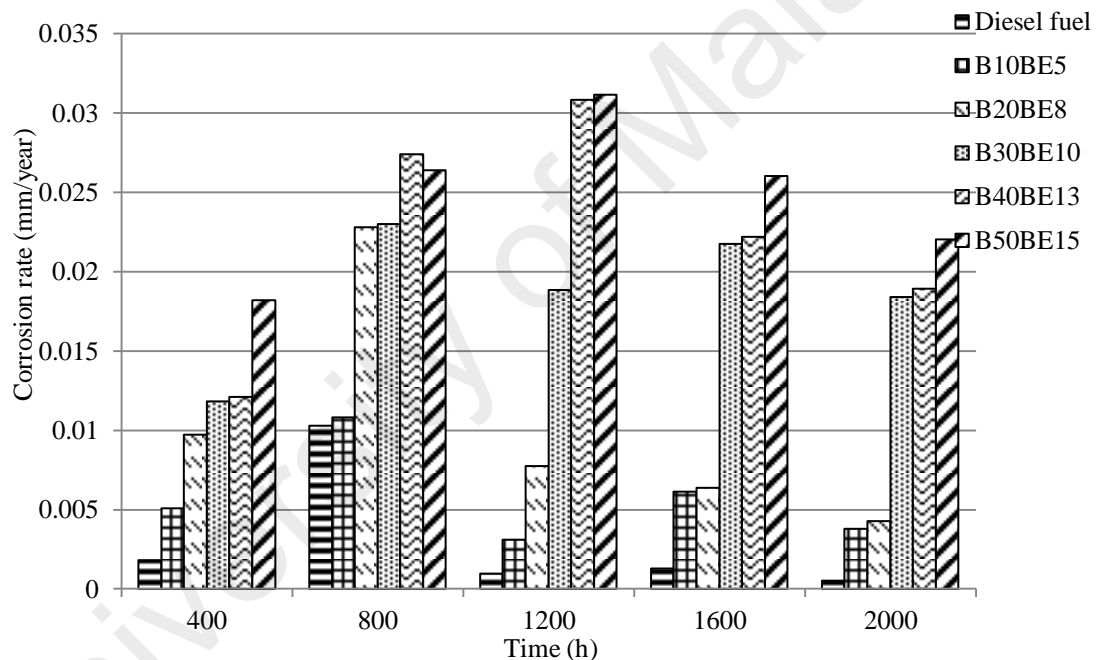
4.5 Biodiesel-diesel fuel blends and biodiesel-bioethanol-diesel fuel blends corrosion

4.5.1 Corrosion rate

Characters of corrosive metal is crucial for long-term durability of engine parts when using biodiesel or bioethanol as a fuel engine. Comparison of corrosion rate of J50C50 biodiesel blended with diesel fuel for some variations (B0, B10, B20, B30, B40 and B50) and addition of bioethanol with a percentage of 5–15% at ambient temperature are shown in **Figure 4.14**.



(a)



(b)

Figure 4.14: Corrosion rate of mild steel in (a) biodiesel-diesel blends, and (b) biodiesel-bioethanol-diesel blends after immersion for 400, 800, 1200, 1600 and 2000 hours

In this study, the measurement of weight lost during the immersion became the basis in calculating the corrosion rate. Figure 4.14 (a) shows that the corrosion rate of mild steel for the entire fuel mixture (B0, B10, B20, B30, B40 and B50) appears higher at 400 hours of immersion at 0.0018 mm/year, 0.0011 mm/year, 0.0198 mm/year, 0.0200 mm/year, 0.0220 mm/year, and 0.0290 mm/year, respectively.

0.0199 mm/year, 0.0222 mm/year and 0.0289 mm/year, respectively. The corrosion rate of mild steel immersed in B50 was 15 times faster than with diesel fuel. This mixture also had the fastest corrosion rate compared to other fuels. Meanwhile, the B10 had the lowest corrosion rate, of approximately 38% lower compared to diesel fuel.

Meanwhile, the effect of adding bioethanol on biodiesel-diesel fuel blends to corrosion rate of mild steel coupon is shown in **Figure 4.14 (b)**. The corrosion rate appears to be greatly influenced by the immersion time and the bioethanol content in the mixture. It is seen that the corrosion rate had increased at the beginning of immersion to 200 hours of immersion, before decreasing. On average, the addition of bioethanol into the biodiesel-diesel fuel blends increased the corrosion rate by more than 85% compared to the biodiesel-diesel fuel blends. Thangavelu et al. (2015) stated that the rate of corrosion in the use of ethanol fuel is higher than that of petro-diesel. In addition, Baena et al. (2012) stated that the presence of ethanol in fuels causes more susceptibility to corrosion when exposed to ferrous material, due to the occurrence of water and oxygen in ethanol.

Overall, the addition of J50C50 biodiesel into diesel fuel cause increment of corrosion rate on mild steel. The rate of corrosion depends on the volume percentage of biodiesel in the mixture of biodiesel-diesel. The increase in corrosion rate is in line with the increasing content of biodiesel in the mixture (Haseeb, Sia, et al., 2010). The high corrosion rate show that biodiesel is more corrosive than the diesel fuel (Cursaru et al., 2014). Increment of corrosion rate was due to the addition of biodiesel, and this is consistent with studies done by Samuel et al. (2016) who reported that the addition of palm oil biodiesel produced from alkali-catalyzed processes transesterification impact on increasing the corrosion rate was 0.054, 0.0954 and 0.139 mpy for B0, B50 and B100, each. Hu et al. (2012b) also added that mild carbon steel and copper, a material that is easily oxidized compared to aluminium and stainless steel.

Low oxidation stability of biodiesel compared to diesel fuel in the engine triggered some problems such as corrosion, filter plugging and deposit machines. In addition, the content of unsaturated methyl esters such as methyl linoleate (C18: 2) and methyl linolenate (C18: 3) may causes the formation of biodegradable compounds such as acids, aldehydes, esters, ketones, peroxides and alcohols (Sorate et al., 2015). The generated acids could be corrosive for the automotive components though they could improve lubricity in short term operations (Fazal et al., 2013b). **Table 4.2** shows the fatty acid composition of J50C50 biodiesel, which largely consists of oleic acid (36.2%) and linoleic acid (34.3%), while linolenate acid in small amounts is (0.8%) (Dharma, Masjuki, et al., 2016).

On the other hand, the effect of immersion time showed something different. It appeared that the mild steel immersed with a long duration was likely to have a corrosion rate lower than the immersed with a shorter duration, though the data measuring the weight lost from coupons mild steel showed improvement. This indicates that the weight lost was not linear with immersion time, as it tended to experience a slowdown compared to the time that continued to grow. The decline in the corrosion rate could occur, such as the research conducted by Fazal et al. (2010a) which found that a reduction in the rate of corrosion of aluminum, where the rate of corrosion of aluminium at 1200 hours lower than 600 hours. Chew et al. (2013) also said that a decline in the corrosion rate of magnesium and aluminum along with increasing the immersion period.

4.5.2 Surface characteristics

The colour change of coupons mild steel as a result of J50C50 biodiesel-diesel fuel blend of exposure before and after immersion can be seen in **Figure 4.15**. Coupons mild steel immersed in diesel showed fuel barely visible colour change, which was slightly darker. This was in contrast to the coupons mild steel immersed in J50C50 biodiesel-diesel fuel blends as well as with the addition of bioethanol. Clear visible colour degradation appeared in all types of mixtures J50C50 biodiesel and also bioethanol. At the beginning, the immersion changed to slight brownish. The brown colour constantly increased with increasing immersion time. In 2000 hours immersion, there was a thin layer of black color on the surface of the product, especially for some blends such as B40 and B50. Meanwhile, the immersion of mild steel coupons in bioethanol blend oils produced lighter but somewhat blackish coupons, especially on B30BE10, B40BE13 and B50BE15. It is known that immersion of mild steel coupons for a long duration in the biodiesel could cause discoloration and sediment formation. Formation of sediments and gums could cause problems to engine performance including fuel filter plugging (Chew et al., 2013).

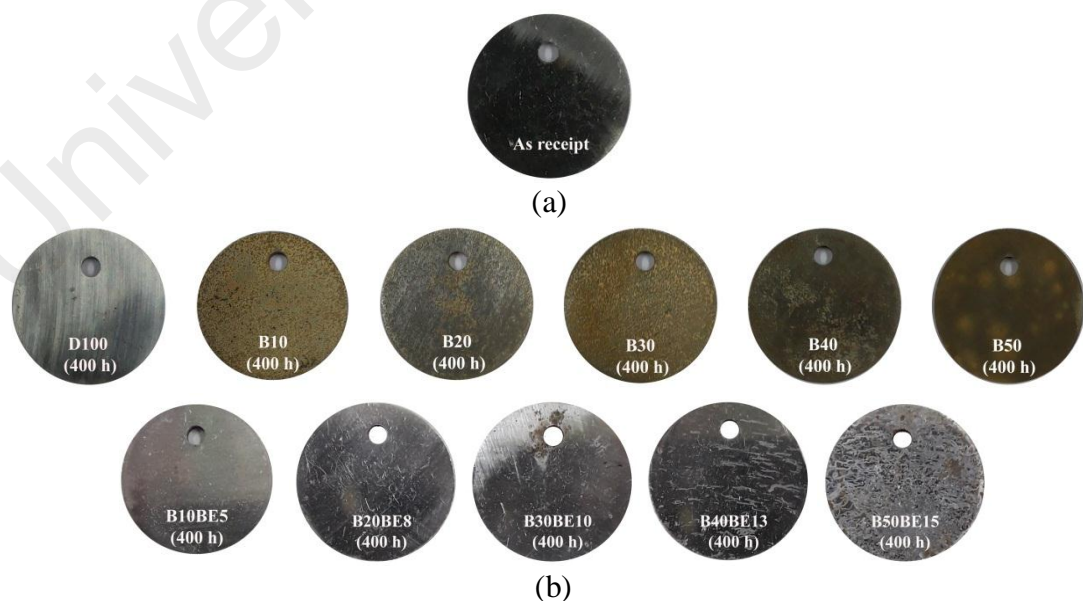


Figure 4.15: Photographs of mild steel coupons are immersed in some fuel mixtures with the immersion time duration of (a) 0 hour (as receipt), (b) 400 hours, (c) 2000 hours.



(c)

Figure 4.15: Continued

Scanning electron microscope (SEM) was used to analyse the surface morphology of mild steel which was immersed in biodiesel-diesel fuel blends and biodiesel-bioethanol-diesel fuel blends for 400 hours and 2000 hours as shown in **Figure 4.16** and **Figure 4.17**. These observations were made to analyse the impact of biodiesel fuel against corrosion during static immersion. It is apparent that there was a change in the morphology of the metal surface caused by corrosion. Immersion time showed degradation of mild steel material damage was greater due to immersion in fuel blended with biodiesel and bioethanol. The figures show that magnification of $1000\times$ shows that metal surfaces exposed mild steel to wider corrosion with increasing duration of immersion. Clearly, the corrosion degraded the metal surfaces. Round pits were visible on the surface as an indication of corrosion attack (Chew et al., 2013). Pitting corrosion on metal surfaces could also be caused by mono-carboxylic acids such as formic acid, acetic acid, propionic acid, and caproic acid (Haseeb, Masjuki, et al., 2010; Tsuchiya et al., 2006). Corrosion attack on diesel was less than the mild steel coupon when immersed in the fuel mixture. The duration of immersion time also had considerable influence on changes in surface morphology of coupons. Mild steel coupon immersed at

2000 hours shows the round pits on the full surface with black colour more evenly distributed compared with coupon immersed at 400 hours.

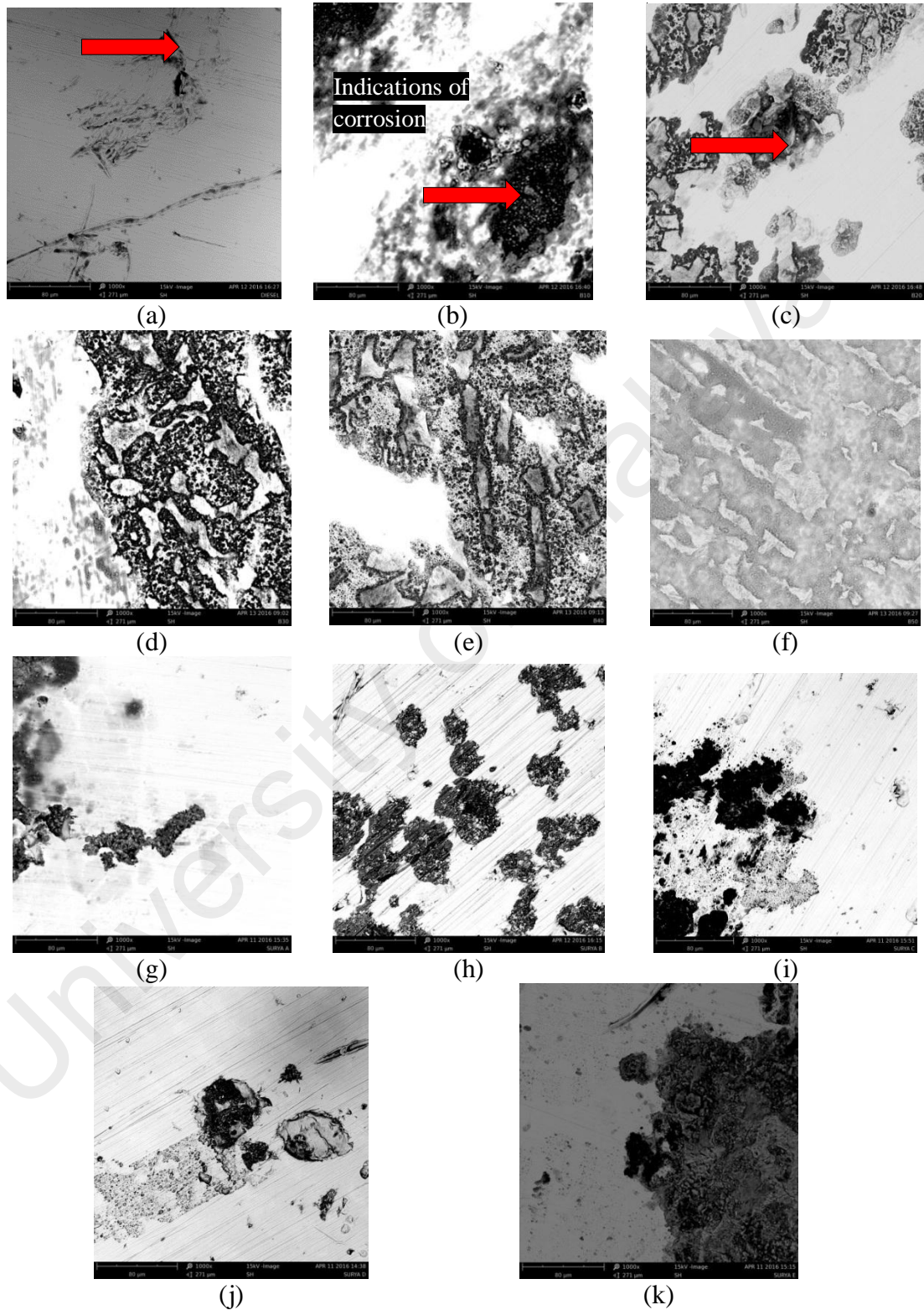


Figure 4.16: Optical photograph (1000 ×) showing the morphology of corrosion products in the surface of mild steel after immersion 400 h at ambient temperature for (a) B0, (b) B10, (c) B20, (d) B30, (e) B40, (f) B50, (g) B10BE5, (h) B20BE8, (i) B30BE10, (j) B40BE13 and (k) B50BE15

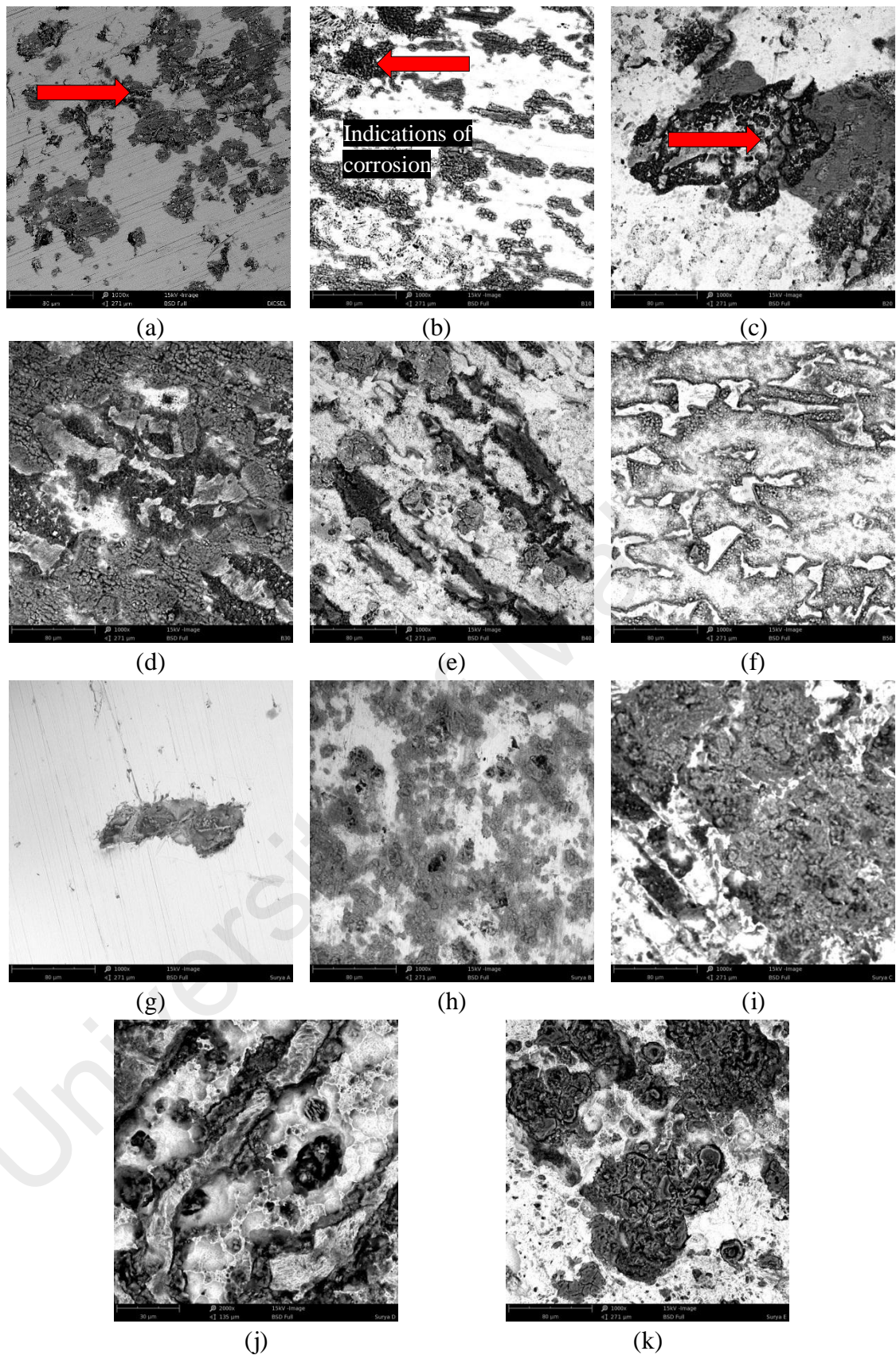


Figure 4.17: Optical photograph (1000 ×) showing the morphology of corrosion products in the surface of mild steel after immersion 2000 h at ambient temperature for (a) B0, (b) B10, (c) B20, (d) B30, (e) B40, (f) B50, (g) B10BE5, (h) B20BE8, (i) B30BE10, (j) B40BE13 and (k) B50BE15

Analysis of mild steel specimens surface immersed in all of fuel mixtures to 2000 hours was done using EDX and presented in **Figure 4.18**. The content of oxygen in mild steel immersed in diesel fuel is 2.54 wt.%, and mild steel immersed in B50 reached 19.16 wt.%, Meanwhile, the oxygen content in mild steel after addition 15% of bioethanol increased up to 20.51 wt.%. This indicates the presence of biodiesel and bioethanol in diesel fuel, which is caused by oxidizable components of biodiesel such as unsaturated fatty acids, active atom oxygen, and others (Hu et al., 2012b; Jin et al., 2015). This oxidation may occur due to the hygroscopic properties of biodiesel that causes water retention. As a result, microbial growth and contamination increases in the biodiesel fuel (Fazal et al., 2016).

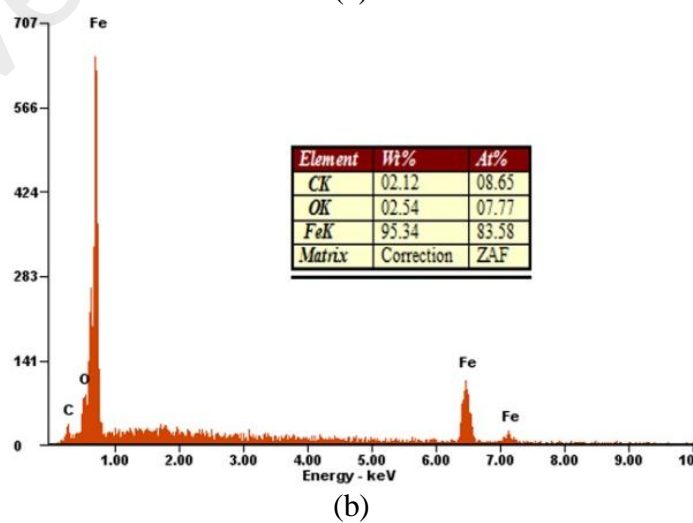
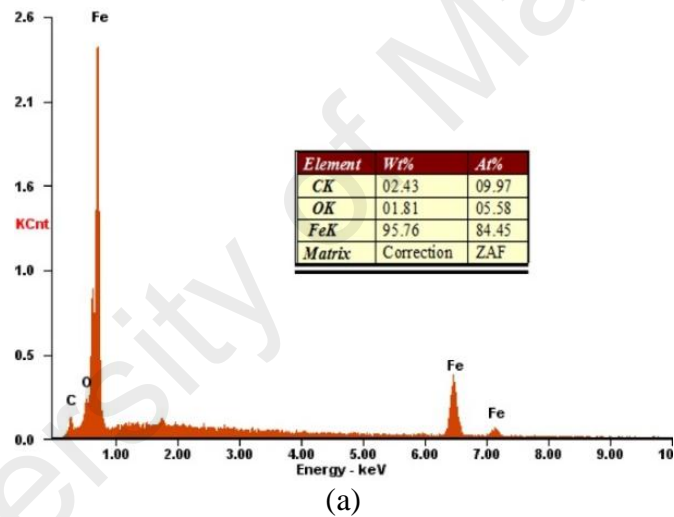


Figure 4.18: Elemental composition of mild steel as received (a) and mild steel after immersion 2000 hours at ambient temperature for (b) B0, (c) B10, (d) B20, (e) B30, (f) B40, (g) B50, (h) B10BBE5, (i) B20BE8, (j) B30BE10, (k) B40BE13, and (l) B50BE15.

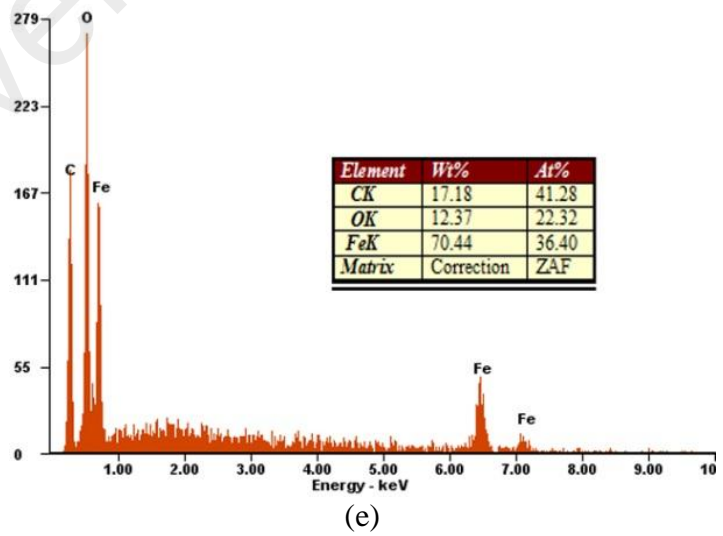
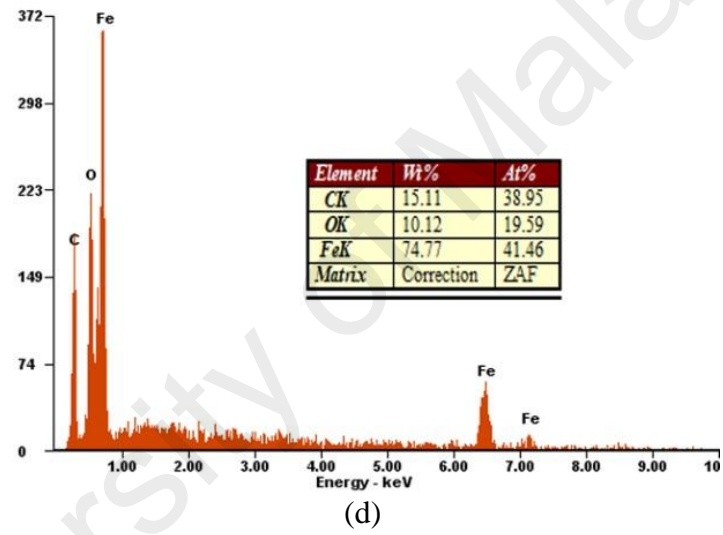
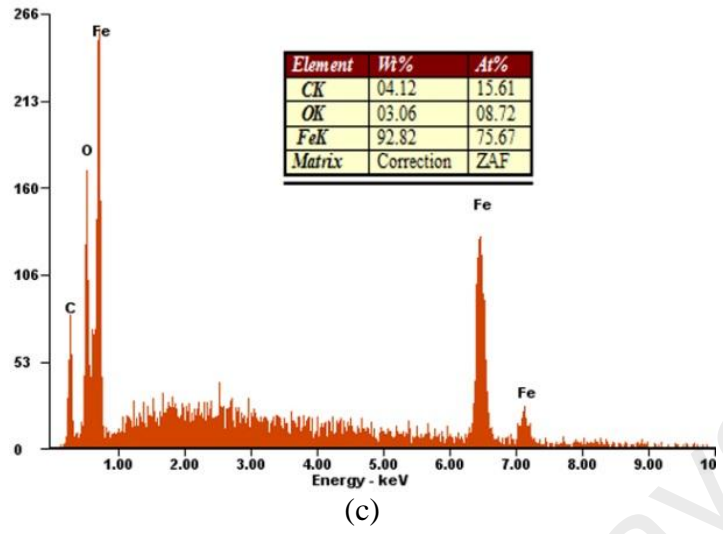
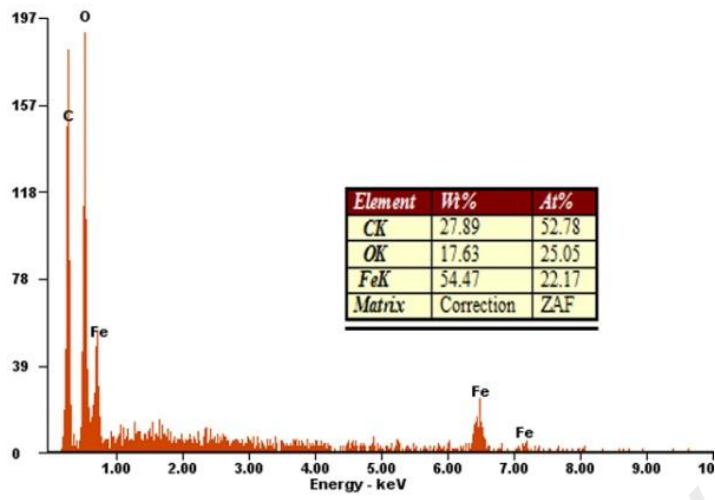
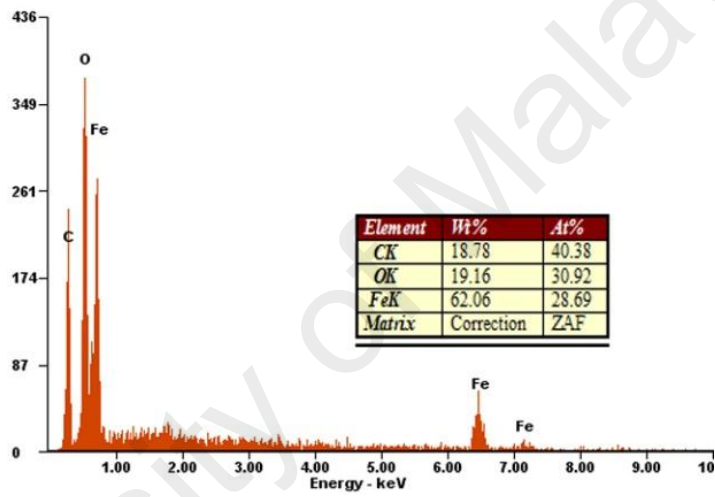


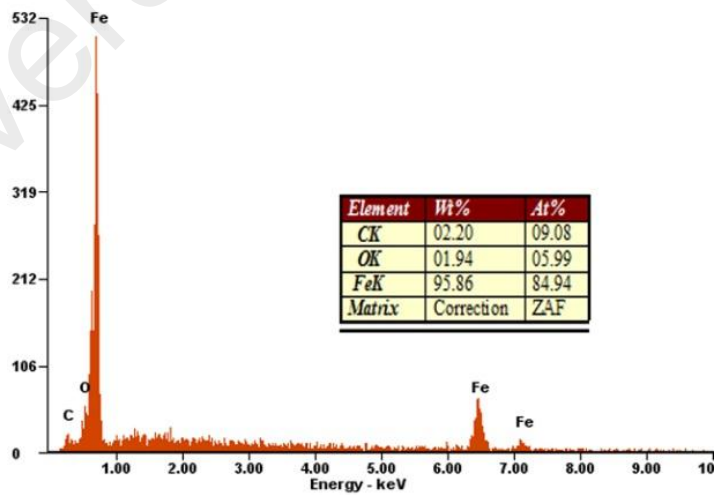
Figure 4.18: Continued



(f)

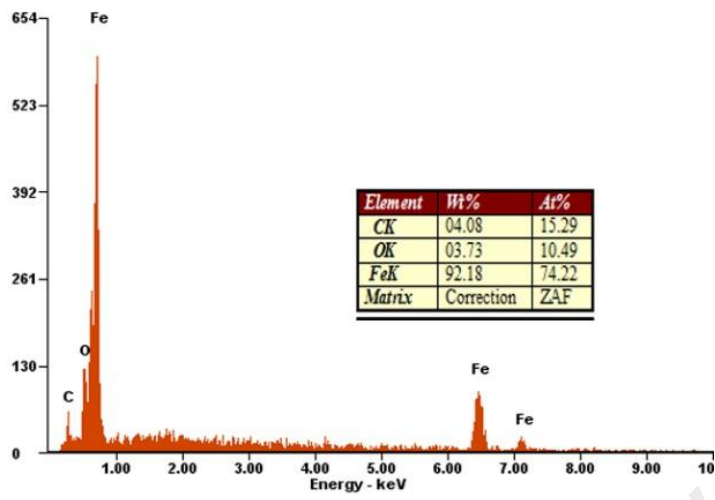


(g)

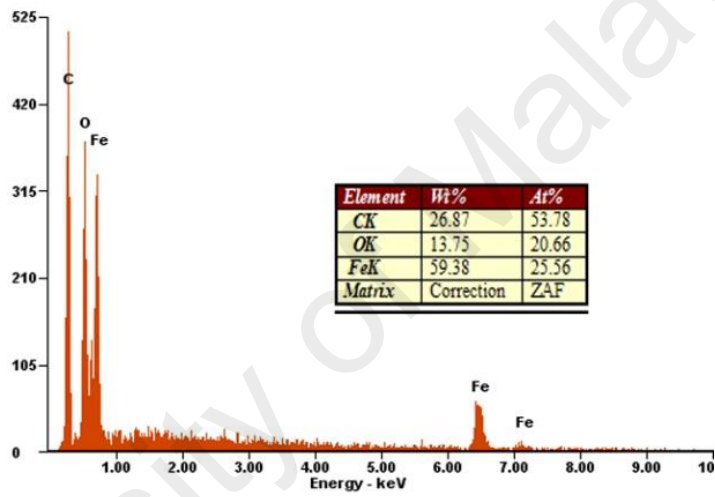


(h)

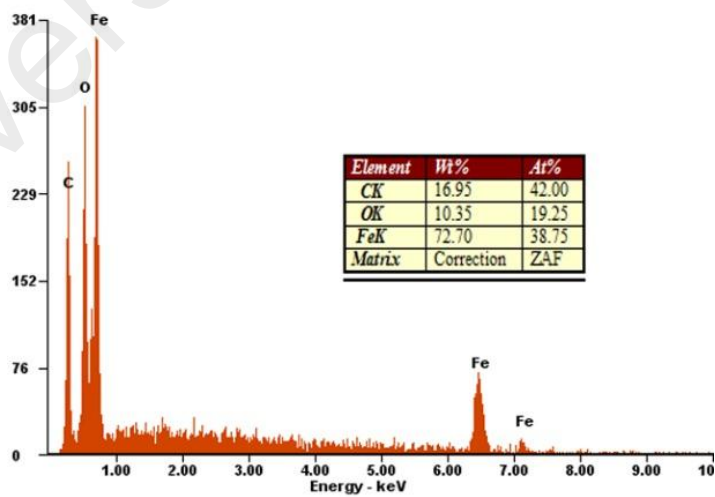
Figure 4.18: Continued



(i)



(j)



(k)

Figure 4.18: Continued

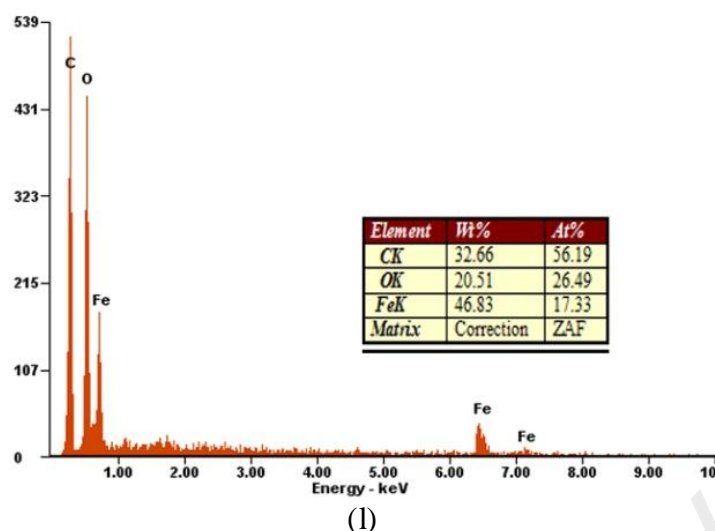


Figure 4.18: Continued

4.5.3 Effects of corrosion on fuel properties

4.5.3.1 Total acid number

TAN is the value of the concentration of acid in a non-aqueous solution. This value is derived by calculating the amount of potassium hydroxide (KOH) needed to neutralize 1 g of sample and indicates the number of carboxylic acid groups in it (Saluja et al., 2016). The standard limit of TAN value in biodiesel blend is 0.5 mg KOH/g for standards ASTM D6751 and EN 14214. TAN values of J50C50 biodiesel-diesel fuel blends and J50C50 biodiesel-bioethanol-diesel fuel blends before and after exposure to mild steel at ambient temperature is shown in **Figure 4.19**. The acid number measured for J50C50 biodiesel-diesel fuel blends for 0 h were 0.17, 0.373, 0.374, 0.428, 0.455 and 0.468 mg KOH/g, for B0, B10, B20, B30, B40 and B50, respectively and in accordance to the standards. TAN value increased with increasing time of immersion of mild steel. From **Figure 4.19**, it is known that an increase in the value of TAN played a very significant role at each time of observation due to the exposure to mild steel. Meanwhile, TAN value for diesel fuel looked more stable and slightly increased. TAN value increased on almost all the fuel indicating that metal coupons (mild steel)

participated in the oxidation process, ultimately increasing the acid concentration in the fuel mixture (Thangavelu et al., 2016). The TAN value for B50 had the highest value for each immersion time from 400 hours to 2000 hours; 1.9618, 1.95798, 2.3378, 2.4206, 2.5152 mg KOH/g, respectively. Meanwhile, the addition of bioethanol increased TAN value by an average of 21.45, 5.39, 19.91, 31.17 and 9.18%, respectively after addition of 5, 8, 10, 13 and 15% of ethanol. According to Fazal et al. (2011b) TAN value increases is caused by the rising levels of biodiesel oxidation to form free fatty acids in the fuel. The presence of corrosive acid in the fuel increased the value of TAN. In addition, the amount of acid could also be used to determine the levels of free fatty acids and other acids, which are responsible for the degradation of biodiesel (Cursaru et al., 2014).

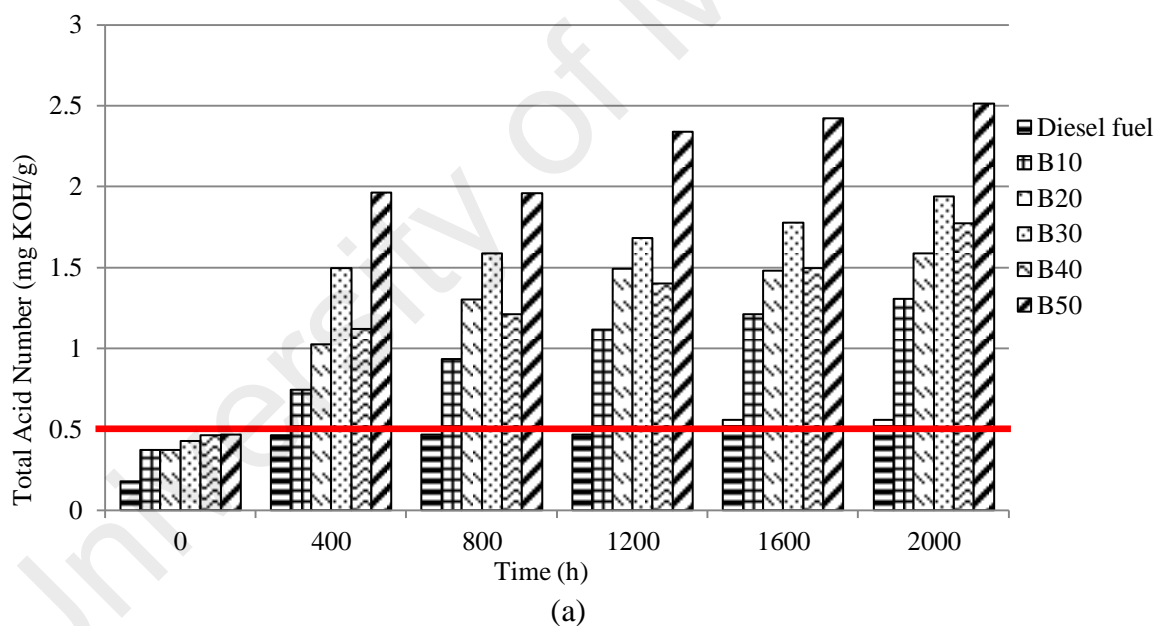


Figure 4.19: Changes in total acid number (TAN) of (a) J50C50 biodiesel-diesel fuel blends and (b) J50C50 biodiesel-bioethanol-diesel fuel blends before and after exposure to mild steel at ambient temperature for 0, 400, 800, 1200, 1600 and 2000 hours of immersion

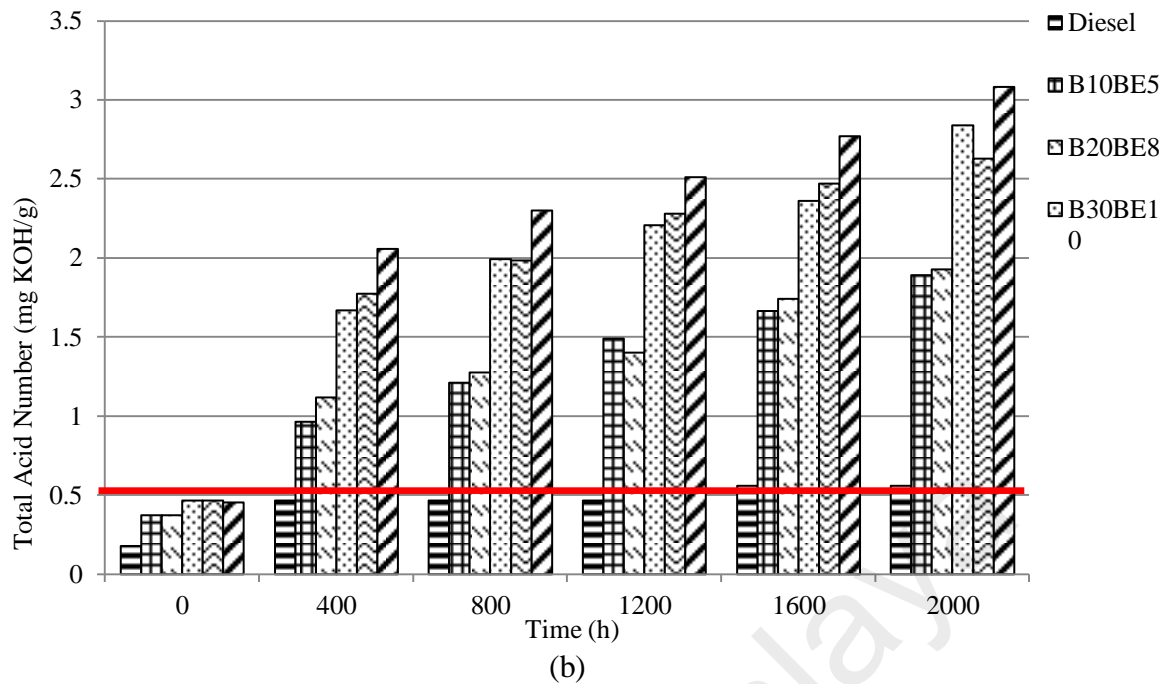


Figure 4.19: Continued

4.5.3.2 Kinematic viscosity and density

Kinematic viscosity of J50C50 biodiesel-diesel fuel blends and biodiesel-bioethanol-diesel fuel blends before and after exposure to mild steel at ambient temperature is shown in **Figure 4.20**. It is known that viscosity values increase along with the content of biodiesel in the mixture and immersion time. The viscosity for biodiesel-bioethanol-diesel fuel blends is noticeably higher than that of mixed fuels without bioethanol. The value of viscosity for maximum immersion 2000 hours for biodiesel-diesel fuel blends was 3.7096, 3.9096, 4.477, 4.7612, 4.8165 and 5.3053 mm^2/s , respectively for B0, B10, B20, B30, B40 and B50. While the kinematic viscosity for biodiesel-bioethanol-diesel fuel blends was 4.6603, 4.4764, 5.5784, 5.6316, and 6.8944 mm^2/s , respectively for the addition of 5, 8, 10, 13 and 15% of bioethanol. In this case, the change in viscosity grades of fuel mixture due to exposure to the metal which showed that metal particles (mild steel) have a considerable effect on the degradation of the fuel mixture (Thangavelu et al., 2016).

In addition, changes in density of J50C50 biodiesel-diesel fuel blends and biodiesel-bioethanol-diesel fuel blends before and after exposure to mild steel are shown in Figures 4.21 (a) and (b). Figure 4.21 (a) shows the variation of biodiesel-diesel fuel blends against the immersion time, and it is known that the highest density of the fuel for each observation time was owned by B50, 846, 849.8, 849.8, 849.9, 850.3, and 850.3 kg/cm³, respectively for 0 to 2000 hours. In addition, the addition of bioethanol into the mixture affected the density change of the fuel as shown in Figure 4.21 (b). It is known that the density increases as the immersion time increases. Density for B50E15 still looks the highest compared to other mixtures, namely 863, 879.4, 871.9, 885.5, 888.4, and 889.7 kg/cm³, respectively from 0 to 2000 hours.

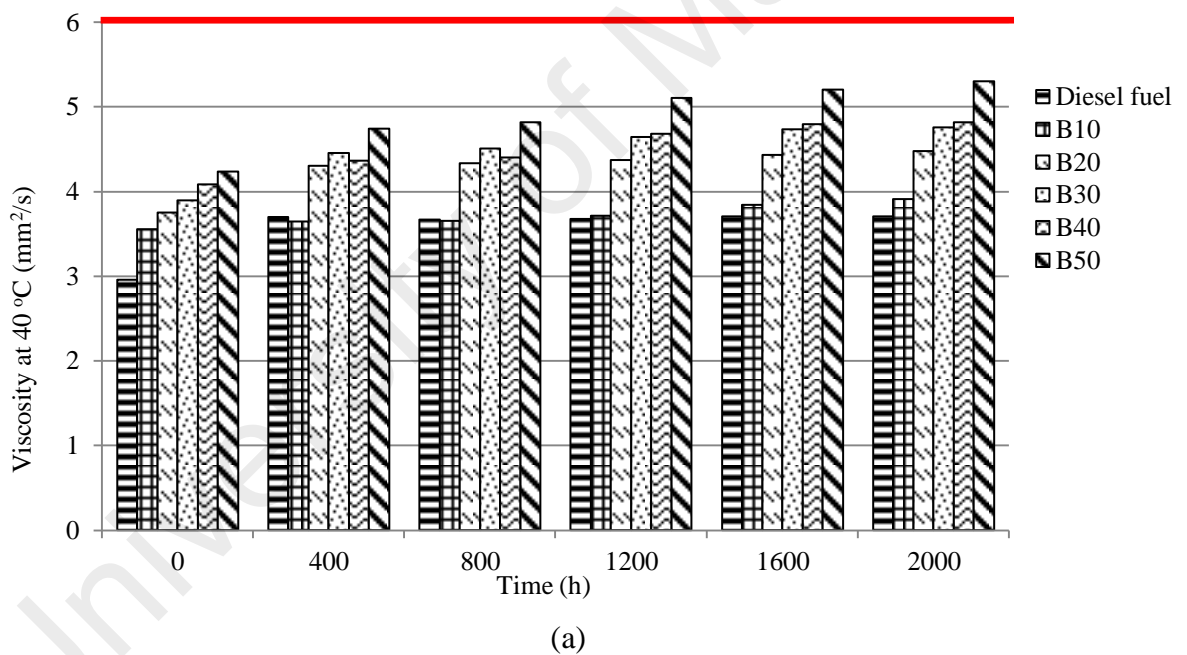
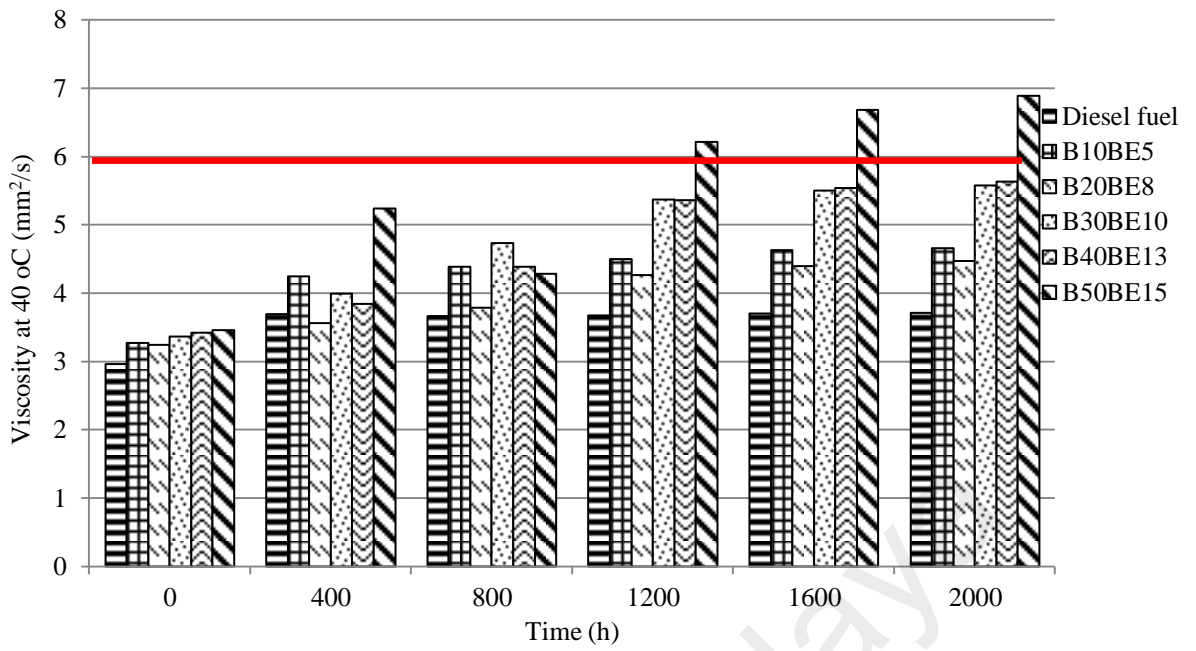
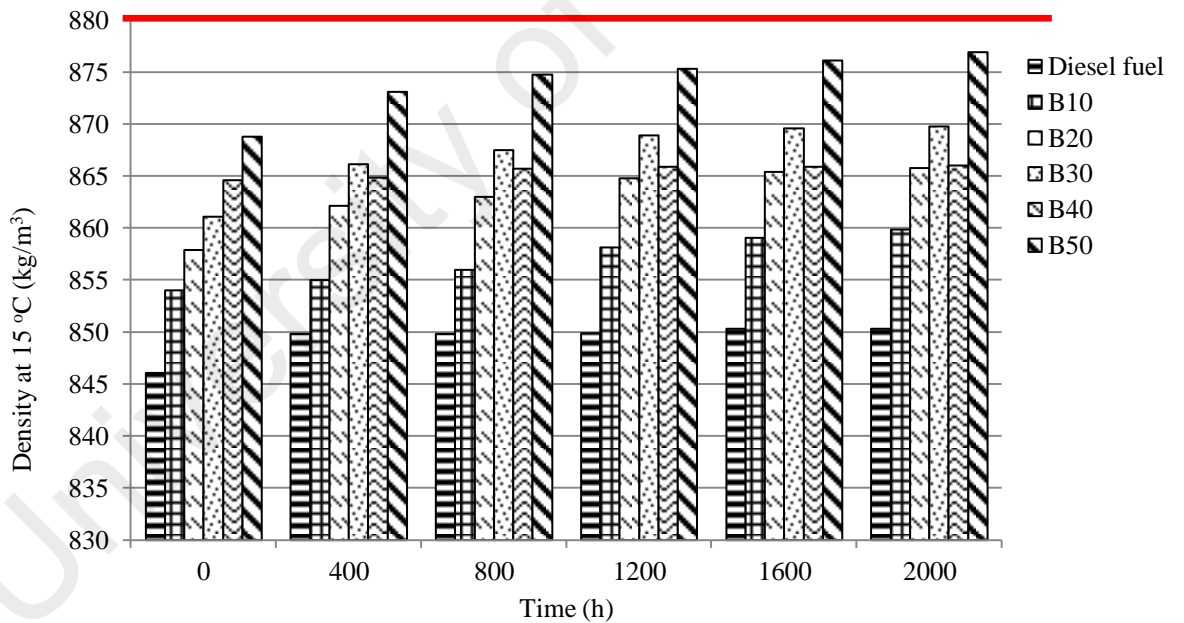


Figure 4.20: Changes in viscosity of (a) J50C50 biodiesel-diesel fuel blends and (b) J50C50 biodiesel-bioethanol-diesel fuel blends before and after exposure to mild steel at ambient temperature for 0, 400, 800, 1200, 1600 and 2000 hours of immersion



(b)

Figure 4.20: Continued



(a)

Figure 4.21: Changes in density (a) J50C50 biodiesel-diesel fuel blends and (b) J50C50 biodiesel-bioethanol-diesel fuel blends before and after exposure to mild steel at ambient temperature for 0, 400, 800, 1200, 1600 and 2000 hours of immersion.

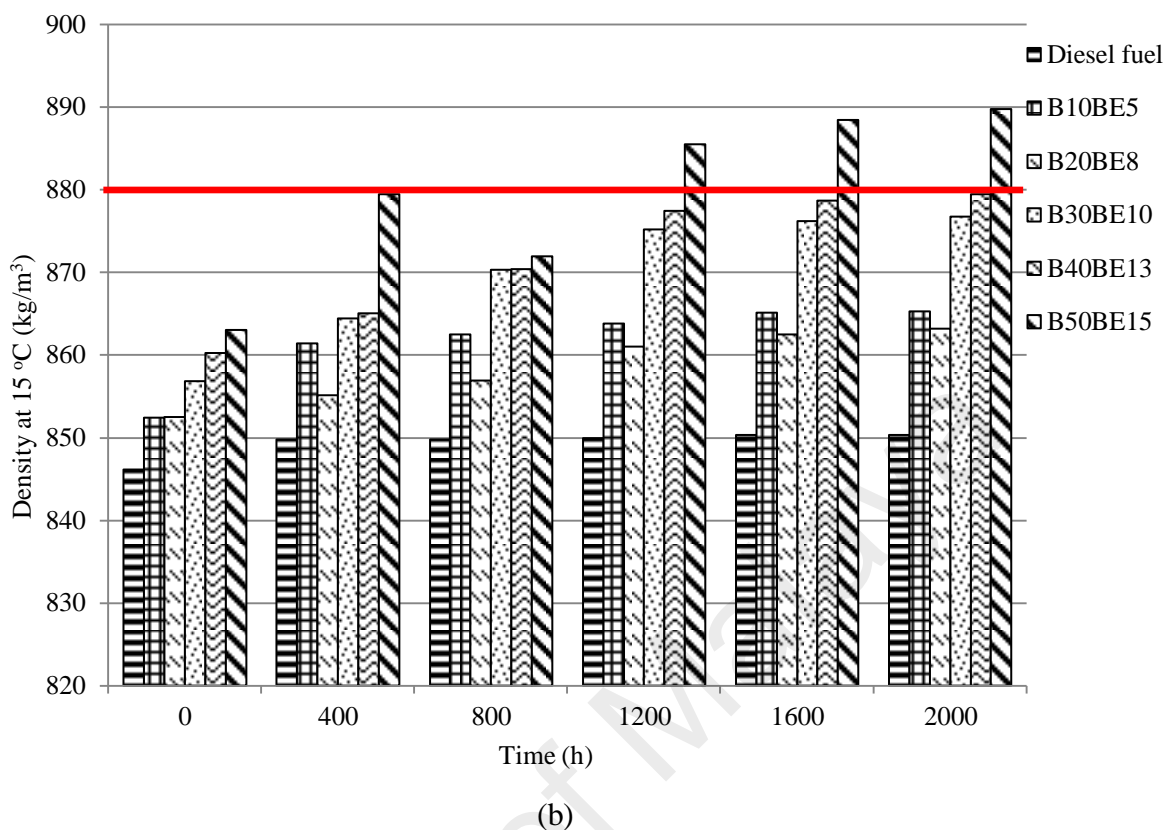


Figure 4.21: Continued

4.5.3.3 Fourier transform infrared (FTIR)

Figure 4.22 shows chemical structure analysis of the spectrum of FTIR of sediment formed on the metal mild steel after exposure to the mixture of diesel oil and J50C50 biodiesel (B0, B10, B20, B30, B40 and B50) for 0, 400, 800, 1200, 1600 and 2000 hours. Wave numbers, functional groups, tasks and absorption band absorption peak intensity were analysed in Fourier transform infrared spectrum of the overall fuel mix and presented in **Table 4.10**. The chemical structure of all types of fuel mixture caused by corrosion immersion tests up to 2000 hours witnessed some changes. Each figure shows a graph of FTIR for each fuel at the time of observation, namely 400, 800, 1200, 1600 and 2000 hours. However, for diesel fuel (B0) immersed at 800 hours, there was an invention of new peaks in the FTIR spectrum at 2359 cm^{-1} . This peak is the stretching vibration of O–H compound in the absorption intensity weak.

FTIR analysis on the overall oil mixture showed the spectrum of a sample mixture of oils wherein the main absorption bands at 2954–2953 cm^{-1} was identified as the stretch of a carbon-carbon double bonds assigned to ($=\text{C}-\text{H}$). Furthermore, the stretch of unsaturated carbon-carbon bonds in the region indicated by spectra 2922 cm^{-1} and 2853 cm^{-1} assigned to ($=\text{C}-\text{H}$). Meanwhile, the peak observed in the 1746-1744 cm^{-1} for the carbonyl functional spectrum that can be attributed to the strain ($-\text{C}=\text{O}$), which is typical esters and commonly encountered in refined oil and FAME (Soares et al., 2008). The absorption in the range of 1800–1670 cm^{-1} suggests the presence of oxidation products including aldehydes, ketones and carboxylic acids (Fazal et al., 2011c). Region 1607–1606 cm^{-1} is a stretch of carbon-carbon double bond with a weak absorption intensity, assigned to ($=\text{CH}$). The range of 1500–900 cm^{-1} , known as "fingerprint" region, was the main spectrum region that allowed for chemical discrimination between J50C50 biodiesel and its respective FAME. 1459–1458 cm^{-1} assigned to ($=\text{C}-\text{H}$) was indicated as the stretch of a carbon-carbon saturated with weak intensity. Furthermore, the stretch of the ester function can be observed in the range of 1170–1169 cm^{-1} were assigned to ($\text{C}-\text{O}-\text{C}$). Meanwhile, 722.37 cm^{-1} was out of the plane stretching of the saturated carbon-carbon bond was assigned to ($=\text{C}-\text{H}$) (Gomez et al., 2011).

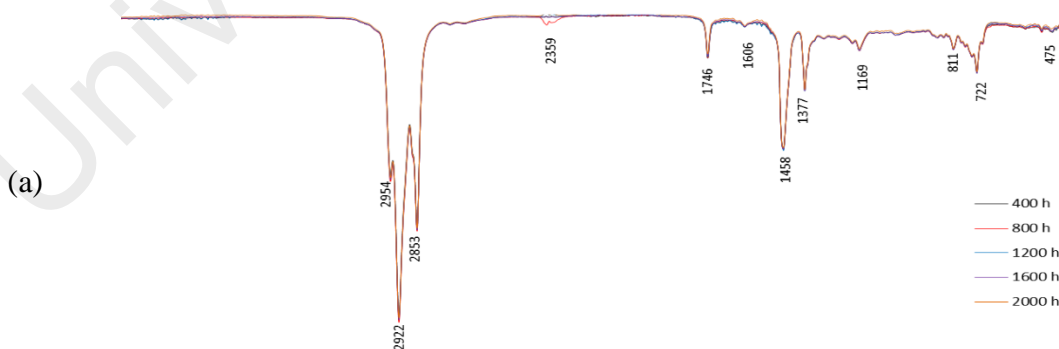


Figure 4.22: Main features of the FTIR spectrum of J50C50 biodiesel-diesel fuel sediment caused by exposure to mild steel to some fuel mixtures (a) Diesel fuel, (b) B10, (c) B20, (d) B30, (e) B40, (f) B50, (g) B10BE5, (h) B20BE8, (i) B30BE10, (j) B40BE13, and (k) B50BE15

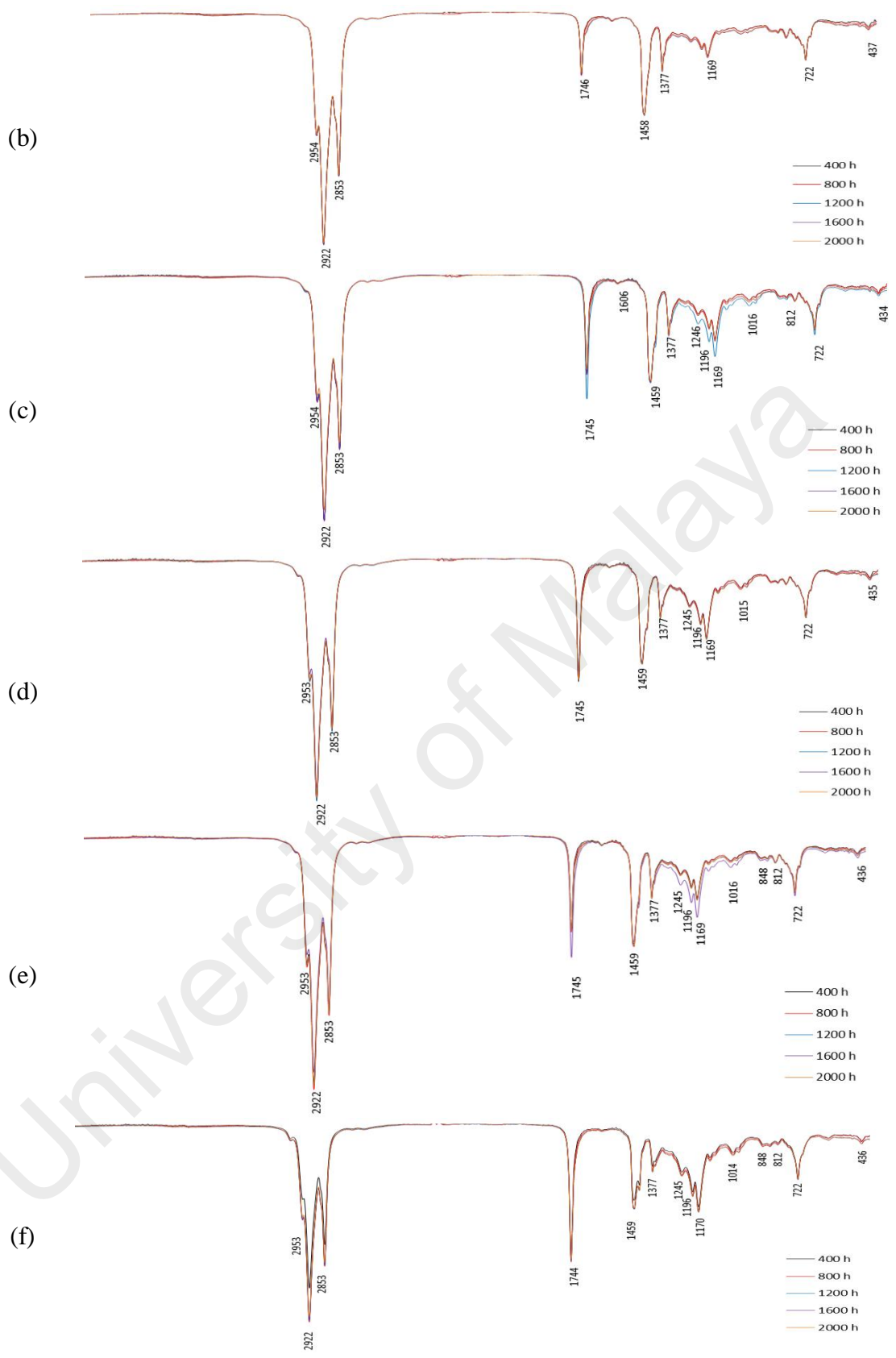


Figure 4.22: Continued

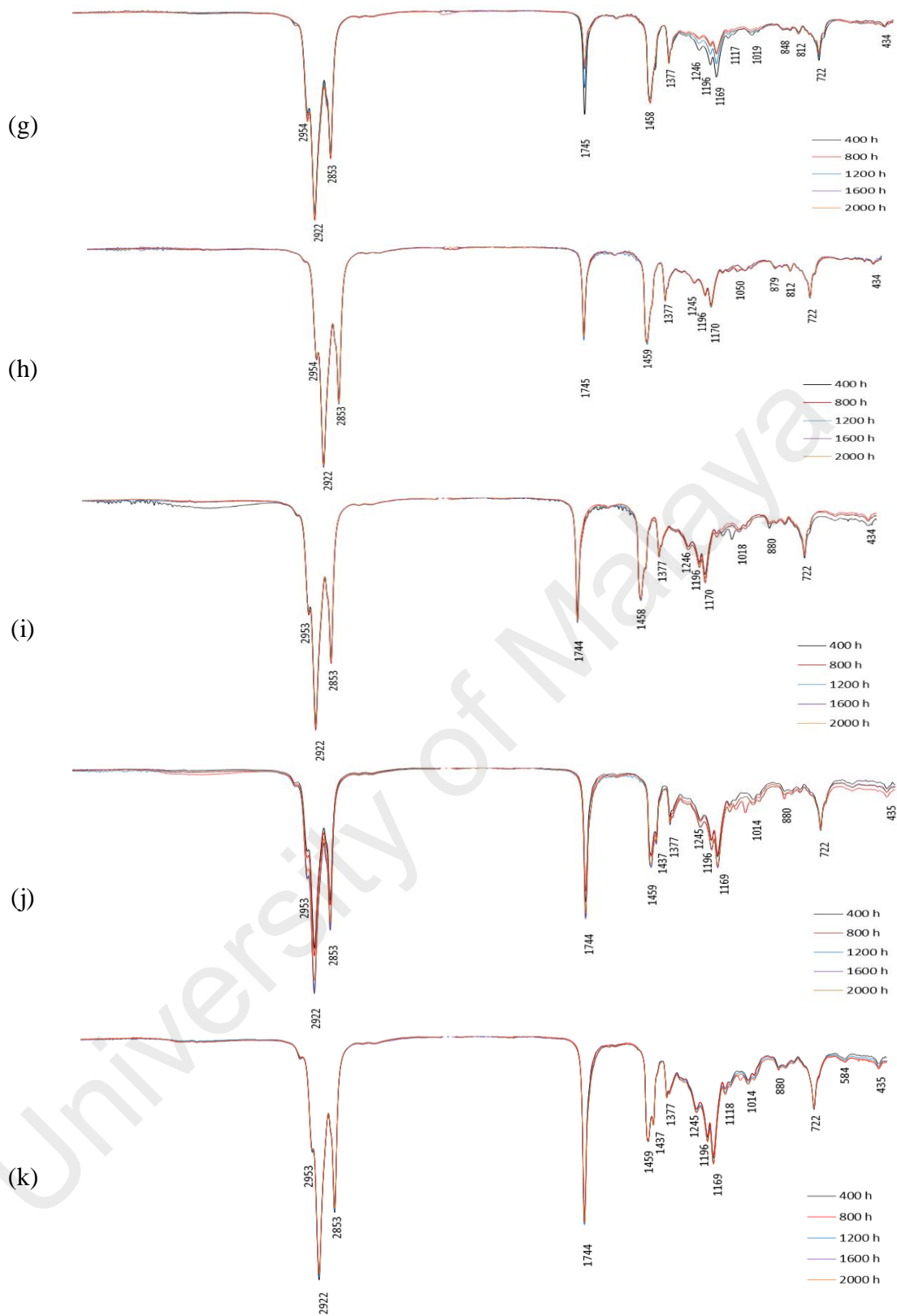


Figure 4.22: Continued

Table 4.10: Wavenumber, functional group, band assignment and absorption intensity of the absorption peaks detected in the Fourier transform infrared spectrum of the J50C50 biodiesel-diesel fuel blends

Wavenumber (cm ⁻¹)											Group attribution	Vibration type	Absorption intensity
B0	B10	B20	B30	B40	B50	B10BE5	B20BE8	B30BE10	B40BE13	B50BE15			
2954	2954	2954	2953	2953	2953	2954	2954	2953	2953	2953	=C-H	Asymmetric stretching vibration	Strong
2922	2922	2922	2922	2922	2922	2922	2922	2922	2922	2922	=C-H	Asymmetric stretching vibration	Strong
2853	2853	2853	2853	2853	2853	2853	2853	2853	2853	2853	-CH ₂	Symmetric stretching vibration	Strong
2359	-	-	-	-	-	-	-	-	-	-	O-H	stretching vibration	Weak
1746	-	1745	1745	1745	1744	1745	1745	1744	1744	1744	-C=O	Stretching	Strong
1606	1607	1606	1606	1606	-	-	-	-	-	-	=C-H	vibration (overtone)	Weak
1458	1458	1459	1459	1459	1459	1458	1459	1458	1459	1459	-CH ₂	Shear-type vibration	Weak
1377	1377	1377	1377	1377	1377	1377	1377	1377	1377	1377	-CH ₃	Bending vibration	Weak
-	1246	1246	1245	1245	1245	1246	1245	1246	1245	1245	=C-H	deformation vibration	Weak
-	-	1196	1196	1196	1196	1196	1196	1196	1196	1196	C-O-C	Anti-symmetric stretching vibration	Middling
1169	1169	1169	1169	1169	1170	1169	1170	1170	1116	1116	C-O-C	Anti-symmetric stretching vibration	Middling
-	1019	1016	1015	1016	1014	1019	-	1018	1014	1014	C-O-C	Anti-symmetric stretching vibration	Weak
811	812	812	812	812	812	848	879	880	880	880	C-O-C	Stretching vibration	Weak
722	722	722	722	722	722	722	722	722	722	722	-CH ₂	Plane rocking vibration	Weak
435	437	434	435	436	436	434	434	434	435	435	C-C	Skeleton vibration	Weak

4.5.4 Summary

The corrosion testing was carried out at temperatures of 25–30 °C (ambient temperature) through immersion of mild steel coupons in biodiesel-diesel blend and biodiesel-bioethanol-diesel fuel blend up to 2000 hours. Analysis of the corrosion rate and fuel properties was performed every 400 h of the immersion period. The main findings of this test series are summarized as follows:

- 1 The mild steel corrosion rate appeared faster for biodiesel diesel fuel blends. However, A 10% biodiesel diesel fuel blends had a smaller corrosion rate (800 hours of initial immersion). Meanwhile, the bioethanol content in the fuel caused higher corrosion rate, the corrosion rate increased as the bioethanol content increased.
- 2 Corrosion analysis using SEM indicated that corrosion occurs on the surface of the material characterized by the change of metal surface color and round pits. Additionally, EDX testing showed the occurrence of increased oxygen on the material after the addition of biodiesel and bioethanol, indicating that mild steel was oxidized.
- 3 The influence of corrosion on fuel properties showed an increase in total acid number, viscosity and density along with increasing duration of immersion time.

CHAPTER 5: CONCLUSION AND RECOMMENDATIONS

5.1 Conclusion

The experiments had been conducted in this study to analyze the potential of combining several types of raw materials such as *J.curcas* and *C. pentandra* based on properties of crude oil. Furthermore, there was also an investigation of engine performance and exhaust emissions on a single-cylinder direct-injection diesel engine using biodiesel-diesel fuel blend and biodiesel-bioethanol-diesel fuel blend. At the final stage, the analysis of the influence of mixed fuel on corrosion of mild steel with static immersion up to 2000 hours was performed. Therefore, from the series of tests above, it can be concluded as follows:

1. Mixing two types of raw materials such as *J. curcas* and *C. pentandra* based on properties crude oil produces a mixture of J50C50 as the best mixture and suitable for conversion into biodiesel.
2. J50C50 oil mixture was selected for biodiesel conversion through a two-steps process (acid-catalysed esterification followed by alkali-catalysed transesterification). Response surface methodology based on Box-Behnken experimental design has been implemented to obtain the maximum yield for the J50C50 biodiesel. The optimum operating parameters for transesterification of the J50C50 oil mixture at 60 ° C over a period of 2 hours were as follows: methanol-to-oil ratio: 30%, agitation speed: 1300 rpm and KOH catalyst concentration: 0.5 wt.%. These optimum operating parameters gave the highest yield for the J50C50 biodiesel, with a value of 93.33%. The physicochemical properties of the produced J50C50 biodiesel fulfilled requirements in ASTM D6751 and EN 14214 standards. As the values are close to the physicochemical properties of diesel and therefore, it can be concluded that the optimized J50C50 biodiesel is a potential substitute of diesel fuel.

3. The effect of biodiesel-diesel fuel blends and biodiesel-bioethanol-diesel fuel blends on the performance of the engine and exhaust emissions of a single-cylinder four-stroke compression ignition engine had been explored thoroughly in this study. In general, all of the fuel blends investigated in this study fulfill the ASTM D6751 and EN 14214 standards. The results show that the B10 blend (10% of J50C50 biodiesel-diesel fuel) has physicochemical properties similar to diesel fuel. The B10 blend has better exhaust emissions compared to diesel fuel such as CO₂ and smoke opacity, which are lower on average by 20.65% and 23.43%, respectively. The B10 blend had higher engine torque, brake power and brake thermal efficiency compared to other fuel blends, with a value of 26.07 Nm, 5.2 kW and 25.79%, respectively. More importantly, the CO and NO_x emissions as well as smoke opacity were the lowest at an engine speed of 1900 rpm for all J50C50 biodiesel-diesel fuel blends investigated in this study, indicating that this speed is an ideal condition for the engine. Overall, the addition of J50C50 biodiesel into diesel fuel reduced CO emissions and smoke opacity. However, it increased the NO_x emissions at full load. Meanwhile, the addition of bioethanol in the mix caused the occurrence of changes in fuel properties occur such as decreased kinematic viscosity, density, and calorific value, while on the other hand it increased flash point and pour point. The engine performance test also shows that the B10BE5 blend had better brake power, engine torque, thermal efficiency of the bakes, NO_x emissions and smoke opacity than the other blends. CO₂ emissions and smoke opacities for The B10BE5 blend are known to be lower than diesel fuels, the decline averaging 49.3% and 28.34%, respectively. Overall, the addition of bioethanol into the mixture showed a significant reduction such as brake power, engine torque, brake thermal efficiency, and exhaust emissions such as NO_x and smoke opacity.

4. Analysis of the corrosion on mild steel immersed in J50C50 biodiesel-diesel fuel blends in the period up to 2000 hours had also been carried out and observed. There were some observations on changes in mild steel coupons and the properties of the fuel mixture, which had been investigated in this study. The results showed that the downward trend in the rate of corrosion due to the increasing immersion time of mild steel coupons in J50C50 biodiesel-diesel fuel blend. It is known that the B10 has a corrosion rate very close to diesel fuel, as even for long periods of immersion 400 hours and 800 hours, B10 was better than diesel fuel with the corrosion rate of 0.0011 and 0.0043 mm/year, respectively. Meanwhile, the addition of bioethanol into the biodiesel-diesel fuel blends showed a rising corrosion rate up to 1200 hours of immersion, after which the corrosion rate was seen to decrease. B10BE5 had a corrosion rate close to diesel fuel, but still higher than the corrosion rate of B10. The surface observation of the mild steel coupons using SEM suggests corrosion attack, which is characterized by the round pits on the surface of the metal. The mild steel corrosion attack was seen more in materials immersed in biodiesel-diesel fuel blends and biodiesel-bioethanol-diesel fuel blends compared with diesel fuel. Overall, the addition of J50C50 biodiesel and bioethanol into diesel fuel caused increased corrosion rate and TAN. Exposure of biodiesel-diesel fuel blends and biodiesel-bioethanol-diesel fuel to mild steel led to changes in fuel properties such as viscosity and density. However, for small amounts of mixtures, the increase in viscosity and density was still within the limits specified by the ASTM D6751 standard.

5.2 Recommendations

The depletion of fossil-based petroleum reserves is the main reason for the development of renewable and biodegradable fuels. Therefore, researchers explore various sources of raw materials to be converted into fuel. Biodiesel is one of the most promising fuel, considering that it is very environmentally friendly. The study provides

several recommendations to improve the quality and production capacity and improvements in its application in the engine. The recommendations are as follows:

1. To obtain optimum methyl ester yield, it is very important to influence biodiesel production parameters such as methanol-to-oil ratio, speed agitation, catalyst concentration, reaction temperature and processing time. In mass production, optimization should be done in advance to obtain optimal parameters.
2. Biodiesel production through esterification and transesterification process using methanol to shorten the reaction of triglyceride convert to methyl ester. Methanol will eventually be separated from methyl esters and is a waste product in the biodiesel production process. Therefore, a more in-depth study is needed to make use of residual methanol production through purification and separation processes from homogeneous catalysts and other impurities, to be reused in further biodiesel production processes.
3. Biodiesel-diesel and biodiesel-bioethanol-diesel fuel blends had been tested in the engine to determine changes in engine performance and exhaust emissions. In this case, exhaust emissions have decreased significantly. However, the use of such mixed fuels over a long period of time will inevitably have an impact on engine components and material durability, albeit in very small percentages. Therefore, there is a need for advanced researches that focuses on the observation of material durability to produce biodiesel that is feasible and safe to use.

Finally, this study is expected to be a reference to produce biodiesel from multiple feedstocks to increase production, improve its characteristic properties, improve engine performance and reduce exhaust emissions.

REFERENCES

- Acevedo, J. C., Hernández, J. A., Valdés, C. F., & Khanal, S. K. (2015). Analysis of operating costs for producing biodiesel from palm oil at pilot-scale in Colombia. *Bioresource Technol.*, *188*, 117-123.
- Adewale, P., Dumont, M.-J., & Ngadi, M. (2015). Recent trends of biodiesel production from animal fat wastes and associated production techniques. *Renew Sust Energ Rev.*, *45*, 574-588.
- Agarwal, A. K., Dhar, A., Gupta, J. G., Kim, W. I., Choi, K., Lee, C. S., & Park, S. (2015). Effect of fuel injection pressure and injection timing of Karanja biodiesel blends on fuel spray, engine performance, emissions and combustion characteristics. *Energ Convers Manage*, *91*, 302-314.
- Agarwal, A. K., Gupta, T., Shukla, P. C., & Dhar, A. (2015). Particulate emissions from biodiesel fuelled CI engines. *Energ Convers Manage*, *94*, 311-330.
- Ahmad, A., Yasin, N. M., Derek, C., & Lim, J. (2011). Microalgae as a sustainable energy source for biodiesel production: a review. *Renew Sust Energ Rev.*, *15*(1), 584-593.
- Ahmad, J., Yusup, S., Bokhari, A., & Kamil, R. N. M. (2014). Study of fuel properties of rubber seed oil based biodiesel. *Energ Convers Manage*, *78*, 266-275.
- Al-Hamamre, Z., & Yamin, J. (2014). Parametric study of the alkali catalyzed transesterification of waste frying oil for Biodiesel production. *Energ Convers Manage*, *79*, 246-254.
- Al-Hasan, M. (2003). Effect of ethanol–unleaded gasoline blends on engine performance and exhaust emission. *Energ Convers Manage*, *44*(9), 1547-1561.
- Al-Hassan, M., Mujafet, H., & Al-Shannag, M. (2012). An Experimental Study on the Solubility of a Diesel-Ethanol Blend and on the Performance of a Diesel Engine Fueled with Diesel-Biodiesel-Ethanol Blends. *Jordan Journal of Mechanical & Industrial Engineering*, *6*(2), 147 - 153.
- Al Basir, F., Datta, S., & Roy, P. K. (2015). Studies on biodiesel production from *Jatropha curcas* oil using chemical and biochemical methods—A mathematical approach. *Fuel*, *158*, 503-511.

- Alicke, A. A., Leopércio, B. C., Marchesini, F. H., & de Souza Mendes, P. R. (2015). Guidelines for the rheological characterization of biodiesel. *Fuel*, *140*, 446-452.
- Altenburg, T. (2010). Biodiesel policies for India: achieving optimal socio-economic and environmental impact. *Journal of Biofuels*, *1*(1), 163-171.
- Altun, Ş., & Lapuerta, M. (2014). Properties and emission indicators of biodiesel fuels obtained from waste oils from the Turkish industry. *Fuel*, *128*, 288-295.
- An, H., Yang, W., Maghbouli, A., Li, J., Chou, S., & Chua, K. (2013). Performance, combustion and emission characteristics of biodiesel derived from waste cooking oils. *Appl Energ*, *112*, 493-499.
- Anand, K., Sharma, R., & Mehta, P. S. (2011). Experimental investigations on combustion, performance and emissions characteristics of neat karanja biodiesel and its methanol blend in a diesel engine. *Biomass bioenerg*, *35*(1), 533-541.
- Anderson, J., DiCicco, D., Ginder, J., Kramer, U., Leone, T., Raney-Pablo, H., & Wallington, T. (2012). High octane number ethanol-gasoline blends: Quantifying the potential benefits in the United States. *Fuel*, *97*, 585-594.
- Armas, O., Martínez-Martínez, S., & Mata, C. (2011). Effect of an ethanol-biodiesel-diesel blend on a common rail injection system. *Fuel Process Technol*, *92*(11), 2145-2153.
- Ashokkumar, V., Salam, Z., Sathishkumar, P., Hadibarata, T., Yusoff, A. R. M., & Ani, F. N. (2015). Exploration of fast growing *Botryococcus sudeticus* for upstream and downstream process in sustainable biofuels production. *J Clean Prod*, *92*, 162-167.
- Ashraful, A. M., Masjuki, H., Kalam, M., Fattah, I. R., Imtenan, S., Shahir, S., & Mobarak, H. (2014). Production and comparison of fuel properties, engine performance, and emission characteristics of biodiesel from various non-edible vegetable oils: a review. *Energ Convers Manage*, *80*, 202-228.
- ASTM. (2004). Standard Practice for Laboratory Immersion Corrosion Testing of Metals. Annual Book of ASTM Standards. *ASTM, Philadelphia, PA, G31-72*.
- Atabani, A., & da Silva César, A. (2014). *Calophyllum inophyllum* L.—A prospective non-edible biodiesel feedstock. Study of biodiesel production, properties, fatty acid composition, blending and engine performance. *Renew Sust Energ Rev.*, *37*, 644-655.

- Atabani, A., Mahlia, T., Badruddin, I. A., Masjuki, H., Chong, W., & Lee, K. T. (2013). Investigation of physical and chemical properties of potential edible and non-edible feedstocks for biodiesel production, a comparative analysis. *Renew Sust Energ Rev.*, *21*, 749-755.
- Atabani, A., Mahlia, T., Masjuki, H., Badruddin, I. A., Yussof, H. W., Chong, W., & Lee, K. T. (2013). A comparative evaluation of physical and chemical properties of biodiesel synthesized from edible and non-edible oils and study on the effect of biodiesel blending. *Energy*, *58*, 296-304.
- Atabani, A., Silitonga, A., Ong, H., Mahlia, T., Masjuki, H., Badruddin, I. A., & Fayaz, H. (2013). Non-edible vegetable oils: a critical evaluation of oil extraction, fatty acid compositions, biodiesel production, characteristics, engine performance and emissions production. *Renew Sust Energ Rev.*, *18*, 211-245.
- Atabani, A. E., Silitonga, A. S., Badruddin, I. A., Mahlia, T., Masjuki, H., & Mekhilef, S. (2012). A comprehensive review on biodiesel as an alternative energy resource and its characteristics. *Renew Sust Energ Rev.*, *16*(4), 2070-2093.
- Attia, A. M., & Hassaneen, A. E. (2016). Influence of diesel fuel blended with biodiesel produced from waste cooking oil on diesel engine performance. *Fuel*, *167*, 316-328.
- Awad, S., Loubar, K., & Tazerout, M. (2014). Experimental investigation on the combustion, performance and pollutant emissions of biodiesel from animal fat residues on a direct injection diesel engine. *Energy.*, *69*, 826-836.
- Awad, S., Paraschiv, M., Varuvel, E. G., & Tazerout, M. (2013). Optimization of biodiesel production from animal fat residue in wastewater using response surface methodology. *Bioresource Technol.*, *129*, 315-320.
- Aydin, C. (2007). Some engineering properties of peanut and kernel. *J Food Eng*, *79*(3), 810-816.
- Aydın, F., & Öğüt, H. (2017). Effects of using ethanol-biodiesel-diesel fuel in single cylinder diesel engine to engine performance and emissions. *Renew Energ*, *103*, 688-694.
- Aydın, H., & Bayindir, H. (2010). Performance and emission analysis of cottonseed oil methyl ester in a diesel engine. *Renew Energ*, *35*(3), 588-592.

- Aydın, S., & Sayın, C. (2014). Impact of thermal barrier coating application on the combustion, performance and emissions of a diesel engine fueled with waste cooking oil biodiesel–diesel blends. *Fuel*, 136, 334-340.
- Aydoğan, H., & Acaroglu, M. (2013). Effects of bioethanol-diesel fuel blends containing beramid ED10 additive on engine performance. *International Journal of Arts & Sciences*, 6(1), 57.
- Badday, A. S., Abdullah, A. Z., & Lee, K.-T. (2013). Optimization of biodiesel production process from Jatropha oil using supported heteropolyacid catalyst and assisted by ultrasonic energy. *Renew Energ*, 50, 427-432.
- Baena, L., Gómez, M., & Calderón, J. (2012). Aggressiveness of a 20% bioethanol–80% gasoline mixture on autoparts: I behavior of metallic materials and evaluation of their electrochemical properties. *Fuel*, 95, 320-328.
- Balat, M. (2007). Global bio-fuel processing and production trends. *Energ Explor Exploit*, 25(3), 195-218.
- Balat, M. (2009). Global status of biomass energy use. *Energ Source Part A*, 31(13), 1160-1173.
- Balat, M. (2011). Production of bioethanol from lignocellulosic materials via the biochemical pathway: a review. *Energ Convers Manage*, 52(2), 858-875.
- Balat, M., Balat, H., & Öz, C. (2008). Progress in bioethanol processing. *Prog energ combust*, 34(5), 551-573.
- Banapurmath, N., Tewari, P., & Hosmath, R. (2008). Performance and emission characteristics of a DI compression ignition engine operated on Honge, Jatropha and sesame oil methyl esters. *Renew Energ*, 33(9), 1982-1988.
- Banerjee, M., Dey, B., Talukdar, J., & Kalita, M. C. (2014). Production of biodiesel from sunflower oil using highly catalytic bimetallic gold–silver core–shell nanoparticle. *Energy*, 69, 695-699.
- Banković-Ilić, I. B., Stojković, I. J., Stamenković, O. S., Veljković, V. B., & Hung, Y.-T. (2014). Waste animal fats as feedstocks for biodiesel production. *Renew Sust Energ Rev.*, 32, 238-254.

- Barabás, I. (2015). Liquid densities and excess molar volumes of ethanol+ biodiesel binary system between the temperatures 273.15 K and 333.15 K. *J Mol Liq*, 204, 95-99.
- Barabas, I., Todoruț, A., & Băldean, D. (2010). Performance and emission characteristics of an CI engine fueled with diesel–biodiesel–bioethanol blends. *Fuel*, 89(12), 3827-3832.
- Bari, S. (2014). Performance, combustion and emission tests of a metro-bus running on biodiesel-ULSD blended (B20) fuel. *Appl Energ*, 124, 35-43.
- Bari, S., & Saad, I. (2015). Performance and emissions of a compression ignition (CI) engine run with biodiesel using guide vanes at varied vane angles. *Fuel*, 143, 217-228.
- Bayraktar, H. (2005). Experimental and theoretical investigation of using gasoline–ethanol blends in spark-ignition engines. *Renew Energ*, 30(11), 1733-1747.
- Behçet, R. (2011). Performance and emission study of waste anchovy fish biodiesel in a diesel engine. *Fuel Process Technol*, 92(6), 1187-1194.
- Betiku, E., Omilakin, O. R., Ajala, S. O., Okeleye, A. A., Taiwo, A. E., & Solomon, B. O. (2014). Mathematical modeling and process parameters optimization studies by artificial neural network and response surface methodology: a case of non-edible neem (*Azadirachta indica*) seed oil biodiesel synthesis. *Energy*, 72, 266-273.
- Betiku, E., & Taiwo, A. E. (2015). Modeling and optimization of bioethanol production from breadfruit starch hydrolyzate vis-à-vis response surface methodology and artificial neural network. *Renew Energ*, 74, 87-94.
- Bhardwaj, M., Gupta, P., & Kumar, N. (2014). Compatibility of metals and elastomers in biodiesel-a review. *Int J Res*, 1, 376-391.
- Bilgen, S. (2014). Structure and environmental impact of global energy consumption. *Renew Sust Energ Rev.*, 38, 890-902.
- Bindhu, C., Reddy, J., Rao, B., Ravinder, T., Chakrabarti, P., Karuna, M., & Prasad, R. (2012). Preparation and evaluation of biodiesel from *Sterculia foetida* seed oil. *J Am Oil Chem Soc*, 89(5), 891-896.

- Binod, P., Sindhu, R., Singhanian, R. R., Vikram, S., Devi, L., Nagalakshmi, S., . . . Pandey, A. (2010). Bioethanol production from rice straw: an overview. *Bioresource Technol.*, *101*(13), 4767-4774.
- Boey, P.-L., Ganesan, S., Maniam, G. P., Khairuddean, M., & Efendi, J. (2013). A new heterogeneous acid catalyst for esterification: optimization using response surface methodology. *Energ Convers Manage*, *65*, 392-396.
- Boniatti, R., Bandeira, A. L., Crespi, Â. E., Aguzzoli, C., Baumvol, I. J., & Figueroa, C. A. (2013). The influence of surface microstructure and chemical composition on corrosion behaviour in fuel-grade bio-ethanol of low-alloy steel modified by plasma nitro-carburizing and post-oxidizing. *Appl Surf Sci*, *280*, 156-163.
- Boog, J. H. F., Silveira, E. L. C., De Caland, L. B., & Tubino, M. (2011). Determining the residual alcohol in biodiesel through its flash point. *Fuel*, *90*(2), 905-907.
- Bora, D. K., Baruah, D., Das, L., & Babu, M. (2012). Performance of diesel engine using biodiesel obtained from mixed feedstocks. *Renew Sust Energ Rev.*, *16*(8), 5479-5484.
- Bracco, S. (2015). Effectiveness of EU biofuels sustainability criteria in the context of land acquisitions in Africa. *Renew Sust Energ Rev.*, *50*, 130-143.
- Buyukkaya, E. (2010). Effects of biodiesel on a DI diesel engine performance, emission and combustion characteristics. *Fuel*, *89*(10), 3099-3105.
- Campanelli, P., Banchero, M., & Manna, L. (2010). Synthesis of biodiesel from edible, non-edible and waste cooking oils via supercritical methyl acetate transesterification. *Fuel*, *89*(12), 3675-3682.
- Can, Ö. (2014). Combustion characteristics, performance and exhaust emissions of a diesel engine fueled with a waste cooking oil biodiesel mixture. *Energ Convers Manage*, *87*, 676-686.
- Canakci, M., Ozsezen, A. N., Arcaklioglu, E., & Erdil, A. (2009). Prediction of performance and exhaust emissions of a diesel engine fueled with biodiesel produced from waste frying palm oil. *Expert Syst Appl*, *36*(5), 9268-9280.
- Canakci, M., & Sanli, H. (2008). Biodiesel production from various feedstocks and their effects on the fuel properties. *J Ind Microbiol Biot*, *35*(5), 431-441.

- Cao, L., Frankel, G., & Sridhar, N. (2013). Effect of chloride on stress corrosion cracking susceptibility of carbon steel in simulated fuel grade ethanol. *Electrochim Acta*, 104, 255-266.
- Carareto, N. D., Kimura, C. Y., Oliveira, E. C., Costa, M. C., & Meirelles, A. J. (2012). Flash points of mixtures containing ethyl esters or ethylic biodiesel and ethanol. *Fuel*, 96, 319-326.
- Caspeta, L., Buijs, N. A., & Nielsen, J. (2013). The role of biofuels in the future energy supply. *Energ Environ Sci*, 6(4), 1077-1082.
- Černoch, M., Hájek, M., & Skopal, F. (2010). Relationships among flash point, carbon residue, viscosity and some impurities in biodiesel after ethanolysis of rapeseed oil. *Bioresource Technol.*, 101(19), 7397-7401.
- Chattopadhyay, S., & Sen, R. (2013). Fuel properties, engine performance and environmental benefits of biodiesel produced by a green process. *Appl Energ*, 105, 319-326.
- Chellamboli, C., & Perumalsamy, M. (2014). Application of response surface methodology for optimization of growth and lipids in *Scenedesmus abundans* using batch culture system. *RSC Adv*, 4(42), 22129-22140.
- Chen, H., Xie, B., Ma, J., & Chen, Y. (2018). NO_x emission of biodiesel compared to diesel: higher or lower? *Appl Therm Eng*.
- Chen, H., Zhou, D., Luo, G., Zhang, S., & Chen, J. (2015). Macroalgae for biofuels production: Progress and perspectives. *Renew Sust Energ Rev.*, 47, 427-437.
- Chen, Y.-H., & Luo, Y.-M. (2011). Oxidation stability of biodiesel derived from free fatty acids associated with kinetics of antioxidants. *Fuel Process Technol*, 92(7), 1387-1393.
- Cheng, J. J., & Timilsina, G. R. (2011). Status and barriers of advanced biofuel technologies: a review. *Renew Energ*, 36(12), 3541-3549.
- Chetty, C., Rossin, C., Gruissem, W., Vanderschuren, H., & Rey, M. (2013). Empowering biotechnology in southern Africa: establishment of a robust transformation platform for the production of transgenic industry-preferred cassava. *New Biotechnol*, 30(2), 136-143.

- Chew, K., Haseeb, A., Masjuki, H., Fazal, M., & Gupta, M. (2013). Corrosion of magnesium and aluminum in palm biodiesel: A comparative evaluation. *Energy*, 57, 478-483.
- Chhetri, A., & Watts, K. (2012). Densities of canola, jatropha and soapnut biodiesel at elevated temperatures and pressures. *Fuel*, 99, 210-216.
- Chotwichien, A., Luengnaruemitchai, A., & Jai-In, S. (2009). Utilization of palm oil alkyl esters as an additive in ethanol–diesel and butanol–diesel blends. *Fuel*, 88(9), 1618-1624.
- Conde-Mejia, C., Jimenez-Gutierrez, A., & El-Halwagi, M. (2012). A comparison of pretreatment methods for bioethanol production from lignocellulosic materials. *Process Saf Environ*, 90(3), 189-202.
- Corseuil, H. X., Monier, A. L., Gomes, A. P., Chiaranda, H. S., do Rosario, M., & Alvarez, P. J. (2011). Biodegradation of soybean and castor oil biodiesel: implications on the natural attenuation of monoaromatic hydrocarbons in groundwater. *Groundwater Monitoring & Remediation*, 31(3), 111-118.
- Costa, R. C., & Sodr e, J. R. (2011). Compression ratio effects on an ethanol/gasoline fuelled engine performance. *Appl Therm Eng*, 31(2), 278-283.
- Costagliola, M., De Simio, L., Iannaccone, S., & Prati, M. (2013). Combustion efficiency and engine out emissions of a SI engine fueled with alcohol/gasoline blends. *Appl Energ*, 111, 1162-1171.
- Council, W. E. (2013). World Energy Resources, Survey, 2013
- Cursaru, D.-L., Br noiu, G., Ramadan, I., & Miculescu, F. (2014). Degradation of automotive materials upon exposure to sunflower biodiesel. *Ind Crop Prod*, 54, 149-158.
- da Silva Ara ujo, F. D., Ara ujo, I. C., Costa, I. C. G., de Moura, C. V. R., Chaves, M. H., & Ara ujo, E. C. E. (2014). Study of degumming process and evaluation of oxidative stability of methyl and ethyl biodiesel of *Jatropha curcas* L. oil from three different Brazilian states. *Renew Energ*, 71, 495-501.
- da Silva C sar, A., de Azedias Almeida, F., de Souza, R. P., Silva, G. C., & Atabani, A. (2015). The prospects of using *Acrocomia aculeata* (maca uba) a non-edible biodiesel feedstock in Brazil. *Renew Sust Energ Rev.*, 49, 1213-1220.

- Dantas, M., Albuquerque, A., Barros, A., Rodrigues Filho, M., Antoniosi Filho, N., Sinfrônio, F., . . . Souza, A. (2011). Evaluation of the oxidative stability of corn biodiesel. *Fuel*, 90(2), 773-778.
- de Almeida, V. F., García-Moreno, P. J., Guadix, A., & Guadix, E. M. (2015). Biodiesel production from mixtures of waste fish oil, palm oil and waste frying oil: Optimization of fuel properties. *Fuel Process Technol*, 133, 152-160.
- de Souza, A. P., Leite, D. C., Pattathil, S., Hahn, M. G., & Buckeridge, M. S. (2013). Composition and structure of sugarcane cell wall polysaccharides: implications for second-generation bioethanol production. *Bioenerg Res*, 6(2), 564-579.
- Demirbas, A. (2008). Relationships derived from physical properties of vegetable oil and biodiesel fuels. *Fuel*, 87(8), 1743-1748.
- Deyab, M. (2016). The inhibition activity of butylated hydroxytoluene towards corrosion of carbon steel in biodiesel blend B20. *J Taiwan Inst Chem E*, 60, 369-375.
- Dharma, S., Masjuki, H., Ong, H. C., Sebayang, A., Silitonga, A., Kusumo, F., & Mahlia, T. (2016). Optimization of biodiesel production process for mixed *Jatropha curcas*-*Ceiba pentandra* biodiesel using response surface methodology. *Energ Convers Manage*, 115, 178-190.
- Dharma, S., Ong, H. C., Masjuki, H., Sebayang, A., & Silitonga, A. (2016). An overview of engine durability and compatibility using biodiesel-bioethanol-diesel blends in compression-ignition engines. *Energ Convers Manage*, 128, 66-81.
- Dias, M. O., Junqueira, T. L., Cavalett, O., Cunha, M. P., Jesus, C. D., Mantelatto, P. E., . . . Bonomi, A. (2013). Cogeneration in integrated first and second generation ethanol from sugarcane. *Chem Eng Res Des*, 91(8), 1411-1417.
- Dias, M. O., Modesto, M., Ensinas, A. V., Nebra, S. A., Maciel Filho, R., & Rossell, C. E. (2011). Improving bioethanol production from sugarcane: evaluation of distillation, thermal integration and cogeneration systems. *Energy*, 36(6), 3691-3703.
- Dillon, H. S., Laan, T., & Dillon, H. S. (2008). Biofuels, at what cost?: government support for ethanol and biodiesel in Indonesia: Citeseer.
- Dunn, R. O. (2005). Effect of antioxidants on the oxidative stability of methyl soyate (biodiesel). *Fuel Process Technol*, 86(10), 1071-1085.

- Dwivedi, G., & Sharma, M. (2014). Impact of cold flow properties of biodiesel on engine performance. *Renew Sust Energ Rev.*, 31, 650-656.
- Dwivedi, G., & Sharma, M. P. (2015). Application of Box–Behnken design in optimization of biodiesel yield from Pongamia oil and its stability analysis. *Fuel*, 145, 256-262.
- Dyer, J., Vergé, X., Desjardins, R., Worth, D., & McConkey, B. (2010). The impact of increased biodiesel production on the greenhouse gas emissions from field crops in Canada. *Energ Sust Develop*, 14(2), 73-82.
- EIA, U. S. E. I. A. (2016). International Energy Outlook 2016. Retrieved accessed January 2017.
- Energy, U. S. D. o. (2016). Energy Sources. Retrieved accessed February 2017.
- Enweremadu, C., & Rutto, H. (2010). Combustion, emission and engine performance characteristics of used cooking oil biodiesel—a review. *Renew Sust Energ Rev.*, 14(9), 2863-2873.
- Eurostat. (2015). EU energy in figures statistical pocketbook 2015.
- Fan, X., Wang, X., & Chen, F. (2011). Biodiesel production from crude cottonseed oil: an optimization process using response surface methodology. *The Open Fuels & Energy Science Journal*, 4.
- Fang, Q., Fang, J., Zhuang, J., & Huang, Z. (2013). Effects of ethanol–diesel–biodiesel blends on combustion and emissions in premixed low temperature combustion. *Appl Therm Eng*, 54(2), 541-548.
- Farooq, M., & Ramli, A. (2015). Biodiesel production from low FFA waste cooking oil using heterogeneous catalyst derived from chicken bones. *Renew Energ*, 76, 362-368.
- Fasogbon, S., & Olagoke, O. (2016). Influence of Temperature on Corrosion Characteristics of Metals in Used Cooking Oil Methyl Ester. *The International Journal Of Engineering And Science (IJES)*, 5(4), 71-75.

- Fattah, I. R., Masjuki, H., Kalam, M., Hazrat, M., Masum, B., Imtenan, S., & Ashraful, A. (2014). Effect of antioxidants on oxidation stability of biodiesel derived from vegetable and animal based feedstocks. *Renew Sust Energ Rev.*, 30, 356-370.
- Fazal, M., Haseeb, A., & Masjuki, H. (2010a). Comparative corrosive characteristics of petroleum diesel and palm biodiesel for automotive materials. *Fuel Processing Technology*, 91(10), 1308-1315.
- Fazal, M., Haseeb, A., & Masjuki, H. (2010b). Comparative corrosive characteristics of petroleum diesel and palm biodiesel for automotive materials. *Fuel Process Technol*, 91(10), 1308-1315.
- Fazal, M., Haseeb, A., & Masjuki, H. (2011a). Biodiesel feasibility study: an evaluation of material compatibility; performance; emission and engine durability. *Renew Sust Energ Rev.*, 15(2), 1314-1324.
- Fazal, M., Haseeb, A., & Masjuki, H. (2011b). Effect of different corrosion inhibitors on the corrosion of cast iron in palm biodiesel. *Fuel Process Technol*, 92(11), 2154-2159.
- Fazal, M., Haseeb, A., & Masjuki, H. (2011c). Effect of temperature on the corrosion behavior of mild steel upon exposure to palm biodiesel. *Energy*, 36(5), 3328-3334.
- Fazal, M., Haseeb, A., & Masjuki, H. (2012). Degradation of automotive materials in palm biodiesel. *Energy*, 40(1), 76-83.
- Fazal, M., Haseeb, A., & Masjuki, H. (2013a). Corrosion mechanism of copper in palm biodiesel. *Corrosion Science*, 67, 50-59.
- Fazal, M., Haseeb, A., & Masjuki, H. (2013b). Investigation of friction and wear characteristics of palm biodiesel. *Energ Convers Manage*, 67, 251-256.
- Fazal, M., Rathinee, B., & Masjuki, H. (2016). Corrosion of phosphorus bronze in different biodiesel blends and its remedial measures.
- Fernando, S., & Hanna, M. (2004). Development of a novel biofuel blend using ethanol– biodiesel– diesel microemulsions: EB-diesel. *Energ Fuel*, 18(6), 1695-1703.
- Fernando, S., Karra, P., Hernandez, R., & Jha, S. K. (2007). Effect of incompletely converted soybean oil on biodiesel quality. *Energy*, 32(5), 844-851.

- Ganapathy, T., Gakkhar, R., & Murugesan, K. (2011). Influence of injection timing on performance, combustion and emission characteristics of Jatropha biodiesel engine. *Appl Energ*, 88(12), 4376-4386.
- Gandure, J., Ketlogetswe, C., & Temu, A. (2014). Fuel properties of biodiesel produced from selected plant kernel oils indigenous to Botswana: A comparative analysis. *Renew Energ*, 68, 414-420.
- Gautam, A., & Agarwal, A. K. (2015). Determination of important biodiesel properties based on fuel temperature correlations for application in a locomotive engine. *Fuel*, 142, 289-302.
- Geacai, S., Iulian, O., & Nita, I. (2015). Measurement, correlation and prediction of biodiesel blends viscosity. *Fuel*, 143, 268-274.
- Ghadge, S. V., & Raheman, H. (2005). Biodiesel production from mahua (*Madhuca indica*) oil having high free fatty acids. *Biomass bioenerg*, 28(6), 601-605.
- Ghadge, S. V., & Raheman, H. (2006). Process optimization for biodiesel production from mahua (*Madhuca indica*) oil using response surface methodology. *Bioresource Technol.*, 97(3), 379-384.
- Ghazali, W. N. M. W., Mamat, R., Masjuki, H., & Najafi, G. (2015). Effects of biodiesel from different feedstocks on engine performance and emissions: A review. *Renew Sust Energ Rev.*, 51, 585-602.
- Ghisi, M., Chaves, E. S., Quadros, D. P., Marques, E. P., Curtius, A. J., & Marques, A. L. (2011). Simple method for the determination of Cu and Fe by electrothermal atomic absorption spectrometry in biodiesel treated with tetramethylammonium hydroxide. *Microchemical Journal*, 98(1), 62-65.
- Gomez, N. A., Abonia, R., Cadavid, H., & Vargas, I. H. (2011). Chemical and spectroscopic characterization of a vegetable oil used as dielectric coolant in distribution transformers. *Journal of the Brazilian Chemical Society*, 22(12), 2292-2303.
- Gonçalves, J. d. A., Gióia, R., & Aranda, D. A. (2012). Properties of soybean biodiesel blended with palm or tallow during long term storage under different conditions. *Int Rev Chem Eng*, 4, 417-422.

- Gui, M. M., Lee, K., & Bhatia, S. (2008). Feasibility of edible oil vs. non-edible oil vs. waste edible oil as biodiesel feedstock. *Energy*, 33(11), 1646-1653.
- Gülüm, M., & Bilgin, A. (2015). Density, flash point and heating value variations of corn oil biodiesel–diesel fuel blends. *Fuel Process Technol*, 134, 456-464.
- Gumus, M. (2010). A comprehensive experimental investigation of combustion and heat release characteristics of a biodiesel (hazelnut kernel oil methyl ester) fueled direct injection compression ignition engine. *Fuel*, 89(10), 2802-2814.
- Gunatilake, H., Roland-Holst, D., & Sugiyarto, G. (2014). Energy security for India: Biofuels, energy efficiency and food productivity. *Energ Policy*, 65, 761-767.
- Gupta, A., & Verma, J. P. (2015). Sustainable bio-ethanol production from agro-residues: a review. *Renew Sust Energ Rev.*, 41, 550-567.
- Gutiérrez-Rivera, B., Ortiz-Muñiz, B., Gómez-Rodríguez, J., Cárdenas-Cágal, A., González, J. M. D., & Aguilar-Uscanga, M. G. (2015). Bioethanol production from hydrolyzed sugarcane bagasse supplemented with molasses “B” in a mixed yeast culture. *Renew Energ*, 74, 399-405.
- Hamze, H., Akia, M., & Yazdani, F. (2015). Optimization of biodiesel production from the waste cooking oil using response surface methodology. *Process Saf Environ*, 94, 1-10.
- Hansen, A. C., Zhang, Q., & Lyne, P. W. (2005). Ethanol–diesel fuel blends—a review. *Bioresource Technol.*, 96(3), 277-285.
- Haseeb, A., Fazal, M., Jahirul, M., & Masjuki, H. (2011). Compatibility of automotive materials in biodiesel: a review. *Fuel*, 90(3), 922-931.
- Haseeb, A., Masjuki, H., Ann, L., & Fazal, M. (2010). Corrosion characteristics of copper and leaded bronze in palm biodiesel. *Fuel Process Technol*, 91(3), 329-334.
- Haseeb, A., Sia, S., Fazal, M., & Masjuki, H. (2010). Effect of temperature on tribological properties of palm biodiesel. *Energy*, 35(3), 1460-1464.
- Haşimoğlu, C., Ciniviz, M., Özsert, İ., İcingür, Y., Parlak, A., & Salman, M. S. (2008). Performance characteristics of a low heat rejection diesel engine operating with biodiesel. *Renew Energ*, 33(7), 1709-1715.

- Hoekman, S. K., & Robbins, C. (2012). Review of the effects of biodiesel on NO_x emissions. *Fuel Process Technol*, 96, 237-249.
- Hu, E., Xu, Y., Hu, X., Pan, L., & Jiang, S. (2012a). Corrosion behaviors of metals in biodiesel from rapeseed oil and methanol. *Renew Energ*, 37(1), 371-378.
- Hu, E., Xu, Y., Hu, X., Pan, L., & Jiang, S. (2012b). Corrosion behaviors of metals in biodiesel from rapeseed oil and methanol. *Renewable Energy*, 37(1), 371-378.
- Hulwan, D. B., & Joshi, S. V. (2011). Performance, emission and combustion characteristic of a multicylinder DI diesel engine running on diesel–ethanol–biodiesel blends of high ethanol content. *Appl Energ*, 88(12), 5042-5055.
- Iglesias, L., Laca, A., Herrero, M., & Díaz, M. (2012). A life cycle assessment comparison between centralized and decentralized biodiesel production from raw sunflower oil and waste cooking oils. *J Clean Prod*, 37, 162-171.
- Ileri, E., Atmanli, A., & Yilmaz, N. (2016). Comparative analyses of n-butanol–rapeseed oil–diesel blend with biodiesel, diesel and biodiesel–diesel fuels in a turbocharged direct injection diesel engine. *J Energy Inst*, 89(4), 586-593.
- Imahara, H., Minami, E., & Saka, S. (2006). Thermodynamic study on cloud point of biodiesel with its fatty acid composition. *Fuel*, 85(12), 1666-1670.
- Iqbal, M. A., Varman, M., Hassan, M. H., Kalam, M. A., Hossain, S., & Sayeed, I. (2015). Tailoring fuel properties using jatropha, palm and coconut biodiesel to improve CI engine performance and emission characteristics. *J Clean Prod*, 101, 262-270.
- Jain, S., & Sharma, M. (2011). Correlation development for effect of metal contaminants on the oxidation stability of Jatropha curcas biodiesel. *Fuel*, 90(5), 2045-2050.
- Jansson, C., Westerbergh, A., Zhang, J., Hu, X., & Sun, C. (2009). Cassava, a potential biofuel crop in (the) People's Republic of China. *Appl Energ*, 86, S95-S99.
- Jayed, M., Masjuki, H., Kalam, M., Mahlia, T., Husnawan, M., & Liaquat, A. (2011). Prospects of dedicated biodiesel engine vehicles in Malaysia and Indonesia. *Renew Sust Energ Rev.*, 15(1), 220-235.

- Jena, P. C., Raheman, H., Kumar, G. P., & Machavaram, R. (2010). Biodiesel production from mixture of mahua and simarouba oils with high free fatty acids. *Biomass bioenerg*, 34(8), 1108-1116.
- Ji, L.-Q. (2015). An assessment of agricultural residue resources for liquid biofuel production in China. *Renew Sust Energ Rev.*, 44, 561-575.
- Jin, D., Zhou, X., Wu, P., Jiang, L., & Ge, H. (2015). Corrosion behavior of ASTM 1045 mild steel in palm biodiesel. *Renew Energ*, 81, 457-463.
- Jindal, M., Rosha, P., Mahla, S., & Dhir, A. (2015). Experimental investigation of performance and emissions characteristics of waste cooking oil biodiesel and n-butanol blends in a compression ignition engine. *RSC Adv*, 5(43), 33863-33868.
- Jones, C. S., & Mayfield, S. P. (2012). Algae biofuels: versatility for the future of bioenergy. *Curr Opin Biotech*, 23(3), 346-351.
- Kabbashi, N. A., Mohammed, N. I., Alam, M. Z., & Mirghani, M. E. S. (2015). Hydrolysis of *Jatropha curcas* oil for biodiesel synthesis using immobilized *Candida cylindracea* lipase. *Journal of Molecular Catalysis B: Enzymatic*, 116, 95-100.
- Kafuku, G., & Mbarawa, M. (2010). Biodiesel production from *Croton megalocarpus* oil and its process optimization. *Fuel*, 89(9), 2556-2560.
- Kakati, J., & Gogoi, T. (2016). Biodiesel production from Kutkura (*Meyna spinosa* Roxb. Ex.) fruit seed oil: Its characterization and engine performance evaluation with 10% and 20% blends. *Energ Convers Manage*, 121, 152-161.
- Kalam, M., Ahamed, J., & Masjuki, H. (2012). Land availability of *Jatropha* production in Malaysia. *Renew Sust Energ Rev.*, 16(6), 3999-4007.
- Kalam, M., Masjuki, H., Jayed, M., & Liaquat, A. (2011). Emission and performance characteristics of an indirect ignition diesel engine fuelled with waste cooking oil. *Energy*, 36(1), 397-402.
- Kalghatgi, G. T., Risberg, P., & Ångström, H.-E. (2006). *Advantages of Fuels with High Resistance to Auto-ignition in Late-injection, Low-temperature, Compression Ignition Combustion.*
- Kannan, G., & Anand, R. (2011). Experimental investigation on diesel engine with diestrol–water micro emulsions. *Energy*, 36(3), 1680-1687.

- Karunanithy, C., Muthukumarappan, K., & Julson, J. (2008). *Enzymatic hydrolysis of corn stover pretreated in high shear bioreactor*. Paper presented at the Proceedings of the American Society of Agricultural and Biological Engineers Annual International Meeting.
- Kaul, S., Saxena, R., Kumar, A., Negi, M., Bhatnagar, A., Goyal, H., & Gupta, A. (2007). Corrosion behavior of biodiesel from seed oils of Indian origin on diesel engine parts. *Fuel Process Technol*, 88(3), 303-307.
- Kaya, C., Hamamci, C., Baysal, A., Akba, O., Erdogan, S., & Saydut, A. (2009). Methyl ester of peanut (*Arachis hypogea* L.) seed oil as a potential feedstock for biodiesel production. *Renew Energ*, 34(5), 1257-1260.
- Khan, T. Y., Atabani, A., Badruddin, I. A., Ankalgi, R., Khan, T. M., & Badarudin, A. (2015). *Ceiba pentandra*, *Nigella sativa* and their blend as prospective feedstocks for biodiesel. *Ind Crop Prod*, 65, 367-373.
- Kim, H., & Choi, B. (2010). The effect of biodiesel and bioethanol blended diesel fuel on nanoparticles and exhaust emissions from CRDI diesel engine. *Renew Energ*, 35(1), 157-163.
- Knothe, G. (2005). Dependence of biodiesel fuel properties on the structure of fatty acid alkyl esters. *Fuel Process Technol*, 86(10), 1059-1070.
- Knothe, G. (2010). Biodiesel and renewable diesel: a comparison. *Prog energ combust*, 36(3), 364-373.
- Knothe, G., & Steidley, K. R. (2011). Kinematic viscosity of fatty acid methyl esters: prediction, calculated viscosity contribution of esters with unavailable data, and carbon-oxygen equivalents. *Fuel*, 90(11), 3217-3224.
- Koutinas, A. A., Vlysidis, A., Pleissner, D., Kopsahelis, N., Garcia, I. L., Kookos, I. K., . . . Lin, C. S. K. (2014). Valorization of industrial waste and by-product streams via fermentation for the production of chemicals and biopolymers. *Chem Soc Rev*, 43(8), 2587-2627.
- Krishnamurthy, S. R. (2013). A comparison of corrosion behavior of copper and its alloy in *Pongamia pinnata* oil at different conditions. *J Energy*, 2013, 1-4.
- Kristensen, S. B. P., Birch-Thomsen, T., Rasmussen, K., Rasmussen, L. V., & Traoré, O. (2014). Cassava as an energy crop: A case study of the potential for an

expansion of cassava cultivation for bioethanol production in Southern Mali. *Renew Energ*, 66, 381-390.

Krüger, L., Tuchscheerer, F., Mandel, M., Müller, S., & Liebsch, S. (2012). Corrosion behaviour of aluminium alloys in ethanol fuels. *J Mater Sci*, 47(6), 2798-2806.

Kulkarni, M. G., & Dalai, A. K. (2006). Waste cooking oil an economical source for biodiesel: a review. *Ind Eng Chem Res*, 45(9), 2901-2913.

Kumar, N., & Chauhan, S. R. (2015). Evaluation of endurance characteristics for a modified diesel engine runs on jatropha biodiesel. *Appl Energ*, 155, 253-269.

Kumar, T. S., Kumar, P. S., & Annamalai, K. (2015). Experimental study on the performance and emission measures of direct injection diesel engine with Kapok methyl ester and its blends. *Renew Energ*, 74, 903-909.

Kwanchareon, P., Luengnaruemitchai, A., & Jai-In, S. (2007). Solubility of a diesel–biodiesel–ethanol blend, its fuel properties, and its emission characteristics from diesel engine. *Fuel*, 86(7), 1053-1061.

Labeckas, G., Slavinskas, S., & Mažeika, M. (2014). The effect of ethanol–diesel–biodiesel blends on combustion, performance and emissions of a direct injection diesel engine. *Energ Convers Manage*, 79, 698-720.

Lapuerta, M., Armas, O., & García-Contreras, R. (2009). Effect of ethanol on blending stability and diesel engine emissions. *Energ Fuel*, 23(9), 4343-4354.

Lapuerta, M., Herreros, J. M., Lyons, L. L., García-Contreras, R., & Briceño, Y. (2008). Effect of the alcohol type used in the production of waste cooking oil biodiesel on diesel performance and emissions. *Fuel*, 87(15), 3161-3169.

Leung, D., & Guo, Y. (2006). Transesterification of neat and used frying oil: optimization for biodiesel production. *Fuel Process Technol*, 87(10), 883-890.

Li, L., Wang, J., Wang, Z., & Xiao, J. (2015). Combustion and emission characteristics of diesel engine fueled with diesel/biodiesel/pentanol fuel blends. *Fuel*, 156, 211-218. doi: <https://doi.org/10.1016/j.fuel.2015.04.048>

Likožar, B., & Levec, J. (2014). Transesterification of canola, palm, peanut, soybean and sunflower oil with methanol, ethanol, isopropanol, butanol and tert-butanol to biodiesel: Modelling of chemical equilibrium, reaction kinetics and mass transfer based on fatty acid composition. *Appl Energ*, 123, 108-120.

- Limayem, A., & Ricke, S. C. (2012). Lignocellulosic biomass for bioethanol production: current perspectives, potential issues and future prospects. *Prog energ combust*, 38(4), 449-467.
- Lin, C.-Y., & Fan, C.-L. (2011). Fuel properties of biodiesel produced from *Camellia oleifera* Abel oil through supercritical-methanol transesterification. *Fuel*, 90(6), 2240-2244.
- Lin, L., Cunshan, Z., Vittayapadung, S., Xiangqian, S., & Mingdong, D. (2011). Opportunities and challenges for biodiesel fuel. *Appl Energ*, 88(4), 1020-1031.
- Lin, R., Zhu, Y., & Tavlarides, L. L. (2014). Effect of thermal decomposition on biodiesel viscosity and cold flow property. *Fuel*, 117, 981-988.
- Lin, Y.-C., Hsu, K.-H., & Chen, C.-B. (2011). Experimental investigation of the performance and emissions of a heavy-duty diesel engine fueled with waste cooking oil biodiesel/ultra-low sulfur diesel blends. *Energy*, 36(1), 241-248.
- Lin, Y.-C., Yang, P.-M., Chen, S.-C., & Lin, J.-F. (2013). Improving biodiesel yields from waste cooking oil using ionic liquids as catalysts with a microwave heating system. *Fuel Process Technol*, 115, 57-62.
- Liu, B., Wang, F., Zhang, B., & Bi, J. (2013). Energy balance and GHG emissions of cassava-based fuel ethanol using different planting modes in China. *Energ Policy*, 56, 210-220.
- Love, N., Parthasarathy, R., & Gollahalli, S. (2009). Effect of iodine number on NO_x formation in laminar flames of oxygenated biofuels. *Int J Green Energy*, 6(4), 323-332.
- Macedo, I. C., Seabra, J. E., & Silva, J. E. (2008). Green house gases emissions in the production and use of ethanol from sugarcane in Brazil: the 2005/2006 averages and a prediction for 2020. *Biomass bioenerg*, 32(7), 582-595.
- Mangus, M., Kiani, F., Mattson, J., Tabakh, D., Petka, J., Depcik, C., . . . Stagg-Williams, S. (2015). Investigating the compression ignition combustion of multiple biodiesel/ULSD (ultra-low sulfur diesel) blends via common-rail injection. *Energy*, 89, 932-945.

- Manzetti, S., & Andersen, O. (2015). A review of emission products from bioethanol and its blends with gasoline. Background for new guidelines for emission control. *Fuel*, *140*, 293-301.
- Maran, J. P., & Priya, B. (2015). Modeling of ultrasound assisted intensification of biodiesel production from neem (*Azadirachta indica*) oil using response surface methodology and artificial neural network. *Fuel*, *143*, 262-267.
- Martínez, G., Sánchez, N., Encinar, J., & González, J. (2014). Fuel properties of biodiesel from vegetable oils and oil mixtures. Influence of methyl esters distribution. *Biomass bioenerg*, *63*, 22-32.
- Maryana, R., Ma'rifatun, D., Wheni, A., Satriyo, K., & Rizal, W. A. (2014). Alkaline pretreatment on sugarcane bagasse for bioethanol production. *Enrgy Proced*, *47*, 250-254.
- Masum, B., Masjuki, H., Kalam, M., Fattah, I. R., Palash, S., & Abedin, M. (2013). Effect of ethanol-gasoline blend on NOx emission in SI engine. *Renew Sust Energ Rev.*, *24*, 209-222.
- Math, M., Kumar, S. P., & Chetty, S. V. (2010). Technologies for biodiesel production from used cooking oil—A review. *Energ Sust Develop*, *14*(4), 339-345.
- Meher, L., Dharmagadda, V. S., & Naik, S. (2006). Optimization of alkali-catalyzed transesterification of *Pongamia pinnata* oil for production of biodiesel. *Bioresource Technol.*, *97*(12), 1392-1397.
- Mejía, J., Salgado, N., & Orrego, C. (2013). Effect of blends of Diesel and Palm-Castor biodiesels on viscosity, cloud point and flash point. *Ind Crop Prod*, *43*, 791-797.
- Micic, R. D., Tomić, M. D., Kiss, F. E., Nikolić-Djorić, E. B., & Simikić, M. Đ. (2015). Optimization of hydrolysis in subcritical water as a pretreatment step for biodiesel production by esterification in supercritical methanol. *The Journal of Supercritical Fluids*, *103*, 90-100.
- Mittelbach, M., & Remschmidt, C. (2004). Biodiesel: the comprehensive handbook: Martin Mittelbach.
- Mofijur, M., Atabani, A., Masjuki, H., Kalam, M., & Masum, B. (2013). A study on the effects of promising edible and non-edible biodiesel feedstocks on engine performance and emissions production: a comparative evaluation. *Renew Sust Energ Rev.*, *23*, 391-404.

- Mofijur, M., Masjuki, H., Kalam, M., & Atabani, A. (2013). Evaluation of biodiesel blending, engine performance and emissions characteristics of *Jatropha curcas* methyl ester: Malaysian perspective. *Energy*, *55*, 879-887.
- Mofijur, M., Masjuki, H., Kalam, M., Atabani, A., Fattah, I. R., & Mobarak, H. (2014). Comparative evaluation of performance and emission characteristics of *Moringa oleifera* and Palm oil based biodiesel in a diesel engine. *Ind Crop Prod*, *53*, 78-84.
- Mofijur, M., Masjuki, H., Kalam, M., Atabani, A., Shahabuddin, M., Palash, S., & Hazrat, M. (2013). Effect of biodiesel from various feedstocks on combustion characteristics, engine durability and materials compatibility: A review. *Renew Sust Energ Rev.*, *28*, 441-455.
- Mofijur, M., Rasul, M., Hyde, J., Azad, A., Mamat, R., & Bhuiya, M. (2016). Role of biofuel and their binary (diesel–biodiesel) and ternary (ethanol–biodiesel–diesel) blends on internal combustion engines emission reduction. *Renew Sust Energ Rev.*, *53*, 265-278.
- Mojović, L., Nikolić, S., Rakin, M., & Vukasinović, M. (2006). Production of bioethanol from corn meal hydrolyzates. *Fuel*, *85*(12–13), 1750-1755.
- Mood, S. H., Golfeshan, A. H., Tabatabaei, M., Jouzani, G. S., Najafi, G. H., Gholami, M., & Ardjmand, M. (2013). Lignocellulosic biomass to bioethanol, a comprehensive review with a focus on pretreatment. *Renew Sust Energ Rev.*, *27*, 77-93.
- Mosarof, M., Kalam, M., Masjuki, H., Alabdulkarem, A., Ashraful, A., Arslan, A., . . . Monirul, I. (2016). Optimization of performance, emission, friction and wear characteristics of palm and *Calophyllum inophyllum* biodiesel blends. *Energy Convers Manage*, *118*, 119-134.
- Moser, B. R. (2012). Preparation of fatty acid methyl esters from hazelnut, high-oleic peanut and walnut oils and evaluation as biodiesel. *Fuel*, *92*(1), 231-238.
- Mukhopadhyay, K., & Forssell, O. (2005). An empirical investigation of air pollution from fossil fuel combustion and its impact on health in India during 1973–1974 to 1996–1997. *Ecol Econ*, *55*(2), 235-250.
- Muralidharan, K., Vasudevan, D., & Sheeba, K. (2011). Performance, emission and combustion characteristics of biodiesel fuelled variable compression ratio engine. *Energy*, *36*(8), 5385-5393.

- Najafi, G., Ghobadian, B., Tavakoli, T., Buttsworth, D., Yusaf, T., & Faizollahnejad, M. (2009). Performance and exhaust emissions of a gasoline engine with ethanol blended gasoline fuels using artificial neural network. *Appl Energ*, 86(5), 630-639.
- Nalgundwar, A., Paul, B., & Sharma, S. K. (2016). Comparison of performance and emissions characteristics of DI CI engine fueled with dual biodiesel blends of palm and jatropha. *Fuel*, 173, 172-179.
- Nanaki, E. A., & Koroneos, C. J. (2012). Comparative LCA of the use of biodiesel, diesel and gasoline for transportation. *J Clean Prod*, 20(1), 14-19.
- Nigam, P. S., & Singh, A. (2011). Production of liquid biofuels from renewable resources. *Prog energ combust*, 37(1), 52-68.
- Nikolić, S., Mojović, L., Rakin, M., & Pejin, D. (2009). Bioethanol production from corn meal by simultaneous enzymatic saccharification and fermentation with immobilized cells of *Saccharomyces cerevisiae* var. *ellipsoideus*. *Fuel*, 88(9), 1602-1607.
- Nizah, M. R., Taufiq-Yap, Y., Rashid, U., Teo, S. H., Nur, Z. S., & Islam, A. (2014). Production of biodiesel from non-edible *Jatropha curcas* oil via transesterification using Bi₂O₃-La₂O₃ catalyst. *Energ Convers Manage*, 88, 1257-1262.
- Noraini, M., Ong, H. C., Badrul, M. J., & Chong, W. (2014). A review on potential enzymatic reaction for biofuel production from algae. *Renew Sust Energ Rev.*, 39, 24-34.
- Nurfitri, I., Maniam, G. P., Hindryawati, N., Yusoff, M. M., & Ganesan, S. (2013). Potential of feedstock and catalysts from waste in biodiesel preparation: a review. *Energ Convers Manage*, 74, 395-402.
- Oliveira, L., & Da Silva, M. (2013). *Comparative study of calorific value of rapeseed, soybean, jatropha curcas and crambe biodiesel*. Paper presented at the International Conference on Renewable Energies and Power Quality (ICREPQ'13) Bilbao (Spain).
- Oncel, S. S. (2013). Microalgae for a macroenergy world. *Renew Sust Energ Rev.*, 26, 241-264.

- Ong, H., Mahlia, T., & Masjuki, H. (2012). A review on energy pattern and policy for transportation sector in Malaysia. *Renew Sust Energ Rev.*, 16(1), 532-542.
- Ong, H., Silitonga, A., Masjuki, H., Mahlia, T., Chong, W., & Boosroh, M. (2013). Production and comparative fuel properties of biodiesel from non-edible oils: *Jatropha curcas*, *Sterculia foetida* and *Ceiba pentandra*. *Energy Convers Manage*, 73, 245-255.
- Ong, H. C., Masjuki, H., Mahlia, T., Silitonga, A., Chong, W., & Yusaf, T. (2014). Engine performance and emissions using *Jatropha curcas*, *Ceiba pentandra* and *Calophyllum inophyllum* biodiesel in a CI diesel engine. *Energy*, 69, 427-445.
- Ong, L. K., Effendi, C., Kurniawan, A., Lin, C. X., Zhao, X. S., & Ismadji, S. (2013). Optimization of catalyst-free production of biodiesel from *Ceiba pentandra* (kapok) oil with high free fatty acid contents. *Energy*, 57, 615-623.
- Ononiwu, I., George, I., Adams, F. V., Joseph, I. V., & Afolabi, A. S. (2015). *Corrosion Behaviour of Mild Steel in Biodiesel Prepared from Ghee Butter*.
- Oo, C. W., Shioji, M., Nakao, S., Dung, N. N., Reksowardojo, I., Roces, S. A., & Dugos, N. P. (2015). Ignition and combustion characteristics of various biodiesel fuels (BDFs). *Fuel*, 158, 279-287.
- Organisation for Economic Co-operation and Development (OECD). (2015). *Agricultural Outlook*. Retrieved accessed February 2017, https://stats.oecd.org/Index.aspx?DataSetCode=HIGH_AGLINK_2012.
- Orozco, F. D. A., Sousa, A. C., Domini, C. E., Araujo, M. C. U., & Band, B. S. F. (2013). An ultrasonic-accelerated oxidation method for determining the oxidative stability of biodiesel. *Ultrason Sonochem*, 20(3), 820-825.
- Özçelik, A. E., Aydoğan, H., & Acaroğlu, M. (2015). Determining the performance, emission and combustion properties of camelina biodiesel blends. *Energy Convers Manage*, 96, 47-57.
- Özener, O., Yüksek, L., Ergenç, A. T., & Özkan, M. (2014). Effects of soybean biodiesel on a DI diesel engine performance, emission and combustion characteristics. *Fuel*, 115, 875-883.
- Pang, X., Shi, X., Mu, Y., He, H., Shuai, S., Chen, H., & Li, R. (2006). Characteristics of carbonyl compounds emission from a diesel-engine using biodiesel-ethanol-diesel as fuel. *Atmos Environ*, 40(36), 7057-7065.

- Park, I.-J., Nam, T.-H., Kim, J.-H., & Kim, J.-G. (2014). Evaluation of corrosion characteristics of aluminum alloys in the bio-ethanol gasoline blended fuel by 2-electrode electrochemical impedance spectroscopy. *Fuel*, *126*, 26-31.
- Park, J.-Y., Kim, D.-K., Lee, J.-P., Park, S.-C., Kim, Y.-J., & Lee, J.-S. (2008). Blending effects of biodiesels on oxidation stability and low temperature flow properties. *Bioresource Technol.*, *99*(5), 1196-1203.
- Patil, P. D., & Deng, S. (2009). Optimization of biodiesel production from edible and non-edible vegetable oils. *Fuel*, *88*(7), 1302-1306.
- Peidong, Z., Yanli, Y., Yongsheng, T., Xutong, Y., Yongkai, Z., Yonghong, Z., & Lisheng, W. (2009). Bioenergy industries development in China: Dilemma and solution. *Renew Sust Energ Rev.*, *13*(9), 2571-2579.
- Pérez, Á., Casas, A., Fernández, C. M., Ramos, M. J., & Rodríguez, L. (2010). Winterization of peanut biodiesel to improve the cold flow properties. *Bioresource Technol.*, *101*(19), 7375-7381.
- Petroleum, B. (2016). Energy Outlook. 2016. Available online: [https://www. bp.com/content/dam/bp/pdf/energy-economics/energy-outlook-2016/bp-energy-outlook-2016.pdf](https://www.bp.com/content/dam/bp/pdf/energy-economics/energy-outlook-2016/bp-energy-outlook-2016.pdf) (accessed on 28 August 2016).
- Pidol, L., Lecoite, B., Starck, L., & Jeuland, N. (2012). Ethanol–biodiesel–diesel fuel blends: performances and emissions in conventional diesel and advanced low temperature combustions. *Fuel*, *93*, 329-338.
- Pinzi, S., Rounce, P., Herreros, J. M., Tsolakis, A., & Dorado, M. P. (2013). The effect of biodiesel fatty acid composition on combustion and diesel engine exhaust emissions. *Fuel*, *104*, 170-182.
- Pradhan, S., Madankar, C., Mohanty, P., & Naik, S. (2012). Optimization of reactive extraction of castor seed to produce biodiesel using response surface methodology. *Fuel*, *97*, 848-855.
- Prieto, N. M., Ferreira, A. G., Portugal, A. T., Moreira, R. J., & Santos, J. B. (2015). Correlation and prediction of biodiesel density for extended ranges of temperature and pressure. *Fuel*, *141*, 23-38.
- Puhan, S., Jegan, R., Balasubramanian, K., & Nagarajan, G. (2009). Effect of injection pressure on performance, emission and combustion characteristics of high

linolenic linseed oil methyl ester in a DI diesel engine. *Renew Energ*, 34(5), 1227-1233.

Pullen, J., & Saeed, K. (2012). An overview of biodiesel oxidation stability. *Renew Sust Energ Rev.*, 16(8), 5924-5950.

Qi, D., Chen, H., Geng, L., & Bian, Y. (2011). Effect of diethyl ether and ethanol additives on the combustion and emission characteristics of biodiesel-diesel blended fuel engine. *Renew Energ*, 36(4), 1252-1258.

Qi, D., Chen, H., Geng, L., & Bian, Y. Z. (2010). Experimental studies on the combustion characteristics and performance of a direct injection engine fueled with biodiesel/diesel blends. *Energ Convers Manage*, 51(12), 2985-2992.

Qi, D., Geng, L., Chen, H., Bian, Y. Z., Liu, J., & Ren, X. C. (2009). Combustion and performance evaluation of a diesel engine fueled with biodiesel produced from soybean crude oil. *Renew Energ*, 34(12), 2706-2713.

Qi, D., & Lee, C. (2014). Influence of soybean biodiesel content on basic properties of biodiesel-diesel blends. *J Taiwan Inst Chem E*, 45(2), 504-507.

Qi, D., Lee, C., Jia, C., Wang, P., & Wu, S. (2014). Experimental investigations of combustion and emission characteristics of rapeseed oil–diesel blends in a two cylinder agricultural diesel engine. *Energ Convers Manage*, 77, 227-232.

Rabelo, S. N., Ferraz, V. P., Oliveira, L. S., & Franca, A. S. (2015). FTIR analysis for quantification of fatty acid methyl esters in biodiesel produced by microwave-assisted transesterification. *International Journal of Environmental Science and Development*, 6(12), 964.

Raheman, H., & Ghadge, S. (2008). Performance of diesel engine with biodiesel at varying compression ratio and ignition timing. *Fuel*, 87(12), 2659-2666.

Ramadhas, A., Muraleedharan, C., & Jayaraj, S. (2005). Performance and emission evaluation of a diesel engine fueled with methyl esters of rubber seed oil. *Renew Energ*, 30(12), 1789-1800.

Ramadhas, A. S., Jayaraj, S., & Muraleedharan, C. (2005). Biodiesel production from high FFA rubber seed oil. *Fuel*, 84(4), 335-340.

Ramírez-Verduzco, L. F., Rodríguez-Rodríguez, J. E., & del Rayo Jaramillo-Jacob, A. (2012). Predicting cetane number, kinematic viscosity, density and higher

heating value of biodiesel from its fatty acid methyl ester composition. *Fuel*, 91(1), 102-111.

Rashedul, H., Masjuki, H., Kalam, M., Ashraful, A., Rashed, M., Sanchita, I., & Shaon, T. (2014). Performance and emission characteristics of a compression ignition engine running with linseed biodiesel. *RSC Adv*, 4(110), 64791-64797.

Rashid, U., & Anwar, F. (2008). Production of biodiesel through optimized alkaline-catalyzed transesterification of rapeseed oil. *Fuel*, 87(3), 265-273.

Rashid, U., Knothe, G., Yunus, R., & Evangelista, R. L. (2014). Kapok oil methyl esters. *Biomass bioenerg*, 66, 419-425.

Rocabruno-Valdés, C., Ramírez-Verduzco, L., & Hernández, J. (2015). Artificial neural network models to predict density, dynamic viscosity, and cetane number of biodiesel. *Fuel*, 147, 9-17.

Romaní, A., Garrote, G., Ballesteros, I., & Ballesteros, M. (2013). Second generation bioethanol from steam exploded Eucalyptus globulus wood. *Fuel*, 111, 66-74.

Rosillo-Calle, F., Pelkmans, L., & Walter, A. (2009). A global overview of vegetable oils, with reference to biodiesel. *A Report for the Bioenergy Task*, 40.

Roy, M. M., Wang, W., & Bujold, J. (2013). Biodiesel production and comparison of emissions of a DI diesel engine fueled by biodiesel–diesel and canola oil–diesel blends at high idling operations. *Appl Energ*, 106, 198-208.

Ruhul, A., Kalam, M., Masjuki, H., Alabdulkarem, A., Atabani, A., Fattah, I. R., & Abedin, M. (2016). Production, characterization, engine performance and emission characteristics of Croton megalocarpus and Ceiba pentandra complementary blends in a single-cylinder diesel engine. *RSC Adv*, 6(29), 24584-24595.

Ruiz-Méndez, M., Marmesat, S., Liotta, A., & Dobarganes, M. C. (2008). Analysis of used frying fats for biodiesel production. *Grasas Aceites*, 59(1), 45-50.

Saboori, B., Sapri, M., & bin Baba, M. (2014). Economic growth, energy consumption and CO₂ emissions in OECD (Organization for Economic Co-operation and Development)'s transport sector: a fully modified bi-directional relationship approach. *Energy*, 66, 150-161.

- Sajjad, H., Masjuki, H., Varman, M., Kalam, M., Arbab, M., Imtenan, S., & Rahman, S. A. (2014). Engine combustion, performance and emission characteristics of gas to liquid (GTL) fuels and its blends with diesel and bio-diesel. *Renew Sust Energ Rev.*, *30*, 961-986.
- Saloua, F., Saber, C., & Hedi, Z. (2010). Methyl ester of [Maclura pomifera (Rafin.) Schneider] seed oil: Biodiesel production and characterization. *Bioresource Technol.*, *101*(9), 3091-3096.
- Saluja, R. K., Kumar, V., & Sham, R. (2016). Stability of biodiesel—A review. *Renew Sust Energ Rev.*, *62*, 866-881.
- Samuel, O., Ashiedu, F., & Oreko, B. (2016). Analysis of coconut ethyl ester (biodiesel) and fossil diesel blending: properties and corrosion characteristic. *Nigerian Journal of Technology*, *35*(1), 107-113.
- Sanford, S. D., White, J. M., Shah, P. S., Wee, C., Valverde, M. A., & Meier, G. R. (2009). Feedstock and biodiesel characteristics report. *Renewable Energy Group*, *416*, 1-136.
- Sanjid, A., Kalam, M. A., Masjuki, H. H., Varman, M., Zulkifli, N. W. B. M., & Abedin, M. J. (2016). Performance and emission of multi-cylinder diesel engine using biodiesel blends obtained from mixed inedible feedstocks. *J Clean Prod*, *112*, 4114-4122.
- Sarkar, N., Ghosh, S. K., Bannerjee, S., & Aikat, K. (2012). Bioethanol production from agricultural wastes: an overview. *Renew Energ*, *37*(1), 19-27.
- Sarve, A., Sonawane, S. S., & Varma, M. N. (2015). Ultrasound assisted biodiesel production from sesame (*Sesamum indicum* L.) oil using barium hydroxide as a heterogeneous catalyst: comparative assessment of prediction abilities between response surface methodology (RSM) and artificial neural network (ANN). *Ultrason Sonochem*, *26*, 218-228.
- Schober, S., & Mittelbach, M. (2004). The impact of antioxidants on biodiesel oxidation stability. *Eur J Lipid Sci Tech*, *106*(6), 382-389.
- Sebayang, A., Masjuki, H., Ong, H. C., Dharma, S., Silitonga, A., Mahlia, T., & Aditiya, H. (2016). A perspective on bioethanol production from biomass as alternative fuel for spark ignition engine. *RSC Adv*, *6*(18), 14964-14992.

- Shahir, S., Masjuki, H., Kalam, M., Imran, A., & Ashraful, A. (2015). Performance and emission assessment of diesel–biodiesel–ethanol/bioethanol blend as a fuel in diesel engines: A review. *Renew Sust Energ Rev.*, *48*, 62-78.
- Shahir, S., Masjuki, H., Kalam, M., Imran, A., Fattah, I. R., & Sanjid, A. (2014). Feasibility of diesel–biodiesel–ethanol/bioethanol blend as existing CI engine fuel: An assessment of properties, material compatibility, safety and combustion. *Renew Sust Energ Rev.*, *32*, 379-395.
- Shanmugaprakash, M., & Sivakumar, V. (2013). Development of experimental design approach and ANN-based models for determination of Cr (VI) ions uptake rate from aqueous solution onto the solid biodiesel waste residue. *Bioresource Technol.*, *148*, 550-559.
- Shi, X., Yu, Y., He, H., Shuai, S., Wang, J., & Li, R. (2005). Emission characteristics using methyl soyate–ethanol–diesel fuel blends on a diesel engine. *Fuel*, *84*(12), 1543-1549. doi: <http://dx.doi.org/10.1016/j.fuel.2005.03.001>
- Silitonga, A., Masjuki, H., Mahlia, T., Ong, H., Atabani, A., & Chong, W. (2013). A global comparative review of biodiesel production from jatropha curcas using different homogeneous acid and alkaline catalysts: Study of physical and chemical properties. *Renew Sust Energ Rev.*, *24*, 514-533.
- Silitonga, A., Masjuki, H., Mahlia, T., Ong, H., Chong, W., & Boosroh, M. (2013). Overview properties of biodiesel diesel blends from edible and non-edible feedstock. *Renew Sust Energ Rev.*, *22*, 346-360.
- Silitonga, A., Ong, H., Mahlia, T., Masjuki, H., & Chong, W. (2013). Characterization and production of Ceiba pentandra biodiesel and its blends. *Fuel*, *108*, 855-858.
- Singh, A., Nigam, P. S., & Murphy, J. D. (2011). Renewable fuels from algae: an answer to debatable land based fuels. *Bioresource Technol.*, *102*(1), 10-16.
- Singh, B., Korstad, J., & Sharma, Y. (2012). A critical review on corrosion of compression ignition (CI) engine parts by biodiesel and biodiesel blends and its inhibition. *Renew Sust Energ Rev.*, *16*(5), 3401-3408.
- Singh, V. (2012). Effect of corn quality on bioethanol production. *Biocatalysis and Agricultural Biotechnology*, *1*(4), 353-355.
- Sirisomboonchai, S., Abuduwayiti, M., Guan, G., Samart, C., Abliz, S., Hao, X., . . . Abudula, A. (2015). Biodiesel production from waste cooking oil using calcined scallop shell as catalyst. *Energ Convers Manage*, *95*, 242-247.

- Soares, I. P., Rezende, T. F., Silva, R. C., Castro, E. V. R., & Fortes, I. C. (2008). Multivariate calibration by variable selection for blends of raw soybean oil/biodiesel from different sources using fourier transform infrared spectroscopy (FTIR) spectra data. *Energ Fuel*, 22(3), 2079-2083.
- Solís, J. C., & Sheinbaum, C. (2013). Energy consumption and greenhouse gas emission trends in Mexican road transport. *Energy Sustain Develop*, 17(3), 280-287.
- Sorate, K. A., & Bhale, P. V. (2015). Biodiesel properties and automotive system compatibility issues. *Renew Sust Energ Rev.*, 41, 777-798.
- Srithar, K., Balasubramanian, K. A., Pavendan, V., & Kumar, B. A. (2014). Experimental investigations on mixing of two biodiesels blended with diesel as alternative fuel for diesel engines. *Journal of King Saud University-Engineering Sciences*.
- Sterpu, A.-E., Dumitru, A. I., & Popa, M.-F. (2012). Corrosion behavior of steel in biodiesel of different origin. *Analele Universitatii" Ovidius" Constanta-Seria Chimie*, 23(2), 143-148.
- Su, J., Zhu, H., & Bohac, S. V. (2013). Particulate matter emission comparison from conventional and premixed low temperature combustion with diesel, biodiesel and biodiesel–ethanol fuels. *Fuel*, 113, 221-227.
- Subbaiah, G. V., Gopal, K. R., Hussain, S. A., Prasad, B. D., & Reddy, K. T. (2010). Rice bran oil biodiesel as an additive in diesel-ethanol blends for diesel engines. *International journal of research and reviews in Applied sciences*, 3(3), 334-342.
- Sulistyo, H., Almeida, M. F., & Dias, J. M. (2015). Influence of synthetic antioxidants on the oxidation stability of biodiesel produced from acid raw *Jatropha curcas* oil. *Fuel Process Technol*, 132, 133-138.
- Sundaresan, M., Chandrasekaran, S., & Porai, P. T. (2007). Analysis of combustion, performance and emission characteristics of blends of methyl esters of *jatropha* oil (MEJ) in DI diesel engine: SAE Technical Paper, No. 2007-32-0066.
- Surisetty, V. R., Dalai, A. K., & Kozinski, J. (2011). Alcohols as alternative fuels: An overview. *Applied Catalysis A: General*, 404(1), 1-11.

- Takase, M., Zhao, T., Zhang, M., Chen, Y., Liu, H., Yang, L., & Wu, X. (2015). An expatiate review of neem, jatropha, rubber and karanja as multipurpose non-edible biodiesel resources and comparison of their fuel, engine and emission properties. *Renew Sust Energ Rev.*, 43, 495-520.
- Talebian-Kiakalaieh, A., Amin, N. A. S., & Mazaheri, H. (2013). A review on novel processes of biodiesel production from waste cooking oil. *Appl Energ*, 104, 683-710.
- Tan, I. S., & Lee, K. T. (2014). Enzymatic hydrolysis and fermentation of seaweed solid wastes for bioethanol production: An optimization study. *Energy*, 78, 53-62.
- Tan, Y. H., Abdullah, M. O., Nolasco-Hipolito, C., Zauzi, N. S. A., & Abdullah, G. W. (2017). Engine performance and emissions characteristics of a diesel engine fueled with diesel-biodiesel-bioethanol emulsions. *Energ Convers Manage*, 132, 54-64.
- Tangka, J., Berinyuy, J., & Okale, A. (2011). Physico-chemical properties of bio-ethanol/gasoline blends and the qualitative effect of different blends on gasoline quality and engine performance. *Journal of petroleum Technology and Alternative fuels*, 2(2), 35-44.
- Teoh, Y., Masjuki, H., Kalam, M., Amalina, M., & How, H. (2014). Effects of Jatropha biodiesel on the performance, emissions, and combustion of a converted common-rail diesel engine. *RSC Adv*, 4(92), 50739-50751.
- Thangavelu, S. K., Ahmed, A. S., & Ani, F. N. (2016). Impact of metals on corrosive behavior of biodiesel–diesel–ethanol (BDE) alternative fuel. *Renew Energ*, 94, 1-9.
- Thangavelu, S. K., Chelladorai, P., & Ani, F. N. (2015). *Corrosion Behaviour of Carbon Steel in Biodiesel-Diesel-Ethanol (BDE) Fuel Blend*. Paper presented at the MATEC Web Conf.
- Topgül, T., Yücesu, H. S., Cinar, C., & Koca, A. (2006). The effects of ethanol–unleaded gasoline blends and ignition timing on engine performance and exhaust emissions. *Renew Energ*, 31(15), 2534-2542.
- Torres-Jimenez, E., Jerman, M. S., Gregorc, A., Lisec, I., Dorado, M. P., & Kegl, B. (2011). Physical and chemical properties of ethanol–diesel fuel blends. *Fuel*, 90(2), 795-802.

- Tosun, E., Yilmaz, A. C., Ozcanli, M., & Aydin, K. (2014). Determination of effects of various alcohol additions into peanut methyl ester on performance and emission characteristics of a compression ignition engine. *Fuel*, *126*, 38-43.
- Tsuchiya, T., Shiotani, H., Goto, S., Sugiyama, G., & Maeda, A. (2006). Japanese standards for diesel fuel containing 5% FAME: Investigation of acid generation in FAME blended diesel fuels and its impact on corrosion: SAE Technical Paper.
- Tubino, M., & Aricetti, J. A. (2013). A green potentiometric method for the determination of the iodine number of biodiesel. *Fuel*, *103*, 1158-1163.
- Turkcan, A., Ozsezen, A. N., & Canakci, M. (2013). Effects of second injection timing on combustion characteristics of a two stage direct injection gasoline–alcohol HCCI engine. *Fuel*, *111*, 30-39.
- Turkcan, A., Ozsezen, A. N., & Canakci, M. (2014). Experimental investigation of the effects of different injection parameters on a direct injection HCCI engine fueled with alcohol–gasoline fuel blends. *Fuel Process Technol*, *126*, 487-496.
- Turner, D., Xu, H., Cracknell, R. F., Natarajan, V., & Chen, X. (2011). Combustion performance of bio-ethanol at various blend ratios in a gasoline direct injection engine. *Fuel*, *90*(5), 1999-2006.
- Tye, Y. Y., Lee, K. T., Abdullah, W. N. W., & Leh, C. P. (2012). Potential of Ceiba pentandra (L.) Gaertn.(kapok fiber) as a resource for second generation bioethanol: Effect of various simple pretreatment methods on sugar production. *Bioresource Technol.*, *116*, 536-539.
- Vedharaj, S., Vallinayagam, R., Yang, W., Chou, S., Chua, K., & Lee, P. (2013). Experimental investigation of kapok (Ceiba pentandra) oil biodiesel as an alternate fuel for diesel engine. *Energ Convers Manage*, *75*, 773-779.
- Verduzco, L. F. R. (2013). Density and viscosity of biodiesel as a function of temperature: empirical models. *Renew Sust Energ Rev.*, *19*, 652-665.
- Vieira da Silva, M. A., Lagnier Gil Ferreira, B., da Costa Marques, L. G., Lamare Soares Murta, A., & Vasconcelos de Freitas, M. A. (2017). Comparative study of NOx emissions of biodiesel-diesel blends from soybean, palm and waste frying oils using methyl and ethyl transesterification routes. *Fuel*, *194*, 144-156. doi: <https://doi.org/10.1016/j.fuel.2016.12.084>

- Vilutienė, V., Labeckas, G., & Slavinskas, S. (2015). The influence of the cetane number and lubricity improving additives on the quality parameters of aviation-turbine fuel. *Aviation*, 19(2), 72-77.
- Wang, L.-b., Yu, H.-y., He, X.-h., & Liu, R.-y. (2012). Influence of fatty acid composition of woody biodiesel plants on the fuel properties. *Journal of Fuel Chemistry and Technology*, 40(4), 397-404.
- Wang, R., Zhou, W.-W., Hanna, M. A., Zhang, Y.-P., Bhadury, P. S., Wang, Y., . . . Yang, S. (2012). Biodiesel preparation, optimization, and fuel properties from non-edible feedstock, *Datura stramonium* L. *Fuel*, 91(1), 182-186.
- Wang, W., Jenkins, P. E., & Ren, Z. (2012). Electrochemical corrosion of carbon steel exposed to biodiesel/simulated seawater mixture. *Corros Sci*, 57, 215-219.
- Wi, S. G., Kim, H. J., Mahadevan, S. A., Yang, D.-J., & Bae, H.-J. (2009). The potential value of the seaweed Ceylon moss (*Gelidium amansii*) as an alternative bioenergy resource. *Bioresource Technol.*, 100(24), 6658-6660.
- Xue, J. (2013). Combustion characteristics, engine performances and emissions of waste edible oil biodiesel in diesel engine. *Renew Sust Energ Rev*, 23, 350-365.
- Xue, J., Grift, T. E., & Hansen, A. C. (2011a). Effect of biodiesel on engine performances and emissions. *Renew Sust Energ Rev.*, 15(2), 1098-1116.
- Xue, J., Grift, T. E., & Hansen, A. C. (2011b). Effect of biodiesel on engine performances and emissions. *Renew Sust Energ Rev*, 15(2), 1098-1116. doi: <https://doi.org/10.1016/j.rser.2010.11.016>
- Yaakob, Z., Narayanan, B. N., & Padikkaparambil, S. (2014). A review on the oxidation stability of biodiesel. *Renew Sust Energ Rev.*, 35, 136-153.
- Yahagi, Y., & Mizutani, Y. (1984). Corrosive wear of steel in gasoline-ethanol-water mixtures. *Wear*, 97(1), 17-25.
- Yanowitz, J., & McCormick, R. L. (2009). Effect of biodiesel blends on North American heavy- duty diesel engine emissions. *Eur J Lipid Sci Tech*, 111(8), 763-772.
- Yilmaz, N. (2012). Comparative analysis of biodiesel–ethanol–diesel and biodiesel–methanol–diesel blends in a diesel engine. *Energy*, 40(1), 210-213.

- Yilmaz, N., & Vigil, F. M. (2014). Potential use of a blend of diesel, biodiesel, alcohols and vegetable oil in compression ignition engines. *Fuel*, 124, 168-172.
- Yilmaz, N., Vigil, F. M., Benalil, K., Davis, S. M., & Calva, A. (2014). Effect of biodiesel–butanol fuel blends on emissions and performance characteristics of a diesel engine. *Fuel*, 135, 46-50.
- Yilmaz, N., Vigil, F. M., Donaldson, A. B., & Darabseh, T. (2014). Investigation of CI engine emissions in biodiesel–ethanol–diesel blends as a function of ethanol concentration. *Fuel*, 115, 790-793.
- Yoon, S., Ha, S., Roh, H., & Lee, C. (2009). Effect of bioethanol as an alternative fuel on the emissions reduction characteristics and combustion stability in a spark ignition engine. *Proceedings of the Institution of Mechanical Engineers, Part D: Journal of Automobile Engineering*, 223(7), 941-951.
- Yoon, S. H., & Lee, C. S. (2011). Lean combustion and emission characteristics of bioethanol and its blends in a spark ignition (SI) engine. *Energ Fuel*, 25(8), 3484-3492.
- Yoon, S. H., & Lee, C. S. (2012). Effect of undiluted bioethanol on combustion and emissions reduction in a SI engine at various charge air conditions. *Fuel*, 97, 887-890.
- Yücesu, H. S., Topgül, T., Cinar, C., & Okur, M. (2006). Effect of ethanol–gasoline blends on engine performance and exhaust emissions in different compression ratios. *Appl Therm Eng*, 26(17), 2272-2278.
- Yusoff, M. H. M., Abdullah, A. Z., Sultana, S., & Ahmad, M. (2013). Prospects and current status of B5 biodiesel implementation in Malaysia. *Energ Policy*, 62, 456-462.
- Zeng, J., Wang, X., Zhao, B., Sun, J., & Wang, Y. (2008). Rapid in situ transesterification of sunflower oil. *Ind Eng Chem Res*, 48(2), 850-856.
- Zhang, Y., Dube, M., McLean, D., & Kates, M. (2003). Biodiesel production from waste cooking oil: 2. Economic assessment and sensitivity analysis. *Bioresource Technol.*, 90(3), 229-240.
- Zhu, L., Cheung, C., Zhang, W., & Huang, Z. (2010). Emissions characteristics of a diesel engine operating on biodiesel and biodiesel blended with ethanol and methanol. *Sci Total Environ*, 408(4), 914-921.

Zhu, L., Cheung, C., Zhang, W., & Huang, Z. (2011). Combustion, performance and emission characteristics of a DI diesel engine fueled with ethanol–biodiesel blends. *Fuel*, 90(5), 1743-1750.

Ziolkowska, J. R. (2014). Prospective technologies, feedstocks and market innovations for ethanol and biodiesel production in the US. *Biotechnology Reports*, 4, 94-98.

University of Malaya

LIST OF PUBLICATIONS AND PAPERS PRESENTED

Journal articles:

1. Dharma, S., Masjuki, H., Ong, H.C., Sebayang, A., Silitonga, A., Kusumo, F., Mahlia, T., 2016. Optimization of biodiesel production process for mixed *Jatropha curcas*–*Ceiba pentandra* biodiesel using response surface methodology. *Energy Conversion and Management* 115, 178-190.
2. Dharma, S., Ong, H.C., Masjuki, H., Sebayang, A., Silitonga, A., 2016. An overview of engine durability and compatibility using biodiesel–bioethanol–diesel blends in compression-ignition engines. *Energy Conversion and Management* 128, 66-81.
3. Dharma, S., Hassan, M. H., Ong, H. C., Sebayang, A. H., Silitonga, A. S., Kusumo, F., & Milano, J. (2017). Experimental study and prediction of the performance and exhaust emissions of mixed *Jatropha curcas*-*Ceiba pentandra* biodiesel blends in diesel engine using artificial neural networks. *Journal of Cleaner Production*.
4. Dharma, S., Hassana, M. H., Onga, H. C., & Hanra, A. (2017). Optimization of Biodiesel Production from Mixed *Jatropha curcas*–*Ceiba pentandra* Using Artificial Neural Network-Genetic Algorithm: Evaluation of Reaction Kinetic Models. *Chemical Engineering Transaction*, 56.

Collaborated journal articles

1. A.H. Sebayang, H. H. Masjuki, Hwai Chyuan Ong, S. Dharma, A. S. Silitonga, et al. (2016), A perspective on bioethanol production from biomass as alternative fuel for spark ignition engine. RSC Advances, Vol. **6** Pages: 14964-14992.
2. A.H. Sebayang, H. H. Masjuki, Hwai Chyuan Ong, S. Dharma, A. S. Silitonga, et al. (2017), Optimization of bioethanol production from sweet sorghum grains using artificial neural networks integrated with ant colony. Industrial Crops and Products Vol. 97 Pages: 146–155.
3. Abdi Hanra Sebayang, Masjuki Haji Hassan, Hwai Chyuan Ong, Surya Dharma, Arridina Susan Silitonga, et al. (2017) Optimization of reducing sugar production from manihot glaziovii starch using response surface methodology. Energies, Vol. 10 (1) Pages: 1-13.
4. Sebayang, A.H., Masjuki, H.H., Ong, H.C., Dharma, S., Aditiya Harjon Bahar., Silitonga, A.S., Kusumo, F., 2017. Enzymatic Hydrolysis Using Ultrasound for Bioethanol Production from Durian (*Durio zibethinus*) Seeds as Potential Biofuel. Chemical Engineering Transactions 56.
5. Hasni, K., Ilham, Z., Dharma, S., Varman, M., 2017. Optimization of biodiesel production from Brucea javanica seeds oil as novel non-edible feedstock using response surface methodology. Energy Conversion and Management 149, 392-400.
6. Abdi Hanra Sebayang, Masjuki Haji Hassan, Hwai Chyuan Ong, Surya Dharma, Arridina Susan Silitonga, et al. (2017), Prediction of Engine Performance and Emissions with *Manihot Glaziovii* Bioethanol–Gasoline blended using Extreme Learning Machine. Fuel, <https://doi.org/10.1016/j.fuel.2017.08.102>

Conference paper

Surya Dharma, Masjuki Haji Hassan, Hwai Chyuan Ong, Abdi Hanra Sebayang, et al. Optimization of biodiesel production from mixed *Jatropha curcas*–*Ceiba pentandra* using artificial neural network-genetic algorithm: Evaluation of reaction kinetic models Paper 123. 2nd International Conference of Low Carbon Asia (ICLCA'16), Universiti Teknologi Malaysia, Kuala Lumpur, Malaysia. 23-25 Nov 2016.

Under review:

1. Corrosion behaviours of mild steel in mixed *Jatropha curcas*–*Ceiba pentandra* biodiesel blend with diesel fuel. (Manuscript CST2868).

Forthcoming papers:

Experimental study on the performance, exhaust emissions and corrosion of mixed *Jatropha curcas*-*Ceiba pentandra* biodiesel-bioethanol-diesel fuel blends in diesel engine.